

Some pages of this thesis may have been removed for copyright restrictions.

If you have discovered material in AURA which is unlawful e.g. breaches copyright, (either yours or that of a third party) or any other law, including but not limited to those relating to patent, trademark, confidentiality, data protection, obscenity, defamation, libel, then please read our [Takedown Policy](#) and [contact the service](#) immediately

CONFORMATIONAL ANALYSIS AND DIELECTRIC RELAXATION
OF
POLYCARBOSILANES AND RELATED MATERIALS

DAVID JOHN ELSBY BSc

A THESIS SUBMITTED FOR THE DEGREE OF

DOCTOR OF PHILOSOPHY

THE UNIVERSITY OF ASTON IN BIRMINGHAM

JUNE 1994

This copy of the thesis has been supplied on condition that anyone who consults it is understood to recognise that its copyright rests with its author and that no quotation from the thesis and no information derived from it may be published without proper acknowledgement.

THE UNIVERSITY OF ASTON IN BIRMINGHAM
CONFORMATIONAL ANALYSIS AND DIELECTRIC RELAXATION
OF POLYCARBOSILANES AND RELATED MATERIALS

A thesis submitted for the degree of Doctor of Philosophy

by

DAVID JOHN ELSBY JUNE 1994

SUMMARY

The conformational characteristics of poly(dimethylsilmethylene), poly(dimethylsilethene), poly(dimethylsilethane) and a related material, poly(2,2,5,5-tetramethyl-1-oxa-2,5-disilapentane), have been investigated using the method of molecular mechanics. In this method, a quantitative analysis of the factors affecting the nature and magnitude of the bond rotation potentials governing their conformational behaviour has been undertaken. Along with their structural data, the results obtained were employed to calculate a variety of conformationally-dependent properties for these polymers, including the characteristic ratio, the dipole moment ratio and the mean-square radius of gyration.

In addition, the dielectric relaxation behaviour of two samples of poly(2,2,5,5-tetramethyl-1-oxa-2,5-disilapentane) with molar masses $M_w = 28000$ and $M_w = 46000$ respectively, have been studied as a function of temperature (179K-205K) and frequency (100-10⁵Hz). Activation energies for the α -relaxation process and Davidson-Cole empirical distribution factors, β , have been calculated.

KEYWORDS: STATISTICAL WEIGHT, CHARACTERISTIC RATIO, DIPOLE MOMENT RATIO, DAVIDSON-COLE RELAXATION, ACTIVATION ENERGIES.

Dedicated to my parents, especially my father the late Mr. John Edward Elsby

ACKNOWLEDGEMENTS

I wish to express my thanks and gratitude to my supervisor, Dr. M. S. Beevers for his excellent guidance and numerous invaluable suggestions throughout this project.

My thanks are also extended to the Science and Engineering Research Council for providing the funding for my research project. I am also indebted to Dow Corning for their generous financial support throughout my term at Aston University.

Finally, I would like to especially thank my parents for their encouragement and their financial support.

LIST OF CONTENTS

	Page
Title Page	1
Summary	2
Dedication	3
Acknowledgements	4
List of Contents	5
List of Figures	12
List of Tables	18
CHAPTER1: INTRODUCTION	19
CHAPTER2: THEORETICAL CONCEPTS OF CONFORMATIONAL ANALYSIS	31
2.1 Introduction	31
2.2 Bond Rotation Potentials	32
2.3 The Rotational Isomeric State Approximation	34
2.4 Effect of Independent and Interdependent Bond Rotational Potentials on the Conformational Energy of a Polymer Molecule	36
2.5 The Statistical Weight Matrix	37
2.6 The Configuration Partition Function	39
2.7 Mean Square Moments of Chain Molecules	40
2.7.1. Mean Square Moments of Chains with Independent Bond Rotation Potentials	45

	Page
2.7.2. Mean Square Moments of Chains with Interdependent Bond Rotation Potentials	46
2.8 Polycarbosilanes and Related Materials	49
CHAPTER 3: COMPUTER PROGRAM DEVELOPMENT	52
3.1 Introduction	52
3.2 Conformational Analysis of Poly(dimethylsilmethylene) and Poly(dimethylsilethene)	52
3.2.1. Polymethylene	55
3.2.2. Polysilane	56
3.2.3. Polypropylene	57
3.3 The Calculation of Characteristic Ratios and Dipole Moment Ratios	58
3.3.1. Polymethylene	58
3.3.2. Poly(dimethylsiloxane)	58
3.4 Conclusion	59
CHAPTER 4: CONFORMATIONAL ANALYSIS OF POLY(DIMETHYLSILMETHYLENE)	60
4.1 Introduction	60
4.2 Molecular Geometry	61
4.3 Conformational Energy	63
4.4 Rotational States	69
4.5 Statistical Weights	71
4.6 Characteristic Ratio of Poly(dimethylsilmethylene)	76

	Page
4.7 Dipole Moment Ratio of Poly(dimethylsilmethylene)	78
4.8 Discussion of Results	78
CHAPTER5: CONFORMATIONAL ANALYSIS OF POLY(DIMETHYLSILETHENE)	82
5.1 Introduction	82
5.2 Molecular Geometry	84
5.3 Conformational Energy	88
5.4 Configurational Statistics of Poly(dimethylsilethene)	94
5.5 Calculation of the Characteristic Ratio and Mean-Square Radius of Gyration for Poly(dimethylsilethene)	99
5.6 Discussion of Results	102
CHAPTER6: CONFORMATIONAL ANALYSIS OF POLY(DIMETHYLSILETHANE) AND POLY(2,2,5,5-TETRAMETHYL-1-OXA-2,5-DISILAPENTANE) USING THE HARD-SPHERE MODEL	103
6.1 Introduction	103
6.2 The Hard-Sphere Model	104
6.3 Poly(dimethylsilethane)	105
6.3.1. Molecular Geometry	107
6.3.2. Construction of the Statistical Weight Matrices	108
6.3.3. Characteristic Ratio	113
6.4 Poly(2,2,5,5-tetramethyl-1-oxa-2,5-disilapentane)	114
6.4.1. Molecular Geometry	114

	Page
6.4.2. Construction of the Statistical Weight Matrices	116
6.4.3. Characteristic Ratio	123
6.4.4. Dipole Moment Ratio	124
6.5 Discussion of Results	124
CHAPTER 7: MATERIALS	126
7.1 Introduction	126
7.2 Poly(2,2,5,5-tetramethyl-1-oxa-2,5-disilapentane)	126
7.2.1. G.P.C. Analysis of the Samples 10423-1 and 10423-9	126
7.3 A Synthetic Route to Poly(dimethylsilmethylene)	129
7.4 Preparation of 1,1,3,3-tetramethyl-1,3-disilacyclobutane	130
7.4.1. Infra-red Spectroscopy	131
7.4.2. Nuclear Magnetic Resonance Spectroscopy	131
7.5 Polymerisation of 1,1,3,3-tetramethyl-1,3-dilacyclobutane	131
7.5.1. Infra-red Spectroscopy	133
7.5.2. Gel Permeation Chromatography	135
CHAPTER 8: DIELECTRIC RELAXATION	137
8.1 Introduction	137
8.2 Dielectrics in Static Electric Fields	137
8.3 Dielectrics in Time Varying Electric Fields	140
8.3.1. Single Relaxation Behaviour	142
8.3.2. Multiple Relaxation Behaviour	144

	Page
8.4 Temperature and Dielectric Relaxation	148
CHAPTER9: EXPERIMENTAL METHODS	150
9.1 Introduction	150
9.2 Dielectric Apparatus for the Measurement of C_p and $\tan \delta$ at Various Frequencies	150
9.3 The Dielectric Cell	151
9.4 Temperature Control in the Region 203K-298K	153
9.5 Measurement of Electrical Capacitance and Dissipation Factor in the Range 203K-298K	155
9.6 Apparatus for Temperature Control Below 203K	155
9.7 Measurement of Electrical Capacitance and Dissipation Factor Below 203K	157
9.8 Measurement of Dielectric Permittivities	158
CHAPTER10: DIELECTRIC RESULTS	160
10.1 Dielectric Properties of Dow Polymer Samples 10423-1 and 10423-9	160
10.2 Dielectric Loss Results	160
10.3 Measurement of Dielectric Relaxation Activation Energy	163
10.4 Cole-Cole Plots	163
10.5 Calculation of Dielectric Activation Energies	170
10.6 Davidson-Cole Analysis of the Dielectric Data	170

	Page
10.7 Discussion of Results	171
CHAPTER 11: DISCUSSION/FURTHER WORK	172
LIST OF REFERENCES	177
APPENDIX A: THE USE OF EXPERIMENTAL TECHNIQUES TO DETERMINE CONFORMATIONAL BEHAVIOUR	181
A.1. Introduction	181
A.2. Infrared Spectroscopy	181
A.3. High Resolution Spectroscopy	184
A.4. Calorimetry	186
APPENDIX B: COMPUTER SIMULATION OF POLY(DIMETHYLSILMETHYLENE) AND POLY(DIMETHYLSILETHENE)	188
B.1. Introduction	188
B.2. A Brief Description of the Important Subroutines	188
B.3. Computer Simulation of poly(dimethylsilmethylene)	190
B.4. Computer Simulation of poly(dimethylsilethene)	204
APPENDIX C: COMPUTER PROGRAMS	224
C.1. Introduction	224
C.2. Davidson-Cole Analysis	224
C.3. Calculation of the Characteristic Ratio and Dipole Moment of Poly(dimethylsilmethylene)	231
C.4. Calculation of the Characteristic Ratio of Poly(dimethylsilethane)	241

	Page
C.5. Calculation of the Characteristic Ratio and Dipole Moment Ratio of Poly(2,2,5,5-tetramethyl-1-oxa-2,5-disilapentane)	253
APPENDIX D: DIELECTRIC RELAXATION OF THE POLYMER SYSTEM PPG2025 + 1 MOLE %HgCl₂	269
D.1. Introduction	269
D.2. Dielectric Loss Results	269
D.3. Conclusion	271
APPENDIX E: SPECIFICATIONS OF THE DIELECTRIC CELL	272
E.1. Factors Effecting the Design of the Dielectric Cell	272
E.2. Dimensions of the Cell	273
APPENDIX F: EXPERIMENTAL DIELECTRIC DATA	274

LIST OF FIGURES

Figure no.		Page
(1-1)	Proposed mechanism for the success of inverse addition	27
(1-2)	The synthesis of 1,1,3,3-tetramethyl-1,3-disilacyclobutane	28
(1-3)	Synthesis of poly(dimethylsilethene)	28
(1-4)	Illustration of the crankshaft mechanism	30
(2-1)	The conformational energy of n-butane as a function of the rotation angle ϕ_2 about the central bond	35
(2-2)	Schematic representation of a long chain molecule	40
(2-3)	Cartesian coordinate system assigned to bond i	42
(3-1)	Computer program development	54
(3-2)	Section of polymethylene used in the calculations	55
(3-3)	Section of polysilane used in the calculations	56
(3-4)	Section of syndiotactic polypropylene used in the calculations	57
(4-1)	Molecular structure of bis(trimethylsilyl)methane	61
(4-2)	Poly(dimethylsilmethylene) dyad used in the calculations	63

Figure no.	Page
(4-3) Conformational energy map for the poly(dimethylsilmethylene) dyad as determined by the partial relaxation (PR) calculations	67
(4-4) Regions representing isomeric states for the poly(dimethylsilmethylene) dyad	70
(4-5) Newman projections along bond <i>i</i> illustrating the basic first-order interactions	72
(4-6) Interdependent bond pair flanking a Si(CH ₃) ₂ -	73
(4-7) Characteristic ratio of PDMSM at 300K, 400K and 500K	77
(4-8) Dipole moment ratio of PDMSM at 300K, 400K and 500K	79
(5-1) Spatial arrangement of a section of poly(dimethylsilethene) as described by the virtual bonds <i>i</i> and <i>i</i> + 1	83
(5-2) Dependence of C = C-Si bond angle in the trans-trans conformation	86
(5-3) Dependence of C = C-Si bond angle in the trans-gauche conformation	86

Figure no.	Page
(5-4) Dependence of C=C-Si bond angle in the gauche(-)-gauche(-) conformation	87
(5-5) Dependence of C=C-Si bond angle in the gauche(+)-gauche(-) conformation	87
(5-6) Section of poly(dimethylsilethene) used in the calculations	88
(5-7) Lowest energy conformation for a tetravalent Si atom bonded to a doubly bonded C atom	90
(5-8) Conformational energy map for the pair of rotation angles ϕ_a and ϕ_a as determined by the PR calculations	92
(5-9) The H*-H* interaction occurring in the cis-cis state	93
(5-10) The coordinate system assigned to each virtual bond	95
(5-11) Geometrical representation of the relationship between the virtual bonds i and $i+1$ and the skeletal bonds $C^\alpha-Si^\beta$ and $Si^\beta-C^\gamma$	96
(5-12) Characteristic ratio of poly(dimethylsilethene) at 300K, 400K and 500K	100
(5-13) Mean square radius of gyration of poly(dimethylsilethene) at 300K, 400K and 500K	101

Figure no.	Page
(6-1) Conditions utilized in determining the values of the U-matrix elements when applying the hard-sphere model	106
(6-2) Assigning the U-matrices required to describe poly(dimethylsilethane)	108
(6-3) Assigning the U-matrices required to describe poly(2,2,5,5-tetramethyl-1-oxa-2,5-disilapentane)	116
(7-1) G.P.C. chromatograph of sample 10423-1	127
(7-2) G.P.C. chromatograph of sample 10423-9	128
(7-3) Synthetic route to poly(dimethylsilmethylene)	130
(7-4) Infra-red spectrum of 1,1,3,3-tetramethyl-1,3-disilacyclobutane	132
(7-5) N.M.R. spectrum of 1,1,3,3-tetramethyl-1,3-disilacyclobutane	133
(7-6) Infra-red spectrum of poly(dimethylsilmethylene)	134
(7-7) G.P.C. chromatograph of poly(dimethylsilmethylene)	136
(8-1) Schematic representation of dielectric polarization	138
(8-2) Debye dielectric dispersion curves	143

Figure no.		Page
(8-3)	Cole-Cole plots	145
(9-1)	The dielectric cell prior to wrapping in PTFE thread tape	152
(9-2)	Cross-sectional diagram of the Townson and Mercer bath	154
(9-3)	Apparatus for temperature control below 203K	156
(10-1)	Frequency dependence of $\varepsilon''/\varepsilon''_{(max)}$ for sample 10423-1	161
(10-2)	Frequency dependence of $\varepsilon''/\varepsilon''_{(max)}$ for sample 10423-9	162
(10-3)	$\text{Log}(f_{max}/\text{Hz})$ against $1/T$ (K^{-1}) for sample 10423-1	164
(10-4)	$\text{Log}(f_{max}/\text{Hz})$ against $1/T$ (K^{-1}) for sample 10423-9	165
(10-5)	Cole-Cole plots for sample 10423-1 at various temperatures	166
(10-6)	Cole-Cole plots for sample 10423-1 at various temperatures	167
(10-7)	Cole-Cole plots for sample 10423-9 at various temperatures	168
(10-8)	Cole-Cole plots for sample 10423-9 at various temperatures	169

Figure no.		Page
(A-1)	Infrared spectrum of CD ₂ -doped polyethylene at 120°C.	182
(A-2)	Trans conformation of a section of chlorotrifluoroethylene- isobutylene copolymer.	185
(D-1)	Frequency dependence of $\epsilon''/\epsilon''_{(\max)}$ for the polymer system PPG2025 + 1 mole %HgCl ₂	270
(E-1)	Schematic illustration of one plate of the dielectric cell	273

LIST OF TABLES

Table no.		Page
(4-1)	Geometrical parameters for $\text{CH}_2(\text{Si}(\text{CH}_3)_3)$	62
(4-2)	Non-bonded potential energy parameters	66
(4-3)	Conformational averages for dyad conformations	71
(5-1)	Geometrical parameters for poly(dimethylsilethene)	85
(5-2)	Non-bonded potential energy parameters	91
(6-1)	Geometrical parameters used for poly(dimethylsilethane)	107
(6-2)	Geometrical parameters used for poly(2,2,5,5-tetramethyl-1-oxa-2,5-disilapentane)	115
(10-1)	Davidson-Cole distribution parameter, β , for samples 10423-1 and 10423-9	171
(F-1)	Dielectric data for polymer sample 10423-1	275
(F-2)	Dielectric data for polymer sample 10423-9	277

CHAPTER 1

INTRODUCTION

Computer Simulation of Molecular Systems

Computational chemistry is a branch of chemistry that has enjoyed a growing interest from experimental chemists during recent years¹. In this discipline, chemical problems are investigated by the application of computational methods. In many cases, such investigations involve programming computers to simulate complex molecular systems. The aim of these computer simulations is to compute macroscopic behaviour from microscopic interactions.

The two main contributions that a microscopic analysis can offer is an understanding and interpretation of experimentally determined results and the capability to interpolate or extrapolate experimental data into regions that are extremely difficult to access in the laboratory. With the arrival of ever more powerful computers, many previously unexplored realms of theoretical chemistry are now open to such computational examination.

The recent growth in the number of computer simulation methods used in chemistry and physics is directly related to the rapid increase in computing power over the last three decades. The ratio of price to performance has also increased by an order of magnitude every five to seven

years¹, and there is no sign of any weakening in the trend. As the power and performance of computers continues to increase, the ability of computer simulations to complement experimentally determined results will become more and more prominent.

Conformational Analysis of Polymers

It is well known that the conformational behaviour of a polymer molecule is an important factor in determining its chemical and physical properties. For example, the overall dipole moment of a polymer molecule can be attributed to the vectorial sum of the individual bond dipoles², or the probability that a polymer will dissolve in a particular solvent will be dependent upon how the conformational properties of the polymer are affected in the solvent environment^{3,4}. For this and other reasons, the use of computational methods in the investigation of conformationally-dependent properties of polymers has become increasingly popular during the last twenty years.

Early investigations into conformational behaviour concentrated on the n-alkanes⁵ and simple polymer structures such as polymethylene⁵ and polypropylene⁶. However, during the 1970's and 1980's, the general interest in molecular modelling and conformational analysis techniques increased, and to date many flexible molecules and polymers with very varied molecular structures have been subjected to a theoretical investigation. The current list of polymers that have now been examined in this way includes, polysilanes⁷, polysiloxanes⁸, polyketones⁹ and polypeptides¹⁰.

The three most common conformational-dependent quantities that are usually calculated in order to characterise a polymer chain are

1. The mean-square distance between chain ends, $\langle r^2 \rangle$,
2. The mean-square dipole moment, $\langle \mu^2 \rangle$, and
3. The mean-square radius of gyration, $\langle s^2 \rangle$.

In general, the theoretical calculation of the above three quantities is based on short range interactions occurring between atoms separated by only a few skeletal bonds. Long range interactions between remote sections of the chain and possible solvent effects are ignored. In recognition of this fact, they are commonly referred to as unperturbed quantities and are designated by the subscript zero.

The unperturbed mean-square distance between the chain ends, $\langle r^2 \rangle_0$, is an important quantity in characterising a polymer chain since it is a measure of the average chain dimensions. Polymers for which $\langle r^2 \rangle_0$ is large tend to be stiff, extended chains whereas polymers with low values tend to be chains that are flexible and more coiled.

The unperturbed mean-square dipole moment, $\langle \mu^2 \rangle_0$, is an important quantity when characterising a polymer chain with polar bonds or polar branched side groups. The value of $\langle \mu^2 \rangle_0$ can indicate the potential use of a polymer as a dielectric material and can be an important parameter in the study of polymer liquid-crystals. Polymers with large values of $\langle \mu^2 \rangle_0$ tend to exhibit better dielectric properties when compared to polymers with low values. Since most of the interest in the past has been concerned with the

mechanical properties of polymers, considerable work is now being performed examining their electrical and dielectric properties, particularly their potential use in the electronics industry.

The unperturbed mean-square radius of gyration, $\langle s^2 \rangle_0$, is a measure of the average distance of a chain element from the centre of gravity of the chain, and for sufficiently large chains it is related to the quantity $\langle r^2 \rangle_0$ by the equation

$$\langle r^2 \rangle_0 = 6 \langle s^2 \rangle_0 \quad (1-1)$$

In most scientific literature, the quantities $\langle r^2 \rangle_0$, $\langle \mu^2 \rangle_0$ and $\langle s^2 \rangle_0$ are usually expressed as ratios relative to their random flight statistics. For a polymer chain consisting of identical bonds, the characteristic ratio and mean-square radius of gyration ratio are defined as $\langle r^2 \rangle_0/nl^2$ and $\langle s^2 \rangle_0/nl^2$ respectively, with the denominators representing the product of the number of bonds in the polymer chain and the square of the individual bond lengths. The dipole moment ratio is defined as $\langle \mu^2 \rangle_0/nm^2$. Here m is equal to the magnitude of the individual bond dipoles.

Correlation Between Theory and Experiment

In order to correlate the theoretically calculated values of $\langle r^2 \rangle_0$, $\langle \mu^2 \rangle_0$ and $\langle s^2 \rangle_0$ with experimental results, it is important to consider the perturbation caused by long-range interactions and polymer-solvent effects. In dilute solutions, the extent of coil perturbation by long range interactions

and solvent effects can be measured by an expansion factor, α , first introduced by Flory^{2,11}. The square of the expansion factor is defined as the ratio of the perturbed and unperturbed values of a particular quantity. Hence, if $\langle r^2 \rangle$ represents the perturbed value of the mean-square distance between chain ends with $\langle r^2 \rangle_0$ representing its unperturbed value, the expansion factor may be expressed by the equation²

$$\alpha = (\langle r^2 \rangle / \langle r^2 \rangle_0)^{1/2} \quad (1-2)$$

The extent of coil expansion is determined by two effects. The first results from the physical interaction between two remote parts of the polymer chain. This type of interaction tends to reduce the number of conformations available to the chain and also lowers the probability that tightly coiled conformations will be favoured. The second effect is observed with polymers in solution. In a good solvent, the smaller solvent molecules may become intermingled within the polymer chain causing even more extended conformations to exist. Since these two factors affect the volume a polymer chain may occupy, they are commonly known as excluded volume effects.

The expansion factor α is dependent upon the temperature of the polymer solution and on the particular solvent used. By dissolving a polymer in a poor solvent or theta solvent², in which the solvent molecules do not significantly interact with the polymer molecule, the temperature may be adjusted until the value of the expansion factor becomes unity. At this point,

called the theta point², a direct comparison of theoretically calculated quantities with experimentally determined values becomes possible.

Experimental Determination of $\langle r^2 \rangle_0$, $\langle \mu^2 \rangle_0$ and $\langle s^2 \rangle_0$

A popular experimental method employed to determine $\langle r^2 \rangle_0$ for dilute solutions depends upon the relationship between the viscosity of a polymer solution and its molecular mass. For a polymer dissolved in a suitable theta solvent and if the measurements are carried out at the theta point, then it is assumed that the limiting viscosity¹¹, $[\eta]_\theta$, is proportional to the square root of the molar mass, $M^{1/2}$. Experimental values of $\langle r^2 \rangle_0$ may then be determined from the magnitude of the gradients produced from plots of $[\eta]_\theta$ against $M^{1/2}$.

The mean-square dipole moment, $\langle \mu^2 \rangle_0$, of a polymer chain is usually determined experimentally from various dielectric and density measurements performed on a range polymer fractions. Many different methods are available which may be used to calculate $\langle \mu^2 \rangle_0$ from such data. For instance, for a polymer in solution, $\langle \mu^2 \rangle_0$ may be calculated according to the method proposed by Guggenheim and Smith¹². However, for an undiluted polymer, $\langle \mu^2 \rangle_0$ is usually calculated according to the method of Onsager¹³. The choice of which method to use when calculating $\langle \mu^2 \rangle_0$ is dependent upon the properties and conditions of the polymer system under consideration.

The direct experimental determination of the parameter $\langle s^2 \rangle_0$ can be achieved from light-scattering experiments, since for sufficiently large chains, the intensity distribution of the light scattered by a polymer in solution is dependent upon its molecular shape¹¹.

Polycarbosilanes

During recent years, there has been intense activity into the synthesis, characterisation, and the investigation of the physical properties of polycarbosilanes. Originally, interest focused upon their use as thermally-stable high-tensile fibres¹⁴, and on their importance as precursors for silicon carbide based ceramics¹⁵. However, it is becoming increasingly evident that polycarbosilanes and related materials may have other uses, such as surfactants, liquid-crystals and other electro-active materials. Although a great deal of work has been carried out concerning the measurement of the mechanical properties of polycarbosilanes, relatively little is known about their general chemical and physical properties.

Poly(dimethylsilmethylene)

Initially, interest in this polymer was concerned with its mechanical properties¹⁴, since early experiments suggested that fibre formation in carbon-silicon polymers was a field of considerable potential. Only recently has the focus on poly(dimethylsilmethylene) been concerned with its electrical and dielectric nature. Dielectric measurements^{16,17,18} performed on hexalkyl derivatives of disilamethanes have indicated that a dipole moment of 0.6D is

associated with the Si-C bond in poly(dimethylsilmethylene). Since carbon is more electronegative than silicon, the negative end of the skeletal bond dipole probably exists on the carbon atoms.

A synthetic route commonly used to produce poly(dimethylsilmethylene) involves the ring opening polymerisation of 1,1,3,3-tetramethyl-1,3-disilacyclobutane. The monomer, 1,1,3,3-tetramethyl-1,3-disilacyclobutane¹⁹ is not available commercially, but may be synthesized by the following methods.

The first method relies on a Grignard process using (chloromethyl)dimethylchlorosilane as reported by Kriner²⁰. On investigation of this process, Kriner found that normal Grignard addition gives poor yields, while an inverse addition produced yields approaching 50%. To account for the success of the inverse addition process, Kriner proposed the following mechanism²⁰, illustrated in Figure (1-1).

The mechanism suggests that the reason for the success of inverse addition is that the process favours the production of $\text{ClCH}_2(\text{CH}_3)_2\text{SiCH}_2\text{Si}(\text{CH}_3)_2\text{Cl}$. This is because only small amounts of $\text{ClMgCH}_2\text{Si}(\text{CH}_3)_2\text{Cl}$ will be formed in an environment rich in (chloromethyl)dimethylchlorosilane. This advantage holds until the concentration of $\text{ClCH}_2(\text{CH}_3)_2\text{SiCH}_2\text{Si}(\text{CH}_3)_2\text{Cl}$ becomes appreciable. The normal method, in contrast, produces a relatively high concentration of $\text{ClMgCH}_2\text{Si}(\text{CH}_3)_2\text{Cl}$ resulting in chain lengthening reactions.

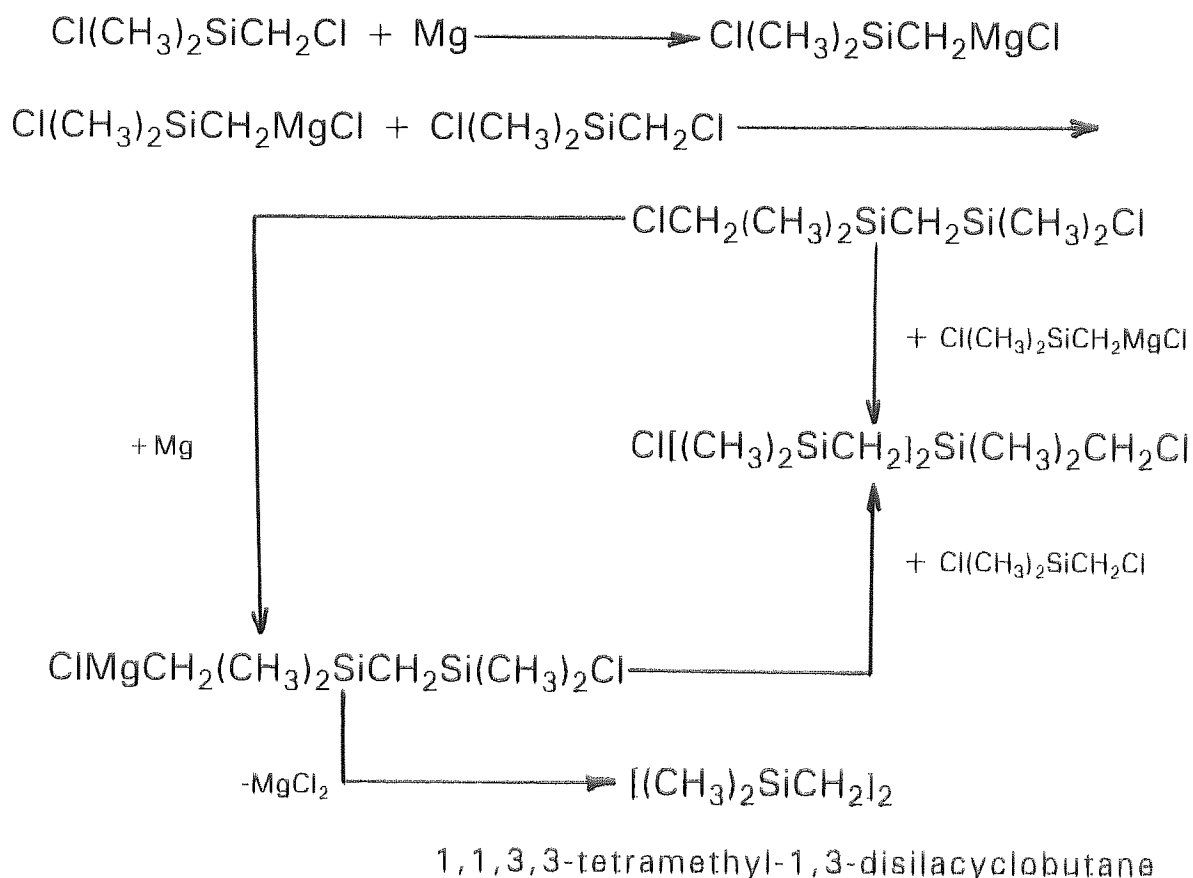


Figure (1-1). Proposed mechanism for the success of inverse addition.

An alternative method to produce 1,1,3,3-tetramethyl-1,3-disilacyclobutane, illustrated in Figure (1-2), was recently proposed by Chmielecka and Stanczyk²¹. Their synthetic approach involves the generation of chloro(lithiomethyl)dimethylsilane from (bromomethyl)chlorodimethylsilane. Chloro(lithiomethyl)dimethylsilane eliminates lithium chloride spontaneously to give an intermediate unsaturated silicon species. This intermediate then undergoes cycloaddition to give the product, 1,1,3,3-tetramethyl-1,3-disilacyclobutane. The resulting yields obtained from this method have been reported as higher than those usually obtained from the inverse Grignard method.

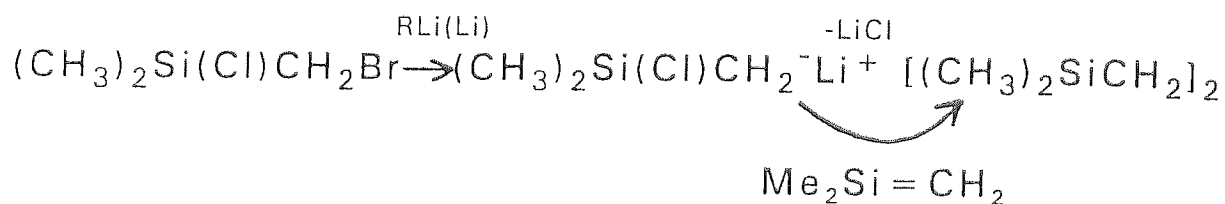


Figure (1-2). Synthesis of 1,1,3,3-tetramethyl-1,3-disilacyclobutane.

Poly(dimethylsilethene)

The synthesis of poly(dimethylsilethene) has been investigated by Andrianov, Pakhomov, Gel'perina and Semenova²². In the presence of catalytic amounts of KOH, they found that at high temperatures alkoxy derivatives of disilylethylenes²³ react with the precipitation of alkoxy silanes and the formation of polymers. The reaction scheme they proposed for the synthesis of poly(dimethylsilethene) is illustrated in Figure (1-3).

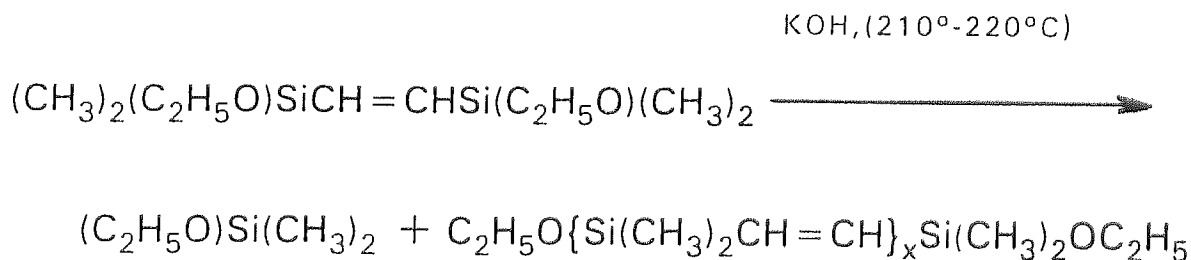


Figure (1-3). Synthesis of poly(dimethylsilethene).

Dielectric Relaxation in Polymers

For polymers in the amorphous state a relaxation region associated with the glass transition is usually observed at temperatures at or around T_g . This relaxation is labelled α and is referred to as the glass-rubber relaxation.

mechanism observed in amorphous polymers. From a molecular point of view it is widely accepted that the α -relaxation process results from large-scale conformational rearrangements of the polymer chain backbone. These rearrangements occur by a mechanism of hindered rotation about the main-chain bonds.

In addition to α -relaxation, many amorphous polymers also exhibit at least one secondary relaxation region. These secondary loss regions (β , γ , δ relaxations) result from motions from within the polymer in the glass-like state. In this state the main chains are effectively 'frozen in' so that these relaxations cannot be due to large scale rearrangements of the main polymer chain. Since the molecules of many amorphous polymers contain branched side groups that are capable of undergoing hindered rotations independently of the chain backbone, these secondary relaxations are often ascribed to such rotations.

However, certain linear polymers considered to be largely amorphous show dielectric β -relaxation that cannot be the result of side-group rotations. Hence, some limited local motions of the chain backbone may be possible in the glassy state.

A third type of relaxation process known as γ -relaxation is often observed in crystalline polymers containing linear $(-\text{CH}_2-)_n$ sequences. These low temperature loss peaks are thought to originate from limited motions of relatively short chain segments. One such mechanism for γ -relaxation proposed

by Schatzki²⁴ is known as the 'crankshaft' mechanism and is illustrated in Figure (1-4).

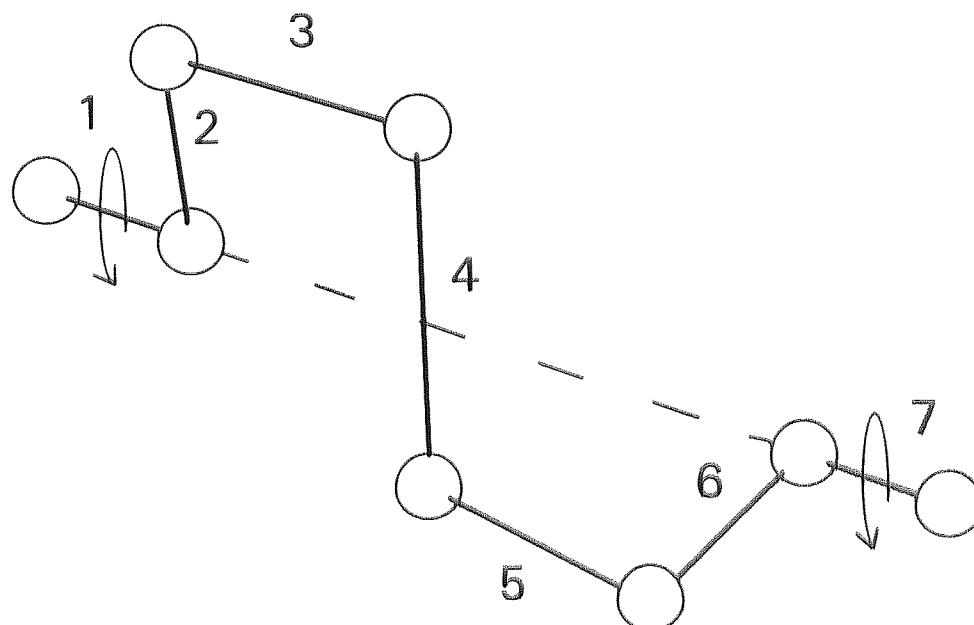


Figure (1-4). Illustration of the crankshaft mechanism.

The crankshaft mechanism involves the simultaneous rotation about the two bonds 1 and 7, such that the intervening carbon atoms move in a manner similar to that of a crankshaft.

Finally, it should be noted that relaxation effects can also arise from the presence of impurities of low molecular weight. The precise mechanism of relaxations of this type are often not clearly understood.

CHAPTER 2

THEORETICAL CONCEPTS OF CONFORMATIONAL ANALYSIS

2.1 Introduction

Most of the conformation-dependent properties of long chain molecules of interest are combinations of vectorial quantities associated with the individual bonds or repeating sequences within the chain. For instance, the overall dipole moment of a molecule may be attributed to the sum of the individual bond dipoles. For chains with fixed bond lengths and fixed bond angles, some correlation exists between these bond vectors in the sense that the direction of a given bond is influenced by the direction of its predecessors. However, the overall magnitude of such a series of bond vectors is primarily dependent upon the molecular conformation of the polymer which in turn is determined by the molecular conformational energy; the majority of polymer molecules tending to exist in the conformations with the lowest energies. It is therefore essential when investigating such properties that a quantitative account of the factors involved in determining the molecular conformation of a polymer is included.

The conformational energy of a polymer molecule originates from the intramolecular interactions between non-bonded atoms within the chain.

These interactions generate rotational energy potentials for all the bonds in the chain. Neighbouring bond rotation potentials interact with each other resulting in the creation of energetically favourable rotational states and energetically unfavourable rotational states for each bond. Since most of the bonds will probably occupy the more favourable rotational states, the molecular conformation of the molecule is established.

Presented in this chapter is a quantitative description of the nature of bond rotation potentials, their interactions with each other and their relationship to the conformational energy of a polymer molecule. Also included is a description of the relative assumptions made and the mathematical methods used which allow us to calculate statistical mean-square moments of vectorial quantities associated with polymer chains.

2.2 Bond Rotation Potentials

Investigations as to the nature of bond rotation potentials of flexible molecules²⁵ have indicated that they may be described generally as mainly repulsive interactions between non-bonded atoms superimposed on an inherent torsional rotation potential. The former may be easily explained as originating from the repulsion between the electron clouds of two or more non-bonded atoms in close proximity to each other and may be expressed, to a good approximation, by the Lennard-Jones²⁶ (6-12) potential

$$E_{NB} = (a_{kl}/r_{kl}^{12}) - (c_{kl}/r_{kl}^6) \quad (2-1)$$

The labels k and l index the atom pair, where r_{kl} is the distance between them and a_{kl} and c_{kl} are constants characteristic of the atom pair.

The latter arises from electron-electron repulsions, nuclei-nuclei repulsions and polarization effects associated with the bonds. It may be expressed mathematically by the empirical equation²⁵

$$E_T = (E^0/2)(1 - \cos n\phi) \quad (2-2)$$

where E^0 is the height of the rotational barrier and ϕ is the angle of rotation. The factor n indicates the number of rotational states the bond may occupy, this usually being three for a simple sp^3 hybridized bond.

In cases where certain bonds of the polymer carry dipole moments, an additional electrostatic term may be required, this being equal to

$$E_S = +/- [(4\pi q_k q_l) / r_{kl}^2] \quad (2-3)$$

where q_k and q_l are the partial charges on atoms k and l respectively, r_{kl} being the distance between them.

Combining these contributions, the bond rotational potential for a particular bond may be expressed as

$$E_{(\phi)} = (E^0/2)(1 - \cos n\phi) + \sum [(a_{kl}/r_{kl}^{12}) - (c_{kl}/r_{kl}^6)] +/- \sum [(4\pi q_k q_l) / r_{kl}^2] \quad (2-4)$$

The first term includes the bond subject to rotation, the second term includes all atom pairs whose distance of separation r_{kl} depends on the rotation angle ϕ and the third term, if necessary, is summed over all atoms assigned a

partial charge, this term being negative for unlike charges and positive for like charges.

2.3 The Rotational Isomeric State Approximation

The rotation potential for n-butane² as a function of the rotation angle ϕ_2 about the central bond is illustrated in Figure (2-1). The height of the barrier occurring at 60° is approximately 3.5 kcal/mol while the barrier height at 180° is unknown but is thought to be large. The curve is shown over the range 0° to 180° for the central bond angle. The region between -180° to 0° may be obtained by reflection through the ordinate axis.

The three potential energy minima, one for the trans (0°) and two for the gauche conformations ($\pm 120^\circ$) are the features of most importance in this example. The potential wells of these three minima are sufficiently steep to confine the majority of the molecules to a state of torsional oscillation about one of these minima. Molecules confined to the regions of the three potential minima in this way are well differentiated, and in this sense three conformations of n-butane may be distinguished. They are designated trans(t), gauche⁺(g⁺) and gauche⁻(g⁻), respectively. On the same basis we would expect six distinguishable rotational conformers for n-pentane, these being tt, tg⁺, tg⁻, g⁺g⁺, g⁻g⁻ and g⁺g⁻. Experimental evidence for the existence of discrete rotational states is presented in Appendix A.

A description of the conformations of these and other simple molecules in terms of distinct rotational isomeric forms is both convenient and well

justified by physical circumstances and it may be applied to long chain molecules where similar potentials affect the rotations of the more numerous skeletal bonds. This is the basis of the rotational isomeric state approximation².

In the rotational isomeric state approximation each molecule, or bond, is treated as occurring in one or another of several discrete rotational states. These states ordinarily are chosen to coincide with potential minima. Fluctuations about the minima are ignored although their occurrence is not denied.

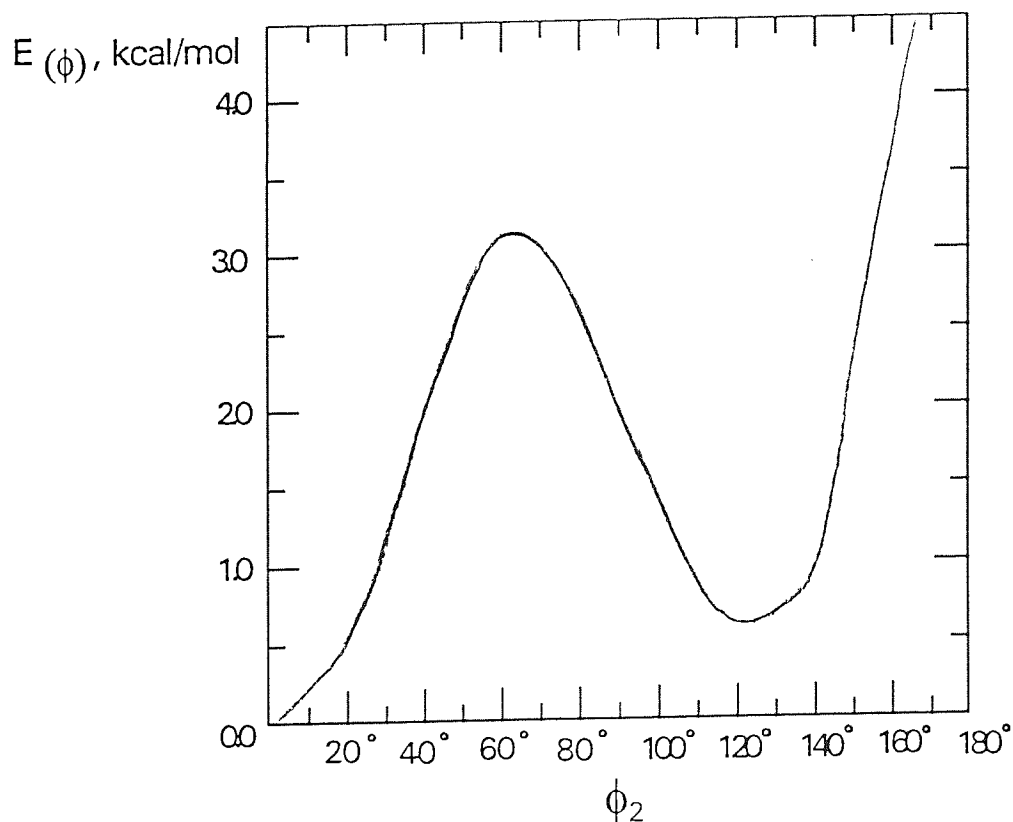


Figure (2-1). The conformational energy of n-butane² as a function of the rotation angle ϕ_2 about the central bond.

2.4 Effect of Independent and Interdependent Bond Rotational Potentials on the Conformational Energy of a Polymer Molecule

For a chain with independent bond rotation potentials the rotational state of a particular bond, say bond i , is totally independent of the rotational states of the neighbouring bonds, both preceding and succeeding bond i . This allows us to separate the overall conformational energy of the chain, $E(\phi)$, into a sum of energies E_i , one such energy contribution being associated with the conformational state of each skeletal bond i in relation to its neighbours, terminal bonds excepted. The conformational energy for bond i may be appropriately designated by $E_i(\phi_i)$, the bond rotational potential for bond i , and according to the assertion that the energy is separable

$$E(\phi) = \sum E_i(\phi_i) , i = 2 \text{ to } n-1 \quad (2-5)$$

This assumption of independence of bond rotational potentials is seldom acceptable. Instead, interdependent bond rotation potentials must be assumed. Interdependence of bond rotation potentials is manifested in the dependence of E_i on ϕ_{i-1} and ϕ_{i+1} as well as on ϕ_i . The total conformational energy of a molecule must then be expressed as a sum of energies for first neighbour pairs. In general²,

$$E(\phi) = \sum E_i(\phi_{i-1}, \phi_i) = \sum E_{\zeta\eta;i} , i = 2 \text{ to } n-1 \quad (2-6)$$

where ζ denotes the state of bond $i-1$ and η that of bond i , with the first term in the sum being a function of one angle only. The energy $E_{\zeta\eta;i} = E_i(\phi_{i-1}, \phi_i)$

is regarded as the contribution to $E(\phi)$ associated with its assignment of bond i to the state η with bond $i-1$ in the state ζ . By adopting this view point the dependence of the energy on ϕ_{i+1} is not overlooked, since the dependence of the energy on ϕ_{i+1} is merely reversed for the next term in the sum. Thus, the total energy for a long chain molecule may be reckoned systematically as a sum of terms each dependent upon a pair of consecutive rotation angles.

2.5 The Statistical Weight Matrix

We may represent the energies $E_{\zeta\eta;i}$ associated with the various rotational states of an interdependent bond pair in terms of statistical weights. For a given state, the statistical weight $u_{\zeta\eta;i}$ corresponding to the energy $E_{\zeta\eta;i}$ may be defined by invoking the relationship²

$$u_{\zeta\eta;i} = \exp(-E_{\zeta\eta;i}/RT) \quad (2-7)$$

The statistical weights assigned in this way may be conveniently expressed in the form of a statistical weight matrix

$$\mathbf{U}_i = [u_{\zeta\eta}]_i \quad (2-8)$$

with states (ζ) for bond $i-1$ indexing the rows and those (η) for bond i the columns. The subscript i may be omitted for a chain in which all the bonds are identical.

The overall statistical weight for a particular conformation of the chain is given by the equation²

$$\Omega_{(\phi)} = \prod u_{\zeta\eta;i}, i = 2 \text{ to } n-1 \quad (2-9)$$

which follows at once from Eq. (2-6). The first term in the product carries a single index for the reason noted earlier. The assigned statistical weights must appropriately take into account neighbour dependence. They must also yield the correct statistical weight for any conformation of the molecule as a whole when they are multiplied in the combination prescribed by the conformation.

The generalised form of the statistical weight matrix² for a polymer chain consisting of identical bonds, each bond occupying one of only three discrete states (t, g⁺ and g⁻) is illustrated in Eq. (2-10)

$$\mathbf{U} = \begin{matrix} & \begin{matrix} (t) & (g^+) & (g^-) \end{matrix} \\ \begin{matrix} (t) \\ (g^+) \\ (g^-) \end{matrix} & \begin{bmatrix} 1 & \sigma & \sigma \\ 1 & \sigma\psi & \sigma\omega \\ 1 & \sigma\omega & \sigma\psi \end{bmatrix} \end{matrix} \quad (2-10)$$

with states for bond i-1 indexing the rows and those for bond i the columns.

The terms σ , ψ and ω are defined by Eq. (2-7) with the energies E_{tg^+} , E_{tg^-} , $E_{g^+g^+}$, $E_{g^-g^-}$ and $E_{g^+g^-}$ being relative to the all trans state. By adopting the convention, whereby the statistical weights are assigned at each step on the premise that all succeeding bonds are trans, renders the elements in the first column equal to unity.

It has been assumed so far that the bond rotational interdependence does not extend beyond first neighbours. Interdependence beyond first neighbours may be safely ignored since intramolecular encounters of much longer range are statistically more improbable.

2.6 The Configuration Partition Function

The configuration partition function, Z , for a particular chain is defined as the sum of all the statistical weights of all the conformations of the chain. It may be expressed by the equation²

$$Z = \sum \Omega_{(\phi)} = \sum \prod u_{\zeta\eta;i}, i = 1 \text{ to } n-1 \quad (2-11)$$

The task of evaluating the partition function by forming the sum of products of statistical weights $u_{\zeta\eta}$ for each conformation as directed by Eq. (2-11) would be very time consuming for a chain having more than about 500 bonds, even with aid of high speed computers. However, the configuration partition function may be alternatively expressed by the equation²

$$Z = \mathbf{J}^* [\prod \mathbf{U}_i] \mathbf{J}, i = 2 \text{ to } n-2 \quad (2-12)$$

where $\mathbf{J}^* = [1 \ 0 \ 0]$ and $\mathbf{J}^T = [1 \ 1 \ 1]$, respectively.

For a flexible chain in which all the bonds are identical Equation (2-12) reduces to

$$Z = \mathbf{J}^* \cdot \mathbf{U}^{(n-1)} \cdot \mathbf{J} \quad (2-13)$$

The evaluation of the configuration partition function for large n may be achieved by consecutive squaring of the matrix \mathbf{U} prior to solving Equation (2-12).

2.7 Mean Square Moments of Chain Molecules

If we consider a long chain molecule as a collection of atoms we may designate the spatial arrangement of these atoms by the term configuration. The configuration of a long chain molecule may be determined by specifying the relative positions of all the atoms in the chain. In a hypothetical chain consisting of n bonds, illustrated in Figure (2-2), the bonds may be represented by bond vectors \mathbf{l}_i numbered from 1 to n . The configuration of the chain is therefore determined by the set of bond vectors $\{\mathbf{l}_1, \mathbf{l}_2, \mathbf{l}_3, \dots, \mathbf{l}_n\}$.

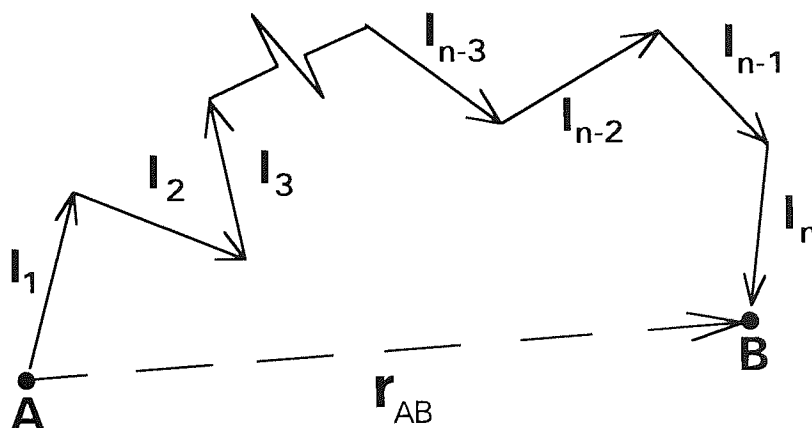


Figure (2-2). Schematic representation of a long chain molecule.

By assigning a bond vector to each bond in the chain, the displacement between the terminal atoms, r_{AB} , may be represented by the equation

$$r_{AB} = l_1 + l_2 + l_3 \dots\dots + l_{n-1} + l_n \quad (2-14)$$

$$= \sum l_i, i = 1 \text{ to } n \quad (2-15)$$

The square of the distance between the terminal atoms of the chain, r_{AB} , may now be calculated by evaluating the dot product of the vector r_{AB} with itself

$$(r_{AB})^2 = r_{AB} \cdot r_{AB} = \sum l_i \cdot l_j, i \& j = 1 \text{ to } n \quad (2-16)$$

Due to the equivalence of $l_i \cdot l_j$ and $l_j \cdot l_i$, Eq. (2-16) may be rewritten as

$$(r_{AB})^2 = \sum l_i^2 + 2\sum (l_i \cdot l_j), i \& j = 1 \text{ to } n \text{ with } i < j \quad (2-17)$$

In order to construct a scheme for formulating the required scalar products $l_i \cdot l_j$, we must define a coordinate system (x, y, z) for each bond in the chain. Each bond vector may then be expressed in its own coordinate system. For simplicity, let the axis x_i of the coordinate system affixed to bond i be taken in the direction of the bond. Let the axis y_i lie in the plane of bonds $i-1$ and i , with its positive direction chosen to render its projection on x_{i-1} positive. The axis z_i may then be directed to complete a right-handed Cartesian coordinate system as shown in Figure (2-3).

Each bond may now be treated as a vector l with components l_x , l_y and l_z in its respective coordinate system and expressed as a column matrix

$$\mathbf{l} = \begin{bmatrix} l_x \\ l_y \\ l_z \end{bmatrix} \quad (2-18)$$

where l_x is the bond length, $l_y = l_z = 0$.

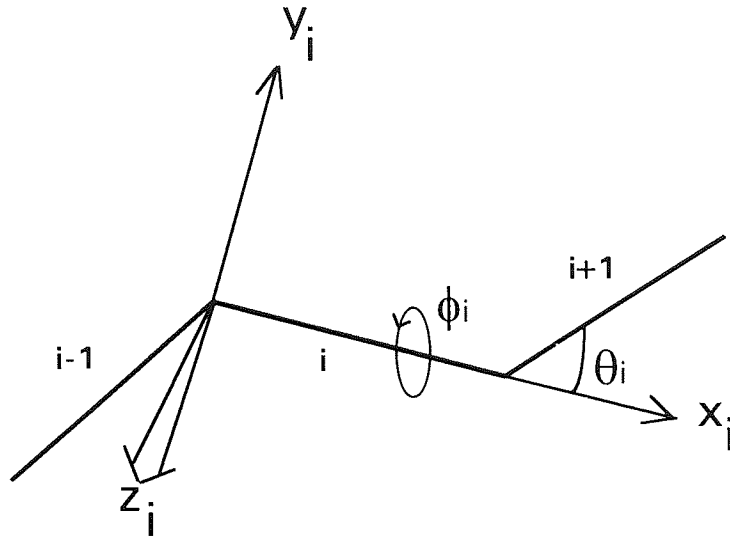


Figure (2-3). Cartesian coordinate system assigned to bond i .

A transformation matrix, \mathbf{T}_i , may now be introduced. The transformation matrix² is an orthogonal matrix which by premultiplication transforms a vector \mathbf{l} , with components l_x , l_y and l_z expressed in reference frame $i+1$, to its representation \mathbf{l}' , with coordinates l'_x , l'_y and l'_z in the reference frame i . Mathematically,

$$\mathbf{l}'_i = \mathbf{T}_i \cdot \mathbf{l}_{i+1} \quad (2-19)$$

The matrix \mathbf{T}_i

$$\mathbf{T}_i = \begin{bmatrix} \cos\theta_i & \sin\theta_i & 0 \\ \sin\theta_i \cdot \cos\phi_i & -\cos\theta_i \cdot \cos\phi_i & \sin\phi_i \\ \sin\theta_i \cdot \sin\phi_i & -\cos\theta_i \cdot \sin\phi_i & -\cos\phi_i \end{bmatrix} \quad (2-20)$$

is dependent on θ_i , the bond angle supplement, and ϕ_i , the bond rotation angle for bond i as defined in Figure (2-3). By assigning a transformation matrix to each bond in the chain, we may evaluate the scalar products $\mathbf{l}_i \cdot \mathbf{l}_j$

$$\mathbf{l}_i \cdot \mathbf{l}_j = \mathbf{l}_i^T (\mathbf{T}_i \cdot \mathbf{T}_{i+1} \cdot \mathbf{T}_{i+2} \cdots \mathbf{T}_{j-1}) \cdot \mathbf{l}_j, \quad i < j \quad (2-21)$$

where \mathbf{l}_i^T denotes the transpose of \mathbf{l}_i (ie. its row matrix representation).

Equation (2-21) is limited in the sense that it represents only one configuration of the chain. However, Eq. (2-21) is considerably simplified when applied to real polymer chains. This is due to real polymer chains having fixed bond lengths and bond angles and although the bond rotation angles (ϕ 's) may take on a number of values, this number is usually limited due to the nature of the rotation potentials for each bond. These simplifications allow the term configuration (dependent on ϕ , θ and \mathbf{l}) to be replaced by the term conformation (dependent on ϕ only). Equation (2-21) now becomes

$$\mathbf{l}_i \cdot \mathbf{l}_j = \mathbf{l}_i^T \langle \mathbf{T}_i \cdot \mathbf{T}_{i+1} \cdot \mathbf{T}_{i+2} \cdots \mathbf{T}_{j-1} \rangle \mathbf{l}_j \quad (2-22)$$

where the angled brackets denote the statistical mechanical average over all conformations of the chain.

By substituting Eq. (2-22) into Eq. (2-17) the expression for the mean-square average distance $\langle r^2 \rangle$ becomes

$$\langle r^2 \rangle = \sum \mathbf{l}_i^2 + 2 \sum (\mathbf{l}_i^T \langle \mathbf{T}_i \cdots \mathbf{T}_{j-1} \rangle \mathbf{l}_j), \quad i \& j = 1 \text{ to } n \text{ with } i < j \quad (2-23)$$

The forgoing expressions are applicable also, with only nominal alterations, to the scalar product of any pair of vectors associated with bonds i and j . Suppose \mathbf{m}_i and \mathbf{m}_j to be two such vectors which are uniquely defined in the respective reference frames of bonds i and j . Then,

$$\langle M^2 \rangle = \sum m_i^2 + 2\sum (\mathbf{m}_i^T \langle \mathbf{T}_i \dots \mathbf{T}_{j-1} \rangle \mathbf{m}_j), \quad i \& j = 1 \text{ to } n \text{ with } i > j \quad (2-24)$$

The vectors \mathbf{m}_i and \mathbf{m}_j may, for example, be dipole moments associated with the respective bonds and the substituents rigidly attached to them. In this case, $\langle M^2 \rangle$ would represent $\langle \mu^2 \rangle$, the mean-square dipole moment for the polymer chain.

Equations (2-23) and (2-24) are quite general. No assumptions have been made concerning the nature of the bond rotation potentials. It is only in the determination of the statistical average of the product of transformation matrices, $\langle \mathbf{T}_i \dots \mathbf{T}_{j-1} \rangle$, that the nature of the bond rotation potentials has to be established.

In the following sections, this term $\langle \mathbf{T}_i \dots \mathbf{T}_{j-1} \rangle$ shall be evaluated for two cases,

1. Chains with independent bond rotation potentials, and
2. Chains with interdependent bond rotation potentials.

For simplicity it will be assumed that in both cases of the above the chain under consideration contains identical bonds connected to identical atoms, that the bond rotation potential for each bond is 3-fold, and that a

vector m is associated with each bond in the chain, this vector being invariant to the chain conformation.

2.7.1. Mean Square Moments of Chains with Independent Bond Rotation Potentials

By assuming the independence of the bond rotation potentials (or the separability of the conformational energy, see section 2.4), the statistical average product of transformation matrices may be replaced by the product of the averages of the individual transformation matrices, i.e.

$$\langle T_i \dots T_{j-1} \rangle = \Pi \langle T_h \rangle, \text{ where } h = i \text{ to } j-1 \quad (2-25)$$

the averaged transformations for the individual bonds being given by the equation²

$$\langle T_h \rangle = \frac{\sum T_h \cdot \exp[-E_h(\phi_h)/RT]}{\sum \exp[-E_h(\phi_h)/RT]} \quad (2-26)$$

The denominator in Eq. (2-26) is frequently referred to as the bond rotational partition function, Z , and the sums extend over all rotation angles.

Treatments of the various properties of chain molecules may be greatly simplified by the forgoing factorisation based on the separability of the conformational energy, however, instances where such separation is justified are the exception rather than the rule.

Under the stated conditions the average of the transformation matrices $\langle T_i \rangle$ are the same for all i . Hence

$$\langle M^2 \rangle = nm^2 + 2\sum m^T \langle T \rangle^{j-1} m, \quad i < j \quad (2-27)$$

or

$$= 1 + (2/nm^2)m^T[\sum_n \langle T \rangle^k - \sum_k \langle T \rangle^k]m, \quad k = 1 \text{ to } n-1 \quad (2-28)$$

Evaluation of these two sums gives²

$$\begin{aligned} \langle M^2 \rangle / n &= m^T [(\mathbf{E} + \langle T \rangle)(\mathbf{E} - \langle T \rangle)^{-1} \\ &\quad - (2\langle T \rangle / n)(\mathbf{E} - \langle T \rangle^n)(\mathbf{E} - \langle T \rangle)^{-2}] m \end{aligned} \quad (2-29)$$

If \mathbf{m} is to be identified as the bond vector \mathbf{l} , which is expressed in its own coordinate system by Eq. (2-18), then the preceding results take the form

$$\begin{aligned} C_n = \langle r^2 \rangle_0 / nl^2 &= [(\mathbf{E} + \langle T \rangle)(\mathbf{E} - \langle T \rangle)^{-1} \\ &\quad - (2\langle T \rangle / n)(\mathbf{E} - \langle T \rangle^n)(\mathbf{E} - \langle T \rangle)^{-2}]_{11} \end{aligned} \quad (2-30)$$

where C_n is known as the characteristic ratio and the subscripts on the brackets denotes the 1,1 element.

Equations (2-27) to (2-30) may be applied to any chain for which the separate averaging of the \mathbf{T} matrices is legitimate. They hold, irrespective of the nature of the geometrical constraints on the bond connections. Separability of energy according to Eq. (2-5) is the necessary condition.

2.7.2. Mean Square Moments of Chains with Interdependent Bond Rotation Potentials

General relationships were derived in section 2.7.1 for chains in which the bond rotations are independent, and the statistical average of the product

of transformation matrices may be replaced by the product of averages of the individual transformation matrices. For chains of interdependent bond rotations such separation is not possible and the unfactored product must be averaged over all conformations of the chain.

The statistical mechanical average of the product of orthogonal matrices, $\langle T_i \dots T_j \rangle$, is expressed to a good approximation² by the equation

$$\langle T_i \dots T_j \rangle = \frac{\sum \dots \sum (T_i \dots T_j) \cdot \exp[-E\{\phi\}/RT] \cdot d\{\phi\}}{\sum \dots \sum \exp[-E\{\phi\}/RT] \cdot d\{\phi\}} \quad (2-31)$$

where $E\{\phi\}$ is the energy of the conformation $\{\phi\}$, R is the gas constant, and T is the absolute temperature. By substituting $u_{\zeta\eta;i} = \exp(-E_{\zeta\eta;i}/RT)$ into Eq. (2-31), we find that the denominator is equivalent to the configuration partition function, Z

$$Z = \sum \prod u_{\zeta\eta;i}, \quad i = 1 \text{ to } n-1 \quad (2-32)$$

which may be solved by the well known scheme presented in section 2.6 for generating all of the statistical weights by multiplication of the matrices \mathbf{U}

$$Z = \mathbf{J}^* [\prod \mathbf{U}_i] \mathbf{J}, \quad i = 2 \text{ to } n-2 \quad (2-33)$$

By applying the same scheme to the numerator, Eq. (2-31) reduces to

$$\langle T_i^{(j-i)} \rangle = Z^{-1} [(\mathbf{J}^* \mathbf{U}^{(i-2)}) \times \mathbf{E}] [(\mathbf{U} \times \mathbf{E}) \prod \mathbf{U}_i]^{(j-i)} [(\mathbf{U}^{(n-j)} \mathbf{J}) \times \mathbf{E}] \quad (2-34)$$

where \mathbf{E} is the identity matrix and is required only to make the matrix \mathbf{U} conformable with $\prod \mathbf{U}_i$, this being equal to

$$\|T\| = \begin{bmatrix} T(\phi_1) & & \\ & T(\phi_2) & \\ & & T(\phi_3) \end{bmatrix} \quad (2-35)$$

Substitution of Eq. (2-34) into Eq. (2-24), derived in section 2.7, gives the mean square moment for a polymer chain with interdependent bond rotation potentials

$$\begin{aligned} \langle M^2 \rangle &= nm^2 \\ &+ 2Z^{-1} \mathbf{J}^* \{ \sum \mathbf{U}^{(i-1)} (\mathbf{E} \otimes \mathbf{m}^T) [(\mathbf{U} \otimes \mathbf{E}) \|T\|]^{(j-i)} (\mathbf{E} \otimes \mathbf{m}) \mathbf{U}^{(n-j)} \} \mathbf{J} \end{aligned} \quad (2-36)$$

where the sum extends over the range $0 < i < j-1 < n$.

Equation (2-36) is very difficult to solve in its present form. However, mathematical methods have been devised² which allow Eq. (2-36) to be expressed in the more convenient form

$$\langle M^2 \rangle = 2Z^{-1} \mathfrak{G}^* \mathbf{G}^{(n)} \mathfrak{G} \quad (2-37)$$

where \mathfrak{G}^* and \mathfrak{G} are the row and column matrices

$$\mathfrak{G}^* = [1 \ 0]$$

$$\mathfrak{G}^T = [0 \ 0 \ 0 \ 0 \ 0 \ 0 \ 0 \ 0 \ 0 \ 0 \ 0 \ 0 \ 0 \ 0 \ 1 \ 1 \ 1 \ 1 \ 1 \ 1 \ 1 \ 1]$$

respectively, and the matrix² \mathbf{G} is

$$\mathbf{G} = \begin{bmatrix} \mathbf{U} & (\mathbf{U} \otimes \mathbf{m}^T) \|T\| & (m^2/2) \mathbf{U} \\ 0 & (\mathbf{U} \otimes \mathbf{E}) \|T\| & \mathbf{U} \otimes \mathbf{m} \\ 0 & 0 & \mathbf{U} \end{bmatrix} \quad (2-38)$$

Equation (2-38) is exact in the sense that no mathematical approximations have been introduced in its derivation. It is applicable to chains of any length consisting of any variety of skeletal bonds in any specified order, provided only that their rotational potentials admit of approximation by a set of discrete rotational states.

The supermatrix \mathbf{G} is often referred to as the generator matrix since it generates all the correct matrix products in the correct order, one such matrix being defined for each bond pair in the chain of interest. The orders of the submatrices comprising this supermatrix for a bond with a v -fold rotational potential is as follows

$$\begin{bmatrix} v \times v & v \times 3v & v \times v \\ 3v \times v & 3v \times 3v & 3v \times v \\ v \times v & v \times 3v & v \times v \end{bmatrix}$$

the order of \mathbf{G} as a whole being $5v \times 5v$. If v differs for successive bonds, the corresponding \mathbf{G} -matrices (and \mathbf{U} -matrices) will be rectangular instead of square. The generator matrix \mathbf{G}_i contains all the required information relating to bond i . It combines geometrical parameters ($\phi_{\eta,i}$ and θ_i) from the \mathbf{T}_i for the various rotational states accorded to bond i , the statistical weights form \mathbf{U}_i , and the bond moments m_i associated with bond i and as with the \mathbf{U} -matrix, it may be solved for large n by consecutive matrix squaring.

2.8 Polycarbosilanes and Related Materials

In order to apply the principles described in this chapter to polycarbosilanes, certain information concerning the polymers under

examination must be established. Since the projected analysis is conceived in terms of the structure of the molecule under examination, data for polycarbosilanes consisting of bond angles and bond lengths are required for its application to these molecules. Data of this nature is usually at hand with ample accuracy for our purposes. This is not, however, sufficient. Unambiguous deduction of the properties of a chain molecule further requires an adequate understanding of the intramolecular energy as a function of the conformation. The conformational energy is usually described in terms of potentials associated with the various bond rotations, or combinations of such rotations. Enough must be known concerning these potentials to permit the selection of rotational isomeric states at or near potential minima, and also allow the statistical weights for the states so chosen to be evaluated.

Originally, the only case where such information was wholly available was for the n-alkanes. However, in recent years, interest in the structural properties of polycarbosilanes has yielded some information concerning their structure and the nature of their intramolecular interactions.

In general, however, the best that can be done is to outline the qualitative character of the conformational energy on the basis of structure, aided by inferences from the analogous molecules and by approximate estimates of the principal contributions to the energy. These contributions include inherent torsional potentials (see section 2.2) of the various bonds, and steric interactions, etc. Appropriate sets of rotational isomeric states can

usually be selected. Their statistical weights ordinarily cannot be evaluated quantitatively, but may be estimated from inspection of the structure of the molecule and from experimentally determined properties. One such method of evaluating the statistical weights for a polymer chain is known as the hard-sphere model.

In the hard-sphere model, the statistical weights are either assigned a value of zero or one, depending on whether the interaction under consideration is subject to significant steric hinderence, or negligible steric hinderence respectively. In such cases only the structural information for the molecule needs to be known and thus where the data concerning the intramolecular interactions in a particular polymer molecule is scarce or the structure of the molecule is complex, the hard-sphere model will be applied.

CHAPTER 3

COMPUTER PROGRAM DEVELOPMENT

3.1 Introduction

Since a large part of this project was concerned with the development of complicated computer programs, based on the mathematical framework presented in the previous chapter, it was important to establish a firm foundation from which reliable results could be obtained. In many cases, computer software contains small errors or 'bugs' which may severely reduce the performance of the application. It is therefore important to eradicate such errors by developing the software in stages, with each stage undergoing a rigorous test to assess the reliability of the results produced.

In this chapter, a brief description of the methods employed to develop reliable computer programs for use in this work is presented.

3.2 Conformational Analysis of Poly(dimethylsilmethylene) and Poly(dimethylsilethene).

The computer programs required to analyze the conformational properties of poly(dimethylsilmethylene) and poly(dimethylsilethene) were developed by performing similar analyses on polymer molecules that had already been studied. These 'test polymers' were polymethylene, polysilane and polypropylene. By comparing the results obtained from our calculations with

those published for the test polymers, the reliability of the programs could be established.

Of the many structural properties associated with polymers, one property common to all polymer molecules is that each contains a skeletal backbone with branched atoms or side groups attached to it. The simplest polymer exhibiting these properties is polymethylene. Polymethylene has been studied by Jernigan and Flory⁵ and the results of the conformational energy calculations performed on this polymer are well documented. For this reason, polymethylene was the first test polymer used.

Since both poly(dimethylsilmethylene) and poly(dimethylsilethene) contain silicon atoms, the second test polymer to be studied was polysilane. Again this is a relatively simple structure whose conformational and structural properties have recently been studied by Mark, DeBolt and Welsh⁷ and also by Damewood and West²⁷.

The third polymer to be studied was the syndiotactic form of polypropylene whose conformational properties have been studied by Suter and Flory⁶. The reason for studying this polymer stems from the fact that the syndiotactic form of polypropylene exhibits two branched methyl groups, one either side of the skeletal backbone. This structural feature is present in both poly(dimethylsilmethylene) and poly(dimethylsilethene). Figure (3-1) illustrates each stage in the development of the programs.

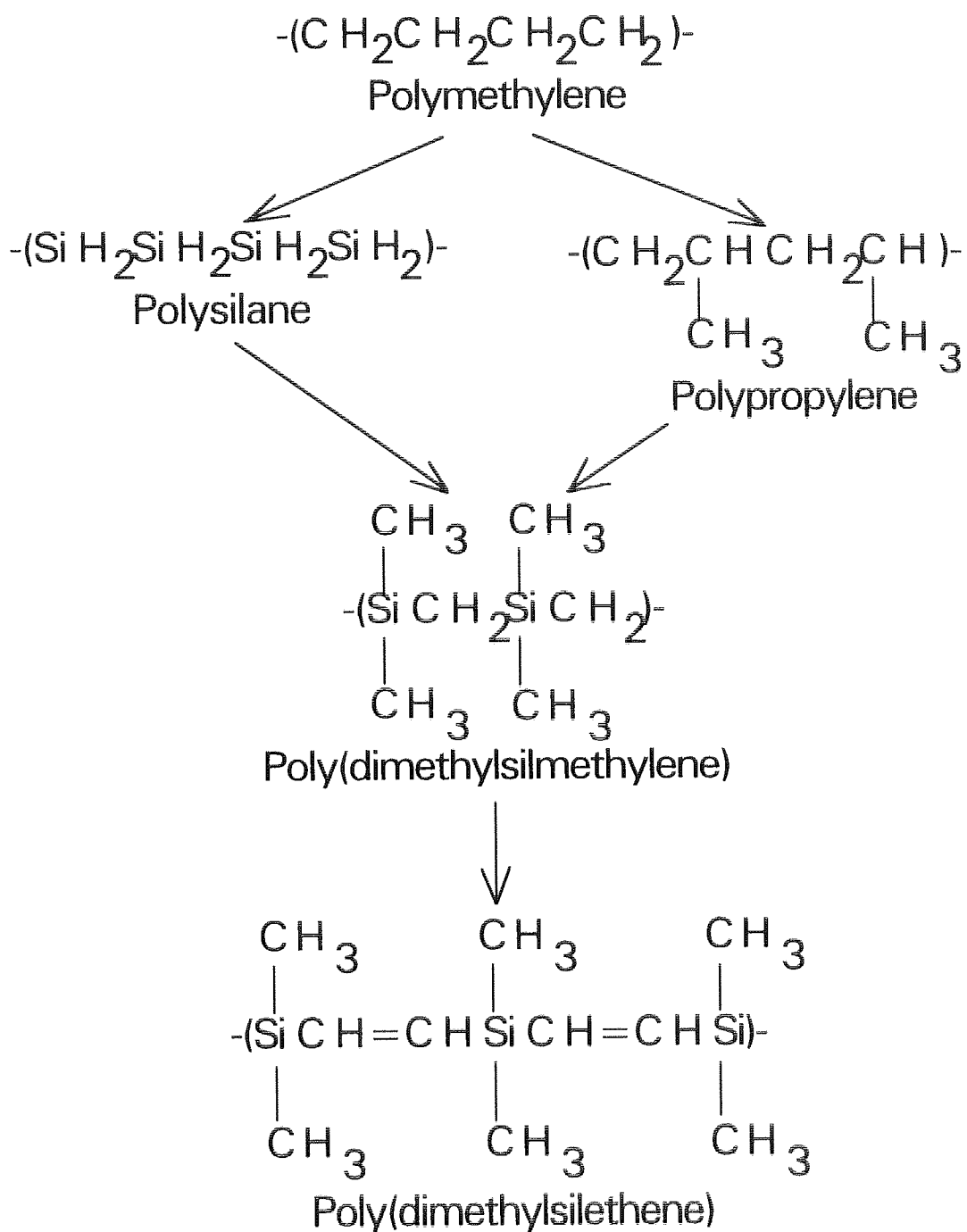


Figure (3-1). The development of the computer programs. At each stage (where possible) the results obtained from our calculations were compared with those published.

3.2.1. Polymethylene

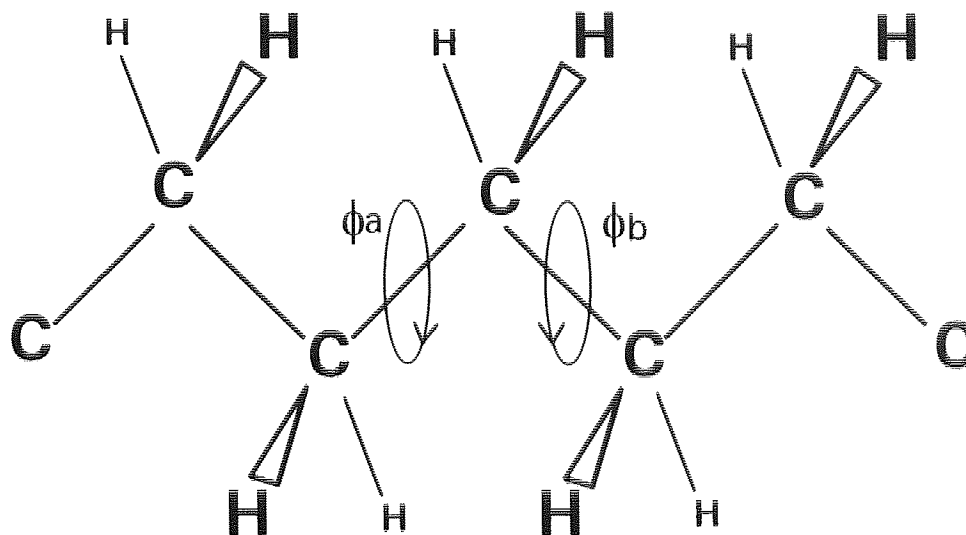


Figure (3-2). Section of polymethylene used in the calculations.

Using the structural and interatomic interaction parameters published by Jernigan and Flory⁵, a conformational energy contour map for the section of polymethylene illustrated in Figure (3-2) was generated. The energies associated with the various conformations were calculated according to the equation⁵

$$E(\phi_a, \phi_b) = \sum (E^0/2)(1 - \cos 3\phi) + \sum [(a_{kl} \exp(-b_{kl} r_{kl}) - (c_{kl}/r_{kl}^6)] \quad (3-1)$$

for $\phi_a = \phi_b = 0^\circ$ to 360° .

The resulting energy map was found to be in exact agreement with that published by Jernigan and Flory⁵.

3.2.2. Polysilane

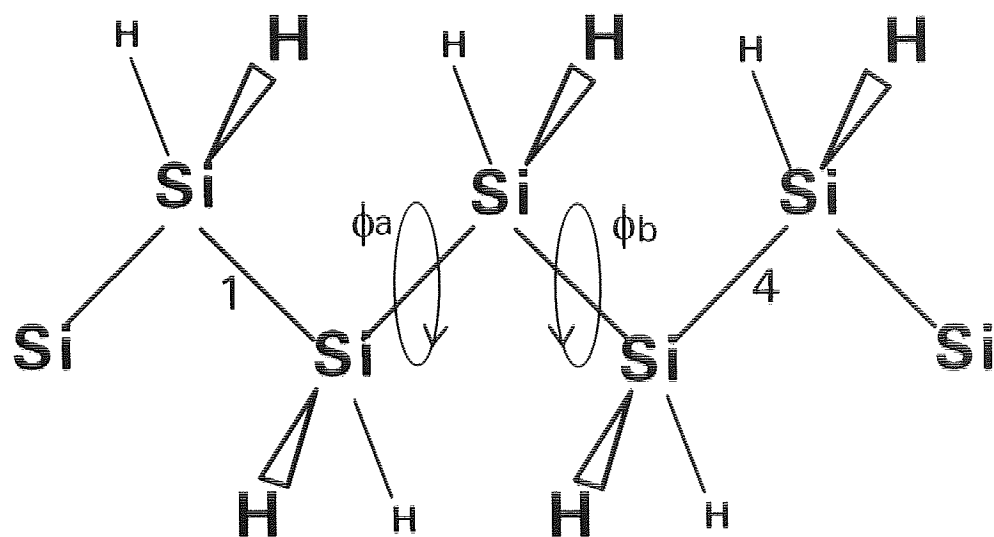


Figure (3-3). Section of polysilane used in the calculations.

The conformational energies for the section of polysilane illustrated in Figure (3-3) were calculated by the equation⁷

$$E(\phi_a, \phi_b) = \Sigma (E^0/2)(1 - \cos 3\phi) + \Sigma [(a_{kl}/r_{kl}^{12}) - (c_{kl}/r_{kl}^6)] \quad (3-2)$$

using parameters published by Mark, DeBolt and Welsh⁷ for $\phi_a = \phi_b = 0^\circ$ to 360° . The resulting energy contour map was compared with that published. Although the two energy maps were nearly identical, small differences were found in the relative positions of the two sets of contour lines. A possible explanation for this discrepancy lies in the fact that Mark's calculations included partial relaxation about the terminal bonds 1 and 4, indicated in

Figure (3-3). In our calculations, the terminal bonds 1 and 4 were fixed in their respective trans conformations.

3.2.3. Polypropylene

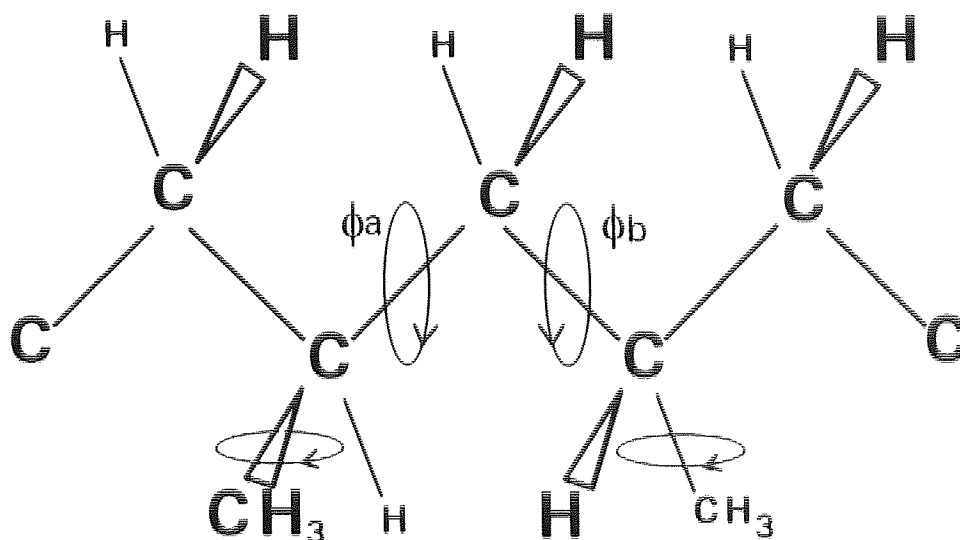


Figure (3-4). Section of syndiotactic polypropylene used in the calculations.

The conformational energy map generated for the section of syndiotactic polypropylene illustrated in Figure (3-4) was calculated according to Eq. (3-2) using the parameters published by Suter and Flory⁶. The conformational energies calculated for each conformation (ϕ_a , ϕ_b) were minimised by allowing partial relaxation about the two pendent methyl groups. The conformational energy map produced from our calculations was identical to that published by Suter and Flory⁶.

3.3 The Calculation of Characteristic Ratios and Dipole Moment Ratios

The development of these computer programs was again based on the results obtained by performing similar calculations on two polymers that had previously been studied; polymethylene and poly(dimethylsiloxane).

3.3.1. Polymethylene

The characteristic ratio of polymethylene was calculated for chains of different lengths according to the equation

$$\langle r^2 \rangle_0/nl^2 = 2(Znl^2)^{-1} \mathfrak{g} * \mathbf{G}_T \mathbf{G}^{(n-2)} \mathbf{G}_n \mathfrak{g} \quad (3-3)$$

The \mathbf{G} -matrices were constructed using parameters published by Flory⁵ at a temperature of 140°C, with the matrices \mathbf{G}_T and \mathbf{G}_n representing the terminal bonds. The results obtained were in exact agreement with the published values.

3.3.2. Poly(dimethylsiloxane)

The characteristic ratios and dipole moment ratios for varying lengths of poly(dimethylsiloxane) chains have been previously calculated by Mark⁸. Using the parameters specified in his work, the characteristic ratio and dipole moment ratio of poly(dimethylsiloxane) were calculated according to the equation⁸

$$\langle M^2 \rangle_0/nm^2 = 2(Znm^2)^{-1} \mathfrak{g} * \mathbf{G}_T (\mathbf{G}_a \mathbf{G}_b)^x \mathbf{G}_a \mathfrak{g} \quad (3-4)$$

at various temperatures for a chain beginning and ending with silicon atoms. The matrix \mathbf{G}_a represents a pair of interdependent bonds flanking an oxygen atom, whereas the matrix \mathbf{G}_b represents a pair of bonds flanking a silicon atom. Again the results were in exact agreement with those published.

3.4 Conclusion

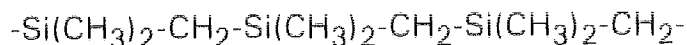
Based on the success of the test programs, it is believed by the author that the results presented in this work concerning the calculation of conformational energy maps, characteristic ratios and dipole moment ratios for polycarbosilanes are both accurate and reliable.

CHAPTER 4

CONFORMATIONAL ANALYSIS OF POLY(DIMETHYLSILMETHYLENE)

4.1 Introduction

The molecular structure of a section poly(dimethylsilmethylene) chain is illustrated below



The skeletal backbone of this polymer chain consists of alternating silicon and carbon atoms with two branched methyl groups attached to each silicon atom. On inspection of the above section, it may be seen that there are two distinguishable interdependent bond pairs, one pair flanking a $-\text{CH}_2-$ group, and one pair flanking a $-\text{Si}(\text{CH}_3)_2-$ group respectively. The bond pair interdependence in poly(dimethylsilmethylene) arises from the severe steric hinderence between the four branched methyl groups attached to a pair of neighbouring silicon atoms.

In this chapter the conformational energy arising from this bond pair interdependence shall be calculated and a set of distinct rotational isomeric states chosen for each bond in the chain. Based on the results obtained the characteristic ratio, $\langle r^2 \rangle / nl^2$, and the dipole moment ratio, $\langle \mu^2 \rangle / nm^2$, for varying chain lengths will be calculated for this polymer, according to the

equations derived in Chapter 2 for a chain with interdependent bond rotational potentials.

4.2 Molecular Geometry

The structural information used in the calculations of the conformational energy of poly(dimethylsilmethylene) were based on the molecular structure of bis(trimethylsilyl)methane, illustrated in Figure (4-1).

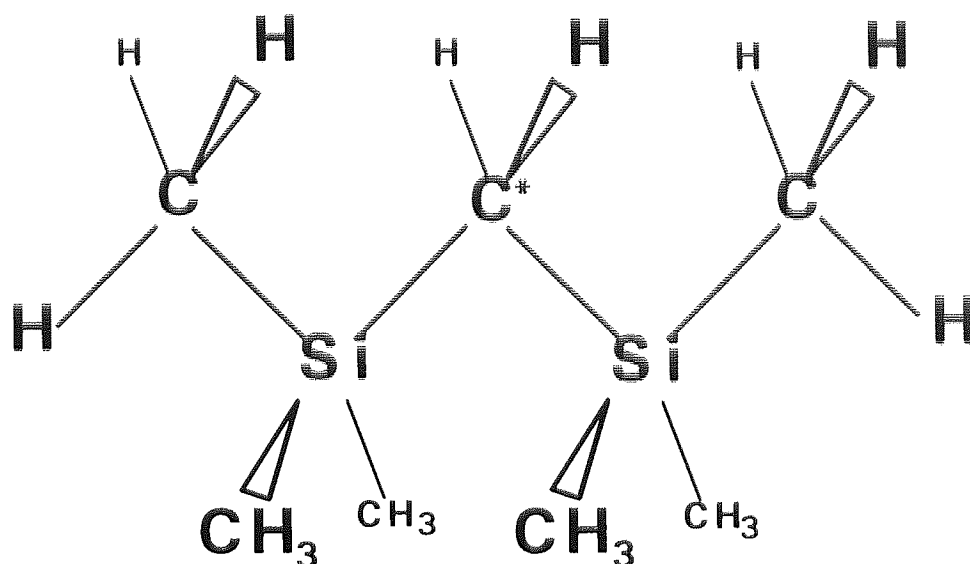


Figure (4-1). Molecular structure of bis(trimethylsilyl)methane.

Fjeldberg, Lappert and Thorne²⁸ investigated the molecular structure of gaseous bis(trimethylsilyl)methane using electron diffraction techniques. One of the most important conclusions derived from their results was that there were severe steric repulsions between the branched methyl groups attached to the neighbouring silicon atoms. The steric hindrance was so severe that the central Si-C*-Si bond angle was found to have an unusually large value,

this value being 123.2° . The large value of this bond angle was explained on the grounds that it allowed partial steric relief between the branched methyl groups. Other investigations²⁹ into the molecular structure of this molecule using Raman infra-red spectroscopy have also indicated an unusually large central bond angle of $\sim 120^\circ$. It therefore seemed logical to assume a similarly large angle for the Si-C-Si bond in poly(dimethylsilmethylene), this value being set at 123° . The values of the parameters calculated by Fjeldberg et al^a and those used in our calculations^b are displayed in Table (4-1).

	Bond Length ^a (Å)	Bond Angle ^a (θ°)	Bond Length ^b (Å)	Bond Angle ^b (θ°)
Si-C*	1.89		1.89	
Si-CH ₃	1.87		1.87	
C-H	1.1		1.1	
Si-C*-Si		123.2		123
C*-Si-C		112.4		110

Table (4-1). Geometrical parameters for $\text{CH}_2(\text{Si}(\text{CH}_3)_3)$.

A value²⁷ of 110° was assigned to the bond angle C*-Si-C rather than the value of 112.4° calculated by Fjeldberg. The reasoning behind this decision lay in the fact that in poly(dimethylsilmethylene) the branched methyl groups are flanked on both sides by the skeletal backbone of the chain,

terminal groups excluded. In bis(trimethylsilyl)methane the methyl groups are only flanked on one side by other structure allowing the bond angle to increase slightly to 112.4° to allow steric relief. All other angles in the chain were set to their normal tetrahedral values.

4.3 Conformational Energy

The conformational energy associated with the interdependent bond pair flanking a $-\text{CH}_2-$ group was calculated using the section of poly(dimethylsilmethylene) illustrated in Figure (4-2).

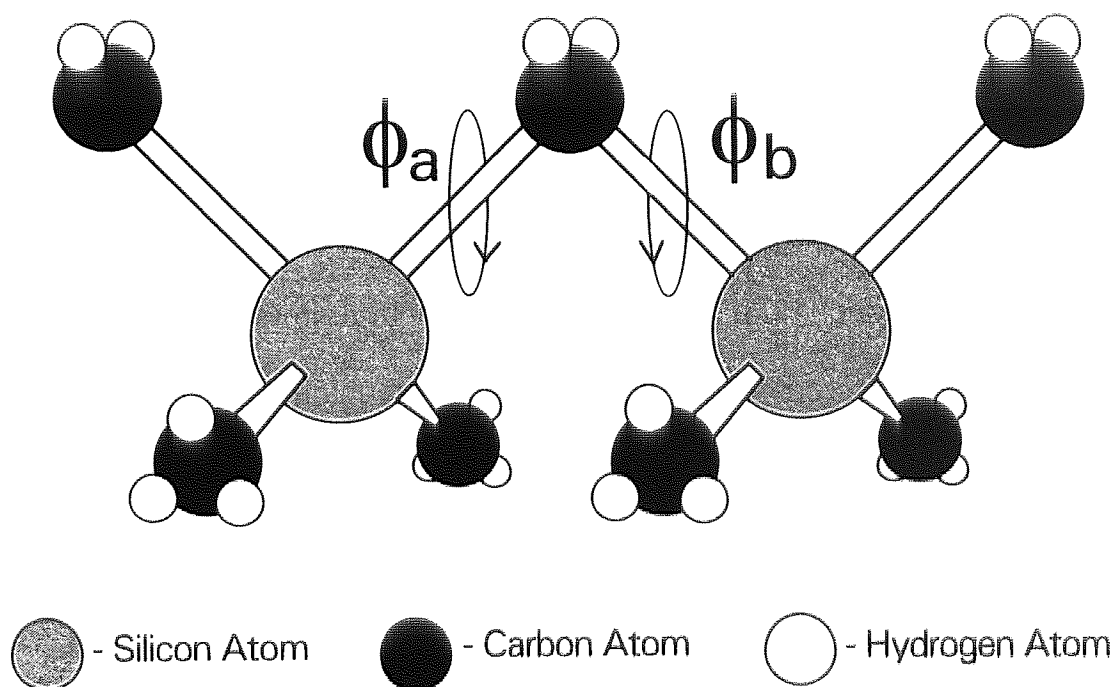


Figure (4-2). Poly(dimethylsilmethylene) dyad used in the calculations.

Sections of polymer chains with two distinguishable interdependent bond pairs, as illustrated in Figure (4-2), are commonly referred to as dyads. Their conformational energies, $E(\phi_a, \phi_b)$, may be calculated by using either the "no relaxation" technique, the "partial relaxation" technique, or the "full relaxation" technique over the range $0^\circ - 360^\circ$ for ϕ_a and ϕ_b .

The "no relaxation" technique, NR, assumes that all the bond lengths and bond angles are rigid and the conformational energy is solely dependent on ϕ_a and ϕ_b . The "partial relaxation" technique, PR, is similar to the NR technique except that the energies of the conformations are minimised with respect to the branched methyl groups, these being allowed to rotate to achieve the lowest conformational energy for a particular state defined by ϕ_a and ϕ_b . The "full relaxation" technique, FR, allows additional relaxation in the dyad by considering flexible bond lengths and flexible bond angles. The latter technique is more computationally intensive and more accurate than either the NR or the PR techniques but it requires an intricate knowledge of the bond length and bond angle force constants. Another difference between the three techniques is that in the NR and PR cases the entire conformational energy space is investigated (ie. ϕ_a and ϕ_b are varied over the range $0^\circ - 360^\circ$), whereas the FR technique is geared to locating local potential energy minima only.

For present purposes it will be sufficient to apply the PR technique in calculating the conformational energies of the poly(dimethylsiloxane)

dyad. This is because the computational speed and affordability of these calculations will permit the use of fine grids to scan the full range of conformational space (rather than seeking local energy minima only). Thus, the entire conformational terrain may be traversed to determine the domain sizes and rotational barriers needed for a complete analysis of the dynamic flexibility of the chain and hence its conformation-dependent properties.

Contributions to the conformational energy of the dyad were considered to arise from three sources, the intrinsic torsional potentials attributable to the bonds themselves, the van der Waals repulsions between non-bonded atoms and the dispersion attractions between non-bonded atoms. The conformational energy of the dyad may therefore be calculated from the equation, (see section 2.2)

$$E(\phi_a, \phi_b) = \sum (E^0/2)(1-\cos 3\phi) + \sum [(a_{kl}/r_{kl}^{12}) - (c_{kl}/r_{kl}^6)] \quad (4-1)$$

The first term in the summation includes all the bonds allowed to rotate; these include the branched methyl groups attached to neighbouring silicon atoms. The second term includes all the non-bonded atom pair interactions, kl , whose distance of separation depends on the rotation angles ϕ_a and ϕ_b .

The torsional barrier height, E^0 , for the Si-C bond was set at 0.5 kcal/mol¹, this value being empirically chosen to fit observed experimental data in substituted disilanes³⁰. The constants a_{kl} and c_{kl} , characteristic of the

¹ kcal/mole are the preferred units in conformational analysis and will be used throughout this work, 1 kcal = 4.185 KJ

Lennard-Jones (6-12) potential²⁶, were calculated from atomic polarizabilities³¹ by application of the Slater-Kirkwood equation²⁵ and are tabulated in Table (4-2).

A conformational energy map, illustrated in Figure (4-3), based on the PR calculations was generated by using Equation (4-1) and scanning the entire conformational energy space, $0^\circ - 360^\circ$, for both ϕ_a and ϕ_b in steps of 10° . The corresponding conformational energies, $E(\phi_a, \phi_b)$, were minimised by allowing rotation of the branched methyl groups between $0^\circ - 360^\circ$ in steps of 5° .

	a_{kl}^*	c_{kl}^*
Si----Si	7.26E + 06	3060
Si----C	1.71E + 06	1050
Si----H	2.62E + 05	374.1
C----C	3.95E + 05	363.0
C----H	5.63E + 04	127.0
H----H	7.27E + 03	47.1

Table (4-2). Non-bonded potential energy parameters. *Units are such to give E_{NB} in kcal/mol for r_{kl} in Å.

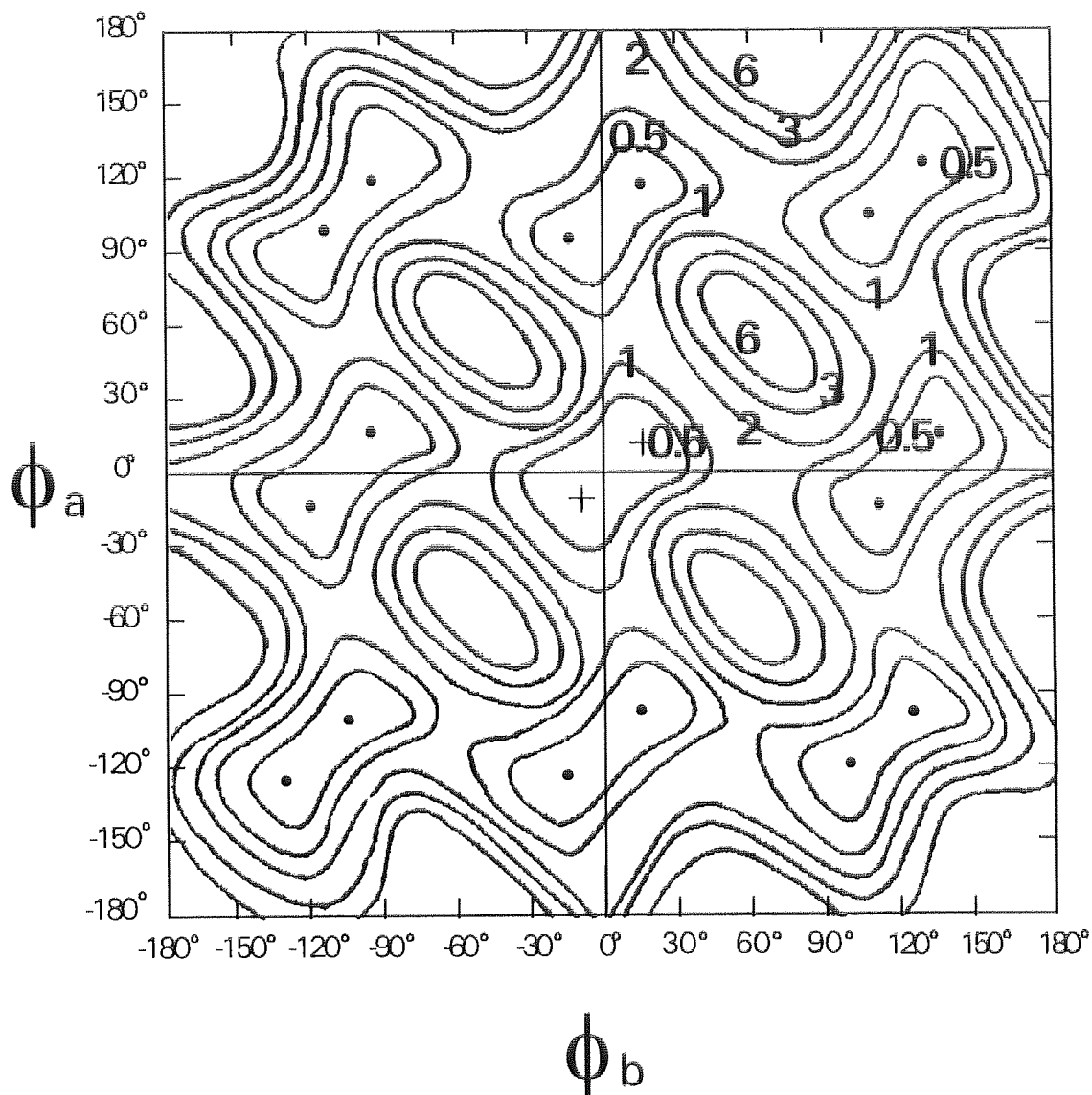


Figure (4-3). Conformational energy map for the poly(dimethylsilmethylene) dyad as determined by the PR calculations. The energy, given in kcal/mol relative to the conformational energy minima designated by "+" on the map, is shown as contour lines with some values illustrated in the top right quadrant. Local potential energy minima are located by the dots.

Analysis of the conformational energy contour map shows the existence of eighteen potential energy minima. These minima approximately occur at the rotation angles, $(15^\circ, 15^\circ)$, $(-15^\circ, -15^\circ)$, $(20^\circ, 130^\circ)$, $(-20^\circ, 105^\circ)$, $(20^\circ, -105^\circ)$, $(-20^\circ, -130^\circ)$, $(105^\circ, -20^\circ)$, $(130^\circ, 20^\circ)$, $(-105^\circ, 20^\circ)$, $(-130^\circ, -20^\circ)$, $(105^\circ, 105^\circ)$, $(135^\circ, 135^\circ)$, $(-105^\circ, -105^\circ)$, $(-135^\circ, -135^\circ)$, $(100^\circ, -130^\circ)$, $(130^\circ, -100^\circ)$, $(-100^\circ, 130^\circ)$ and finally $(-130^\circ, 100^\circ)$, where the angles are expressed in the format (ϕ_a, ϕ_b) . At first this system seems very complicated indeed. However, from a symmetrical point of view the eighteen different potential energy minima may be considered to be equivalent to nine distinguishable energy minima. Each of these nine minima is split into a rapidly interconverting "doublet", the rapidity of the interconversion making it impossible to distinguish between either minima in the doublet. The case for adopting this idea lies in the fact that the potential energy barrier between each minima in a "doublet" is very low (~ 0.2 kcal/mol) when compared to the potential energy barriers between the other minima > 1.5 kcal/mol. This trait has also been observed in polymethylene⁵.

Inspection of the generated potential energy map now reveals that adoption of the familiar three-state (T, G⁺, G⁻) scheme would suffice, each bond allowed to occupy one of three states thus producing nine conformational states for the dyad. These nine states correspond to the nine energy minima on the conformational energy map.

4.4 Rotational States

Incorporation of the results shown in Figure (4-3) in a rotational isomeric state scheme requires allocation of every element of conformational space (ϕ_a, ϕ_b) for which the energy is not excessive to one of the appropriately chosen states, as illustrated in Figure (4-4). All regions for which $E < 6$ kcal/mol relative to the tt state are included in the areas demarcated as shown. The dots denote values of the torsional angles averaged over these regions (see Table (4-3)).

The partition function z , average energy $\langle E \rangle$, and averaged rotation angles $\langle \phi_a, \phi_b \rangle$ for each rotational state s were calculated according to

$$z_s = \sum \sum \exp(-E_k/RT) \quad (4-2)$$

$$\langle E \rangle_s = z_s^{-1} \sum \sum E_k \exp(-E_k/RT) \quad (4-3)$$

$$\langle \phi_j \rangle_s = z_s^{-1} \sum \sum \phi_j \exp(-E_k/RT) \quad (4-4)$$

where the first sum is over all angles ϕ_a , and the second sum is over all angles ϕ_b in each state s . The subscript k refers to the energy of each conformation (ϕ_a, ϕ_b) and j is either a or b . The Boltzmann factors were calculated from the energies $E(\phi_a, \phi_b)$ at 10^0 intervals and the summations were carried out over the regions specified in Figure (4-4).

Partition functions z , average energies $\langle E \rangle$, and average rotation angles $\langle \phi_a, \phi_b \rangle$ calculated at three temperatures (300K, 400K and 500K) for the nine regions or states in Figure (4-4) are listed in Table (4-3).

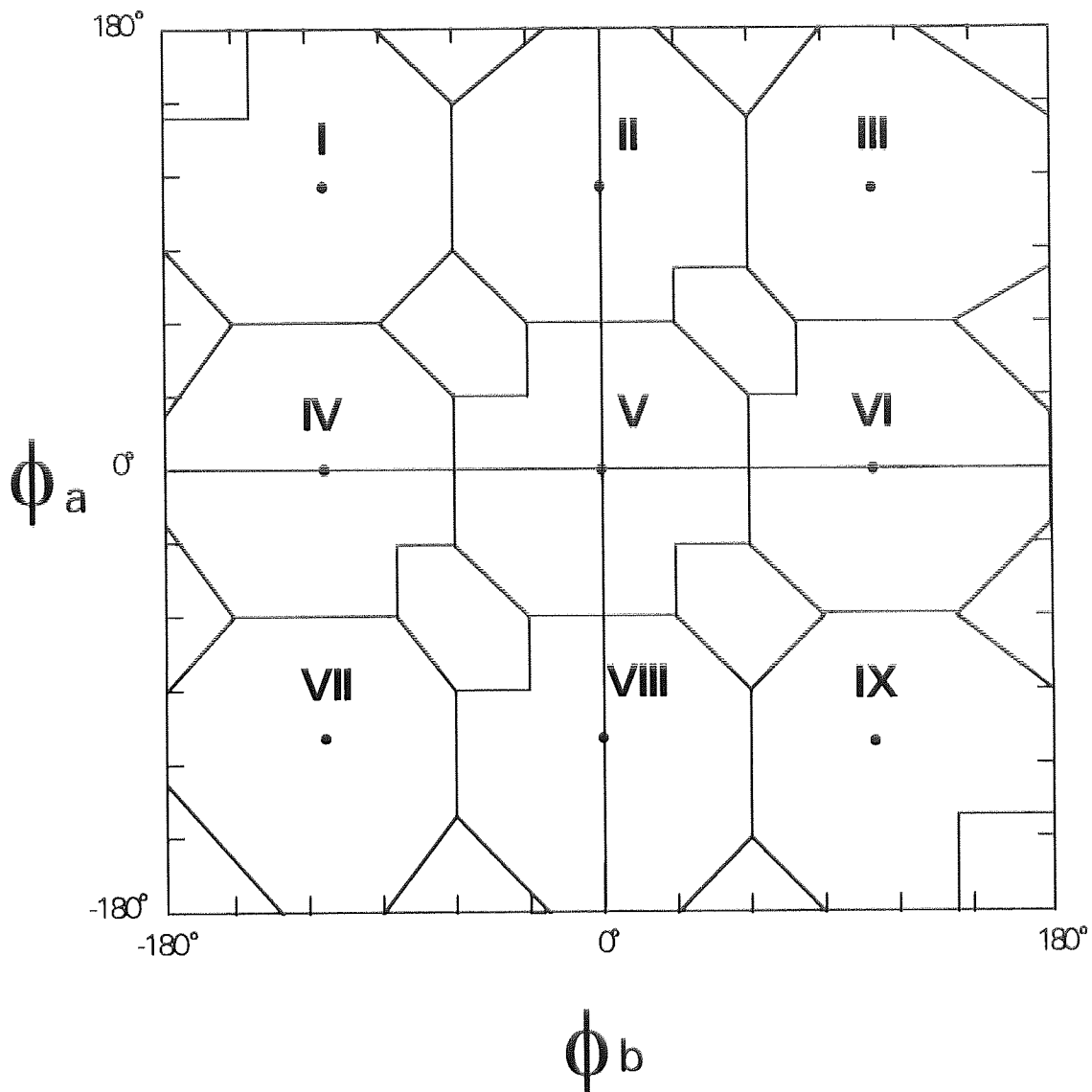


Figure (4-4). Regions representing isomeric states for the poly(dimethylsilmethylene) dyad.

	z			<E>			< ϕ_a, ϕ_b >		
	300K	400K	500K	300K	400K	500K	300K	400K	500K
I	0.73	0.76	0.77	0.63	0.73	0.82	114,-114	114,-114	114,-114
II	0.9	0.92	0.93	0.58	0.68	0.76	116,1	116,1	116,1
III	0.81	0.83	0.84	0.62	0.71	0.78	117,117	117,117	117,117
IV	0.9	0.92	0.93	0.58	0.68	0.76	-1,-116	-1,-116	-1,-116
V	1	1	1	0.54	0.64	0.72	0,0	0,0	0,0
VI	0.9	0.92	0.93	0.58	0.68	0.76	-1,116	-1,116	-1,116
VII	0.81	0.83	0.84	0.62	0.71	0.78	-117,-117	-117,-117	-117,-117
VIII	0.9	0.92	0.93	0.58	0.68	0.76	-116,1	-116,1	-116,1
IX	0.73	0.76	0.77	0.63	0.73	0.82	-114,114	-114,114	-114,114

Table (4-3). Conformational averages for dyad conformation.

Energies are given relative to the tt state in Figure (4-3). The partition functions are expressed relative to a value $z = 1$ for this state. The averaged rotation angles are nearly independent of temperature.

4.5 Statistical Weights

Each of the nine regions in Figure (4-4) may be represented by a combination of rotational isomeric states centred at 0° , 116° and -116° (see Table (4-3)). These states may be denoted by T, G^+ and G^- respectively.

The statistical weights corresponding to first-order interactions (ie. those determined by rotation about one bond only) are illustrated in Figure (4-5). The statistical weights ω , ω' and ω'' may be used for the second-order interactions between the pairs of groups CH_2 and CH_2 , CH_3 and CH_2 , CH_3 and CH_3 respectively, each group separated by four bonds.

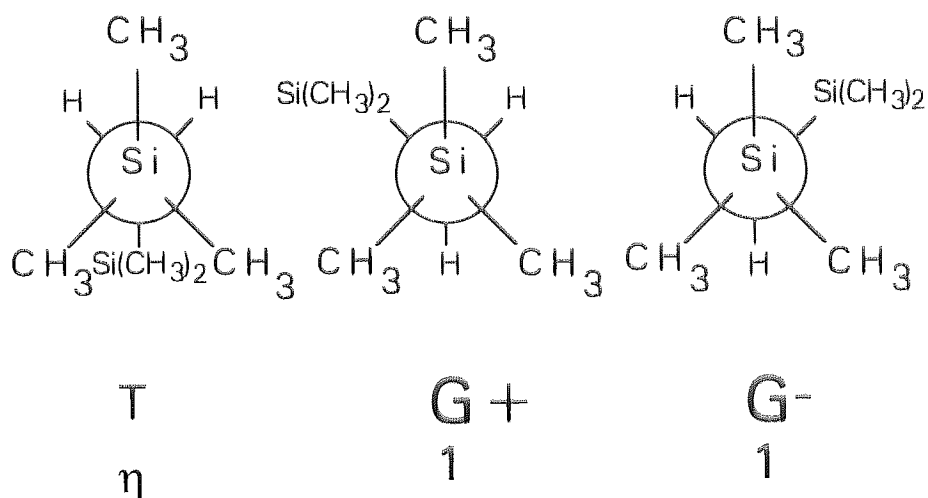


Figure (4-5). Newman projections along bond *i* illustrating the basic first-order interactions.

The features of the conformational energy surface in Figure (4-3) up to at least 6 kcal/mol above the *tt* minimum are well represented by the statistical weight matrix

$$\mathbf{U}'' = \begin{matrix} & \begin{matrix} t & g^+ & g^- \end{matrix} \\ \begin{matrix} t \\ g^+ \\ g^- \end{matrix} & \begin{bmatrix} \eta^2 \omega''^2 & \eta \omega' \omega'' & \eta \omega' \omega'' \\ \eta \omega' \omega'' & \omega'^2 & \omega'' \omega \\ \eta \omega' \omega'' & \omega'' \omega & \omega'^2 \end{bmatrix} \end{matrix} \quad (4-5)$$

The matrix U'' contains all the first-order interactions and second-order interactions that occur within the poly(dimethylsilmethylene) dyad. In addition, it also contains the first-order interactions that would occur between an adjacent pair of dyads in the polymer chain, i.e. the first order interactions for the pair of interdependent bonds flanking a $-\text{Si}(\text{CH}_3)_2-$ group. Since this information is contained in the matrix U'' , the second-order interactions for the interdyad pair illustrated in Figure (4-6) need to be determined. This may be achieved by application of the hard-sphere model.

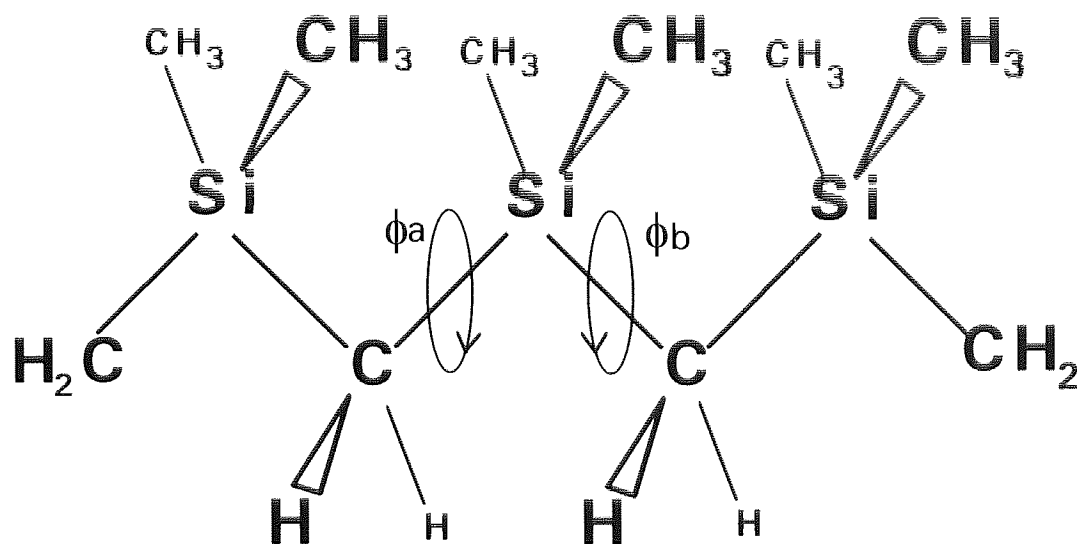


Figure (4-6). Interdependent bond pair flanking a $-\text{Si}(\text{CH}_3)_2-$.

It can be seen that for this interdependent bond pair no significant second-order interactions (interactions between groups separated by four bonds) occur except for the G^+G^-/G^-G^+ conformational states. The steric hindrance between the methyl groups is so severe that a value of zero may

be assigned for the statistical weights of these conformations, all others may be allocated a value of one. The statistical weight matrix containing the second-order interactions for the interdyad pair therefore becomes

$$\mathbf{U}' = \begin{bmatrix} 1 & 1 & 1 \\ 1 & 1 & 0 \\ 1 & 0 & 1 \end{bmatrix} \quad (4-6)$$

Thus, the statistical weight matrix \mathbf{U} that describes all the intramolecular interactions occurring in a section of poly(dimethylsilmethylene) chain containing the two neighbouring interdependent bond pairs, and therefore applicable to the mathematical methods derived in the last chapter, is simply the product of the matrices \mathbf{U}' and \mathbf{U}'' in that order, i.e.

$$\mathbf{U} = \mathbf{U}' \cdot \mathbf{U}'' \quad (4-7)$$

The matrix \mathbf{U}'' may be considerably simplified and its elements directly compared with the calculated values in Table (4-3) by normalising every element in the matrix with respect to the tt state. Mathematically

$$\mathbf{U}'' = \begin{bmatrix} 1 & \alpha & \beta \\ \alpha & \beta & \gamma \\ \alpha & \gamma & \beta \end{bmatrix} \quad (4-8)$$

where $\alpha = \omega' / (\eta\omega'')$, $\beta = \omega'^2 / (\eta^2\omega''^2)$ and $\gamma = \omega / (\eta^2\omega'')$. Since α , β and γ represent the products of statistical weights they may themselves be defined as such by invoking the expressions

$$\alpha = \alpha_0 \exp(-E_\alpha / RT) \quad (4-9)$$

$$\beta = \beta_0 \exp(-E_\beta / RT) \quad (4-10)$$

$$\gamma = \gamma_0 \exp(-E_\gamma / RT) \quad (4-11)$$

The energies E_{α} , E_{β} and E_{γ} were calculated from the averaged energies tabulated in Table (4-3) according to the equations

$$E_{\alpha} = \langle E_{tg+} \rangle - \langle E_{tt} \rangle = 0.04 \text{ kcal/mol}$$

$$E_{\beta} = \langle E_{g+g+} \rangle - \langle E_{tt} \rangle = 0.07 \text{ kcal/mol}$$

$$E_{\gamma} = \langle E_{g+g-} \rangle - \langle E_{tt} \rangle = 0.09 \text{ kcal/mol}$$

these values remaining approximately constant over the three temperatures considered. The factors α_0 , β_0 and γ_0 quantify the relative sizes of the domains or regions defined in Figure (4-4) and were calculated from Equations (4-9) to (4-11), the results being $\alpha_0 = 0.97$, $\beta_0 = 0.91$ and $\gamma_0 = 0.85$.

It is now possible to quantitatively account for the chain statistics of the two neighbouring interdependent bond pairs of poly(dimethylsilmethylene) at any temperature using the matrix \mathbf{U} , where

$$\mathbf{U} = \mathbf{U}' \cdot \mathbf{U}'' = \begin{bmatrix} 1 & 1 & 1 \\ 1 & 1 & 0 \\ 1 & 0 & 1 \end{bmatrix} \begin{bmatrix} 1 & \alpha & \alpha \\ \alpha & \beta & \gamma \\ \alpha & \gamma & \beta \end{bmatrix} \quad (4-12)$$

and $\alpha = 0.97 \exp(-0.04/RT)$, $\beta = 0.91 \exp(-0.07/RT)$ and $\gamma = 0.85 \exp(-0.09/RT)$.

These results may now be used to calculate conformationally-dependent properties of poly(dimethylsilmethylene).

4.6 Characteristic Ratio of Poly(dimethylsilmethylene), (PDMSM)

The characteristic ratio $C_n = \langle r^2 \rangle_0 / nl^2$ for poly(dimethylsilmethylene) was calculated according to the equation

$$\langle r^2 \rangle_0 / nl^2 = 2(Znl^2)^{-1} \mathbf{g}^* \mathbf{G}_T \mathbf{G}^{(n-2)} \mathbf{G}_n \mathbf{g} \quad (4-13)$$

using the three-state model formulated on the potential energy calculations and geometrical parameters derived in the previous sections. The matrices \mathbf{G}_T and \mathbf{G}_n representing the terminal bonds were calculated according to Equation (2-38) by replacing the matrix \mathbf{U} with the identity matrix \mathbf{E} . The matrix \mathbf{G} is defined by the equation

$$\mathbf{G} = \mathbf{G}' \cdot \mathbf{G}'' \quad (4-14)$$

where \mathbf{G}' and \mathbf{G}'' are also calculated by Equation (2-38) by using the matrices \mathbf{U}' and \mathbf{U}'' respectively. The parameters required for construction of the matrices $\mathbf{T}'_1, \mathbf{T}'_2, \mathbf{T}'_3$, and $\mathbf{T}''_1, \mathbf{T}''_2, \mathbf{T}''_3$ were taken from Table (4-1) and the components of the bond vector \mathbf{l} were given the values $l_x = 1.89$, $l_y = 0$ and $l_z = 0$.

Figure (4-7) shows the dependence of C_n on the length of the polymer at the three temperatures 300K, 400K and 500K respectively.

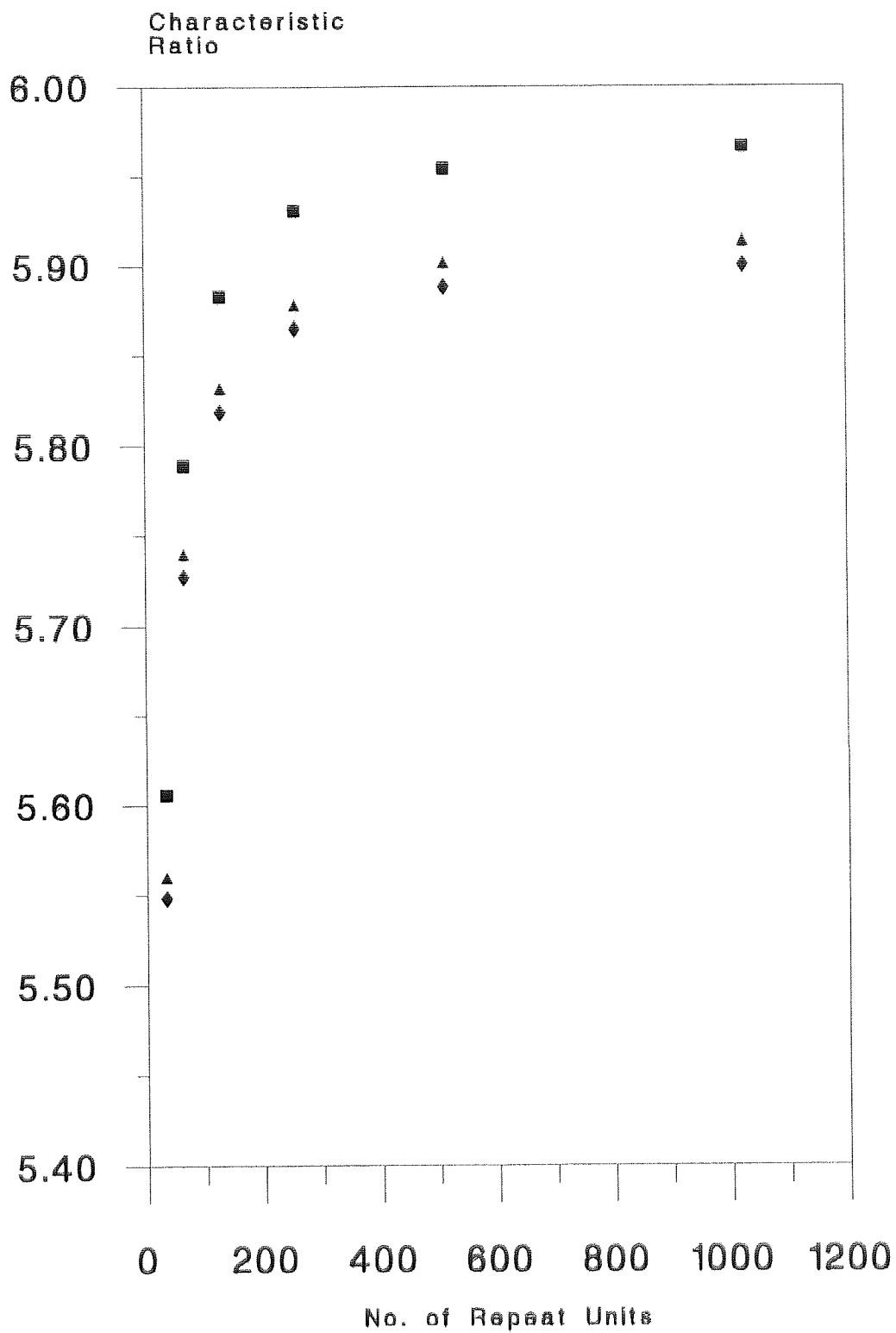


Figure (4-7). Characteristic Ratio of PDMSM at 300K (■), 400K (▲) and 500K (◆).

4.7 Dipole Moment Ratio of Poly(dimethylsilmethylene), (PDMSM)

The dipole moment ratio, $\langle \mu^2 \rangle_0 / nm^2$, for poly(dimethylsilmethylene) was calculated using the equation

$$\langle \mu^2 \rangle_0 / nm^2 = 2(Znm^2)^{-1} \mathbf{g} * \mathbf{G}_T \mathbf{G}^{(n-2)} \mathbf{G}_n \mathbf{g} \quad (4-15)$$

again based on the three state model. The matrices \mathbf{G} , \mathbf{G}_T and \mathbf{G}_n were calculated according to the procedure described in section 4.6.

Investigations into the dielectric behaviour of other organo-silicon compounds^{16,17,18} have indicated that a bond dipole of 0.6D is associated with the Si-C bond. Based on this information the components of the vector \mathbf{m} were given the values $m_x = +0.6$, $m_y = 0$ and $m_z = 0$ for a Si-C bond, and $m_x = -0.6$, $m_y = 0$ and $m_z = 0$ for a C-Si bond.

Figure (4-8) shows the dependence of $\langle \mu^2 \rangle_0 / nm^2$ on chain length at the three temperatures 300K, 400K and 500K respectively.

4.8 Discussion of the Results

The limiting values of $\langle r^2 \rangle_0 / nl^2$ thus obtained in these calculations at 300K, 400K and 500K are 5.97, 5.91 and 5.90 respectively. Similarly the limiting values of $\langle \mu^2 \rangle_0 / nm^2$ at 300K, 400K and 500K are 0.437, 0.432 and 0.430 respectively.

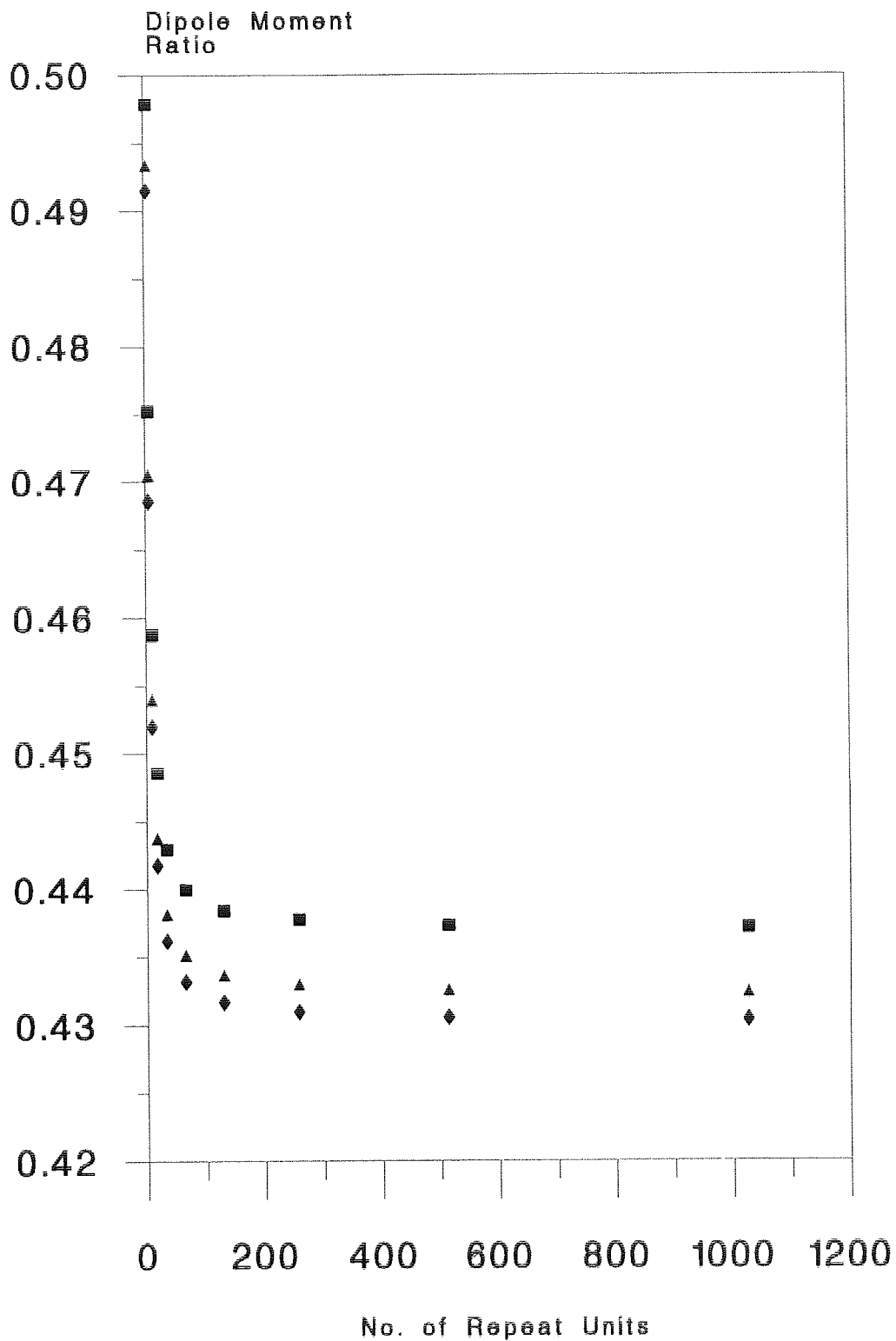


Figure (4-8). Dipole Moment Ratio of PDMSM at 300K (■), 400K (▲) and 500K (◆).

The nature of the results seem to indicate that the characteristic ratio and the dipole moment ratio of poly(dimethylsilmethylene) are very nearly independent of temperature. The near temperature independence of $\langle r^2 \rangle_0/nl^2$ and $\langle \mu^2 \rangle_0/nm^2$ may occur because the rotations about Si-CH₂-Si bond pairs merely serve to interchange CH₂ groups with CH₃ groups and vice versa. Conformational analyses^{6,32} of other chain molecules have employed the reasonable assumption that CH₂ and CH₃ groups are sterically very nearly equivalent.

This assumption may also explain why the characteristic and dipole moment ratios calculated for poly(dimethylsilmethylene) are relatively low compared to values calculated for other polymers at similar temperatures. For instance, the characteristic ratio of polymethylene has been calculated³³ to be 7.9 at 300K. This large value arises since polymethylene shows a strong preference for the all-trans conformation, a distinctive feature of polymers in general. By assuming that CH₂ and CH₃ groups are sterically equivalent, poly(dimethylsilmethylene) shows no preference for any conformation resulting in a lower characteristic ratio.

Values for the characteristic ratio and dipole moment ratio have been experimentally determined for poly(dimethylsilmethylene) by Mark et al³⁴. Using results obtained from viscosity and dipole moment experiments performed on poly(dimethylsilmethylene) fractions, Mark calculated values for $\langle r^2 \rangle_0/nl^2$ and $\langle \mu^2 \rangle_0/nm^2$ at various temperatures. His results for

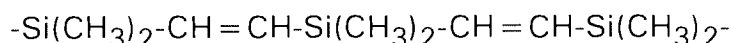
$\langle r^2 \rangle_0/nl^2$ and $\langle \mu^2 \rangle_0/nm^2$ at 303K are 5.32 and 0.355 respectively, compared with the theoretically calculated values of 5.97 and 0.437.

CHAPTER 5

CONFORMATIONAL ANALYSIS OF POLY(DIMETHYLSILETHENE)

5.1 Introduction

The molecular structure of a section of poly(dimethylsilethene) chain is illustrated below



Poly(dimethylsilethene) possesses unusual structural features that make it a very interesting polymer from a conformational point of view. The skeletal backbone of the polymer consists of alternating silicon atoms separated by planar carbon-carbon double bonds which restrict its conformational freedom. In addition, experimental evidence³⁵ obtained from bis(trimethylsilyl)ethene suggests that the carbon-carbon double bonds exist solely in the trans state. This may be expected due to the large steric repulsion between the $\text{Si}(\text{CH}_3)_2$ groups if the double bonds were to exist in the cis conformation. Adherence of all double bonds to the planar trans conformation permits the spatial configuration of the chain to be described in terms of hypothetical virtual bonds^{2,10}, with each virtual bond connecting successive silicon atoms. This is illustrated in Figure (5-1).

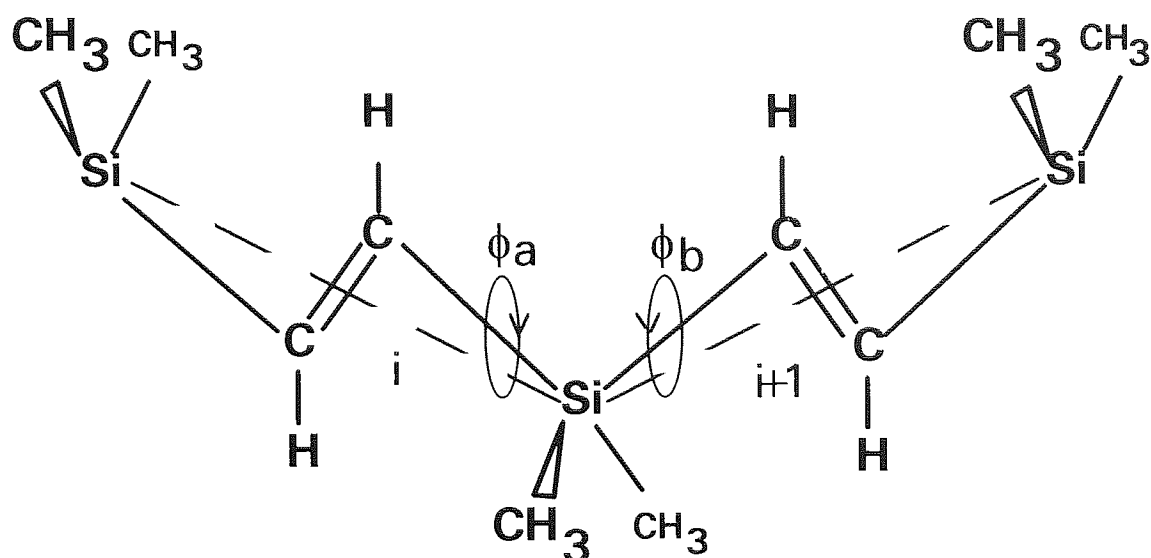


Figure (5-1). Spatial arrangement of a section poly(dimethylsilethene) as described by the virtual bonds i and $i+1$ (dashed lines).

Since each carbon-carbon double bond adopts a planar trans conformation, the virtual bonds i and $i+1$ in Figure (5-1) make up an interdependent bond pair. The conformational energy for such an interdependent bond pair is therefore dependent upon the skeletal bond rotation angles ϕ_a and ϕ_b . However, due to the rigid nature of the planar carbon-carbon double bond, rotations about neighbouring virtual bonds may be ignored. For instance, rotations about the virtual bonds $i-1$ and $i+2$ do not interfere with the intramolecular interactions associated with the virtual bond pair i and $i+1$. The conformational energy of the virtual bond pair i and $i+1$ is therefore unaffected. By treating the polymer as consisting of isolated pairs of rotation angles, with members of the same pair strongly interdependent,

the whole configurational statistics for the chain may be evaluated by quantitatively analysing the interdependence of a virtual bond pair.

In this chapter the conformational energy associated with such an interdependent pair of virtual bonds will be calculated for poly(dimethylsilethene). Based on the results obtained the characteristic ratio, $\langle r^2 \rangle / nl^2$, and the mean-square radius of gyration, $\langle s^2 \rangle / nl^2$, for varying chain lengths will be calculated according to the principles derived in Chapter 2 for a chain with independent bond pairs.

5.2 Molecular Geometry

Due to the small amount of experimental structural data concerning the polycarbosilanes, the structural parameters used in our calculations for poly(dimethylsilethene) were derived from a quantitative study performed by Tribble and Allinger³⁶. In their study of various methylsilanes and vinylsilane, structural parameters such as bond lengths, bond angles and bond angle bending constants were calculated based on experimental data. Some of the structural parameters derived by Tribble and Allinger were used in the present study since it was highly unlikely that they would differ significantly in poly(dimethylsilethene). These are illustrated in Table (5-1).

However, since the steric environment of the double bond in vinylsilane differs somewhat from that in poly(dimethylsilethene), it was important to establish if the value of the bond angles assigned to the Si-C=C-Si groups

would be significantly perturbed by the additional intramolecular energy arising from the different steric surroundings.

	Bond Length (Å)	Bond Angle (θ°)	Angle Bending Constant ³⁶ k _θ (kcal mol ⁻¹ deg ⁻²)
C _{sp3} - Si	1.87	-	-
C _{sp2} - Si	1.85	-	-
C - H	1.1	-	-
C = C	1.34	-	-
C - Si - C	-	110.2	0.022
C = C - Si	-	122.5	0.018
Si - C _{sp2} - H	-	118.4	0.010

Table (5-1). Geometrical parameters used for poly(dimethylsilethene).

Using the parameters displayed in Tables (5-1) and (5-2), the intramolecular energy of the section of poly(dimethylsilethene) illustrated in Figure (5-1) was calculated for the four conformations, tt, tg, g⁻g⁻ and g⁺g⁻, according to the Lennard-Jones (6-12) potential described in Chapter 2. In each case, the C=C-Si bond angles were then varied about their equilibrium values and the intramolecular energy calculated again with the inclusion of the associated bond angle strain³⁶, $E_s = 4 * (0.018/2)(\theta - 122.5^0)$. The results are illustrated in Figures (5-2) to (5-5).

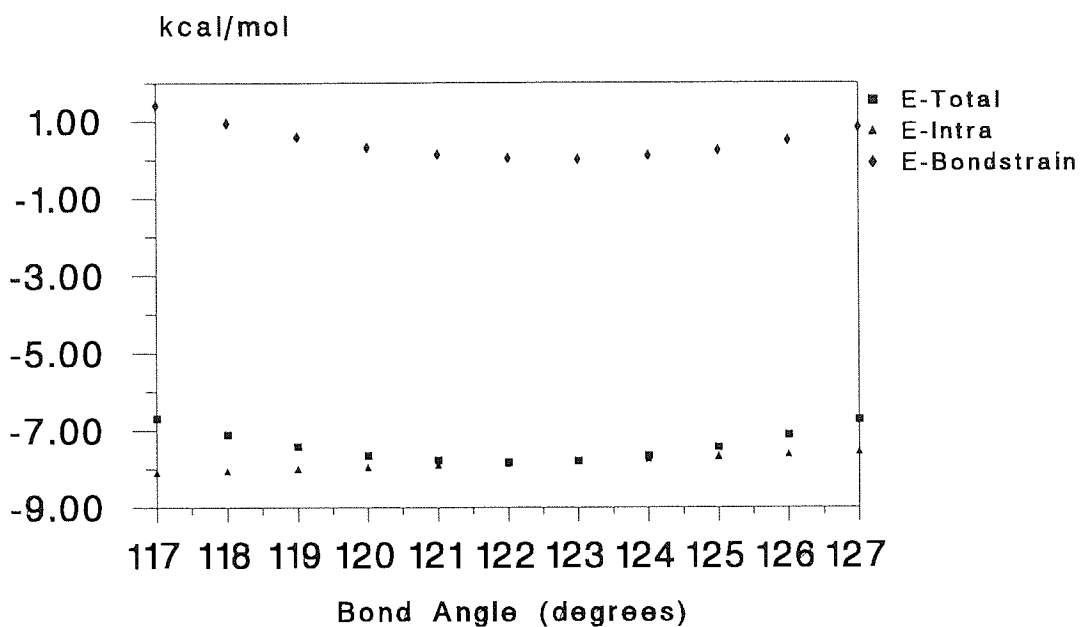


Figure (5-2). Dependence of C=C-Si bond angle in the trans-trans conformation.

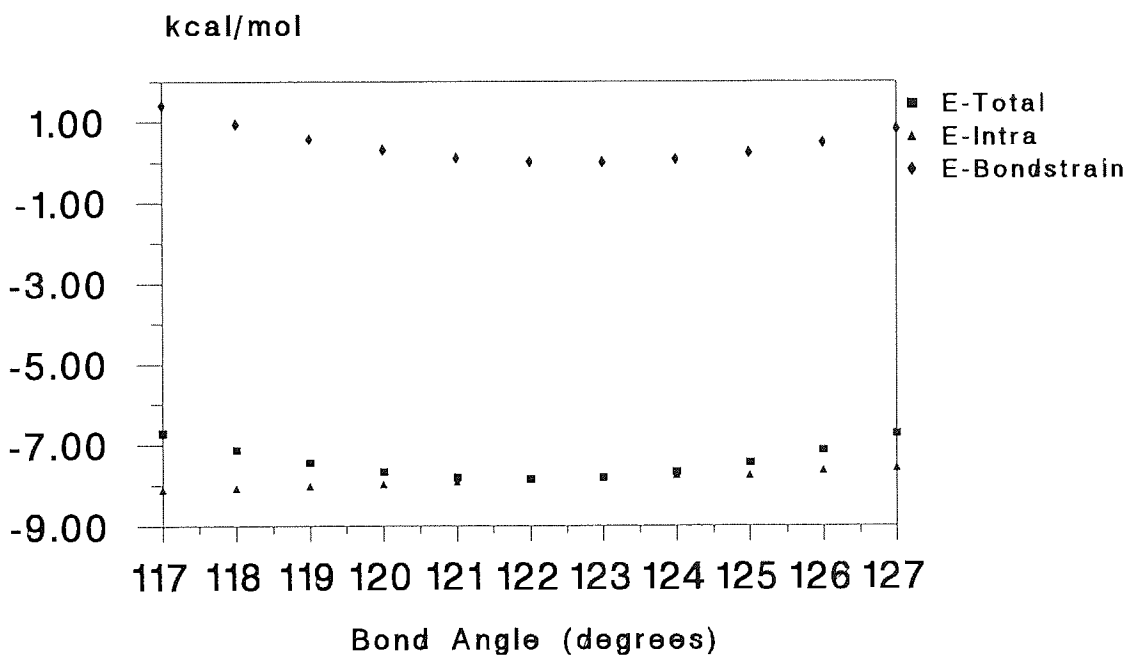


Figure (5-3). Dependence of C=C-Si bond angle in the trans-gauche conformation.

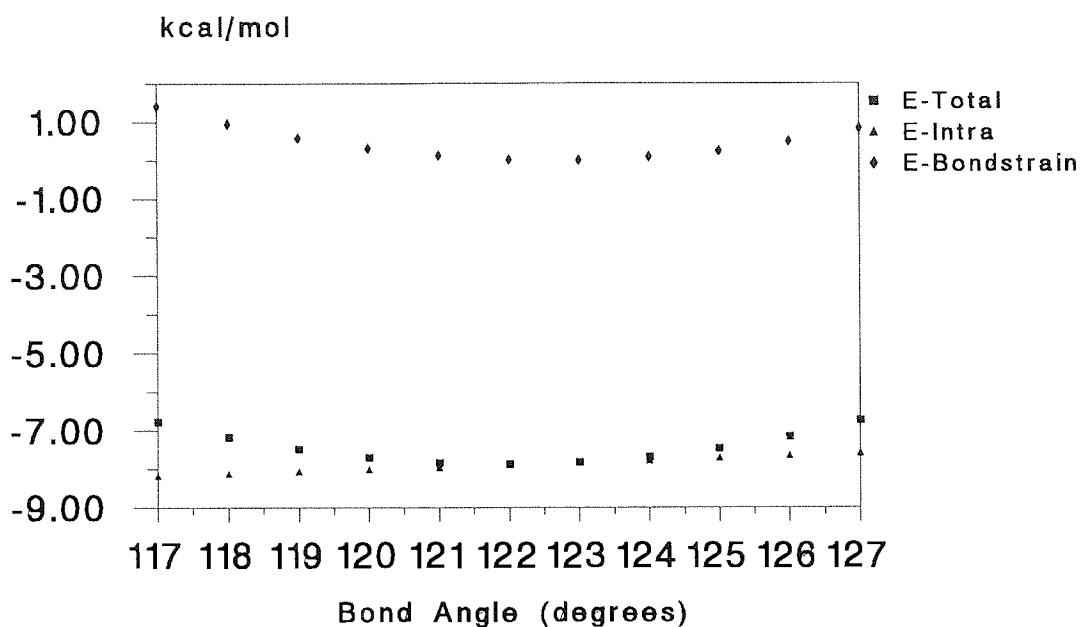


Figure (5-4). Dependence of C=C-Si bond angle in the gauche(-)-gauche(-) conformation.

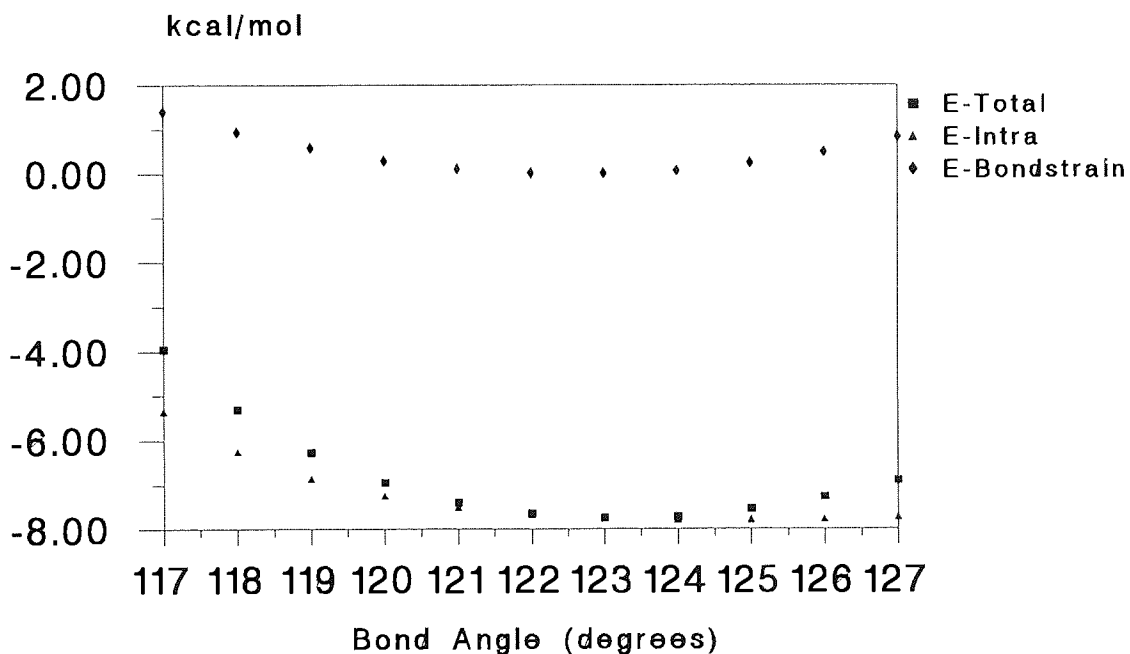


Figure (5-5). Dependence of C=C-Si bond angle in the gauche(+)-gauche(-) conformation.

In three of the conformations, tt, tg, and g^-g^- , the value of the C=C-Si bond angle associated with the minimum conformational energy was the equilibrium value of 122.5° . In the g^+g^- conformation the value of the C=C-Si bond angle generating the minimum energy conformation was distorted to a value of 123° , but since the distortion was very slight it was decided to retain the value of 122.5° for use in the calculations.

5.3 Conformational Energy

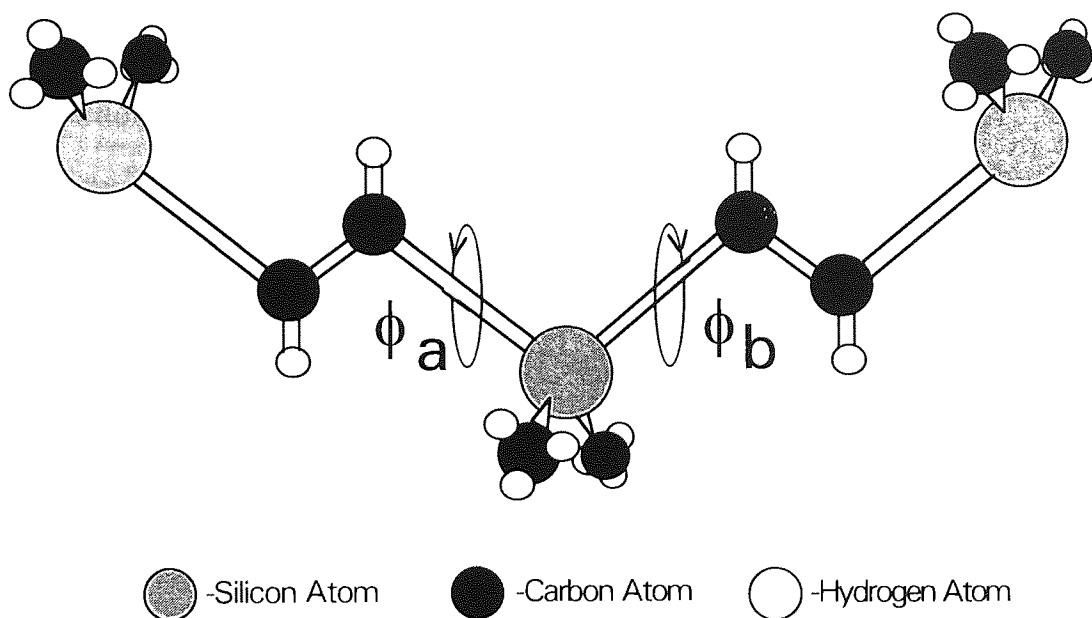


Figure (5-6). Section of poly(dimethylsilethene) used in the calculations.

To investigate the interdependence occurring within a virtual bond pair, the section of poly(dimethylsilethene) illustrated in Figure (5-6) was used as the basis for the calculations.

By assuming that each carbon-carbon double bond adopts a planar trans conformation, and is not subject to rotation, the intramolecular energy for the virtual bond pair in Figure (5-6) is dependent upon the two bond rotation angles ϕ_a and ϕ_b . Since the section of poly(dimethylsilethene) under consideration contains six branched methyl groups, it was decided to calculate the conformational energy for the structure using the "partial relaxation" technique. That is, the conformational energy calculated for each set of bond rotation angles ϕ_a and ϕ_b was minimised by allowing the six branched methyl groups to rotate independently to achieve the lowest conformational energy possible.

It was assumed the conformational energy, $E(\phi_a, \phi_b)$, arising from rotations about ϕ_a and ϕ_b , consisted of a combination of additive contributions from the intrinsic torsional potentials of all rotatable bonds and from the van der Waals interactions between non-bonded atoms. The interactions included in the latter contribution were from those atom pairs whose intramolecular separation depended upon one or more rotatable bonds. Equation (5-1) incorporates all of the contributions described above.

$$E(\phi_a, \phi_b) = \sum (E^0/2)(1-\cos 3\phi) + \sum [(a_{kl}/r_{kl})^{12} - (c_{kl}/r_{kl})^6] \quad (5-1)$$

The intrinsic torsional potential of each pendent Si-C_{sp3} bond was assigned a 3-fold character with a barrier height of 0.5 kcal/mol⁷. Investigations³⁶ into the nature of the Si-C_{sp2} torsional potential have indicated a barrier height of zero. In addition, studies² performed on

analogous structures in which a single bond connects a tetravalent carbon atom to a doubly bonded one, have suggested that the conformation of lowest energy is that in which one of the pendent bonds of the former eclipses the double bond. This is illustrated in Figure (5-7).

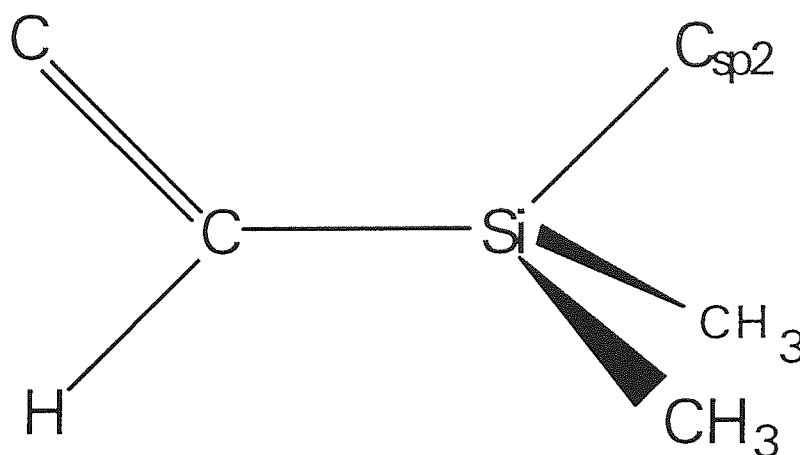


Figure (5-7). Lowest energy conformation for a tetravalent Si atom bonded to a doubly bonded C atom.

This property of rotational potentials for single bonds adjoining double bonds can be reconciled with the bond staggering rule by regarding the double bond as two single bonds drawn together from their normal sp^3 positions.

The constants a_{kl} and c_{kl} characteristic of the Lennard-Jones (6-12) potential were calculated from atomic polarizabilities³¹ by application of the Slater-Kirkwood²⁵ equation and are tabulated in Table (5-2).

	a_{kl}^*	c_{kl}^*
Si-----C _{sp3}	1.71E + 06	1050
Si-----C _{sp2}	1.96E + 06	1300
C _{sp3} ---C _{sp3}	3.95E + 05	363.0
C _{sp3} ---C _{sp2}	4.48E + 05	447.2
C _{sp2} ---C _{sp2}	5.10E + 05	552.9
Si----H	2.62E + 05	374.1
C _{sp3} ----H	5.63E + 04	127.0
C _{sp2} ----H	6.39E + 04	158.8
H-----H	7.27E + 03	47.1

Table (5-2). Non-bonded potential energy parameters. *Units are such as to give E_{NB} in kcal/mol for r_{kl} in Å.

A conformational energy map, illustrated in Figure (5-8), based on the PR calculations was generated by using Eq. (5-1) and scanning the entire conformational energy space, 0° to 360° , for both ϕ_a and ϕ_b in steps of 10° . The corresponding conformational energies, $E(\phi_a, \phi_b)$ were minimised by allowing rotation of the branched methyl groups between 0° and 360° in steps of 5° .

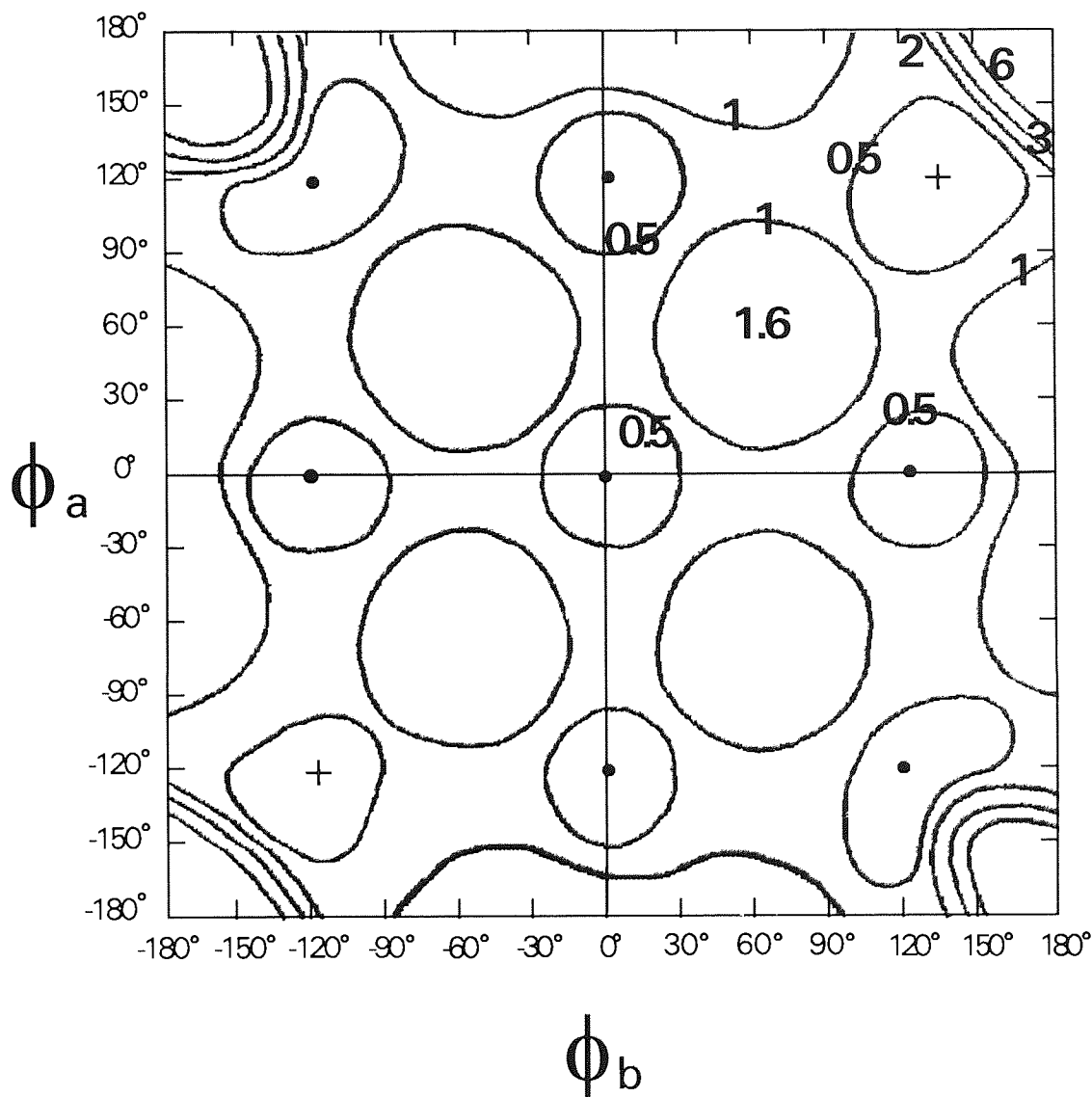


Figure (5-8). Conformational energy map for the pair of bond rotation angles ϕ_a and ϕ_b as determined by the PR calculations. The energy, given in kcal/mol relative to the conformational energy minima designated by "+" on the map, is shown as contour lines with some values illustrated in the top right quadrant. Local potential energy minima are located by the dots.

Analysis of the conformational energy contour map shows the existence of nine potential energy minima. These occur in the tt , tg^+ , tg^- , g^+t , g^-t , g^+g^+ , g^-g^- , g^+g^- and g^-g^+ conformational states with the g^+g^+ and g^-g^- being the lowest energy conformations. Due to the rigid carbon-carbon double bonds restricting the rotational freedom of the molecule, the overall steric hindrance arising from short range intramolecular interactions within the molecule is reduced. This results in the relatively low conformational energies calculated for most of the conformational states (<2 kcal/mol). The only exception occurs when the molecule exists in the cis-cis state where the steric hindrance is so severe that conformational energies greater than 6 kcal/mol have been calculated. The excessive conformational energy calculated for the cis-cis state originates from the intramolecular interaction occurring between the two hydrogen atoms (H^*), illustrated in Figure (5-9).

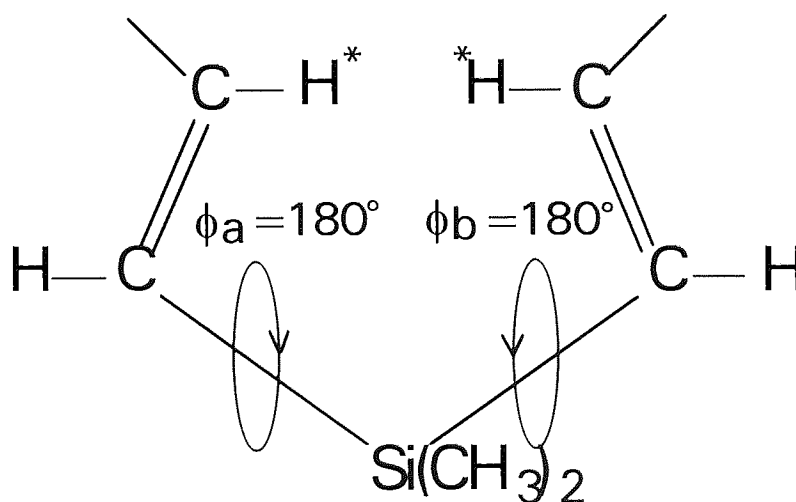


Figure (5-9). The H^*-H^* interaction occurring in the cis-cis state.

In the cis-cis state, the intramolecular distance between the two hydrogen atoms labelled in Figure (5-9) is significantly less than the sum of their van der Waals radii. This leads to severe steric interactions which result in the large conformational energies for this state.

5.4 Configurational Statistics for Poly(dimethylsilethene)

In order to calculate the characteristic ratio and mean-square radius of gyration using the concept of independent virtual bond pairs, it is necessary to derive a transformation matrix, \mathbf{T}_i , dependent upon the bond rotation angles ϕ_a and ϕ_b , which will enable us to transform the representation of a vector quantity in one virtual reference frame, say $i+1$, to its corresponding representation in the preceding virtual reference frame i . To do this a Cartesian coordinate system must be assigned to each virtual bond in the chain. For simplicity, let the X-axis of the coordinate system coincide with the direction of the virtual bond itself. The Y-axis may then be taken in the plane of the carbon-carbon double bond with the Z-axis defined so as to complete an right-handed orthogonal coordinate system as illustrated in Figure (5-10). Let the coordinate systems (xyz) for the various skeletal bonds be defined in accordance with the conventions described in Chapter 2.

Derivation of a virtual bond transformation matrix \mathbf{T}_i , dependent upon the bond rotations of the skeletal bonds, requires that a relationship between the virtual bond coordinate systems and the skeletal bond coordinate systems be developed. Consider two Cartesian reference frames, xyz and x'y'z'. Let

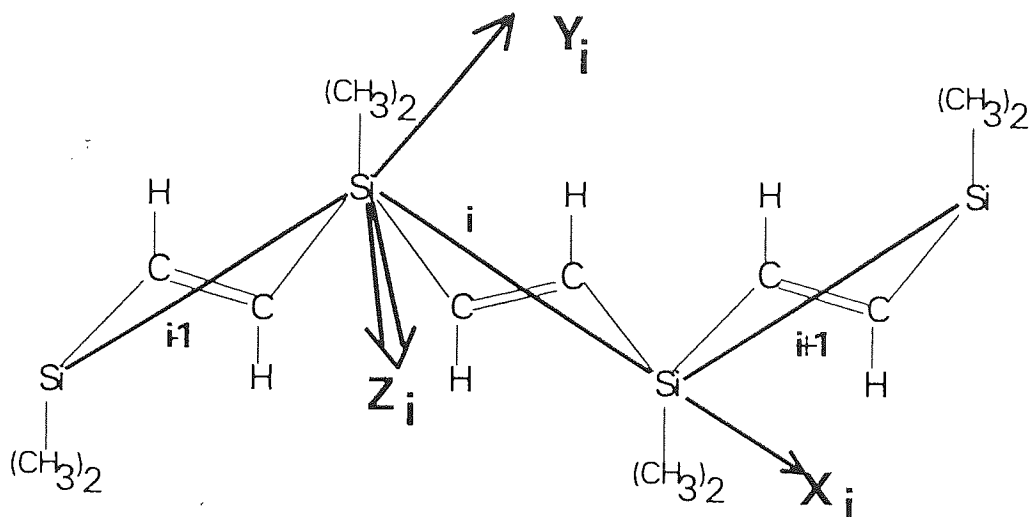


Figure (5-10). The coordinate system assigned to each virtual bond.

the rotation α , centred about the z' -axis of the reference frame $x'y'z'$, render the x -axis of the former reference frame coincident with the x' -axis of the latter reference frame. Now let the rotation β , about the now common x -axes, render the two reference frames coincident. Based on this relationship between the two reference frames, a matrix $\mathbf{R}(\alpha, \beta)$ may be defined that transforms the representation of a vector expressed in the reference frame $x'y'z'$ to its corresponding representation in the reference frame xyz as²

$$\mathbf{R}(\alpha, \beta) = \begin{bmatrix} \cos\alpha & \sin\alpha & 0 \\ -\sin\alpha \cdot \cos\beta & \cos\alpha \cdot \cos\beta & \sin\beta \\ \sin\alpha \cdot \sin\beta & -\cos\alpha \cdot \sin\beta & \cos\beta \end{bmatrix} \quad (5-2)$$

Since the axes X_{i+1} Y_{i+1} Z_{i+1} of the virtual bond $i+1$ are related to the xyz coordinate system of the skeletal bond $\text{Si}^\beta\text{-C}^\gamma$ in the sense that they may be brought into coincidence (see Figure (5-11)), the matrix $\mathbf{R}(\alpha, \beta)$, with $\alpha = -\eta$

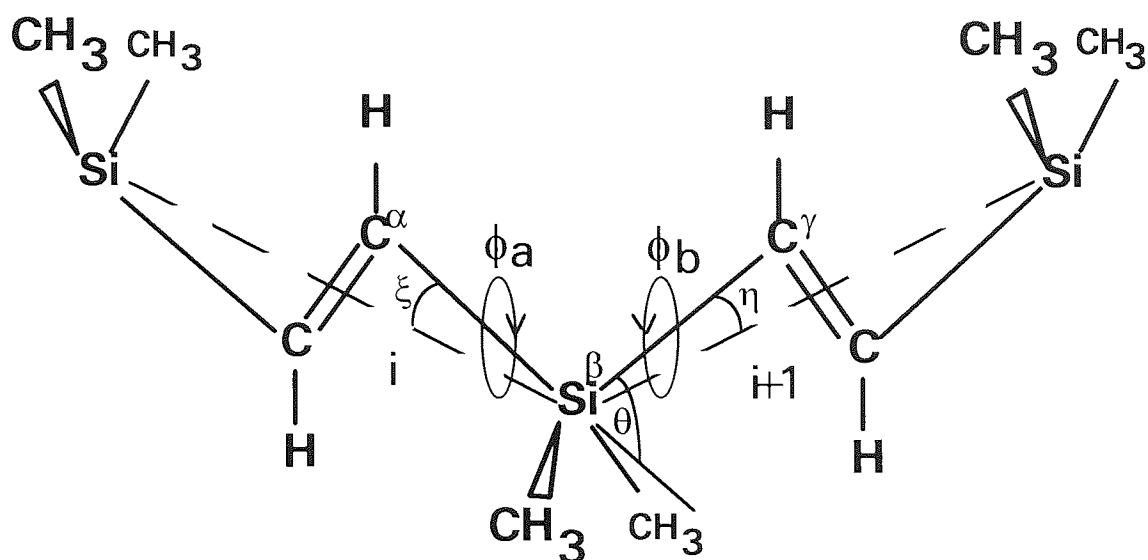


Figure (5-11). Geometrical representation of the relationship between the virtual bonds i and $i+1$ and the skeletal bonds $C^\alpha-Si^\beta$ and $Si^\beta-C^\gamma$.

and $\beta = -\phi_b$, may be used to transform a vector quantity from the reference frame of the virtual bond $i+1$ to the reference frame of the skeletal bond $Si^\beta-C^\gamma$. The matrix $\mathbf{R}(-\eta, -\phi_b)$ is given by the equation²

$$\mathbf{R}(-\eta, -\phi_b) = \begin{bmatrix} \cos\eta & -\sin\eta & 0 \\ \sin\eta \cdot \cos\phi_b & \cos\eta \cdot \cos\phi_b & -\sin\phi_b \\ \sin\eta \cdot \sin\phi_b & \cos\eta \cdot \sin\phi_b & \cos\phi_b \end{bmatrix} \quad (5-3)$$

The transformation of a vector quantity from the reference frame of the skeletal bond $Si^\beta-C^\gamma$ to the reference frame of the preceding skeletal bond $C^\alpha-Si^\beta$, involves the rotations $\alpha = \theta$ and $\beta = \pi - \phi_a$ (the rotation β is displaced by 180° from $-\phi_a$ due to the conventions used). Hence, the matrix $\mathbf{R}(\theta, \pi - \phi_a)$ which performs this task is given by²

$$\mathbf{R}(\theta, \pi - \phi_a) = \begin{bmatrix} \cos\theta & \sin\theta & 0 \\ \sin\theta \cdot \cos\phi_a & -\cos\theta \cdot \cos\phi_a & \sin\phi_a \\ \sin\theta \cdot \sin\phi_a & -\cos\theta \cdot \sin\phi_a & -\cos\phi_a \end{bmatrix} \quad (5-4)$$

Finally, the transformation from the skeletal bond $C^\alpha-Si^\beta$ to the virtual bond i involves a single rotation $\alpha = \xi$, with $\beta = 0$. It is represented by²

$$\mathbf{R}(\xi, 0) = \begin{bmatrix} \cos\xi & \sin\xi & 0 \\ -\sin\xi & \cos\xi & 0 \\ 0 & 0 & 1 \end{bmatrix} \quad (5-5)$$

By combining the above matrices, a transformation matrix, $\mathbf{T}_i(\phi_a, \phi_b)$, may be defined that transforms the representation of a vector quantity from the reference frame of virtual bond $i+1$, to its corresponding coordinates in the reference frame of virtual bond i , by the equation

$$\mathbf{T}_i(\phi_a, \phi_b) = \mathbf{R}(\xi, 0) \cdot \mathbf{R}(\theta, \pi - \phi_a) \cdot \mathbf{R}(-\eta, -\phi_b) \quad (5-6)$$

The above equation is taken to represent the relationship between two vector quantities associated with the pair of virtual bonds i and $i+1$. Since the whole of the poly(dimethylsilolethene) chain may be described in terms of such identical, independent virtual bond pairs, the index i may be dropped since the matrix $\langle \mathbf{T} \rangle$ is the same for all bond pairs. In such cases, the statistical average matrix $\langle \mathbf{T} \rangle$ may be calculated by the equation

$$\begin{aligned} \langle \mathbf{T} \rangle &= \mathbf{R}(\xi, 0) \cdot \langle \mathbf{R}(\theta, \pi - \phi_a) \cdot \mathbf{R}(-\eta, -\phi_b) \rangle \\ &= \mathbf{R}(\xi, 0) \cdot \{ Z^{-1} \sum \mathbf{R}(\theta, \pi - \phi_a) \cdot \mathbf{R}(-\eta, -\phi_b) \cdot \exp[-E(\phi_a, \phi_b)/RT] \} \quad (5-7) \end{aligned}$$

where Z is the partition function and Eq. (5-7) is summed over 0° to 360° , for both ϕ_a and ϕ_b , in steps of 10° .

Calculations performed on poly(dimethylsilethene) resulted in the evaluation of the parameters $\xi = 14^\circ 10'$, $\theta = 69^\circ 48'$ and $\eta = 14^\circ 10'$. Based on these results and the results obtained from the conformational energy calculations, the statistical average transformation matrix, $\langle T \rangle$, for poly(dimethylsilethene) was calculated at three temperatures, 300K, 400K and 500K. The resulting matrices are illustrated below

$$\langle T \rangle_{300K} = \begin{bmatrix} 0.30 & 0.015 & 0 \\ -0.16 & 0.01 & 0 \\ 0 & 0 & 0.022 \end{bmatrix} \quad (5-8)$$

$$\langle T \rangle_{400K} = \begin{bmatrix} 0.313 & 0.0284 & 0 \\ -0.144 & 0.0062 & 0 \\ 0 & 0 & 0.029 \end{bmatrix} \quad (5-9)$$

$$\langle T \rangle_{500K} = \begin{bmatrix} 0.315 & 0.035 & 0 \\ -0.137 & 0.0036 & 0 \\ 0 & 0 & 0.034 \end{bmatrix} \quad (5-10)$$

5.5 Calculation of the Characteristic Ratio and the Mean-Square Radius of Gyration for Poly(dimethylsilethene)

The characteristic ratio for poly(dimethylsilethene) may be calculated according to Eq. (2-30), derived in Chapter 2, for a chain with independent bond rotations

$$C_n = \langle r^2 \rangle_0 / n l_v^2 = [(\mathbf{E} + \langle \mathbf{T} \rangle)(\mathbf{E} - \langle \mathbf{T} \rangle)^{-1} - (2 \langle \mathbf{T} \rangle / n)(\mathbf{E} - \langle \mathbf{T} \rangle)^n (\mathbf{E} - \langle \mathbf{T} \rangle)^{-2}]_{11} \quad (5-11)$$

The corresponding ratio of the mean-square radius of gyration is given by the equation²

$$\begin{aligned} \langle s^2 \rangle_0 / n l_v^2 = & [(n+2)/6(n+1)][(\mathbf{E} + \langle \mathbf{T} \rangle)(\mathbf{E} - \langle \mathbf{T} \rangle)^{-1}]_{11} \\ & - [\langle \mathbf{T} \rangle (\mathbf{E} - \langle \mathbf{T} \rangle)^{-2}]_{11} / (n+1) + 2[\langle \mathbf{T} \rangle^2 (\mathbf{E} - \langle \mathbf{T} \rangle)^{-3}]_{11} / (n+1)^2 \\ & - 2[\langle \mathbf{T} \rangle^3 (\mathbf{E} - \langle \mathbf{T} \rangle)^n (\mathbf{E} - \langle \mathbf{T} \rangle)^{-4}]_{11} / (n(n+1)^2) \end{aligned} \quad (5-12)$$

In both equations, \mathbf{E} is the identity matrix and n is the number of repeat units. The parameter l_v represents the length of the virtual bonds and was calculated to be 4.5\AA .

The characteristic ratio and mean-square radius of gyration were calculated for poly(dimethylsilethene) according to Eq. (5-11) and Eq. (5-12) respectively. The calculations were performed at temperatures of 300K, 400K and 500K using the $\langle \mathbf{T} \rangle$ matrices derived in the previous section. The results are illustrated in Figure (5-12) and Figure (5-13) respectively.

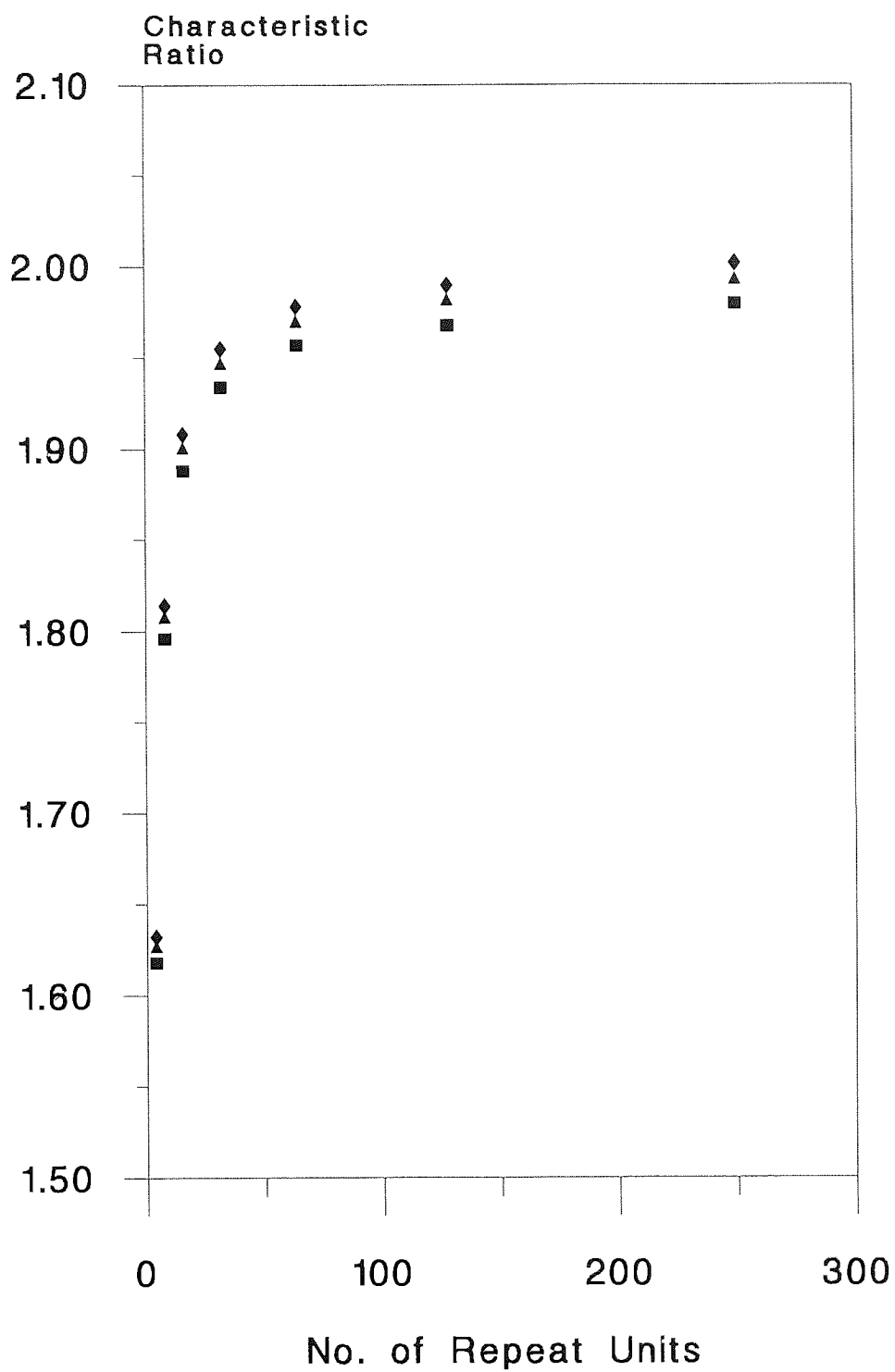


Figure (5-12). Characteristic ratio of poly(dimethylsilethene) at 300K (■), 400K (▲) and 500K (◆).

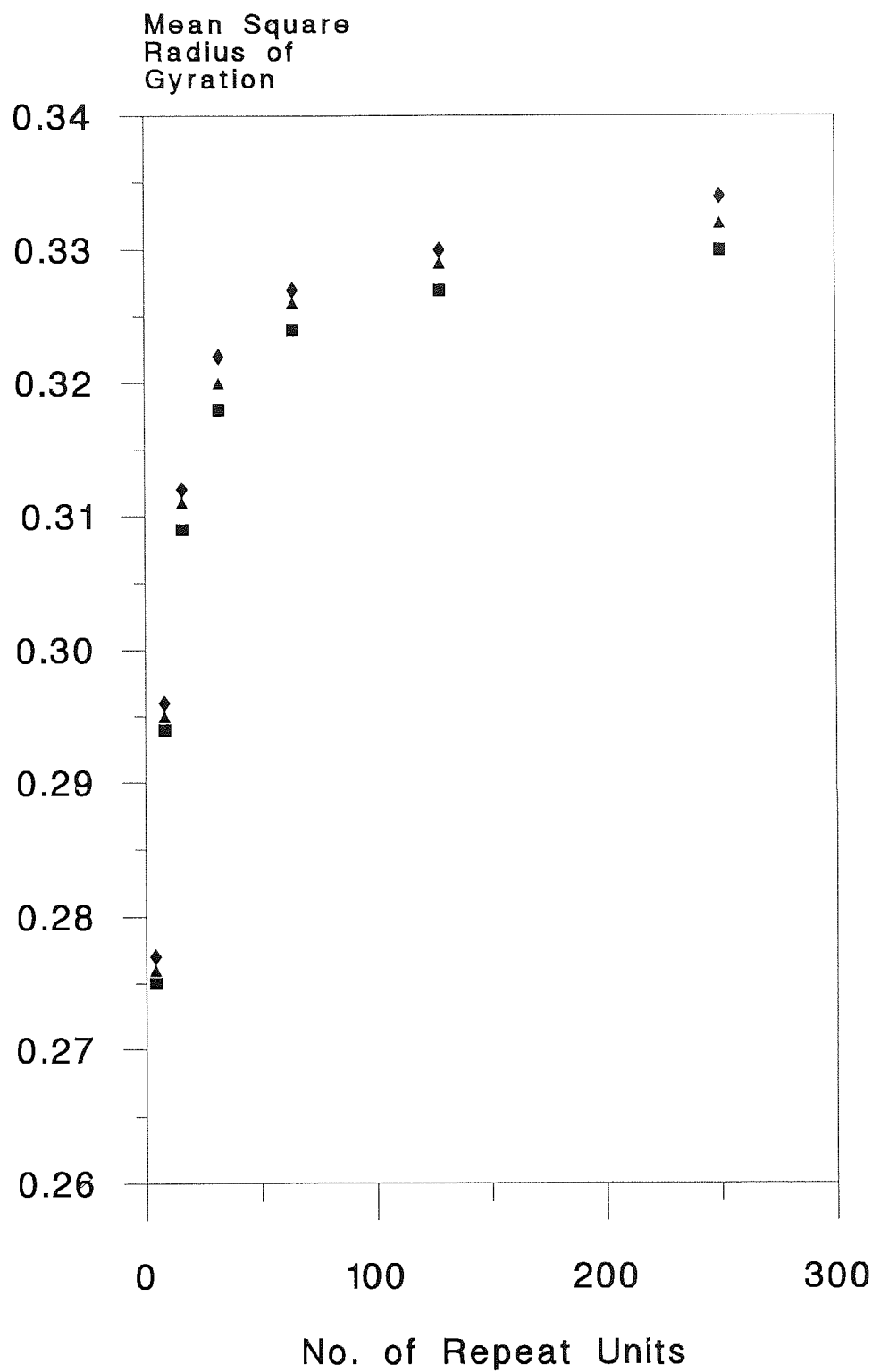


Figure (5-13). Mean-square radius of gyration of poly(dimethylsiloxane) at 300K (■), 400K (▲) and 500K (◆).

5.6 Discussion of Results

The limiting values of the characteristic ratio of poly(dimethylsilethene) at 300K, 400K and 500K are 1.98, 1.99 and 2.00 respectively. The limiting values of the mean-square radius of gyration of poly(dimethylsilethene) at 300K, 400K and 500K are 0.330, 0.332 and 0.334 respectively.

The characteristic ratios calculated for poly(dimethylsilethene) are extremely low compared to those of polymethylene, poly(dimethylsiloxane) and poly(dimethylsilmethylene). In these polymers, bond pair interdependence occurs throughout the chain as a whole. This tends to reduce the number tightly coiled conformations available to the polymers producing more extended chains and large characteristic ratios. By presuming neighbouring bond pairs are independent of each other, the conformational flexibility of the poly(dimethylsilethene) chain is dramatically increased resulting in more tightly coiled conformations and lower characteristic ratios.

Although no experimental data could be found concerning the characteristic ratio of poly(dimethylsilethene), calculations performed on other structures for which the assumption of independent bond pairs is valid, have yielded similar results. These include polyglycine² ($\langle r^2 \rangle_o/nl_v^2 = 1.79$), and poly(L-lactic acid)² ($\langle r^2 \rangle_o/nl_v^2 = 1.24$).

CHAPTER 6

CONFORMATIONAL ANALYSIS OF POLY(DIMETHYLSILETHANE)

AND

POLY(2,2,5,5-TETRAMETHYL-1-OXA-2,5-DISILAPENTANE)

USING THE HARD-SPHERE MODEL

6.1 Introduction

The conformational analyses of poly(dimethylsilmethylene) and poly(dimethylsilethene), described in preceding chapters, have been concerned with polymers with relatively simple molecular structures. The methods employed in the evaluation of the random coil statistics for these polymers have therefore been quite detailed and have involved complicated computational analysis. However, for polymers with more complicated and varied molecular structures, such detailed analyses become extremely difficult to perform. The more complicated and varied the structural backbone of a polymer, the greater the number of **U**-matrices are required to describe it. Since each individual **U**-matrix would have to be evaluated based on the variation of the particular intramolecular interactions involved, the task of evaluating the random coil statistics by this method is very complex and very time consuming.

By analysing the conformational properties of complicated polymers using the hard-sphere model, a less detailed analysis results in a simpler method of evaluating their random coil statistics. Although less detailed, the hard-sphere model is still very useful when determining the characteristic ratio and dipole moment ratio of a polymer and has been used by several workers in the past³².

In this chapter, the principles of the hard-sphere model will be briefly described. This will be followed by the evaluation of the random coil statistics of poly(dimethylsilane), and poly(2,2,5,5-tetramethyl-1-oxa-2,5-disilapentane) using the hard-sphere model.

6.2 The Hard-Sphere Model

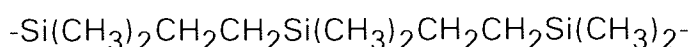
In the hard-sphere model, the individual atoms (or in some cases certain functional groups, *eg.* CH₃) forming a particular polymer structure are assumed to be made of hard spheres, whose radii are equivalent to the van der Waals radii of the atoms or groups involved. When the structure of the polymer in question is then examined, the proximity of particular atoms or groups involved in the determination of the **U**-matrices are compared with the sums of their respective van der Waals radii. For interactions in which the distance of separation between the atoms or groups in a particular conformation are equal to or larger than the sums of their van der Waals radii, a value of unity is assigned to the element of the **U**-matrix responsible for that conformation. In conformations where an interaction between two atoms

or groups has a distance of separation that is significantly less than the sum of their van der Waals radii, a value of zero is assigned to the element of the **U**-matrix responsible for that conformation. A value of zero may also be assigned if there is significant steric hinderence occurring from the interactions of branched groups, usually methyl groups, within a particular conformation. The three cases described above are illustrated in Figures (6-1(a)), (6-1(b)) and (6-1(c)) respectively.

By analysing the conformations of complicated structures in this way, a set of **U**-matrices may be constructed that have values equal to unity or zero. The resulting matrices may then be used to describe the conformational behaviour of the polymer in question. The characteristic ratio and dipole moment ratio can then be determined according to the methods described in Chapter 2.

6.3 Poly(dimethylsilethane)

The molecular structure of a section of poly(dimethylsilethane) is illustrated below



The skeletal backbone of this polymer chain consists of alternating silicon atoms separated by ethane type groups giving this polymer considerable conformational flexibility. In accordance with the rotational isomeric state approximation, each rotational skeletal bond in the chain is assigned to one of a small number of discrete rotational states, in this case three, situated at the

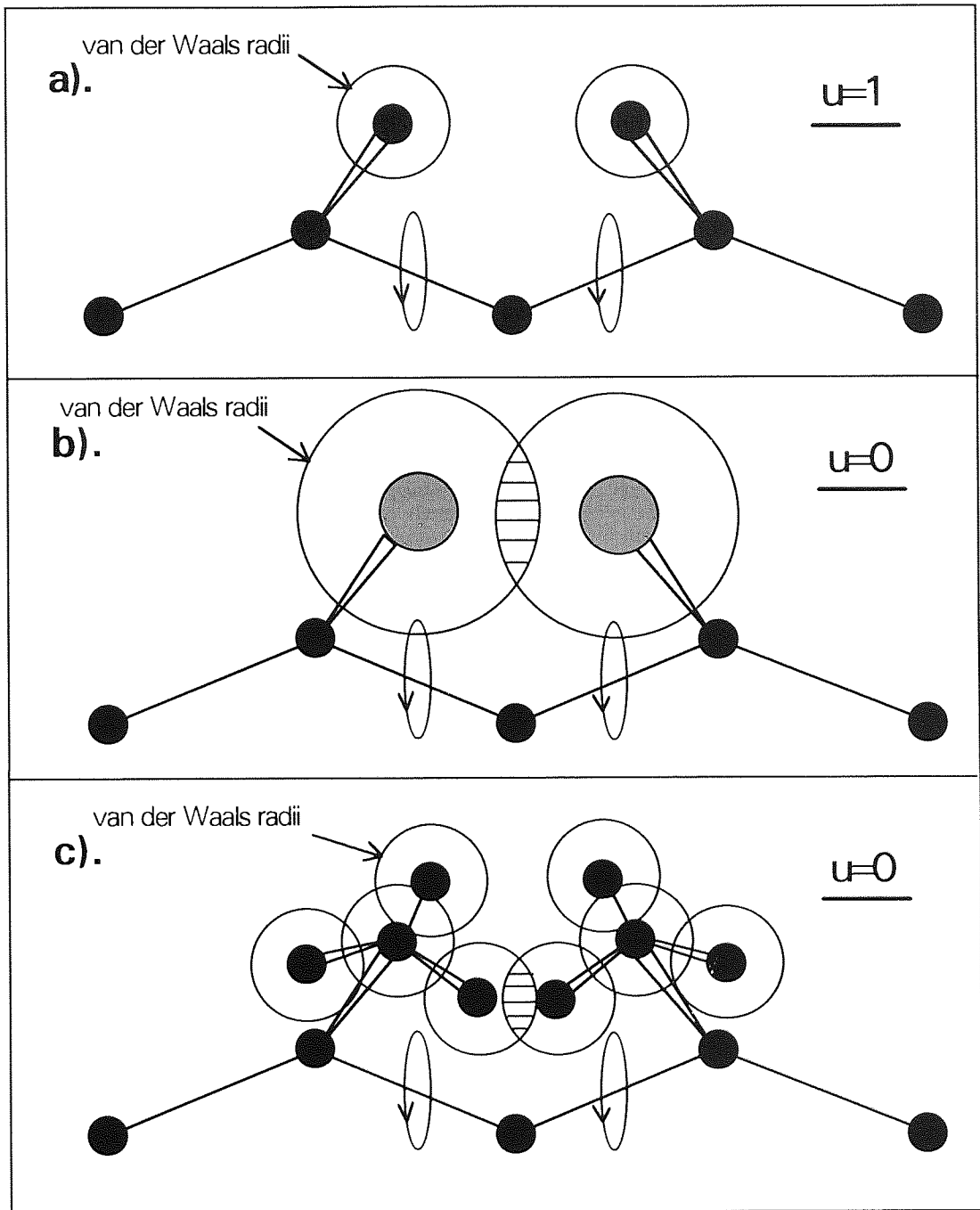


Figure (6-1). The diagrams above illustrate three conditions that may be utilized to determine the values of the U-matrix elements when applying the hard-sphere model. The shaded areas indicate steric hinderence.

rotational angles 0° (t), 120° (g^+) and 240° (g^-).

6.3.1. Molecular Geometry

Some of the structural parameters used in the conformational analysis of poly(dimethylsilethane) were derived from the quantitative study performed by Tribble and Allinger³⁶. The values of the bond lengths and bond angles associated with the skeletal carbon-carbon group were taken to be equivalent to the values found in n-alkanes⁵. The values used in the calculations are illustrated in Table (6-1).

	Bond Length (Å)	Bond Angle (θ°)
Si-C	1.89	-
CH ₂ -CH ₂	1.53	-
C-H	1.1	-
Si-CH ₂ -CH ₂	-	112
CH ₂ -CH ₂ -Si	-	112
CH ₂ -Si-CH ₂	-	110
Si-C-H	-	109

Table (6-1). Geometrical parameters for poly(dimethylsilethane).

6.3.2. Construction of the Statistical Weight Matrices

Since rotations about the Si-CH₂, CH₂-CH₂ and CH₂-Si skeletal bonds all give rise to different intramolecular interactions, the poly(dimethylsilethane) chain requires three **U**-matrices for its characterization. These three matrices, **U**₁, **U**₂ and **U**₃ are illustrated in Figure (6-2).

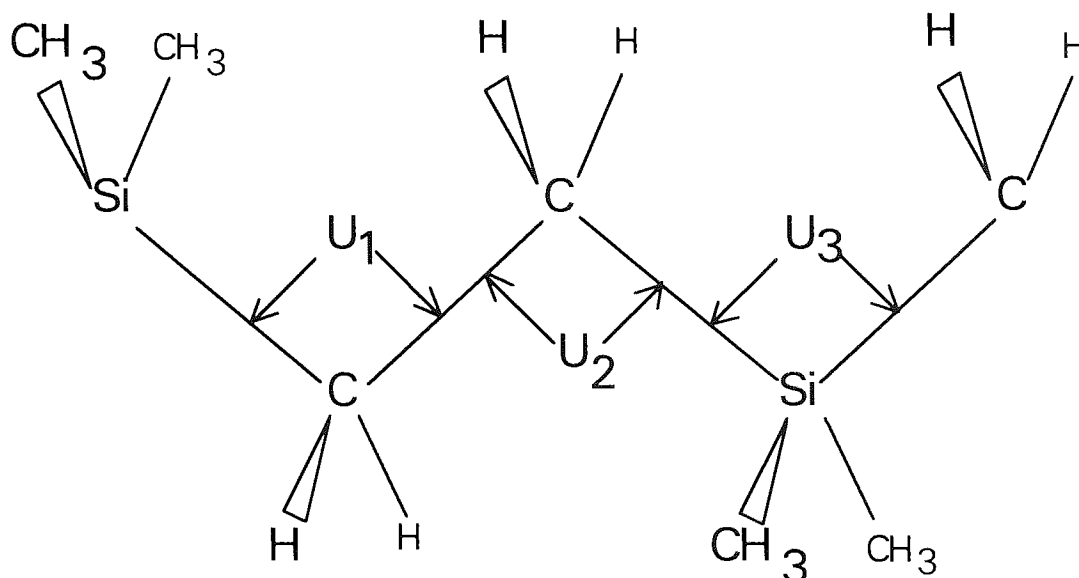
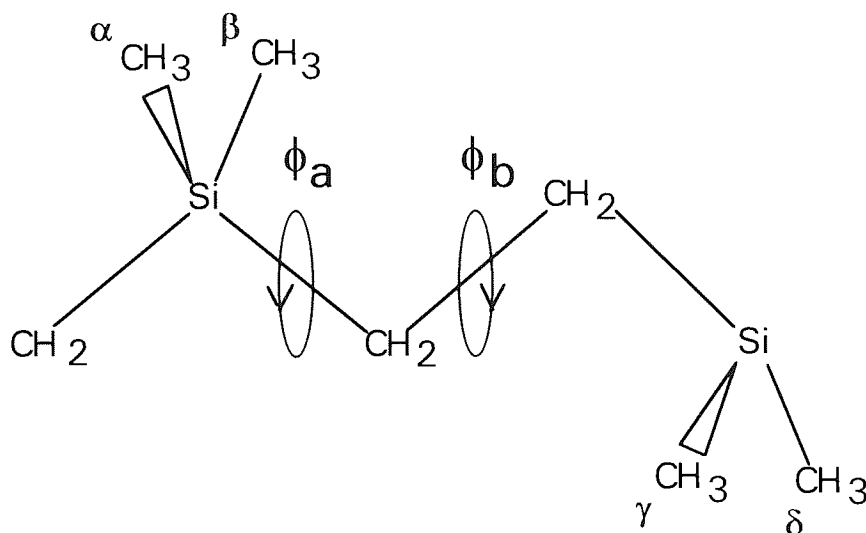


Figure (6-2). Assigning the **U**-matrices required to describe a section of the poly(dimethylsilethane) chain.

Since each rotatable skeletal bond is assumed to exist in one of three distinguishable rotational states (t , g^+ , g^-), each **U**-matrix will consist of nine matrix elements corresponding to the nine conformational states tt , tg^+ , tg^- , g^+t , g^+g^+ , g^+g^- , g^-t , g^-g^+ and g^-g^- . In order to evaluate the value of each matrix element for a particular **U**-matrix, it is necessary to examine the

intramolecular interactions occurring within each of the nine conformations that determine that matrix.

1. The Matrix U_1



In the all-trans conformation, there are no significant intramolecular interactions between any atoms or groups and so the matrix element $u_1(tt)$ was assigned a value of unity.

In the tg^+ conformation, severe intramolecular interactions occur between the two methyl groups CH_3^β and CH_3^δ . Their distance of separation in this conformation was calculated to be 1.78\AA compared with the value of 4.0\AA for the sum of their van der Waals radii³⁷. For this reason a value of zero was assigned to the matrix element $u_1(tg^+)$. Since the conformation tg^- is a mirror image of the conformation tg^+ , a similar interaction occurs in this

conformation between the two methyl groups CH_3^α and CH_3^γ , giving a value of zero for the matrix element $u_1(\text{tg}^-)$.

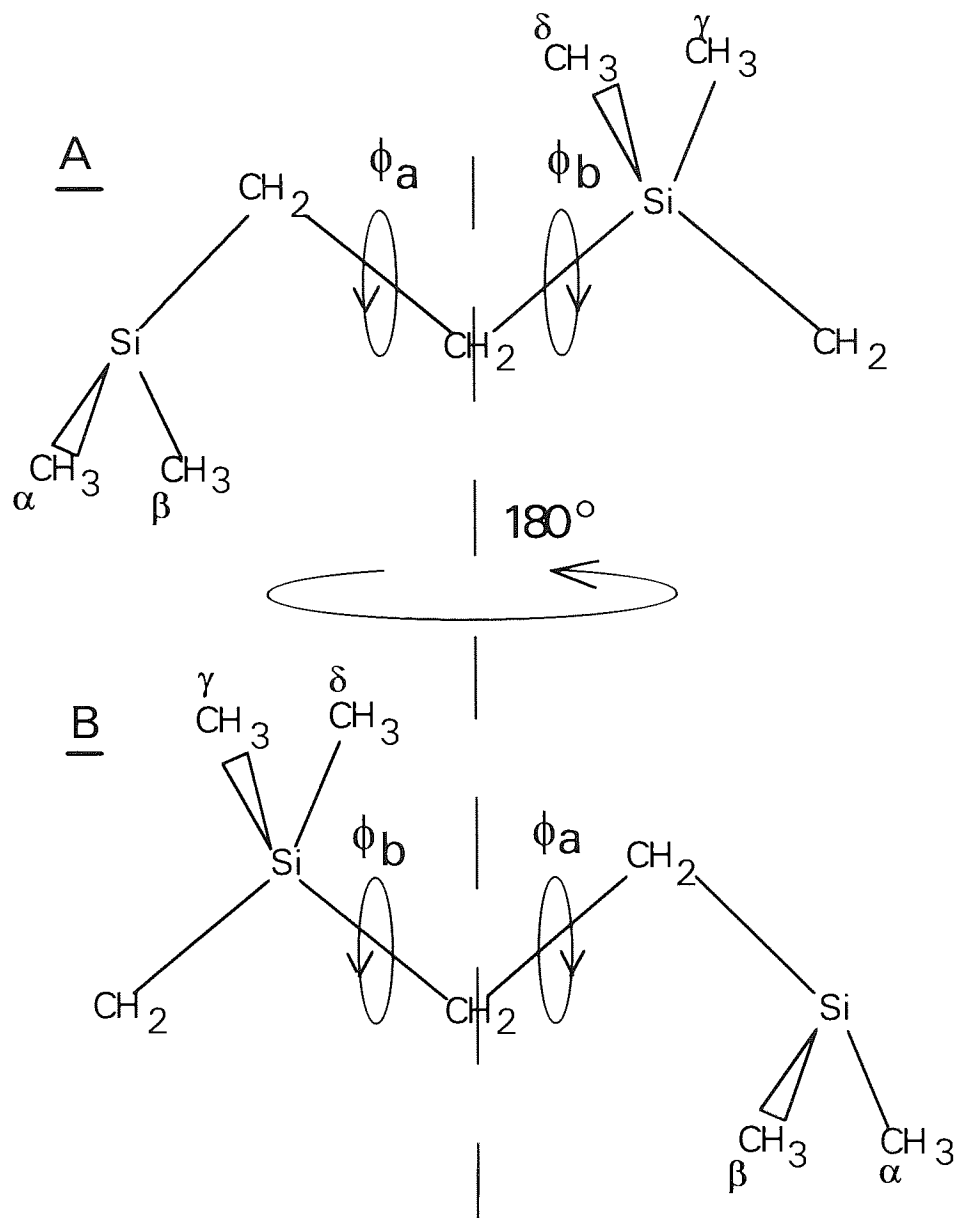
The two conformations g^+t and g^-t are very similar to the all-trans conformation in the sense that rotation about ϕ_a , with ϕ_b remaining equal to zero, simply results in an exchange of positions between the two methyl groups, CH_3^α and CH_3^β , and a CH_2 group. The matrix elements $u_1(g^+t)$ and $u_1(g^-t)$ may therefore be assigned a value of unity.

Due to the similarity between the all-trans, g^+t and g^-t conformations, it will be apparent that in the remaining four conformations, g^+g^+ , g^+g^- , g^-g^+ and g^-g^- , there are severe interactions occurring between the groups, CH_3^α and CH_3^δ , CH_2 and CH_3^γ , CH_2 and CH_3^δ , and CH_3^β and CH_3^γ respectively. In all of these interactions, the distance of separation between each respective group was again calculated to be 1.78A, compared with a value of 4.0A for the sum of the van der Waals radii. Therefore the matrix elements $u_1(g^+g^+)$, $u_1(g^+g^-)$, $u_1(g^-g^+)$ and $u_1(g^-g^-)$ are assigned a value of zero.

The matrix \mathbf{U}_1 may now be represented by the equation

$$\mathbf{U}_1 = \begin{bmatrix} 1 & 0 & 0 \\ 1 & 0 & 0 \\ 1 & 0 & 0 \end{bmatrix} \quad (6-1)$$

2. The Matrix \mathbf{U}_2



After a close inspection of the structure A, defining \mathbf{U}_2 , it became apparent that this structure was related to the structure B, defining \mathbf{U}_1 , via a rotation of 180° about a central axis of symmetry. By invoking this symmetrical relationship between the two structures, the matrix \mathbf{U}_2 may be

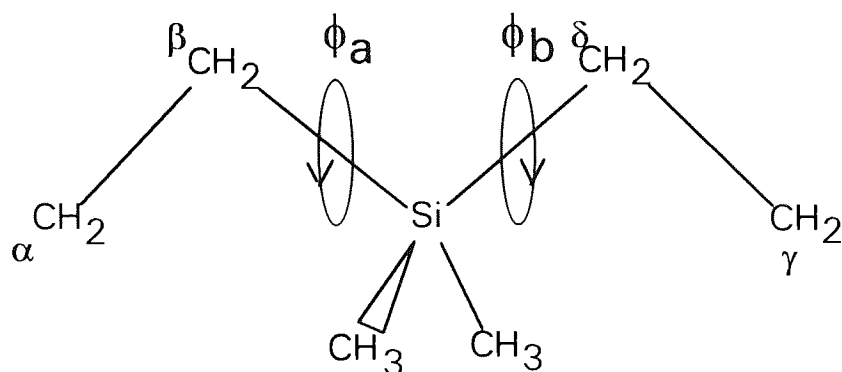
defined as the transpose of the matrix \mathbf{U}_1 , since the net result of this operation is to interchange the rotational angles ϕ_a and ϕ_b . Hence,

$$\mathbf{U}_2(\phi_a, \phi_b) = \mathbf{U}_1(\phi_b, \phi_a) = \mathbf{U}_1^T(\phi_a, \phi_b) \quad (6-2)$$

Since the matrix \mathbf{U}_1 is known, the matrix \mathbf{U}_2 is simply

$$\mathbf{U}_2 = \mathbf{U}_1^T = \begin{bmatrix} 1 & 1 & 1 \\ 0 & 0 & 0 \\ 0 & 0 & 0 \end{bmatrix} \quad (6-3)$$

3. The Matrix \mathbf{U}_3



For the all-trans conformation, the matrix element $u_3(tt)$ was assigned a value of unity, since no significant intramolecular interactions occur in this conformation.

The matrix elements $u_3(tg^+)$, $u_3(tg^-)$, $u_3(g^+t)$ and $u_3(g^-t)$ representing the conformations tg^+ , tg^- , g^+t and g^-t were also assigned values of unity since no significant interactions occur in these conformations.

For the g^+g^+ , g^-g^- , g^+g^- and g^-g^+ conformations any possible intramolecular interactions would occur between the two terminal groups CH_2^α and CH_2^δ . In the g^+g^+ and g^-g^- conformations the distance between these two groups was calculated to be 4.05\AA and so the matrix elements $u_3(g^+g^+)$ and $u_3(g^-g^-)$ were given values of unity. However, the distance between these two groups in the g^+g^- and g^-g^+ conformations was calculated to be 3.22\AA compared with the value of 4.0\AA for the sum of their van der Waals radii. The values of the matrix elements $u_3(g^-g^+)$ and $u_3(g^+g^-)$ were therefore assigned values of zero.

The matrix \mathbf{U}_3 may now be represented by the equation

$$\mathbf{U}_3 = \begin{bmatrix} 1 & 1 & 1 \\ 1 & 1 & 0 \\ 1 & 0 & 1 \end{bmatrix} \quad (6-4)$$

6.3.3. Characteristic Ratio

For an unperturbed poly(dimethylsilethane) chain starting and ending with silicon atoms, the characteristic ratio was calculated according to the equation

$$\langle r^2 \rangle_0/nl^2 = 2(Znl^2)^{-1} \mathbf{1} \cdot \mathbf{G}_T \cdot (\mathbf{G}_1 \cdot \mathbf{G}_2 \cdot \mathbf{G}_3) \cdot \mathbf{G}_1 \cdot \mathbf{G}_2 \cdot \mathbf{1} \quad (6-5)$$

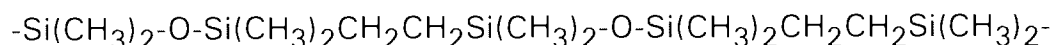
Using the geometrical parameters tabulated in Table (6-1) and the three \mathbf{U} -matrices, \mathbf{U}_1 , \mathbf{U}_2 and \mathbf{U}_3 , the characteristic ratio $\langle r^2 \rangle_0/nl^2$ of poly(dimethylsilethane), in the limit $n \rightarrow$ infinity, was calculated to be 4.63 at all temperatures.

The values of the characteristic ratio calculated for poly(dimethylsilmethylene) were slightly higher than 4.63, indicating increased flexibility in the poly(dimethylsilethane) chain. The reason for the increased flexibility can be seen on examination of the two structures since, in effect, the skeletal CH₂ group is being replaced with the more flexible CH₂-CH₂ group.

Due to the lack of experimental dielectric data concerning this polymer, the dipole moment ratio could not be computed. Its existence, however, cannot be ruled out.

6.4 Poly(2,2,5,5-tetramethyl-1-oxa-2,5-disilapentane)

The molecular structure of a section of poly(2,2,5,5-tetramethyl-1-oxa-2,5-disilapentane) is illustrated below



As in the case of poly(dimethylsilethane), each rotational skeletal bond in this chain was allowed to occupy one of three discrete rotational states situated at 0° (t), 120°(g⁺) and 240°(g⁻).

6.4.1. Molecular Geometry

Some of the structural parameters used in the conformational calculations for poly(dimethylsilethane) were derived from the quantitative study performed by Tribble and Allinger³⁶. The values of the bond lengths and bond angles associated with the skeletal carbon-carbon group were taken

to be equivalent to the values found in n-alkanes⁵, while the bond lengths and bond angles associated with the Si-O-Si link were taken from structural studies performed on poly(dimethylsiloxane)⁸. The values used in the calculations are illustrated in Table (6-2).

	Bond Length (Å)	Bond Angle (θ°)
Si-C	1.89	-
Si-O	1.64	
CH ₂ -CH ₂	1.53	-
C-H	1.1	-
Si-CH ₂ -CH ₂	-	112
CH ₂ -CH ₂ -Si	-	112
CH ₂ -Si-CH ₂	-	110
Si-O-Si	-	143
Si-C-H	-	109

Table (6-2). Geometrical parameters used to describe the structure of poly(2,2,5,5-tetramethyl-1-oxa-2,5-disilapentane).

6.4.2. Construction of the Statistical Weight Matrices

In order to fully characterise poly(2,2,5,5-tetramethyl-1-oxa-2,5-disilapentane), we need to assign five **U**-matrices to account for all of the intramolecular interactions associated with the chain. The allocation of each **U**-matrix is illustrated in Figure (6-3).

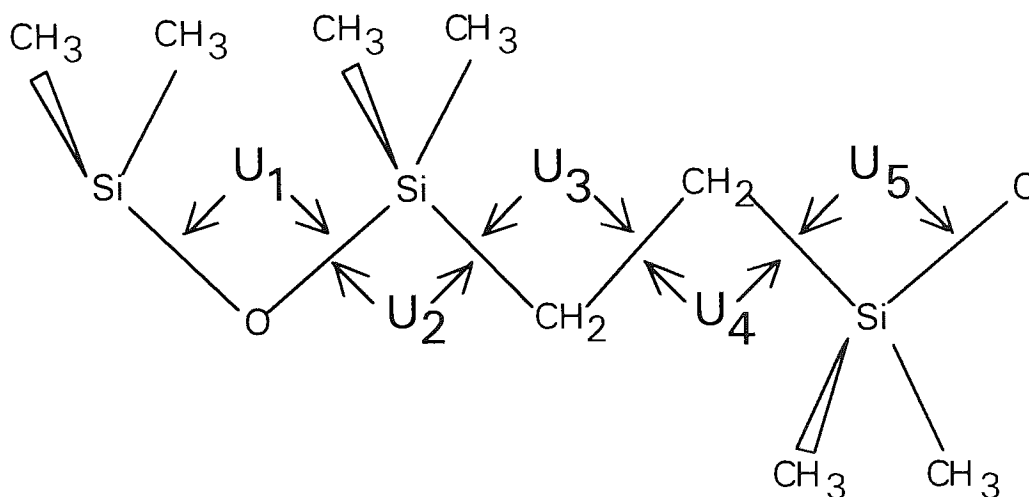
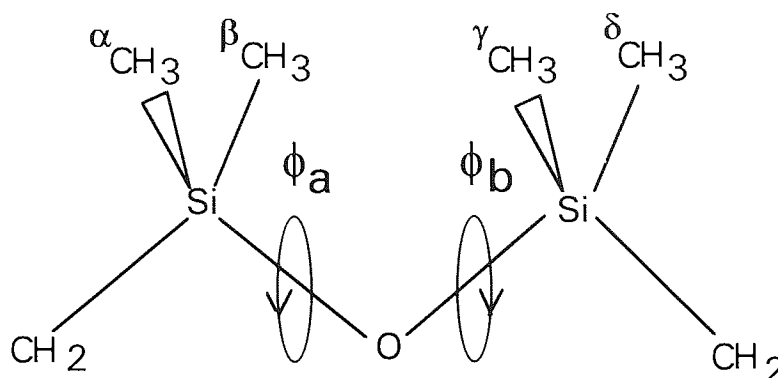


Figure (6-3). Assigning the **U**-matrices required to describe poly(2,2,5,5-tetramethyl-1-oxa-2,5-disilapentane).

Five matrices are required for this polymer since rotations about Si-O-Si, O-Si-CH₂, Si-CH₂-CH₂, CH₂-CH₂-Si and CH₂-Si-O all produce a different combination of intramolecular interactions. Since each skeletal bond is assumed to exist in one of three discrete rotational states (0°, 120° and 240°), each of the five **U**-matrices will consist of nine matrix elements.

1. The matrix \mathbf{U}_1



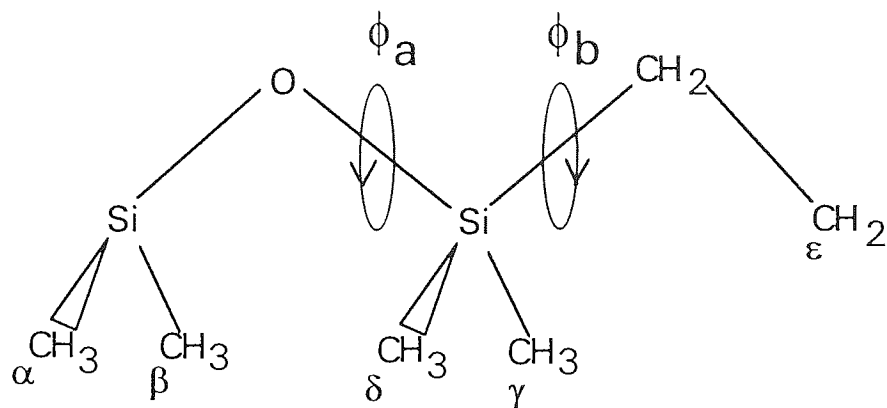
For the all-trans conformation, the distance between the methyl groups CH_3^α and CH_3^δ , and CH_3^α and CH_3^γ , were calculated to be 4.9\AA and 3.95\AA respectively. A similar situation occurs between the methyl groups CH_3^β and CH_3^γ , and CH_3^β and CH_3^δ . Since the sum of the van der Waals radii³⁷ for two methyl groups was calculated to be 4.0\AA , the matrix element $u_1(tt)$ was assigned a value of unity.

Since rotations about ϕ_a and ϕ_b only serve to interchange the positions of CH_3 and CH_2 groups, both of which have the same van der Waals radii (2.0\AA), values of unity were assigned to all the other matrix elements of \mathbf{U}_1 .

The matrix \mathbf{U}_1 is therefore given by the equation

$$\mathbf{U}_1 = \begin{bmatrix} 1 & 1 & 1 \\ 1 & 1 & 1 \\ 1 & 1 & 1 \end{bmatrix} \quad (6-6)$$

2. The matrix U_2



In the all-trans conformation, the distance between the methyl groups CH_3^α , CH_3^β , CH_3^δ and CH_3^γ are the same as those in the structure defining U_1 , hence the matrix element $u_2(\text{tt})$ was assigned a value of unity.

It may be seen from the above diagram that rotations about ϕ_a with $\phi_b = 0$, and rotations about ϕ_b with $\phi_a = 0$, do not produce any significant intramolecular interactions. In fact, the former rotations tend to relieve any steric hinderence present. The matrix elements $u_2(\text{tg}^+)$, $u_2(\text{tg}^-)$, $u_2(\text{g}^+\text{t})$ and $u_2(\text{g}^-\text{t})$ were therefore assigned values of unity.

For the g^+g^+ and g^-g^- conformations, the closest distance of separation occurs between the groups CH_3^α and CH_2^ϵ , and CH_3^β and CH_2^ϵ respectively. The distance between these two pairs of groups was calculated to be 3.95Å. Since this value is nearly identical with the sum of their respective van der

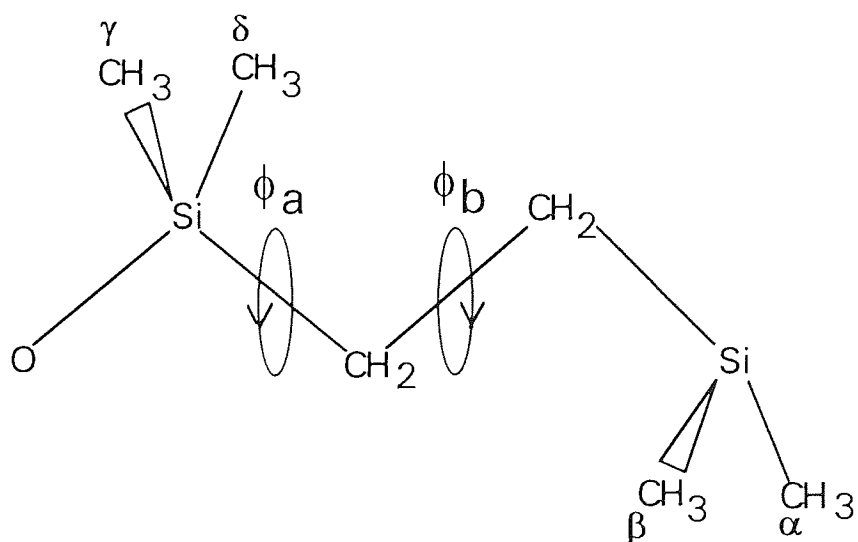
Waals radii, a value of unity was assigned to the matrix elements $u_2(g^+g^+)$ and $u_2(g^-g^-)$.

The only severe intramolecular interactions that are present in this structure occur in the g^+g^- and g^-g^+ conformations. In these conformations, the distance between the groups CH_3^α and CH_2^ϵ , and CH_3^β and CH_2^ϵ were calculated to be 3.11\AA respectively. Since the sum of their van der Waals radii in both cases was calculated to be 4.0\AA , values of zero were assigned to the matrix elements $u_2(g^+g^-)$ and $u_2(g^-g^+)$ respectively.

The matrix \mathbf{U}_2 may now be represented by the equation

$$\mathbf{U}_2 = \begin{bmatrix} 1 & 1 & 1 \\ 1 & 1 & 0 \\ 1 & 0 & 1 \end{bmatrix} \quad (6-7)$$

3. The matrix \mathbf{U}_3



For the all-trans conformation no significant interactions occur. Hence, the matrix element $u_3(tt)$ was assigned a value of unity.

However, in the tg^+ and tg^- conformations, severe intramolecular interactions occur between the methyl groups CH_3^δ and CH_3^α , and CH_3^γ and CH_3^β respectively. The distance between these two pairs of groups was calculated to be 1.78\AA , compared with a value of 4.0\AA for the sum of their van der Waals radii. Values of zero were therefore assigned to the matrix elements $u_3(tg^+)$ and $u_3(tg^-)$ respectively.

Since rotations about ϕ_a , with $\phi_b=0$, serves only to interchange the positions of the three groups O, CH_3^δ and CH_3^γ , the matrix elements $u_3(g^+t)$ and $u_3(g^-t)$ were assigned values of unity.

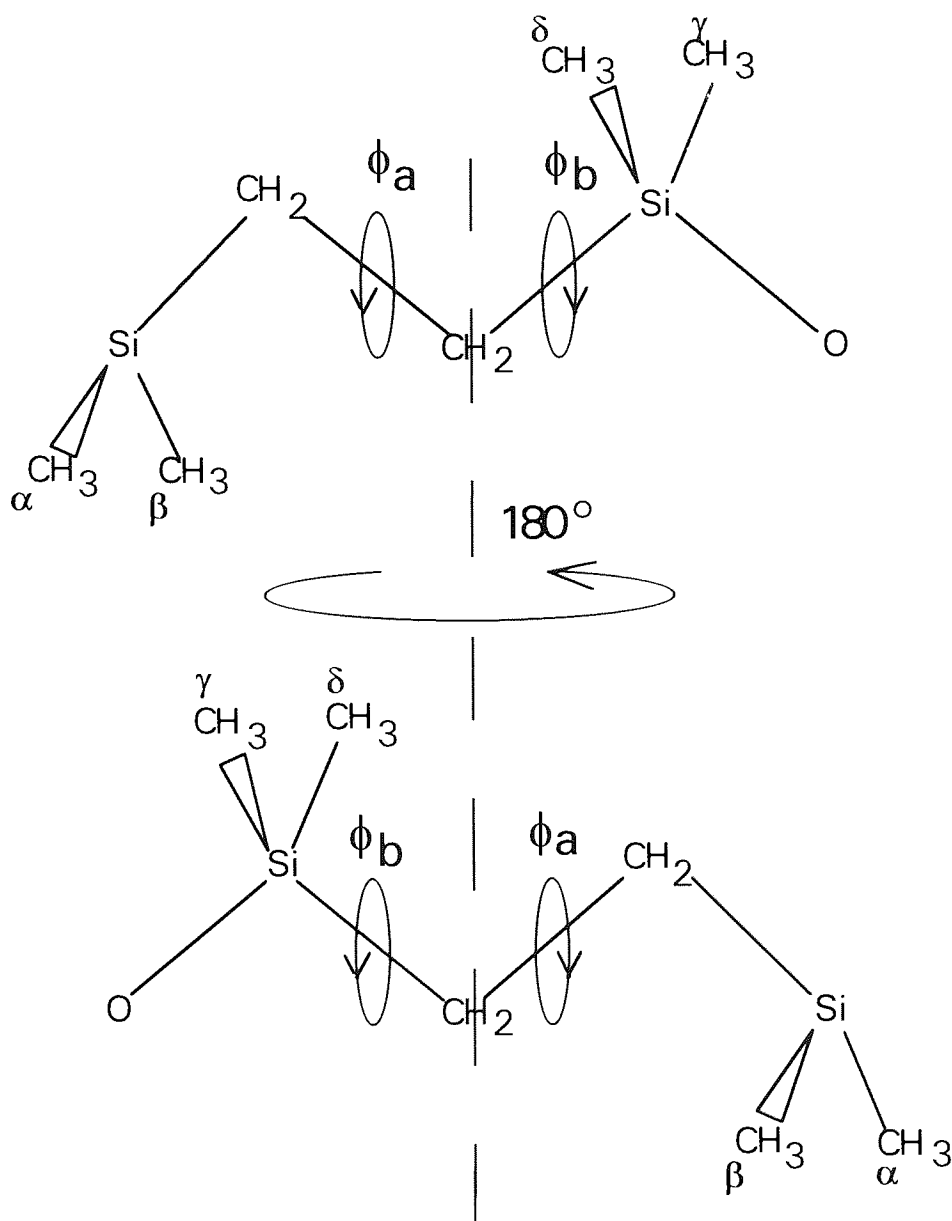
In the g^+g^+ and g^-g^- conformations, the distance between the groups CH_3^γ and CH_3^α , and CH_3^δ and CH_3^β , were both calculated to be 1.78\AA , resulting in values of zero being assigned to the matrix elements $u_3(g^+g^+)$ and $u_3(g^-g^-)$.

Similar interactions occur in the g^+g^- and g^-g^+ conformations between the groups O and CH_3^α , and O and CH_3^β respectively. The distance between these two pairs of groups was calculated to be 1.88\AA , compared to a value of 3.4\AA for the sum of their van der Waals radii. For this reason, the matrix elements $u_3(g^+g^-)$ and $u_3(g^-g^+)$ were also assigned values of zero.

The matrix \mathbf{U}_3 is therefore given by the equation

$$\mathbf{U}_3 = \begin{bmatrix} 1 & 0 & 0 \\ 1 & 0 & 0 \\ 1 & 0 & 0 \end{bmatrix} \quad (6-8)$$

4. The matrix \mathbf{U}_4



It can be seen from inspection that the matrix \mathbf{U}_4 is related to the matrix \mathbf{U}_3 in the same way that the matrix \mathbf{U}_2 was related to \mathbf{U}_1 in the analysis of poly(dimethylsilane). That is the matrix \mathbf{U}_4 is equal to the transpose of the matrix \mathbf{U}_3 due to the fact that the two structures that define the matrices \mathbf{U}_4 and \mathbf{U}_3 are related by a central axis of symmetry. The matrix \mathbf{U}_4 is therefore equal to \mathbf{U}_3^T . Hence,

$$\mathbf{U}_4(\phi_a, \phi_b) = \mathbf{U}_3(\phi_b, \phi_a) = \mathbf{U}_3^T(\phi_a, \phi_b) \quad (6-9)$$

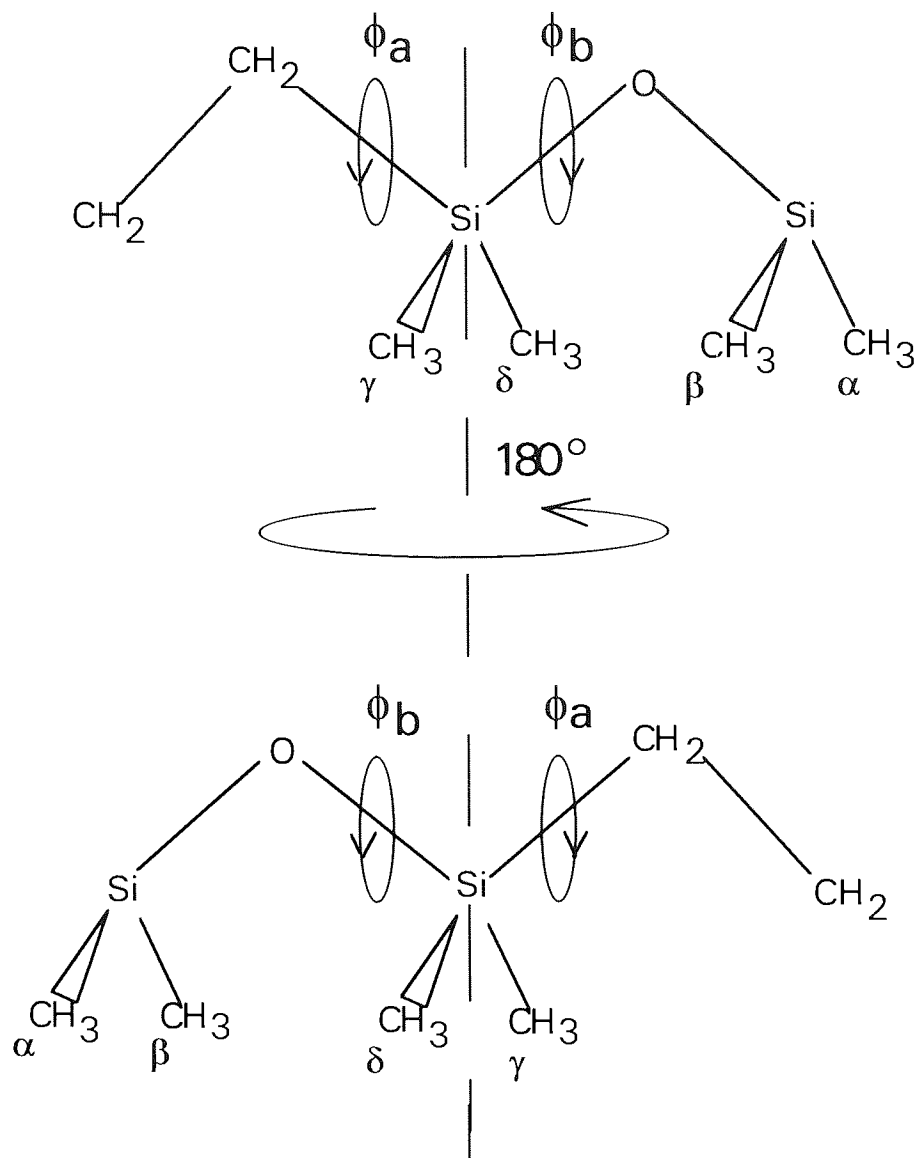
Since the matrix \mathbf{U}_3 is known, the matrix \mathbf{U}_4 is simply

$$\mathbf{U}_4 = \mathbf{U}_3^T = \begin{bmatrix} 1 & 1 & 1 \\ 0 & 0 & 0 \\ 0 & 0 & 0 \end{bmatrix} \quad (6-10)$$

5. The Matrix \mathbf{U}_5

Again, from the diagram overleaf it may be seen that the structure defining \mathbf{U}_5 is related to the structure defining the matrix \mathbf{U}_2 by a central axis of symmetry. Hence, the matrix \mathbf{U}_5 is equal to the transpose of the matrix \mathbf{U}_2 . The matrix \mathbf{U}_5 is therefore given by

$$\mathbf{U}_5 = \mathbf{U}_2^T = \begin{bmatrix} 1 & 1 & 1 \\ 1 & 1 & 0 \\ 1 & 0 & 1 \end{bmatrix} \quad (6-11)$$



6.4.3. Characteristic Ratio

For an unperturbed poly(2,2,5,5-tetramethyl-1-oxa-2,5-disilapentane) chain starting and ending with silicon atoms, the characteristic ratio was calculated according to the equation

$$\langle r^2 \rangle_0 / nl^2 = 2(Znl^2)^{-1} \vartheta * G_T \cdot (G_1 \cdot G_2 \cdot G_3 \cdot G_4 \cdot G_5) \cdot {}^x G_1 \cdot G_2 \cdot G_3 \cdot G_4 \vartheta \quad (6-12)$$

Using the geometrical parameters tabulated in Table (6-2) and the five **U**-matrices, **U**₁, **U**₂, **U**₃, **U**₄ and **U**₅, the characteristic ratio $\langle r^2 \rangle_0/nl^2$ of poly(2,2,5,5-tetramethyl-1-oxa-2,5-disilapentane), in the limit $n \rightarrow$ infinity, was calculated to be 4.79 at all temperatures.

6.4.4. Dipole Moment Ratio

Experimental analyses performed on poly(dimethylsiloxane)³⁸ and other organo-silicon compounds^{16,17} containing a siloxane bond, has revealed that the Si-O bond has a dipole moment of 0.6D. Based on this information, the dipole moment ratio for an unperturbed poly(2,2,5,5-tetramethyl-1-oxa-2,5-disilapentane) chain, starting and ending with silicon atoms, was calculated according to the equation

$$\langle \mu^2 \rangle_0/nm^2 = 2(Znm^2)^{-1} \mathfrak{G} * \mathbf{G}_T \cdot (\mathbf{G}_1 \cdot \mathbf{G}_2 \cdot \mathbf{G}_3 \cdot \mathbf{G}_4 \cdot \mathbf{G}_5) \cdot \mathbf{G}_1 \cdot \mathbf{G}_2 \cdot \mathbf{G}_3 \cdot \mathbf{G}_4 \mathfrak{G} \quad (6-13)$$

Again, the geometrical parameters tabulated in Table (6-2) and the five **U**-matrices **U**₁, **U**₂, **U**₃, **U**₄ and **U**₅, were used in the calculation. The dipole moment ratio was calculated, in the limit $n \rightarrow$ infinity, to be 0.187 at all temperatures.

6.5 Discussion of Results

If the characteristic ratios calculated for poly(dimethylsilmethylene) and poly(dimethylsilethane) are compared, it is seen that the latter value is slightly lower than the former value. As mentioned earlier, this may be due to the increased flexibility of the poly(dimethylsilethane) chain. However, another

factor that may explain the difference in the values is the steric hindrance occurring between the branched methyl groups within each polymer. The steric hindrance occurring between the branched methyl groups in poly(dimethylsilolethane) may be reduced, with respect to that in poly(dimethylsilmethylene), by replacing a $-\text{CH}_2-$ group in the skeletal backbone with a $-\text{CH}_2\text{-CH}_2-$ group.

The same trend is observed when comparing the characteristic ratios and dipole moment ratios of poly(2,2,5,5-tetramethyl-1-oxa-2,5-disilapentane) with those of the closely related structure, poly(dimethylsiloxane)^{8,39}. The characteristic ratio and dipole moment ratio of poly(2,2,5,5-tetramethyl-1-oxa-2,5-disilapentane) are slightly less than the corresponding values of poly(dimethylsiloxane). Again, the introduction of alternate $-\text{CH}_2\text{-CH}_2-$ groups into the skeletal backbone of poly(dimethylsiloxane) to produce poly(2,2,5,5-tetramethyl-1-oxa-2,5-disilapentane), may reduce the overall steric hindrance within the polymer thereby, reducing the calculated characteristic ratio and dipole moment ratio.

CHAPTER 7

MATERIALS

7.1 Introduction

The materials used in this study were a combination of samples of poly(2,2,5,5-tetramethyl-1-oxa-2,5-disilapentane) donated by Dow Corning and one compound, poly(dimethylsilmethylene), synthesized by the author. In this chapter the synthesis and characterisation of poly(dimethylsilmethylene) will be described along with a g.p.c. analysis of the donated polymers.

7.2 Poly(2,2,5,5-tetramethyl-1-oxa-2,5-disilapentane)

Two samples of poly(2,2,5,5-tetramethyl-1-oxa-2,5-disilapentane) were supplied by Dr. D. Thomas of Dow Corning, Barry, South Wales. These experimental samples were labelled sample 10423-1 and sample 10423-9 respectively.

7.2.1. G.P.C. Analysis of the Samples 10423-1 and 10423-9

The distribution of molecular weights in these samples was ascertained using gel permeation chromatography which was performed by RAPRA Technology Ltd. The g.p.c. chromatographs for samples 10423-1 and 10423-9 are illustrated in Figures (7-1) and (7-2) respectively. The results are expressed as the "polystyrene equivalent" molecular masses.

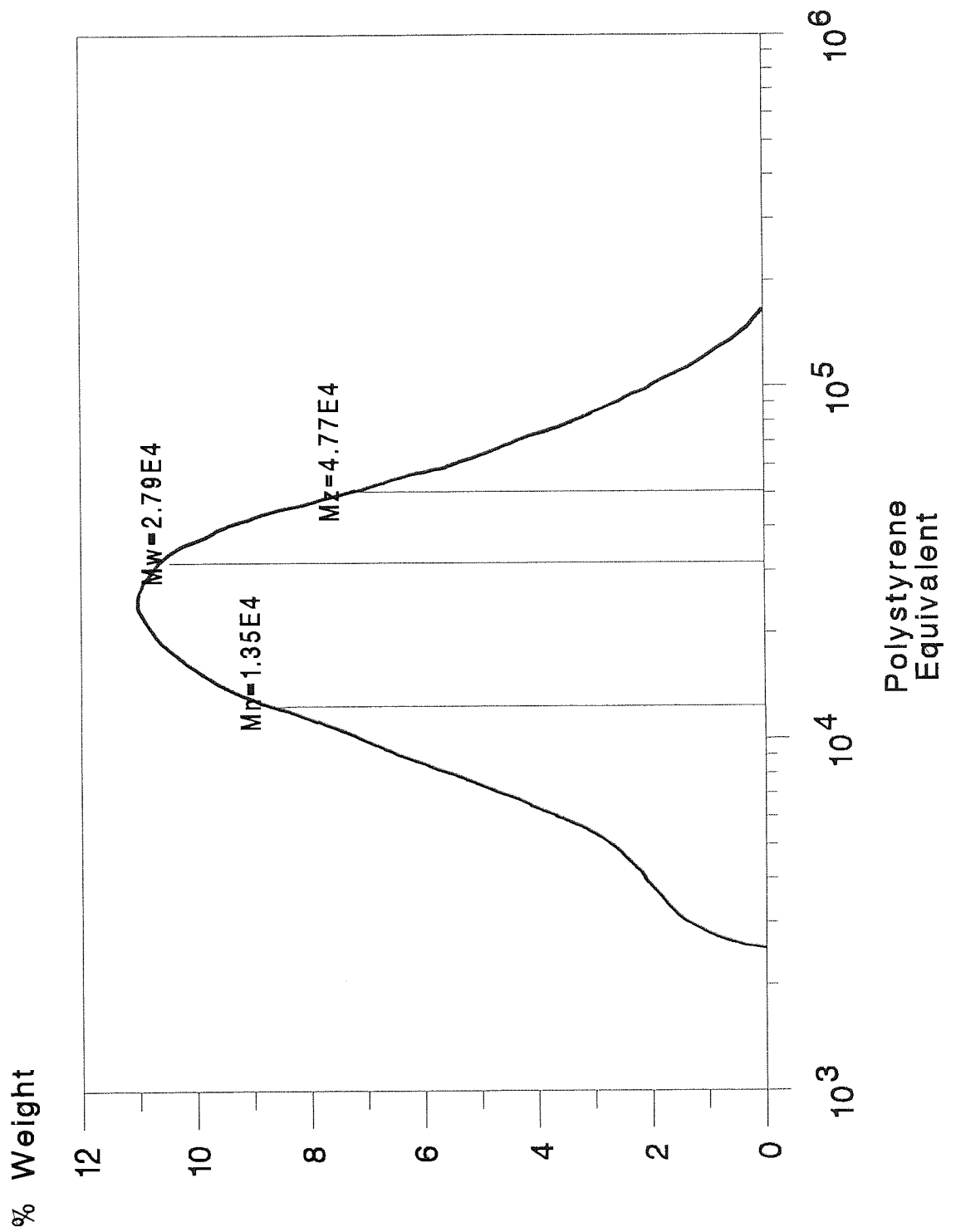


Figure (7-1). G.P.C. chromatogram of sample 10423-1.

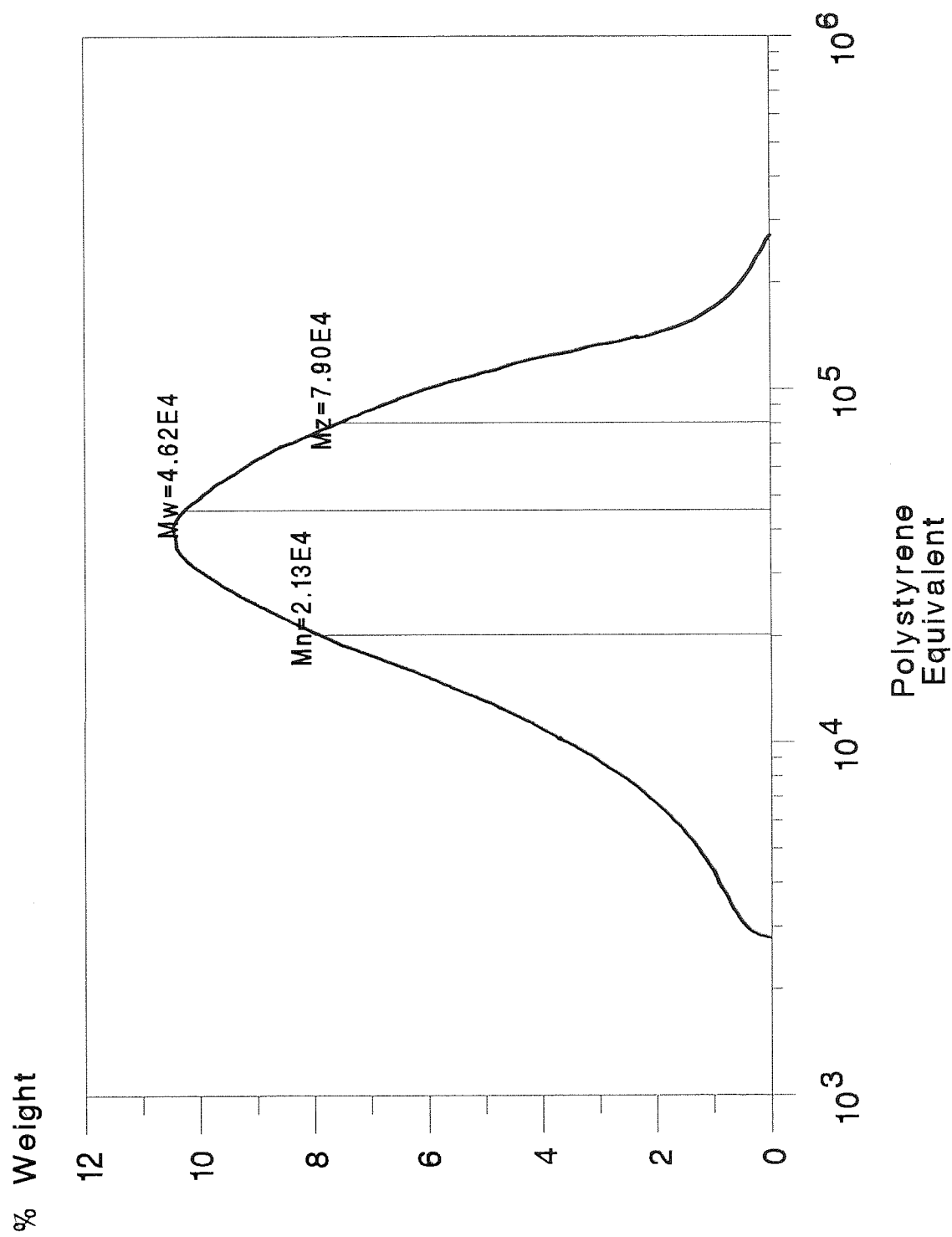


Figure (7-2). G.P.C. chromatograph of sample 10423-9.

The g.p.c. results show that each polymer sample contains a high molecular weight component along with a relatively small amount of low molecular weight material. The average molecular weights, M_w , of the main components in the samples 10423-1 and 10423-9 are approximately 28000 and 46000 respectively.

7.3 A Synthetic Route to Poly(dimethylsilmethylene)

The ring opening polymerisation of 1,1,3,3-tetramethyl-1,3-disilacyclobutane, to produce poly(dimethylsilmethylene) has been investigated by several groups of workers including Kriner²⁰, Weyenberg and Nelson⁴⁰, and Bamford, Lovie and Watt⁴¹. The unusual reactivity of 1,3-disilacyclobutanes is attributed to the severe ring strain present in these rings. The compound 1,1,3,3-tetramethyl-1,3-disilacyclobutane¹⁹ polymerises on heating above 200°C although generally the polymers so obtained are of relatively low molar mass. A popular polymerisation technique involves the use of group VIII metal compounds such as chloroplatinic acid ($H_2PtCl_6 \cdot 6H_2O$).

The compound 1,1,3,3-tetramethyl-1,3-disilacyclobutane is not available commercially and had to be synthesized by an inefficient "inverse" Grignard process²⁰. The synthetic route to poly(dimethylsilmethylene) is illustrated in Figure (7-3).

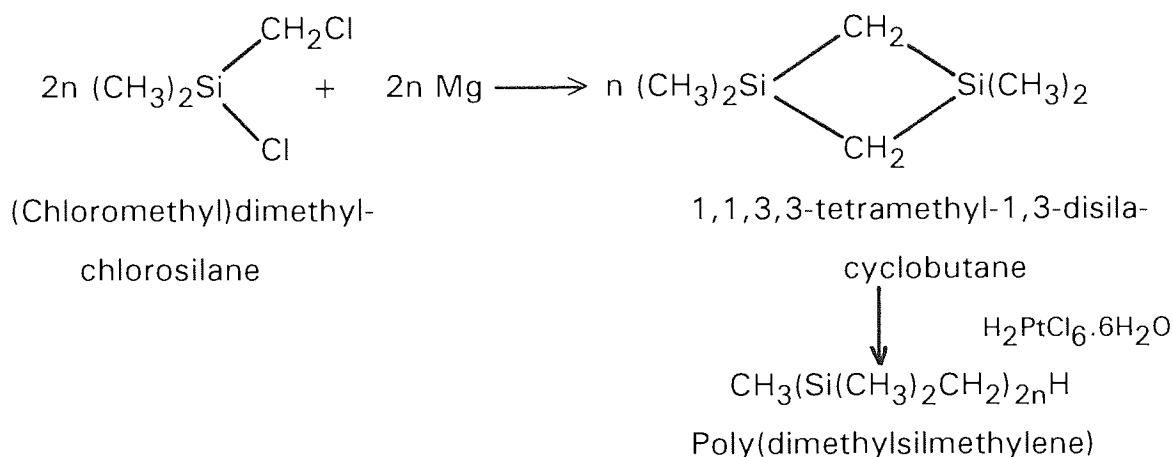


Figure (7-3). Synthetic route to poly(dimethylsilmethylene).

7.4 Preparation of 1,1,3,3-tetramethyl-1,3-disilacyclobutane

(Chloromethyl)dimethylchlorosilane (143g, 1 mol; Dow Corning) in tetrahydrofuran (400 ml) was contained in a 1 litre, three-necked round bottomed flask. Magnesium (26g, 1 mol+excess) was added portion-wise over a two and a half hour period keeping the reaction temperature between 34°C and 36°C by cooling with water. During the addition the reaction mixture was vigorously stirred. The reaction was completed by stirring continuously for two hours with gentle heating to keep the reaction mixture at a temperature of 40° C. When the reaction mixture was cool, three 100ml portions of distilled water were added at 15 minute intervals. The organic layer was separated and washed with distilled water and the monomer was isolated by fractional distillation under reduced pressure (bpt. 59°C, 99 mm/Hg; yield 20%).

7.4.1. Infra-red Spectroscopy

An Infra-red spectrum for the product is shown in Figure (7-4). The spectrum was obtained from the pure product using a Perkin-Elmer 599B infra-red spectrophotometer.

Characteristic absorptions (ν cm^{-1});

2960s, 2900s - C-H stretching; 1250s - symmetrical stretching; 940s- cyclic methylene wagging; 860s, 820s - silicon methyl wagging.

7.4.2. Nuclear Magnetic Spectroscopy

A nuclear magnetic resonance spectrum for the product is shown in Figure (7-5). The spectrum was obtained from the pure product using a Varian EM-300X n.m.r. spectrophotometer operating at 30 MHz.

Characteristic peaks (τ);

10.0 - 12H, strong; 10.3 - 4H, strong;

7.5 Polymerisation of 1,1,3,3-tetramethyl-1,3-disilacyclobutane

The cyclic monomer (6g) with a solution of chloroplatinic acid (0.3% by weight), in propan-2-ol was contained in a sealed dry flask and placed in a water bath at a temperature of 30°C. The pressure in the flask was reduced to approximately half the atmospheric pressure. Subsequent analysis showed that within 30 minutes the monomer had polymerised to form low molecular weight poly(dimethylsilmethylene).

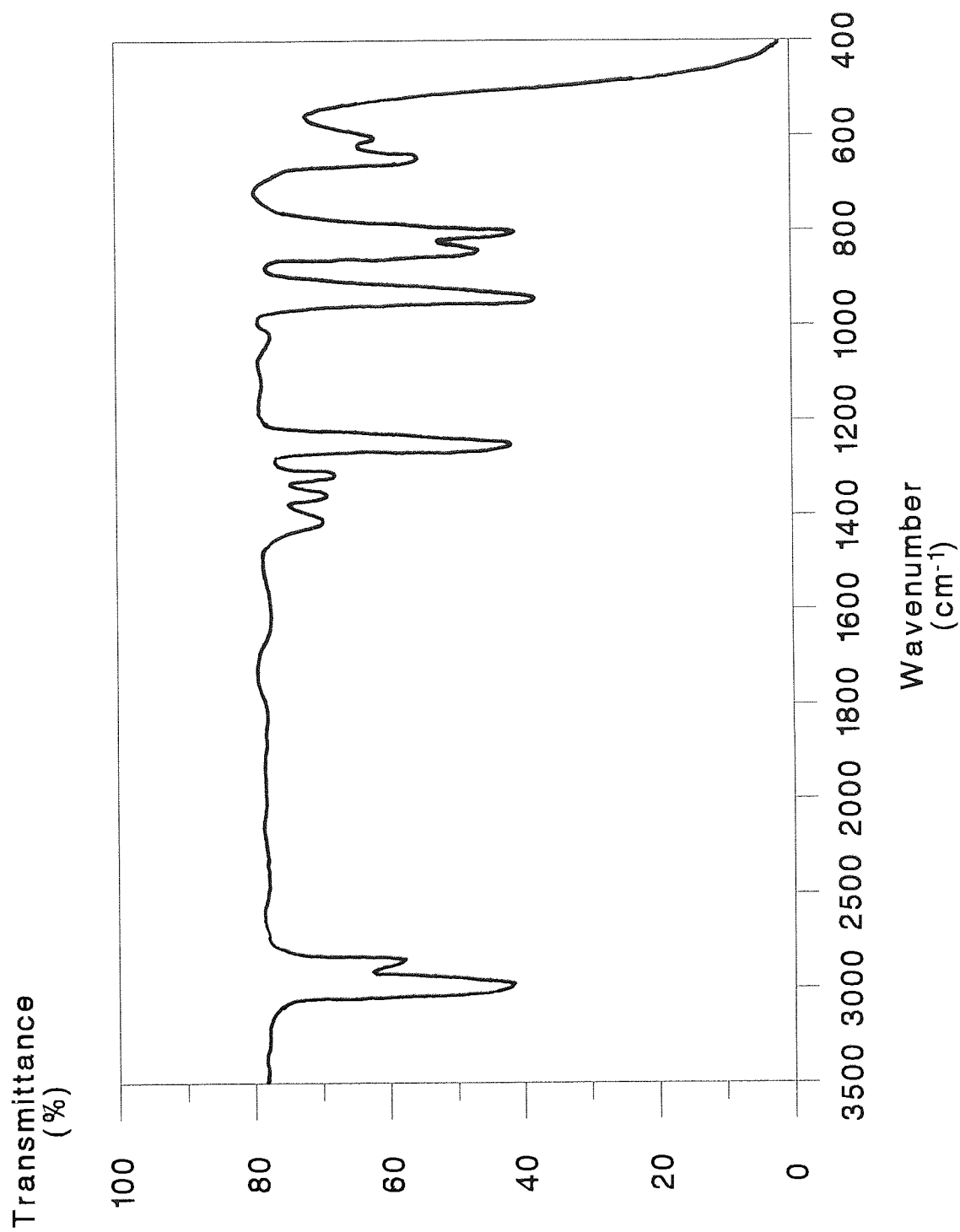


Figure (7-4). Infra-red spectrum of 1,1,3,3-tetramethyl-1,3-disilacyclobutane.

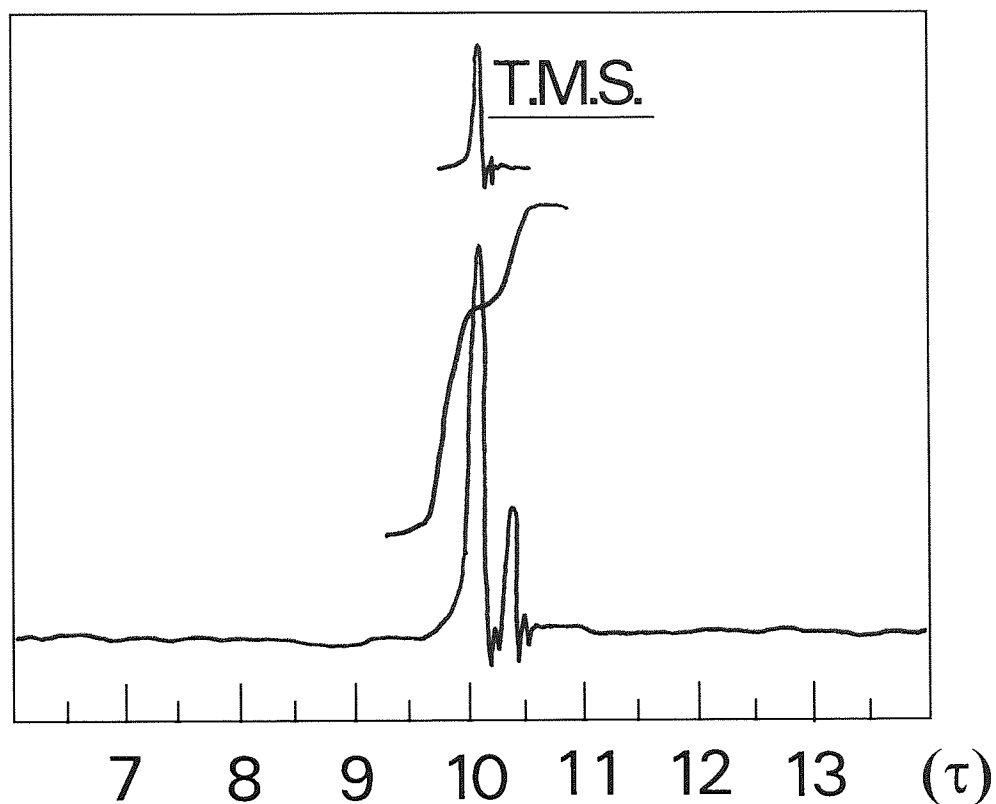


Figure (7-5). N.M.R. spectrum of 1,1,3,3-tetramethyl-1,3-disilacyclobutane relative to T.M.S.

7.5.1. Infra-red Spectroscopy

An infra-red spectrum for poly(dimethylsilmethylene) is shown in Figure (7-6). The spectrum was obtained from the pure product using a Perkin-Elmer 599B infra-red spectrophotometer.

Characteristic absorptions (ν cm^{-1});

2980s, 2950s, 2930s - C-H stretching; 1250s - symmetrical stretching;

1050s- methylene wagging; 840s, 820s - silicon methyl wagging.

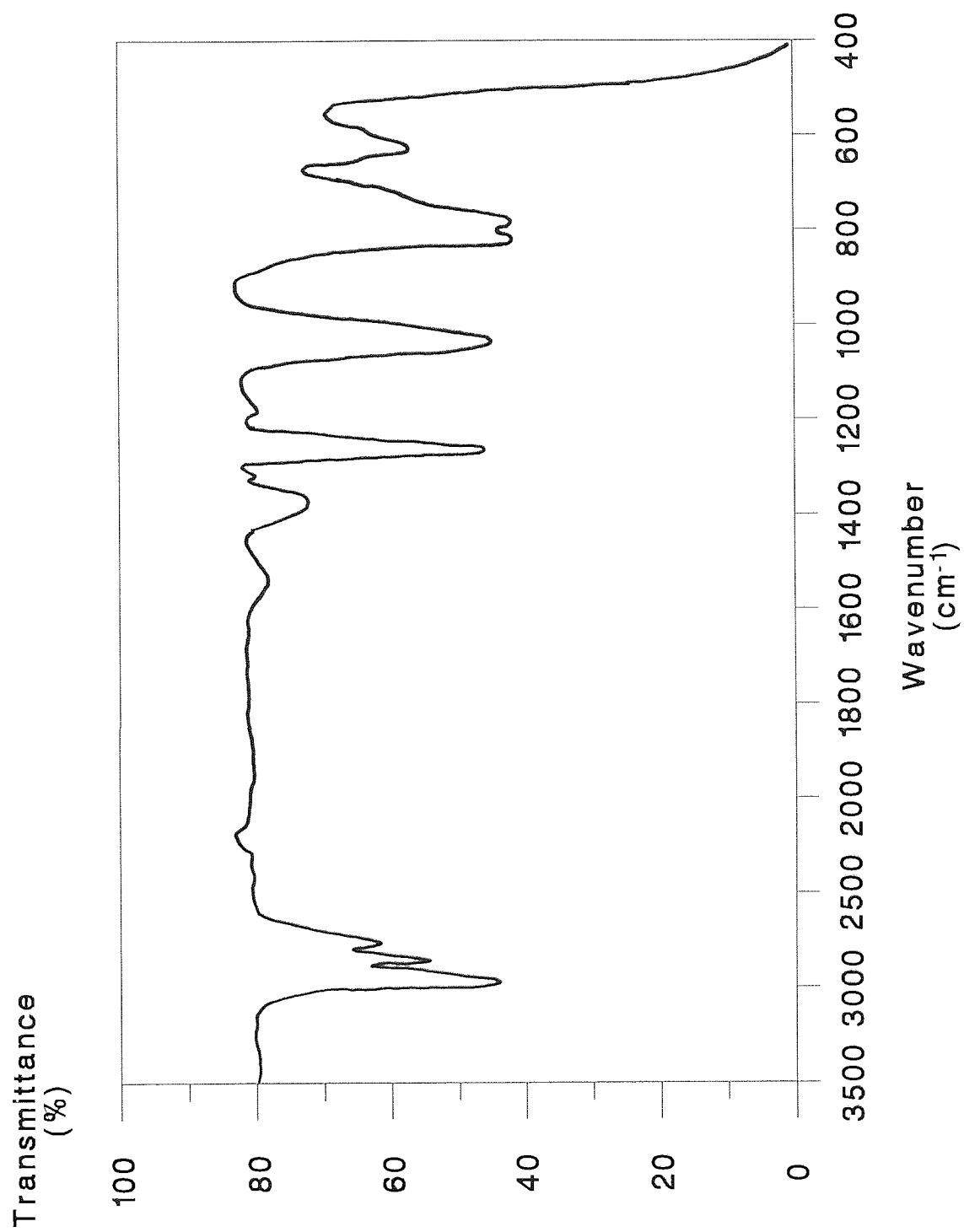


Figure (7-6). Infra-red spectrum of poly(dimethylsilmethylene).

7.5.2. Gel Permeation Chromatography

Samples of the polymer were sent to RAPRA Technology Ltd. for g.p.c. analysis. The results of the analysis are illustrated in Figure (7-7). Again the molecular weights are expressed as the "polystyrene equivalent". The results indicate the sample consists of a major component with a molecular mass of 400, with a high molecular mass 'tail' stretching up to 10^4 .

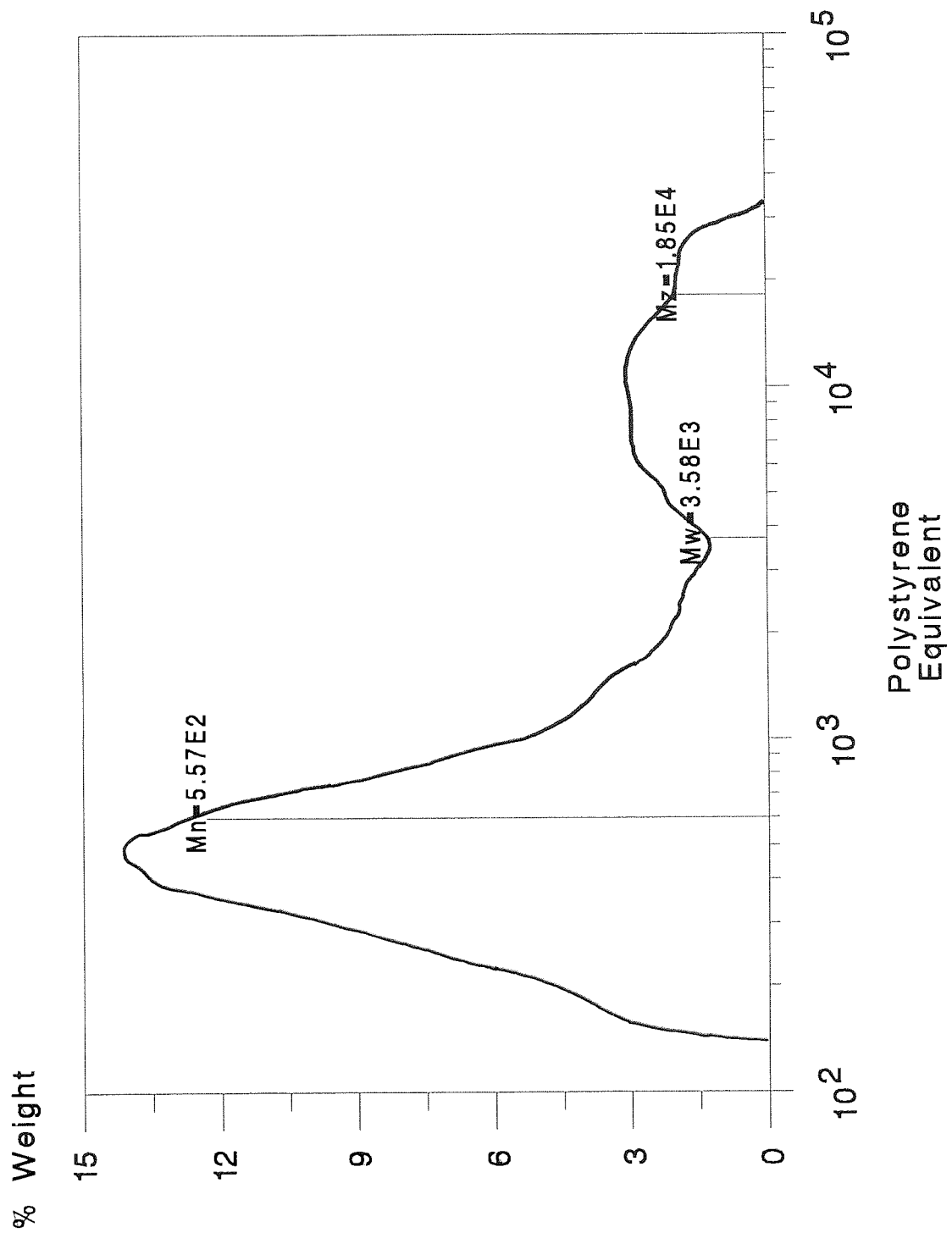


Figure (7-7). G.P.C. chromatograph of poly(dimethylsilmethylene).

CHAPTER 8

DIELECTRIC RELAXATION

8.1 Introduction

In this chapter a theoretical basis will be provided for the interpretation of the dielectric data acquired for the polymer samples.

8.2 Dielectrics in Static Electric Fields

Consider a parallel-plate capacitor consisting of two parallel plates of surface area A , and separation d . On application of a static electric field E_0 the potential difference V_0 between the two plates in vacuo, is given by the product E_0d . Accordingly, the capacitance of the system is defined as⁴²

$$C_0 = Q_0/V_0 \quad (8-1)$$

where Q_0 is known as the true charge since it represents the actual electric charge on each plate of the capacitor.

When the space between the plates of a capacitor is completely filled with an insulating material, called a dielectric, the potential difference across the capacitor is reduced to a value V , with the result that the capacitance of the system is augmented to a value C , given by

$$C = Q_1/V \quad (8-2)$$

where Q_1 is known as the free charge since it is the portion of the true charge which contributes to the voltage V .

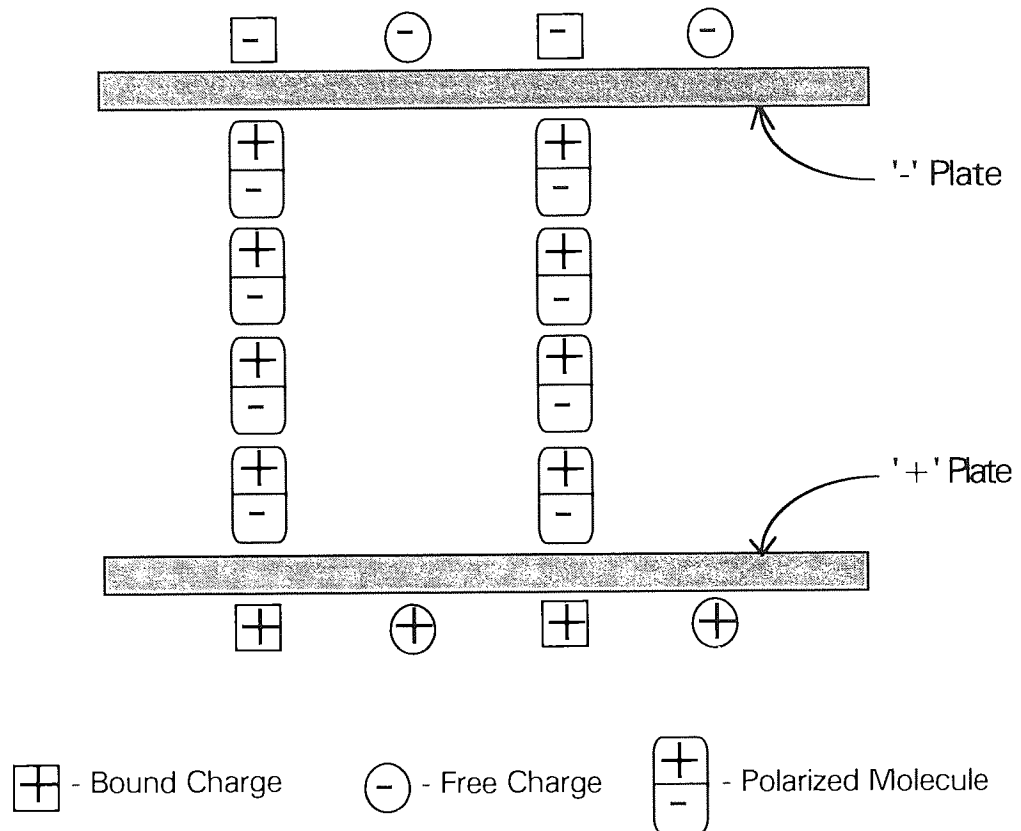


Figure (8-1). Schematic representation of dielectric polarization.

This effect has been described traditionally by introducing the static permittivity, or static dielectric constant, ϵ_s , which is defined as⁴²

$$\epsilon_s = C/C_0 \quad (8-3)$$

The difference between the true and free charges is known as the bound charge ($Q_0 - Q_1$). This charge is bound by an adjacent charge of equal magnitude but of opposite sign which lies at the surface of the dielectric

material and originates from the polarization occurring within the dielectric itself. This is illustrated in Figure (8-1).

The surface density of the bound charge is equal to the polarization of the dielectric P . Hence, if it is assumed the condenser is of a large area so that edge effects may be ignored

$$P = (1/A)(Q_0 - Q_1) \quad (8-4)$$

$$= q_0 - q_1 \quad (8-5)$$

where q_0 and q_1 are the surface densities of the true and free charges. These two charge densities define the electric displacement D_0 and the electric field strength E_0

$$D_0 = 4\pi q_0 \quad (8-6)$$

$$E_0 = 4\pi q_1 \quad (8-7)$$

The relationship between the electric displacement and the electric field strength is given by the equation

$$\epsilon_s = D_0/E_0 \quad (8-8)$$

and it may be shown that

$$D_0 = E_0 + 4\pi P \quad (8-9)$$

The origins of dielectric polarization lie in the nature of the dielectric material and its response when subjected to an applied electric field. For dielectrics that consist of polar molecules with permanent dipole moments,

the applied electric field interacts with the dipoles so that they tend to align against the field. In the case of non-polar dielectrics, the applied electric field induces polarization in the molecules of the dielectric, creating temporary dipoles which tend to align against the field. In both cases the effect is a reduction in the magnitude of the effective electric field between the plates resulting in the reduction of the potential difference across the capacitor.

8.3 Dielectrics in Time Varying Electric Fields

The application of a variable-frequency sinusoidal electric field to a polar liquid dielectric causes the molecules to partly reorientate before the field reverses. At low frequencies there is usually no lag between the reorientation of the molecules and the variation of the alternating electric field. Under these conditions there is no measurable phase difference between the dielectric displacement, D , and the varying electric field, E , and consequently the ratio D/E will be defined by a constant equal to the static value of the dielectric constant ϵ_s . However, as the frequency of the electric field is increased the molecular reorientation fails to keep up with the varying field and a phase angle difference, δ , arises between the D and E vectors. Consequently, the D and E vectors must then be expressed as

$$D_0 \exp[i(\omega t - \delta)] \quad (8-10)$$

and

$$E_0 \exp(i\omega t) \quad (8-11)$$

respectively, so that,

$$D/E = \varepsilon^* = D_0 \exp[i(\omega t - \delta)] / E_0 \exp(i\omega t) \quad (8-12)$$

D_0 and E_0 are the amplitudes of the respective vectors, ω is the angular frequency of the electric field and ε^* is the complex value of the dielectric constant defined by

$$\varepsilon^* = \varepsilon' - i\varepsilon'' \quad (8-13)$$

where ε' is the real part of the dielectric constant and ε'' is the imaginary part of the dielectric constant often referred to as the dielectric loss factor.

The two dielectric constants, ε' and ε'' , are linked by the equation

$$\varepsilon''/\varepsilon' = \tan \delta \quad (8-14)$$

where $\tan \delta$ is known as the dissipation factor. The latter quantity is the ratio of the energy loss per cycle to the energy stored per cycle.

As the frequency of the electric field approaches zero, the present description must become identical with the case of a static electric field, thus

$$\varepsilon'(\omega) \rightarrow \varepsilon_s, \quad \varepsilon''(\omega) \rightarrow 0, \quad \text{as } \omega \rightarrow 0 \quad (8-15)$$

A further relation may be added, namely

$$\varepsilon'(\omega) \rightarrow \varepsilon_i, \quad \text{as } \omega \rightarrow \text{infinity} \quad (8-16)$$

where ε_i is the value that $\varepsilon'(\omega)$ approaches at frequencies that are large relative to $f_{(\max)}$, (see section 8.3.1.).

8.3.1. Single Relaxation Behaviour

The frequency dependence of ϵ' and ϵ'' was first described by Debye⁴³.

For a single relaxation process Debye showed that

$$\epsilon^* = \epsilon_i + [(\epsilon_s - \epsilon_i) / (1 + i\omega\tau)] \quad (8-17)$$

The real and imaginary parts of Eq. (8-17) yield

$$\epsilon'(\omega) = \epsilon_i + [(\epsilon_s - \epsilon_i) / (1 + \omega^2\tau^2)] \quad (8-18)$$

and

$$\epsilon''(\omega) = [\omega\tau(\epsilon_s - \epsilon_i)] / (1 + \omega^2\tau^2) \quad (8-19)$$

where ϵ_i is the high frequency permittivity, ϵ_s is the static permittivity, ω is the angular frequency of the electric field and τ is the relaxation time for the process. The plots of ϵ' and ϵ'' versus $\log \omega$ are illustrated in Figure (8-2). It can be seen that ϵ'' attains a maximum at $\omega = 1/\tau$ or $f = 1/2\pi\tau$, where f is the frequency of the electric field in Hz. At this frequency, the maximum value of ϵ'' becomes equal to

$$\epsilon''(\text{max}) = (\epsilon_s - \epsilon_i)/2 \quad (8-20)$$

and ϵ' assumes the value

$$\epsilon' = (\epsilon_s + \epsilon_i)/2 \quad (8-21)$$

From Eqs. (8-14), (8-18) and (8-19) the dissipation factor may be written as

$$\tan \delta = [\omega\tau(\epsilon_s - \epsilon_i)] / (\epsilon_s + \epsilon_i\omega^2\tau^2) \quad (8-22)$$

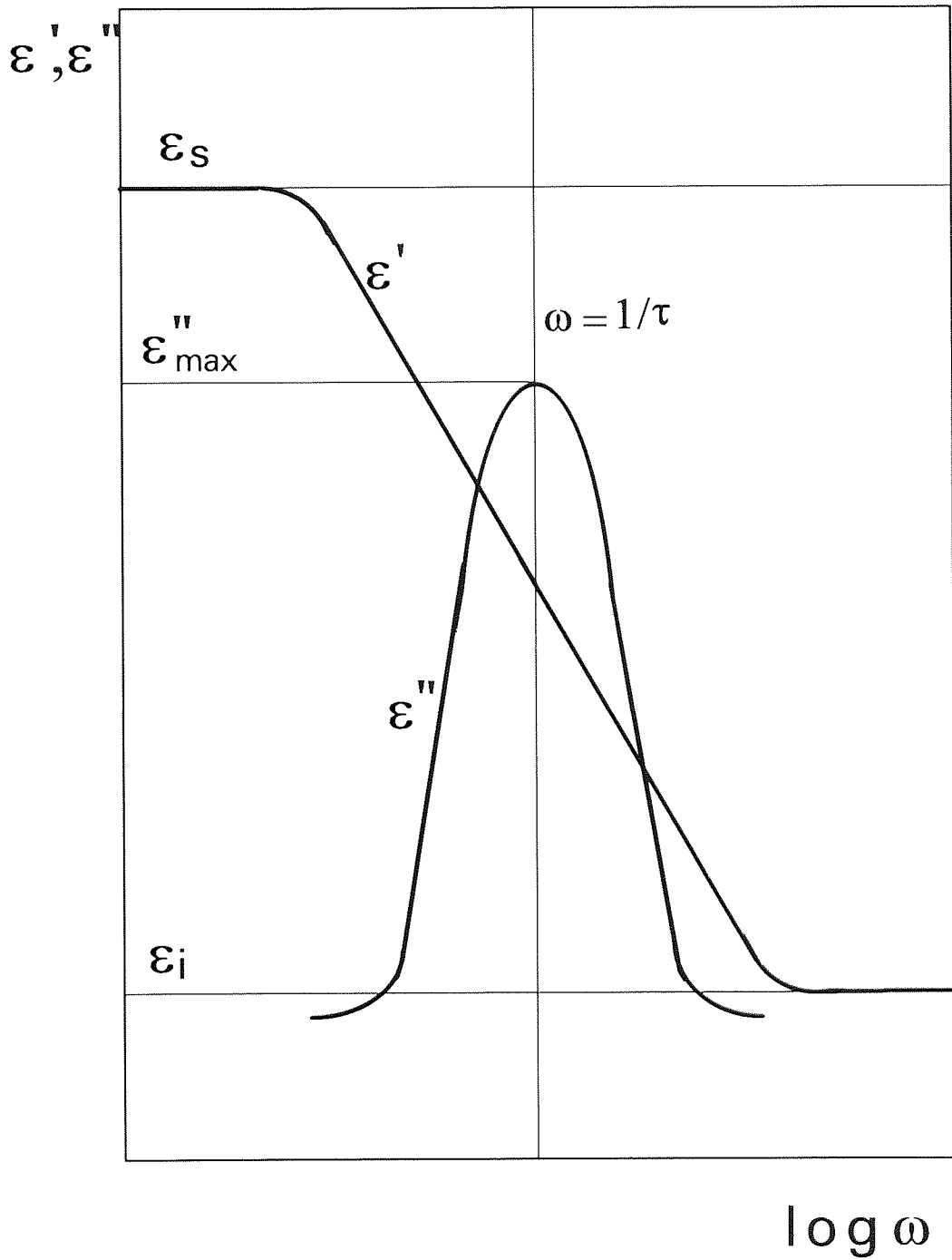


Figure (8-2). Debye dielectric dispersion and absorption curves for a single relaxation process.

The maximum value of $\tan \delta$, at which $d(\tan \delta)/d\omega = 0$, occurs at a frequency

$$\omega_{\max} = (\epsilon_s/\epsilon_i\tau^2)^{1/2} \quad (8-23)$$

attaining a value of

$$(\tan \delta)_{\max} = (\epsilon_s - \epsilon_i) / [2(\epsilon_s\epsilon_i)^{1/2}] \quad (8-24)$$

The frequency portion of the maximum of $\tan \delta$ is not coincident with that of $\epsilon''_{(\max)}$. The displacement of the $\tan \delta$ peak depends upon the difference between the value of ϵ_s and ϵ_i .

The frequency dependence of ϵ'' on ϵ' may be used to test how well the Debye model fits the real case. Eliminating the parameter $\omega\tau$ between Eqs. (8-18) and (8-19) gives

$$[\epsilon' - (\epsilon_s + \epsilon_i)/2] + \epsilon''^2 = [(\epsilon_s - \epsilon_i)/2]^2 \quad (8-25)$$

This is the equation of a circle having a centre at $[(\epsilon_s + \epsilon_i)/2, 0]$ and a radius of $(\epsilon_s - \epsilon_i)/2$. Since negative values of ϵ' are not permissible, a plot of ϵ'' against ϵ' should be a semicircle, as shown in Figure (8-3(a)).

8.3.2. Multiple Relaxation Behaviour

The curves for dielectric loss in polymers are broad and have lower loss maxima than those predicted by the Debye model. This led Cole and Cole⁴⁴ to suggest the following semi-empirical equation for dielectric relaxation in polymers

$$\epsilon^* = \epsilon_i + [(\epsilon_s - \epsilon_i) / (1 + (i\omega\tau)^{1-\alpha})] \quad (8-26)$$

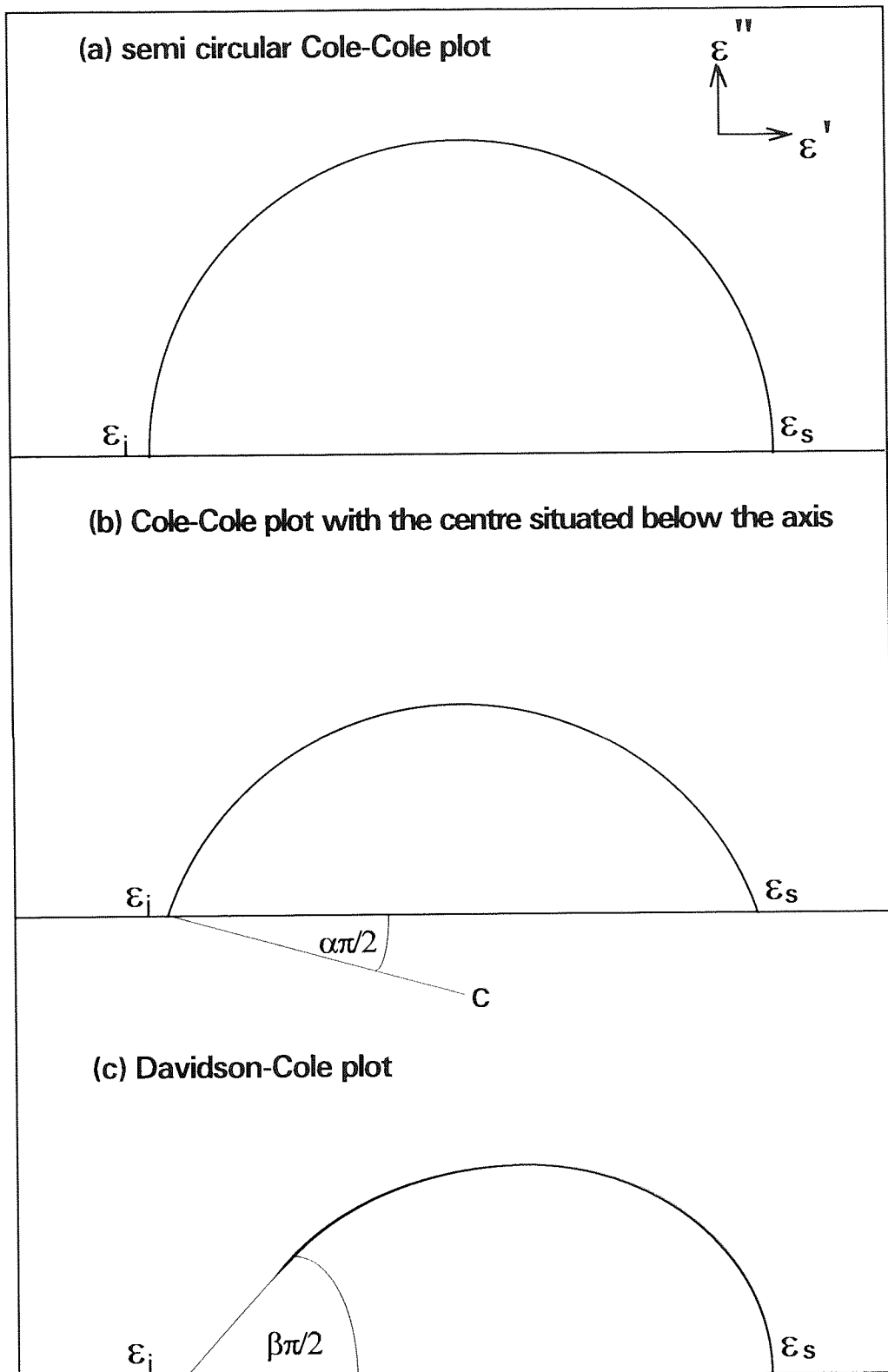


Figure (8-3). Cole-Cole plots.

where $0 < \alpha < 1$, and α is an empirical quantity specifying the broadness of the distribution.

Equation (8-26) better describes a broad dispersion, and gives an ϵ'' versus ϵ' plot in which the centre of the fitted semicircle is depressed below the abscissa, as shown in Figure(8-3(b)).

The flatter or more shallow the circular arc then the greater is the span of relaxation times associated with the relaxation process.

The centre of the semicircle is given by

$$(\epsilon_s - \epsilon_i)/2, -[(\epsilon_s - \epsilon_i)/2]\cotan(\beta\pi/2) \quad (8-27)$$

where $\beta = 1 - \alpha$. The radius of the semicircle is given by

$$[(\epsilon_s - \epsilon_i)/2]\operatorname{cosec}(\beta\pi/2) \quad (8-28)$$

Although the exact form of the distribution of relaxation times in the Cole-Cole equation is not based on any particular molecular model, the empirical parameter α is convenient for specifying the broadness of the experimental relaxation peaks, and it has been extensively used for this purpose.

Referring to Figure (8-3(b)), the angle between the line connecting C to ϵ_i on the real axis is equal to $\alpha\pi/2$. Note that, in the case of $\alpha = 0$, the locus of the Cole-Cole plot approaches the ϵ' axis at 90° and Eq. (8-26) reduces to Eq. (8-17), i.e. single relaxation.

The empirical Cole-Cole equation relates only to dispersion and absorption curves that are symmetrical about the position $\omega\tau = 1$. It is often found, for polymers, that the dielectric loss curves have a high frequency broadening and the Cole-Cole plots are said to be skewed. Davidson and Cole⁴⁵ attempted to fit the experimental results to the following function

$$\varepsilon^*(\omega) = \varepsilon_i + [(\varepsilon_s + \varepsilon_i) / (1 + i\omega\tau)]^\beta \quad (8-29)$$

where β is a parameter, $0 < \beta < 1$.

Also

$$(\varepsilon'(\omega) - \varepsilon_i) / (\varepsilon_s - \varepsilon_i) = (\cos(\phi))^\beta (\cos(\beta\phi)) \quad (8-30)$$

and

$$(\varepsilon''(\omega) - \varepsilon_i) / (\varepsilon_s - \varepsilon_i) = (\cos(\phi))^\beta (\sin(\beta\phi)) \quad (8-31)$$

where $\tan(\phi) = \omega\tau_1$.

For maximum loss $\omega\tau_1 = 1$, but is given by

$$\omega_{\max}\tau_1 = \tan \{1/(\beta + 1)(\pi/2)\} \quad (8-32)$$

where $\omega(\max)$ is the angular frequency corresponding to maximum loss.

Figure (8-3(c)) shows a typical Davidson-Cole arc plot. At low frequencies the curve approaches the abscissa along a straight line. The angle between this line and the abscissa is $\beta\pi/2$. Many measurements on solutions of polymers in low molecular weight solvents often give results that may be fitted by the Davidson-Cole function.

It is apparent from the preceding discussion that Cole-Cole plots are a very convenient graphical method for the representation of the entire dielectric properties of a chemical system. For a complete set of relaxation data, the limiting values of ϵ_s and ϵ_i may be obtained from the intersection of the locus of Cole-Cole plots on the ϵ' axis.

8.4 Temperature and Dielectric Relaxation

The concept of thermal activation over a potential energy barrier was first applied to dielectric phenomena by Eyring⁴⁶. He showed that the rate constant for the movement of molecular dipoles between two or more possible equilibrium positions separated by a potential energy barrier was

$$K_0 = (kT/h)\exp(-\Delta F/RT) \quad (8-33)$$

where k is the Boltzmann constant, h is Planck's constant and R is the gas constant. Here ΔF is the free energy of the dipolar relaxation and is defined as

$$\Delta F = \Delta H - T\Delta S \quad (8-34)$$

where ΔH is the activation energy of dipole relaxation and ΔS is the entropy of activation. In terms of the Eyring model, the dipole relaxation time, τ , is, by definition, the inverse of K_0 , so that

$$\tau = (h/kT)\exp(\Delta H/RT)\exp(-\Delta S/R) \quad (8-35)$$

or, in logarithmic form

$$\ln\tau = (\Delta H/RT) - \ln T + [\ln(h/k) - (\Delta S/R)] \quad (8-36)$$

Since the last term on the right-hand side of Eq. (8-36) is independent of temperature and because the contribution from the $\ln T$ term is small and varies only slowly with changes in temperature, a plot of $\ln\tau$ against $1/T$ would be expected to be a straight line. This is an example of the Arrhenius law, and, in practice it is usual to plot $\log f_{\max}$ against $1/T$ to obtain a straight line possessing a gradient of $-\Delta H/(2.303R)$.

CHAPTER 9

EXPERIMENTAL METHODS

9.1 Introduction

This study is concerned with the measurement of experimentally observable quantities to yield information concerning the structure and dynamic properties of some silicon containing polymers.

The parallel electrical capacitance, C_p , and the dissipation factor, $\tan \delta$, are quantities from which the dielectric constant, ϵ' , and the dielectric loss, ϵ'' , can be calculated. A considerable amount of information concerning the motion and flexibility of polymer molecules can be deduced from the temperature and frequency dependence of ϵ' and ϵ'' . In addition, the activation energies, ΔH , for the molecular processes involved can be calculated.

The apparatus and techniques used to facilitate these measurements will be described in this chapter.

9.2 Dielectric Apparatus for the Measurement of C_p and $\tan \delta$ at Various Frequencies

The measurement of the electrical capacitance and the dissipation factor was carried out using a GenRad 1689 RLC Digibridge connected to a

dielectric cell containing the polymer sample under test. The following sections describe the apparatus used to maintain accurate control of the temperature. The performance and reliability of the dielectric cell was established using a test polymer, PPG2025 + 1 mole %HgCl₂ (see Appendix C), which had been previously subjected to a rigorous dielectric study⁴⁷.

Electrical connections between the Digibridge and the dielectric cell were made using a four-terminal, guarded GenRad 1657-9600 extender cable. The "high", "low" and guard terminals were connected to the cell via a "three way" insulated adapter. The Digibridge was "zeroed" prior to the introduction of the polymer sample to the dielectric cell in order to compensate for stray capacitances occurring in the system.

9.3 The Dielectric Cell

The dielectric cell used in this study was of the parallel-plate capacitor construction, the exact specifications of the cell are described in Appendix D. A diagram of the cell is shown in Figure (9-1).

The cell was constructed from two copper coated glass-fibre plates separated by glass spacers. An epoxy based resin was used to secure the cell together and also to act as a seal to prevent sample leakage. A J-type thermocouple, supplied by RS Components Ltd., with a temperature range -199^o to 199^o C was attached to the side of the cell prior to the cell being wrapped in PTFE sealing tape. The "high" and "low" electrical connections to

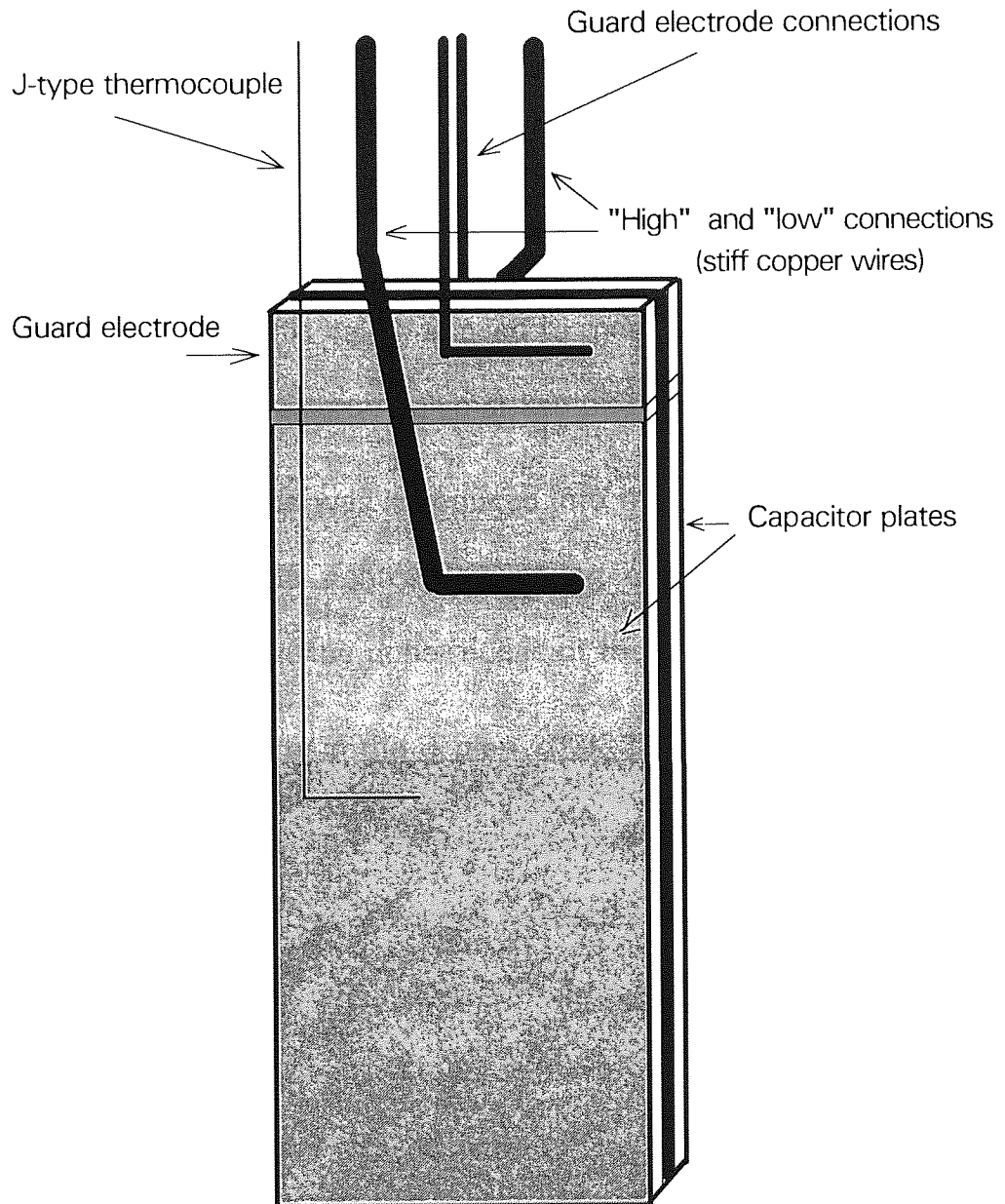


Figure (9-1). The dielectric cell prior to wrapping in PTFE thread tape.

the cell were made using stiff copper wires to minimise possible variable inter lead stray capacitance, while the connection to the guard electrode was made using flexible insulated copper wire. The capacitor had a sample volume of approximately 1.6 cm³ and was contained inside a glass tube containing a silicone oil as a contact fluid. The electrical capacitance of the empty cell was approximately 33pF. This cell was used to measure the electrical capacitance and dissipation factor of three polymer samples.

The guard electrode was introduced into the design of the cell in order to compensate for sample contraction during cooling, and to allow for the distorted electric field at the upper edges of the "high" and "low" electrodes.

9.4 Temperature Control in the Region 203K-298K

Accurate temperature control in the range 203K to 298K was required for the measurement of the dielectric relaxation for the test polymer PPG2025 + 1 mole %HgCl₂. This was achieved using a "Minus Seventy" Thermostat Bath, Bridge Control Model (Townson and Mercer Ltd., Croydon, UK). A cross-sectional diagram of this apparatus showing its general constructional features is shown in Figure (9-2). The heat exchanger vessel was half-filled with acetone and dry ice. The temperature control vessel was filled with acetone. The glass tube containing the dielectric cell was suspended in the temperature control vessel so that the cell was submerged below the level of the acetone. The temperature was measured by a J-type thermocouple connected to a J/K type digital thermometer, both items supplied by RS

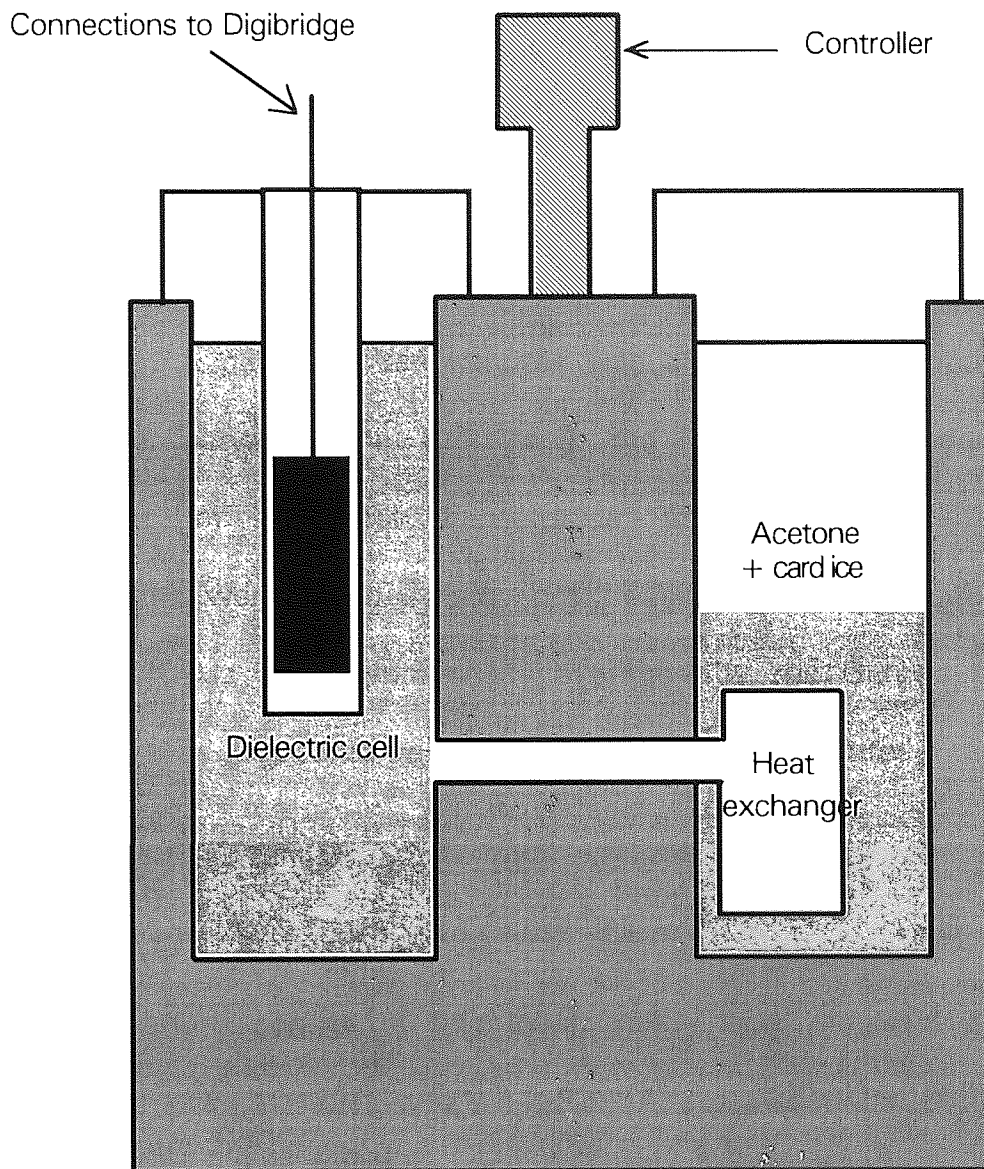


Figure (9-2). Cross-sectional diagram of the "Minus Seventy" bath.

Components Ltd. The temperature control of this apparatus was $\pm 0.1\text{K}$.

9.5 Measurement of Electrical Capacitance and Dissipation Factor in the Range 203K-298K

The acetone in the temperature control vessel was cooled to the required temperature. A period of ten minutes was allowed for the equilibration of temperature between the bath and the cell before undertaking the measurement of electrical capacitance and dissipation factor. Ten measurements were taken at ten spot frequencies in the frequency range 100Hz to 10^5Hz and automatically averaged by the Genrad bridge. This procedure was repeated at five different temperatures spanning the temperature range 203K to 298K.

9.6 Apparatus for Temperature Control Below 203K

Temperature control in this lower range was required for the Dow polymer samples 10423-1 and 10423-9. A cross-sectional diagram of the cooling apparatus designed for this purpose is shown in Figure (9-3). The vessel was constructed using two Dewar flasks, one fitting inside the other. The gap between the Dewar flasks was filled with liquefied N_2 .

Sixty resistors, each of resistance $22\text{k}\Omega$, were connected in parallel to form three resistor "bracelets", each bracelet containing 20 resistors. The three bracelets were then assembled on top of each other and connected in parallel giving the configuration a total resistance of 366Ω . This assembly

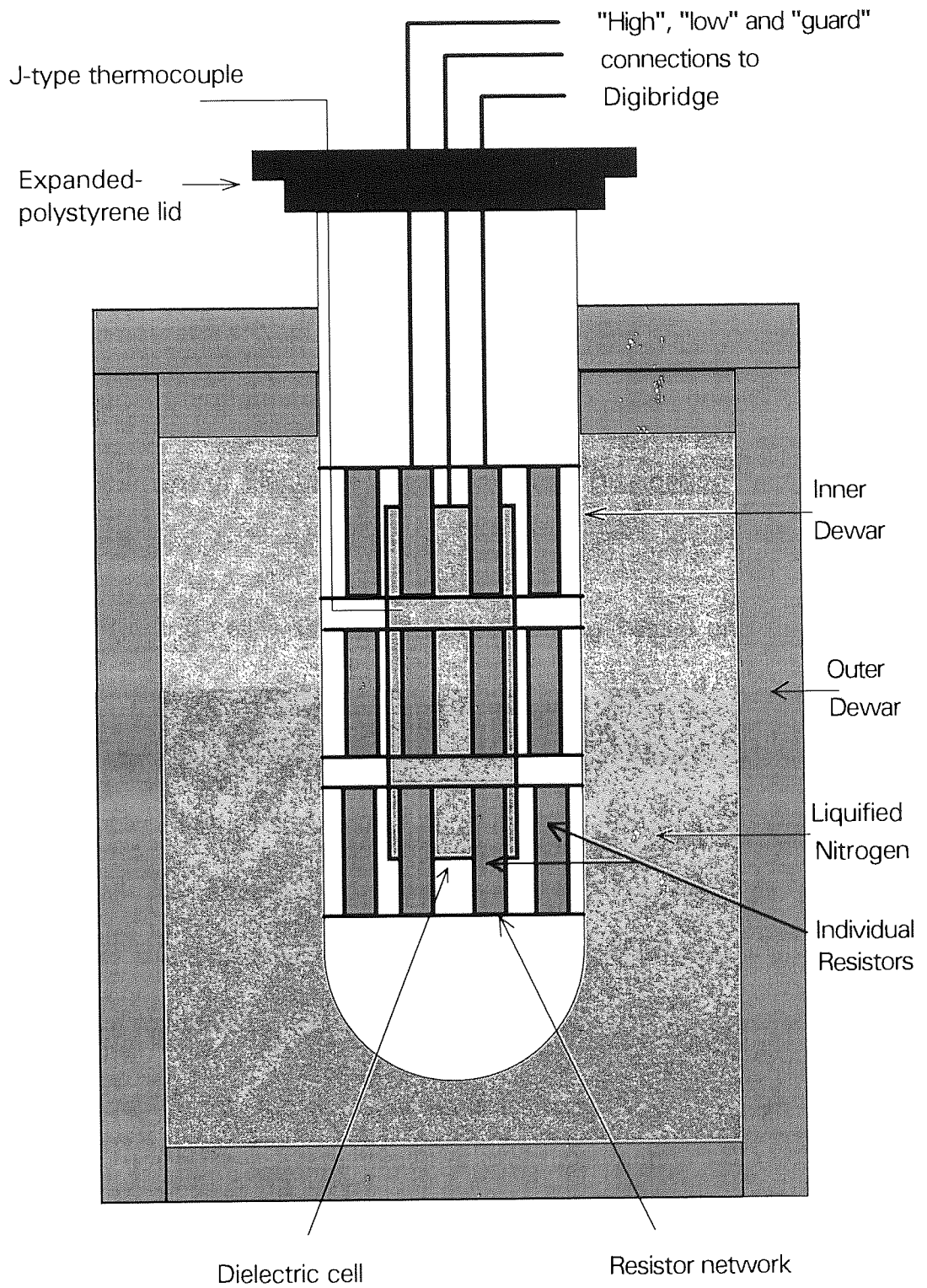


Figure (9-3). Apparatus for temperature control below 203K.

was then inserted into the inner Dewar to form a uniform heating "cage". Electrical connections were made between the resistors and a 30V power supply. The dielectric cell was suspended inside the inner Dewar so as to be completely surrounded by the heating cage. The inner Dewar was then sealed with a lid fashioned from expanded polystyrene.

The temperature was measured using a J-type thermocouple connected to a J/K digital thermometer, both supplied by RS Components Ltd..

9.7 Measurement of Electrical Capacitance and Dissipation Factor Below 203K

The dielectric cell was placed in the cooling vessel and the sample was allowed to cool. A small current, producing approximately 2.5 watts of heating in the resistor network was then applied to stabilize the temperature of the sample in the loss region. At the temperature of interest the power supply was disconnected for measurement purposes, as simultaneous operation of the Digibridge in measure mode and the power supply was not possible due to electrical interference.

The average of ten measurements were taken at up to ten spot frequencies in the frequency range 100Hz to 10^5 Hz. This procedure was repeated at five different temperatures for each sample.

9.8 Measurement of Static Dielectric Permittivities

In order to make accurate measurements of the static dielectric permittivities associated with the polymer samples, the stray capacitance associated with the dielectric cell must be taken into account. The stray capacitance of a dielectric cell originates in the connecting wires which link the cell to the measuring device, in this case a GenRad 1689 precision RLC Digibridge, and also from edge effects inherent to the cell itself. By assuming that the stray capacitance, ΔC , of the dielectric cell does not change upon the introduction a polymer sample, it may be eliminated from the calculations by substitution.

The capacitance of the dielectric cell when empty, C_a , when filled with a standard dielectric (HPLC grade toluene from Aldrich), C_s , and when filled with the polymer sample, C_x , may be expressed by Eqs. (9-1), (9-2) and (9-3) respectively,

$$C_a = (\epsilon_0 A/d) + \Delta C \quad (9-1)$$

$$C_s = (\epsilon_0 \epsilon_s A/d) + \Delta C \quad (9-2)$$

$$C_x = (\epsilon_0 \epsilon_x A/d) + \Delta C \quad (9-3)$$

where ϵ_0 is the permittivity of free space, ϵ_s is the dielectric constant of the standard dielectric, ϵ_x is the dielectric constant of the polymer sample, A is the surface area of the cell plates, and d is the distance between the plates. By manipulating the above equations to eliminate ΔC , it may be shown that

$$(C_x - C_a)/(C_s - C_a) = (\epsilon_x - 1)/(\epsilon_s - 1) \quad (9-4)$$

which gives

$$\epsilon_x = 1 + [(C_x - C_a)/(C_s - C_a)](\epsilon_s - 1) \quad (9-5)$$

For simplicity, the Digibridge was "zeroed" prior to the introduction of the polymer sample under test. This was equivalent to setting C_a to zero. Equation (9-5) then reduces to

$$\epsilon_x = 1 + (C_x / C_s)(\epsilon_s - 1) \quad (9-6)$$

The values of C_x and C_s were taken directly from the Digibridge at the required temperatures while the values of ϵ_s were calculated over the temperature range -90° to 0° using the equation⁴⁸

$$(d\log_{10}\epsilon_s / dT) = -0.045 \quad (9-7)$$

and over the temperature range 0° to $+90^\circ$ using the equation⁴⁸

$$(d\epsilon_s / dT) = -0.243 \quad (9-8)$$

The values listed in Equations (9-7) and (9-8) were obtained from National Bureau of Standards Circular 514 for HPLC grade toluene⁴⁸.

CHAPTER 10

DIELECTRIC RESULTS

10.1 Dielectric Properties of Dow Polymer Samples 10423-1 and 10423-9

The dielectric relaxation behaviour of the two polymer samples of poly(2,2,5,5-tetramethyl-1-oxa-2,5-disilapentane), 10423-1 ($M_w(\text{avg}) = 28000$) and 10423-9 ($M_w(\text{avg}) = 46000$), have been studied, as a function of temperature (205K - 179K) and frequency (100Hz - 10^5 Hz), using the dielectric apparatus described in Chapter 9.

10.2 Dielectric Loss Results

The variation of ϵ'' with respect to $\log f/(\text{Hz})$, at various temperatures, is shown as a series of normalised plots for the Dow polymer samples 10423-1 and 10423-9, in Figures (10-1) and (10-2), respectively.

The presence of a broad α -type relaxation process for these samples is readily discernible. The loss curves are asymmetric, showing broadening on the high frequency side which is typical of the behaviour found for the α -type process in organic amorphous polymers above T_g . The movement of f_{max} , which is the frequency corresponding to maximum loss, within the frequency range $100\text{-}10^5$ Hz, occurs over a temperature interval of approximately 20K. The width of the loss curves at half-height is approximately three decades of frequency.

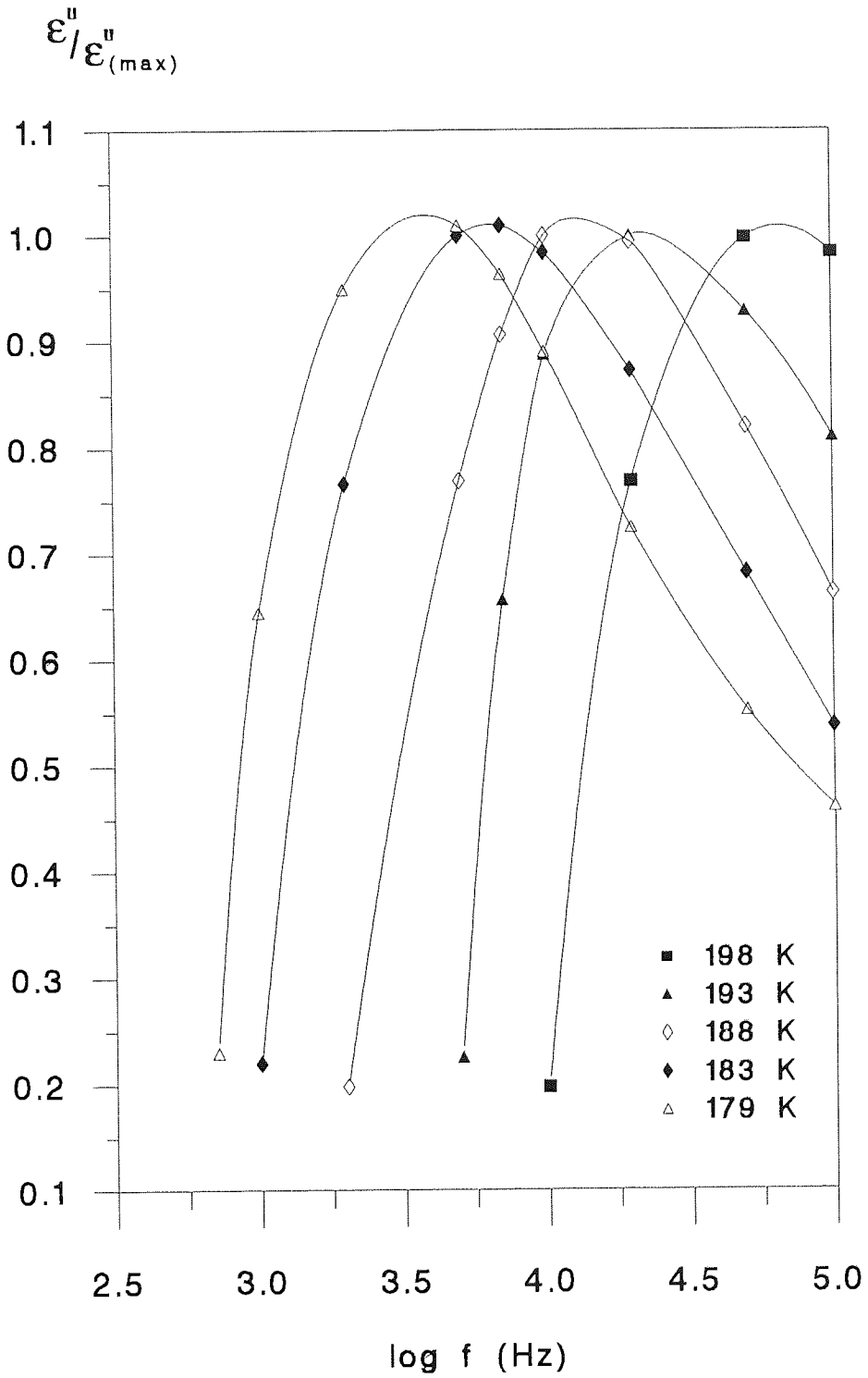


Figure (10-1). Frequency dependence of $\epsilon' / \epsilon''_{(max)}$ for sample 10423-1.

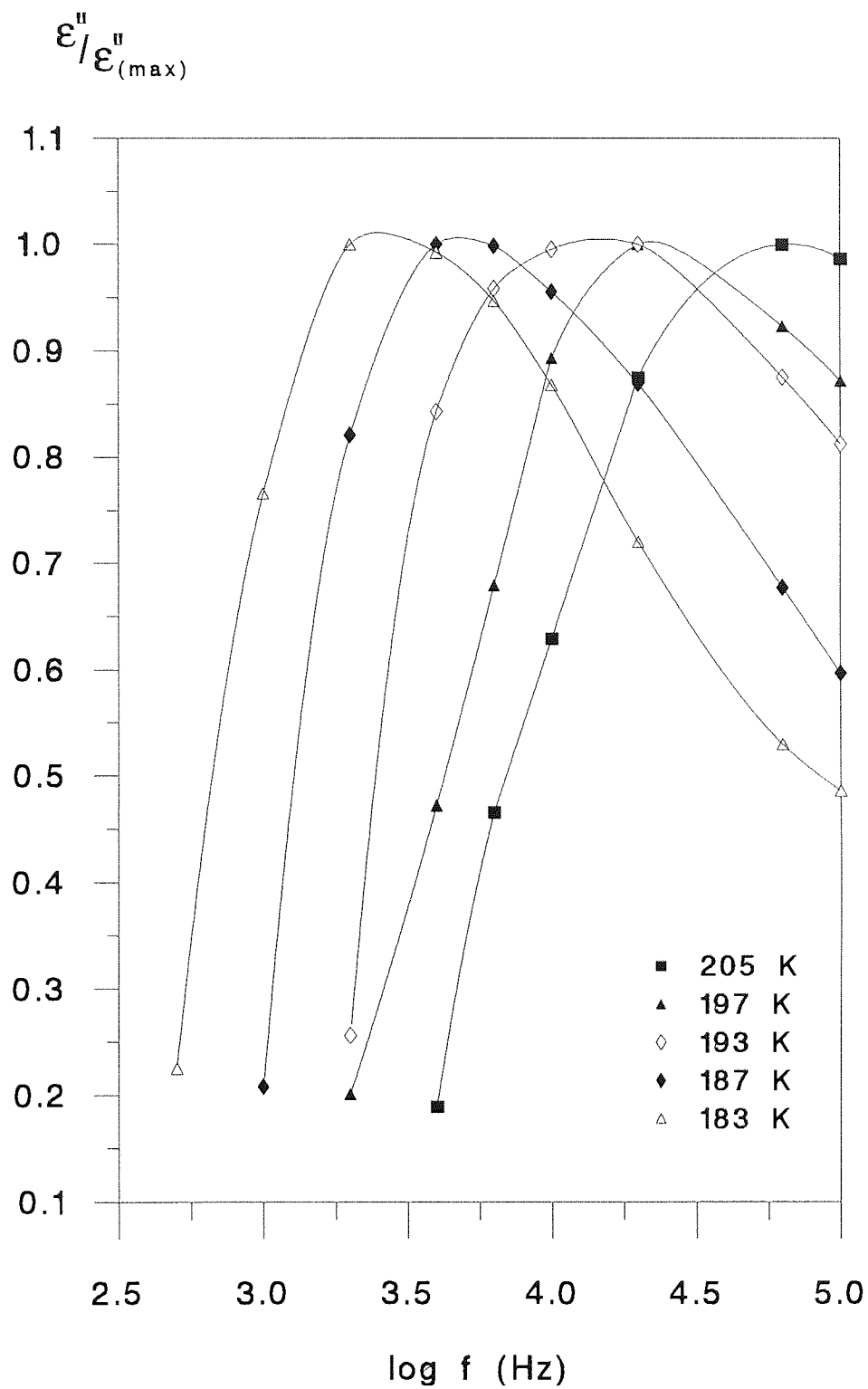


Figure (10-2). Frequency dependence of $\epsilon''/\epsilon''_{(max)}$ for

sample 10423-9.

10.3 Measurement of Dielectric Relaxation Activation Energy

Arrhenius plots of the logarithm of the frequency corresponding to maximum dielectric loss, plotted as a function of the reciprocal of the absolute temperature, for Dow samples 10423-1 and 10423-9, are shown in Figures (10-3) and (10-4) respectively. All plots are linear and have a slope which is proportional to the activation energy for the dielectric loss.

10.4 Cole-Cole Plots

Cole-Cole plots of ϵ'' against ϵ' are presented in Figures (10-5) to (10-8) for the Dow samples at various temperatures. The curves are skewed-arcs and are consistent with the empirical analysis of Davidson and Cole discussed in Chapter 8.

The limiting low frequency permittivity value, ϵ_s , is measured by extrapolating the circular arc onto the ϵ -axis. The limiting high frequency permittivity value, ϵ_i , is estimated from the plots where the data is more complete by a linear extrapolation onto the ϵ -axis. A single ϵ_i is estimated in this way for each sample and is assumed to be constant over the small range of temperatures at which the measurements were carried out. The derivation of ϵ_s and ϵ_i in this manner combined with the values of $f_{(\max)}$, determined from Figures (10-1) and (10-2), permitted the calculation of the Davidson-Cole distribution factor, β , by the computer program listed in Appendix B.

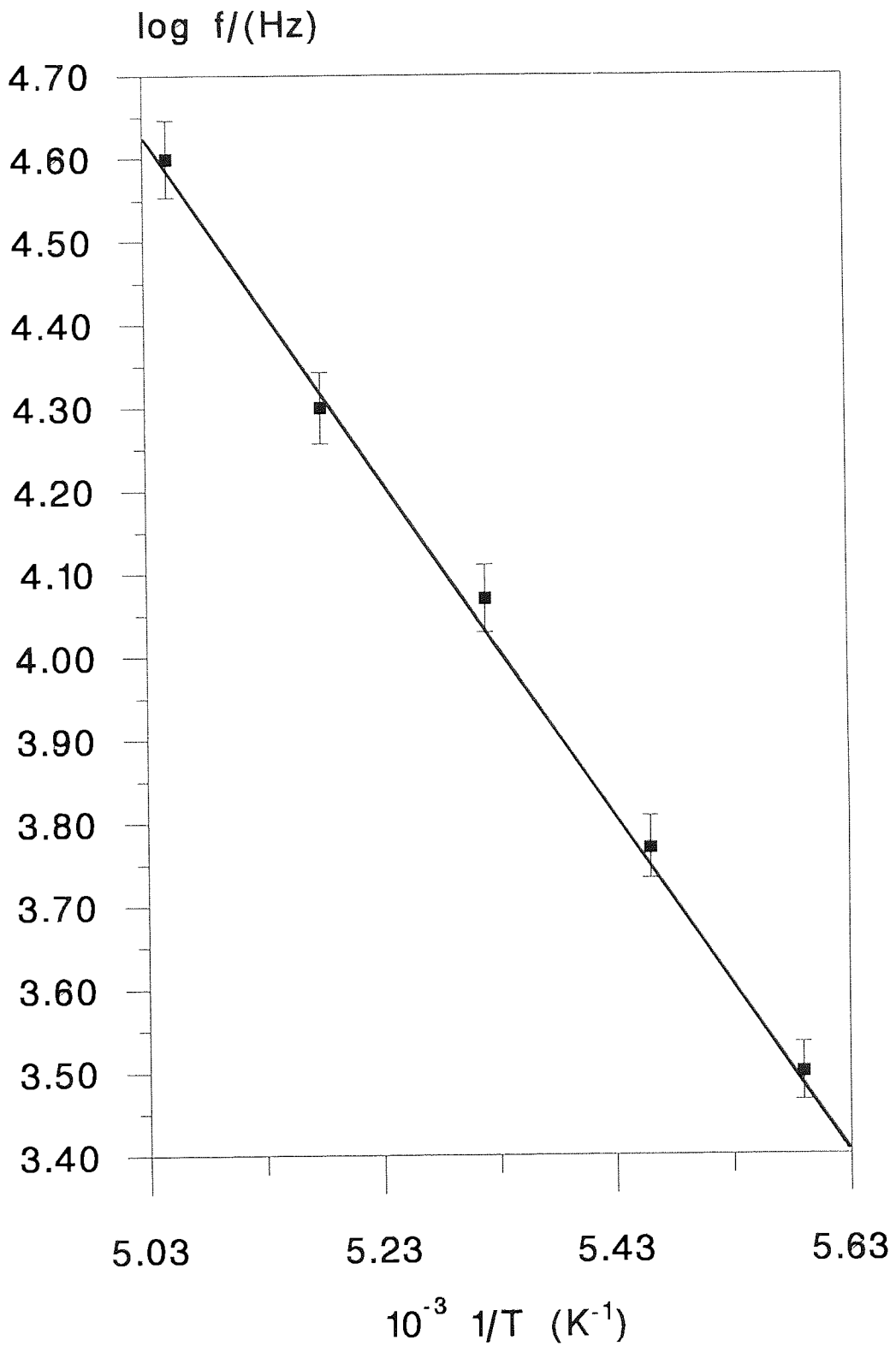


Figure (10-3). $\log(f_{\max}/\text{Hz})$ against $1/T (\text{K}^{-1})$ for sample 10423-1.

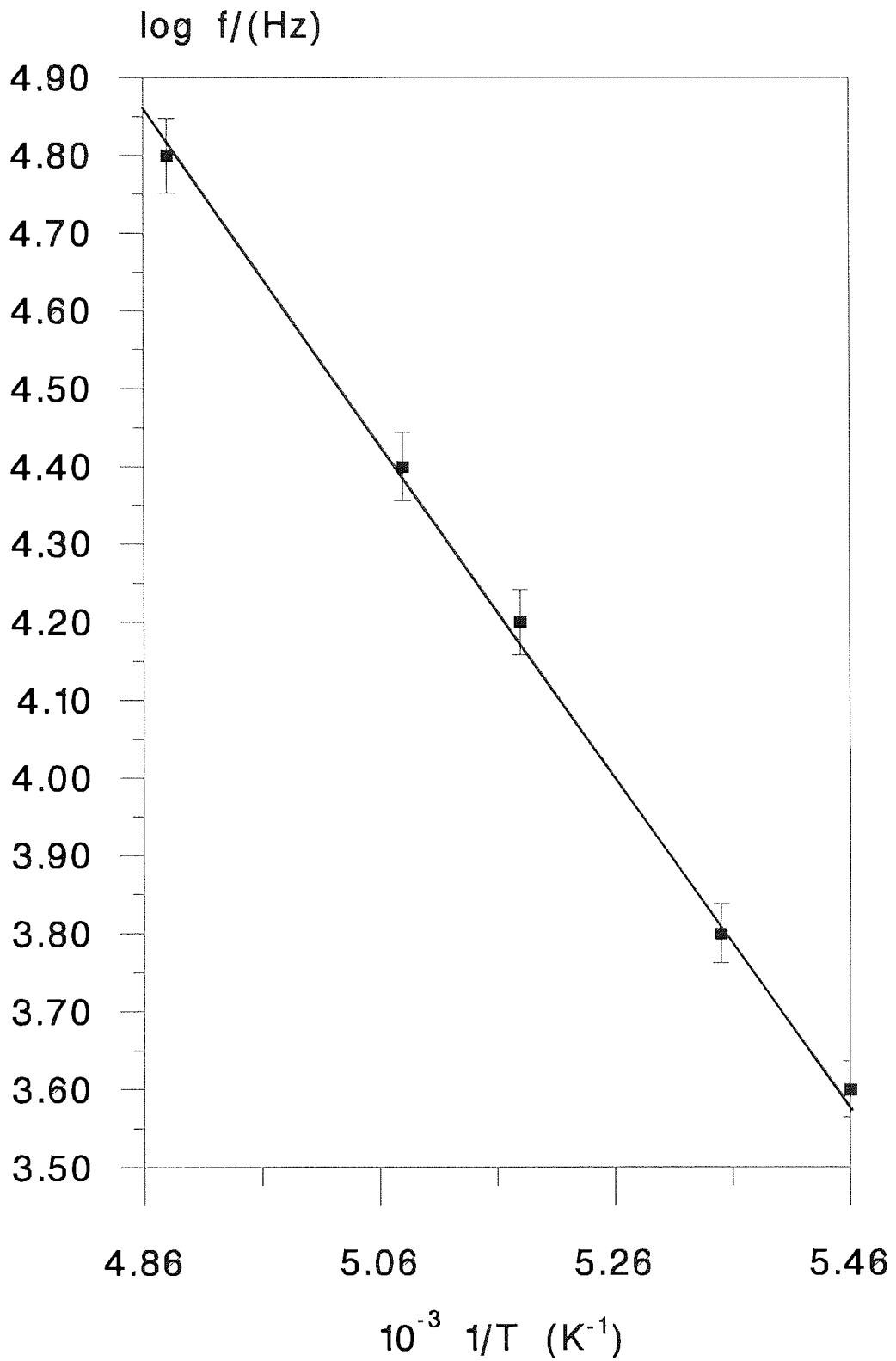


Figure (10-4). $\log(f_{\max}/\text{Hz})$ against $1/T \text{ (K}^{-1}\text{)}$ for sample 10423-9.

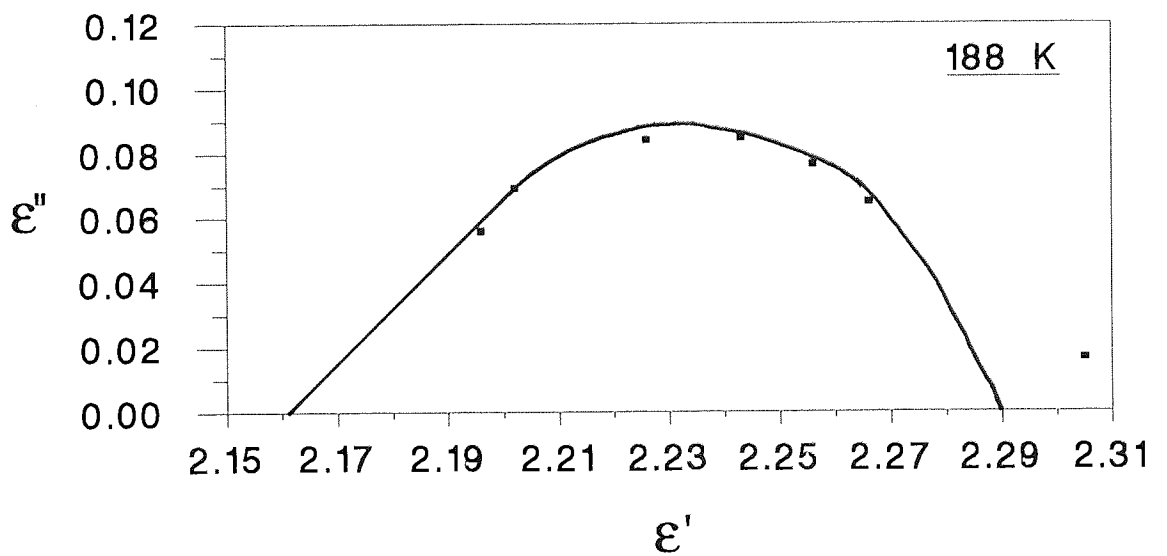
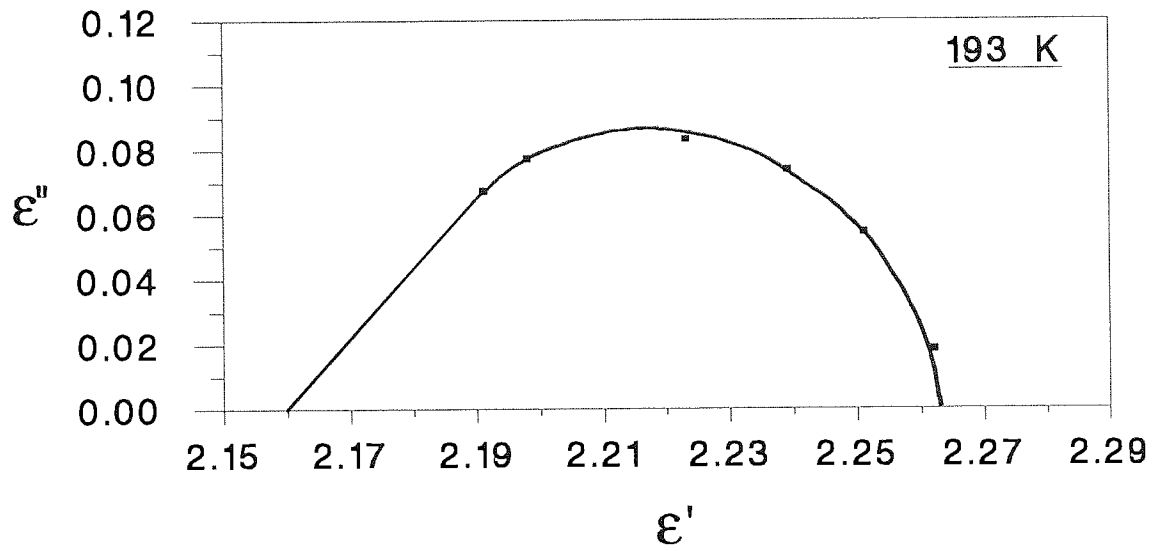


Figure (10-5). Cole-Cole plots for sample 10423-1 at various temperatures.

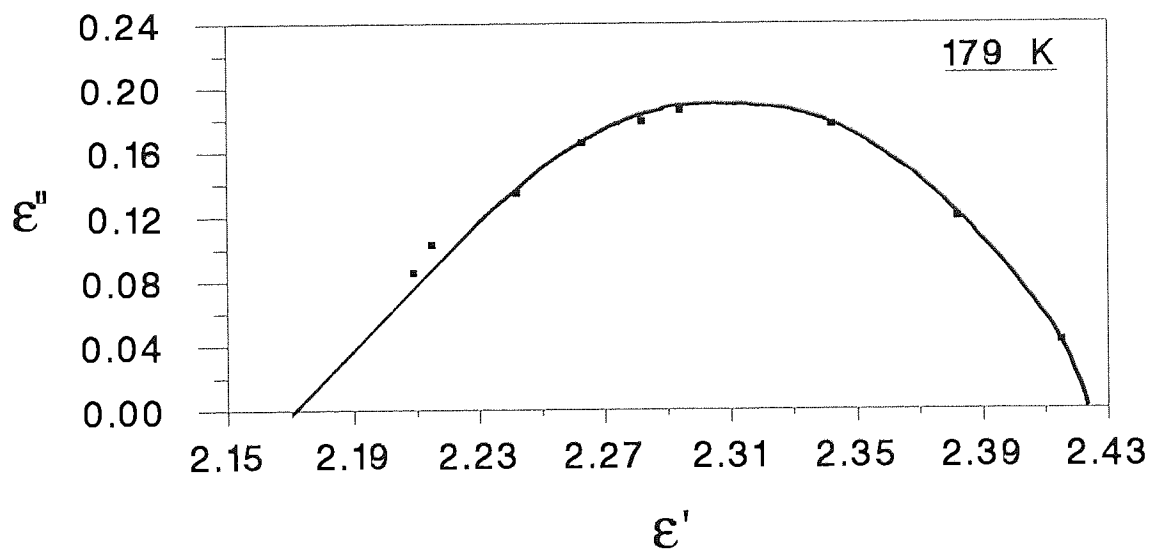
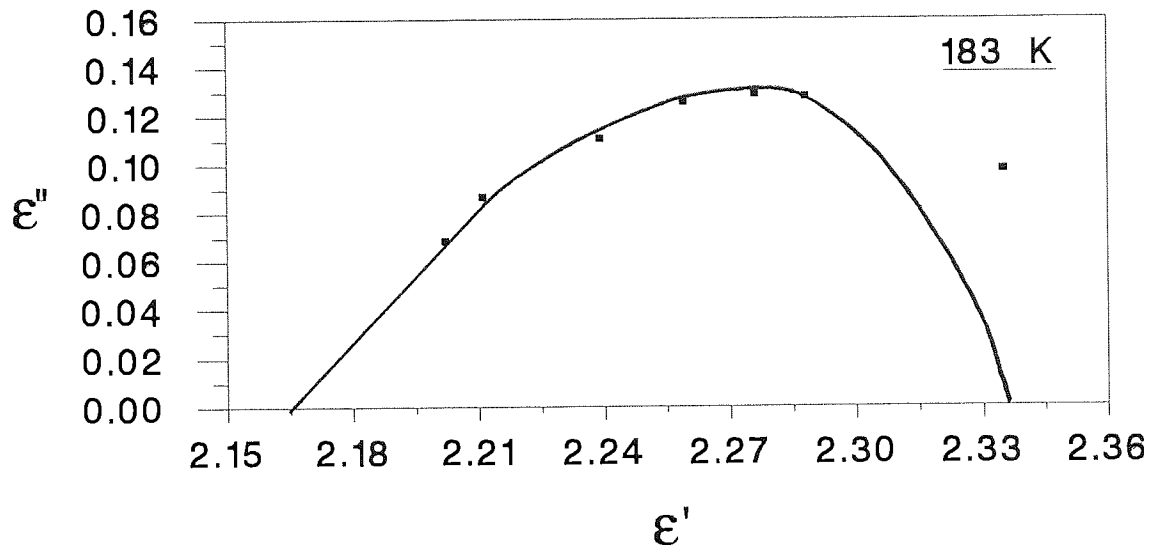


Figure (10-6). Cole-Cole plots of sample 10423-1 at various temperatures.

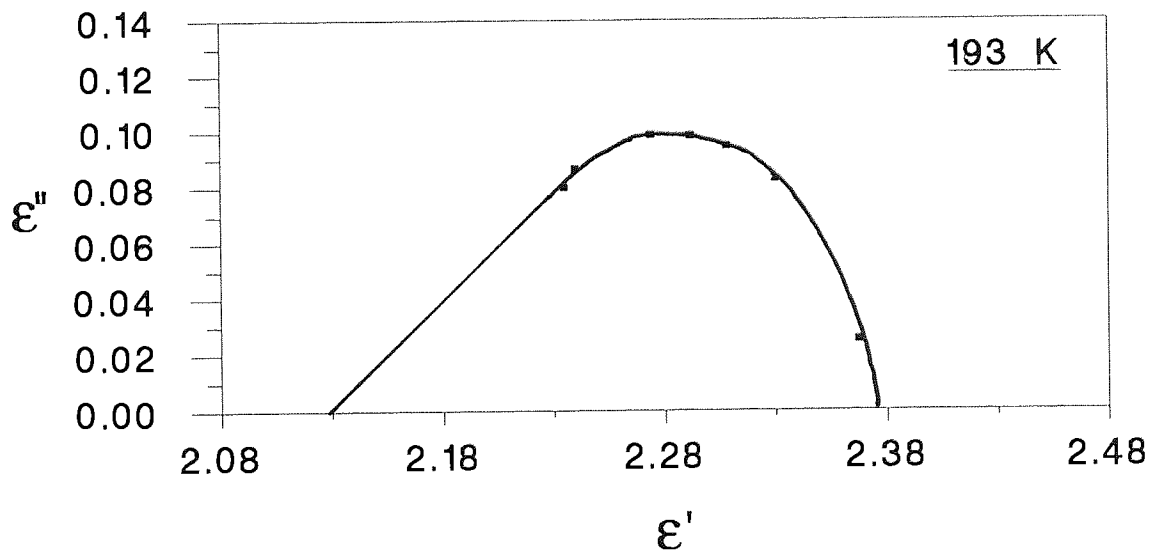
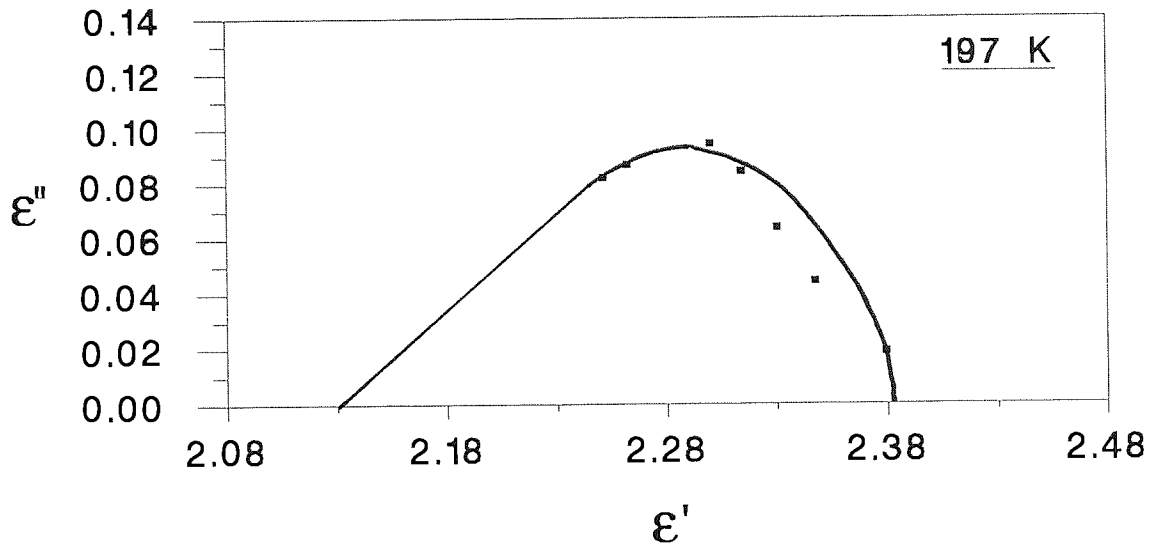


Figure (10-7). Cole-Cole plots for sample 10423-9 at various temperatures.

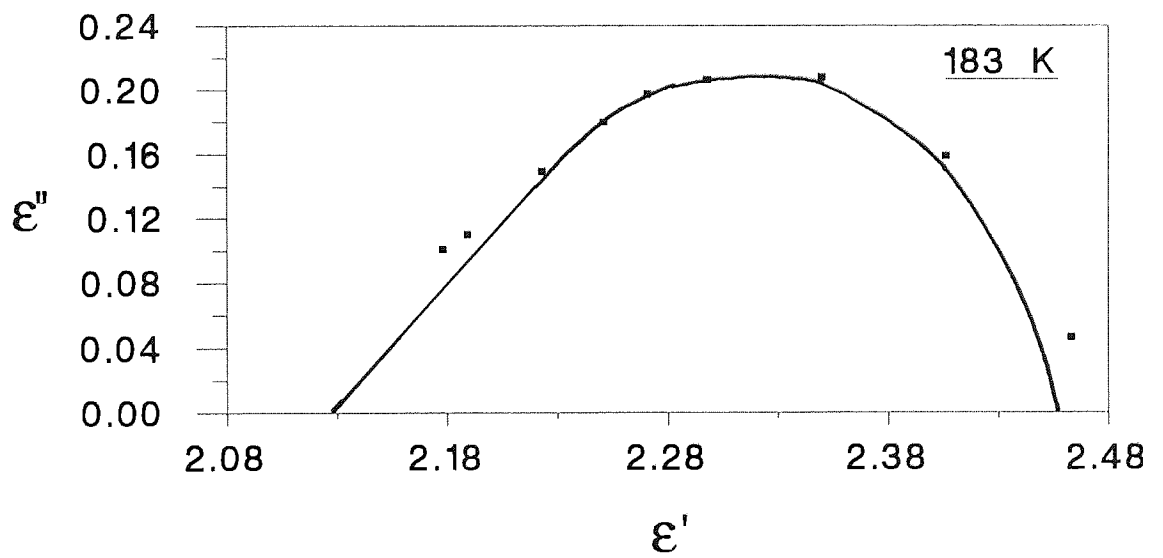
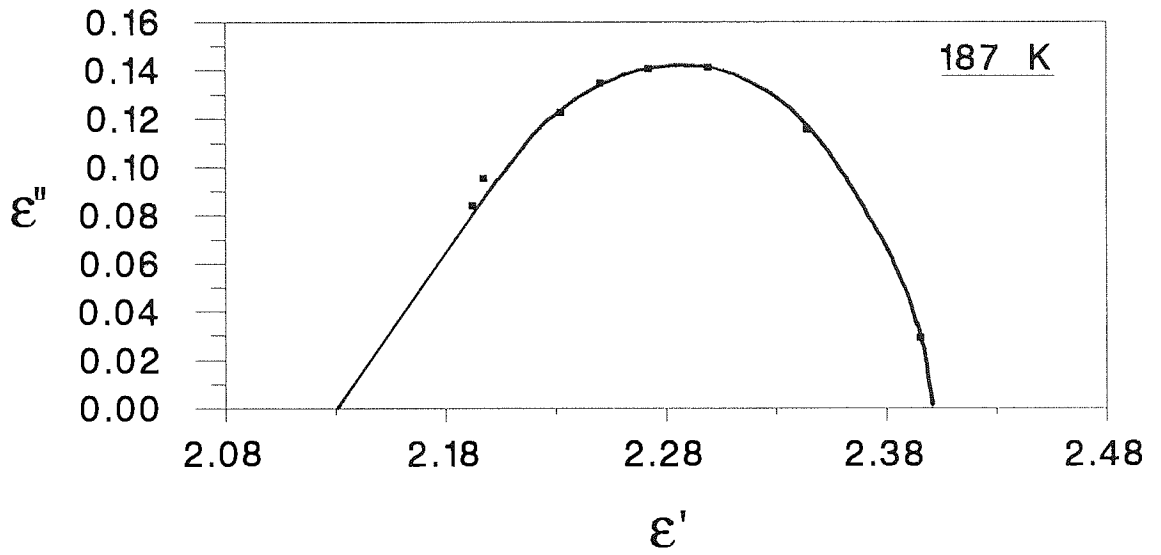


Figure (10-8). Cole-Cole plots for sample 10423-9 at various temperatures.

For the Dow sample 10423-1, ϵ_i has the value 2.16 \pm 0.02 while ϵ_s varies slightly between 2.27 \pm 0.02 and 2.41 \pm 0.02. For the Dow sample 10423-9, ϵ_i has the value 2.13 \pm 0.02 while ϵ_s varies between 2.37 \pm 0.02 and 2.44 \pm 0.02.

An examination of the values of the maximum dielectric loss showed that for both samples this value varied between 0.10 and 0.20 with the changing temperature.

10.5 Calculation of Dielectric Activation Energies

The dielectric activation energies, ΔH_{act} , for polymer samples 10423-1 and 10423-9 were calculated from Eq. (8-36) using Figures (10-3) and (10-4). The results are given below

$$\Delta H_{act}(10423-1) = 39 \text{ kcal/mol}$$

$$\Delta H_{act}(10423-9) = 40 \text{ kcal/mol}$$

As far as the author is aware no studies concerning ΔH_{act} for linear poly(2,2,5,5-tetramethyl-1-oxa-2,5-disilapentane) have been published to date.

10.6 Davidson-Cole Analysis of the Dielectric Data

Values of the Davidson-Cole empirical distribution parameter, β , for polymer samples 10423-1 and 10423-9 are presented in Table (10-1). The values shown are average values of β measured over a small temperature

range. The β values were calculated using the computer program listed in Appendix B.

Sample	M_w	T (K)	β
10423-1	28000	193-179	0.45
10423-9	46000	197-183	0.40

Table (10-1). Davidson-Cole distribution parameter, β , for samples 10423-1 and 10423-9.

10.7 Discussion of Results

Studies^{49,50} performed on amorphous samples of linear poly(dimethylsiloxane) have reported ΔH_{act} values in the range 46-155 kcal/mol. The values of ΔH_{act} calculated for poly(2,2,5,5-tetramethyl-1-oxa-2,5-disilapentane) are considerably lower, 39 kcal/mol and 40 kcal/mol for polymer samples 10423-1 and 10423-9 respectively. This difference may be explained as resulting from the increased flexibility of poly(2,2,5,5-tetramethyl-1-oxa-2,5-disilapentane) compared to poly(dimethylsiloxane) (see section 6.5). The increased flexibility in the former resulting in lower energy barriers for molecular reorientation. However, the corresponding β values calculated for the two polymers are identical, indicating a similar span of relaxation times for the molecular reorientation processes.

CHAPTER 11

DISCUSSION/FURTHER WORK

The major part of this study has been concerned with the development of computer programs with which to simulate and investigate the conformational behaviour of a range of polycarbosilanes and the related material poly(2,2,5,5-tetramethyl-1-oxa-2,5-disilapentane).

The calculation of a series of **U**-matrices describing the intramolecular interactions occurring within each polymer, along with their associated structural data, has permitted the calculation of a variety of macroscopic conformationally-dependent properties from microscopic information.

The reliability of any calculations made concerning the conformationally-dependent properties of polymer molecules using computer simulations will basically depend on two factors;

1. The choice of the molecular model and force field, and
2. A thorough search of the conformational space accessible to the polymer for the conformations of lowest energy.

The selection of a particular model and force field will initially depend upon the availability of the relevant structural information and interatomic interaction parameters for the polymer system under consideration. In

addition, the size of the section of chain to be considered and the complexity of the force field chosen must take into account the type of computer facilities available and the time required for the calculations, since the application of the rotational isomeric state approximation is only valid if the whole of the conformational energy space is analysed.

In the case of poly(dimethylsilmethylene) and poly(dimethylsilethene) the application of these two conditions was achieved. The corresponding characteristic ratio, dipole moment ratio and mean-square radius of gyration, calculated for these polymers were determined by examining the entire conformational energy space associated with each polymer, prior to the application of the rotational isomeric state approximation.

Due to the structural complexity of poly(dimethylsilethane) and poly(2,2,5,5-tetramethyl-1-oxa-2,5-disilapentane) an analysis of their conformational behaviour was not possible according to the factors described above with the computer facilities available. Instead, each rotatable bond was simply assumed to exist in three distinguishable conformations, t , g^+ and g^- . Although this assumption was not based on any examination of the conformational energies of these polymers, it is a valid assumption since each rotatable bond considered in this way was formed by sp^3 hybridized atoms. In general, sp^3 hybridized bonds exhibit a 3-fold rotational potential with the minimum energy conformations at t , g^+ and g^- . However, attention must be

drawn to this fact when considering the conformationally-dependent properties determined for these polymers in this study.

The prediction of conformationally-dependent properties of polymers by computer simulation is certainly not accurate enough to justify abandoning the measurement of such properties experimentally. If a measurement is not too difficult to obtain experimentally, then it should always be preferred to a prediction made by a computer simulation. The utility of computer simulation studies does not lie in the possibility of replacing experimental measurement, but rather in its ability to complement experimental results. For instance, the effects of microscopic quantities that are inaccessible to experimental determination can be monitored or altered in a computer simulation. The resulting consequences for the macroscopic behaviour may be evaluated, with the possibility of gaining valuable insights into the molecular processes occurring. In addition, the computer simulation of a polymer system enables the investigation of its behaviour during extreme conditions that may be inaccessible in the laboratory.

Although the accuracy of a prediction may be estimated by considering the approximations and simplifications of the model and computational procedure, the final test lies in a comparison of theoretically predicted and experimentally measured properties. In order to provide a firm basis for the application of computer simulation methods for the calculation of conformationally-dependent properties of polycarbosilanes, the results should

be compared with experimental data wherever possible. Currently, information of this nature is very scarce and any future work in this subject should concentrate on developing a database of experimentally determined values for comparison. In this context, it must be stressed that good agreement between calculated and experimental data does not necessarily mean that the theoretical model underlying the calculations is correct. Good agreement may be due to a number of reasons. Firstly, the conformationally-dependent property that is compared may be insensitive to the assumptions made or the values of the parameters assigned to that model. Secondly, a compensation of errors, either by chance or by intentionally adjusting the parameters of the model to give the desired properties, may result in a good agreement with experiment. Finally, care must be taken when attempting to ascertain experimental values for conformationally-dependent properties of polymers, since any discrepancy between calculated and experimental values may be due to experimental error.

The measurement of the frequency dependence of the dielectric loss, at various temperatures, for two samples of poly(2,2,5,5-tetramethyl-1-oxa-2,5-disilapentane) has permitted the calculation of the dielectric relaxation energies and the empirical relaxation time distribution factor, β , for this polymer. The relatively low values of ΔH_{act} calculated for this polymer compared to those calculated for the closely related structure, poly(dimethylsiloxane), may result from the increased conformational

flexibility observed in poly(2,2,5,5-tetramethyl-1-oxa-2,5-disilapentane). However, more work must be undertaken to examine the combined conformational and dielectric relaxation behaviour of other polymers to establish a possible link.

LIST OF REFERENCES

1. van Gunsteren, W.F., Berendsen, H.J.C., 'Computer simulation of molecular dynamics: Methodology, applications and perspectives in chemistry.' *Angew. Chem. Int. Ed. Engl.*, Vol. **29**, p992-1023 (1990).
2. Flory, P.J., *Statistical Mechanics of Chain Molecules*, Interscience (1969).
3. Jorgensen, W.L., 'Internal rotation in liquid 1,2 dichloroethane and n-butane.' *J. Am Chem Soc.*, Vol. **103**, p677-679 (1981).
4. Pratt, L.R., Hsu, C.S., Chandler, D. 'Statistical mechanics of small chain molecules in liquids. I. Effects of liquid packing on conformational structures.' *J. Chem. Phys.*, Vol. **68**, p4202-4212 (1978).
5. Flory, P.J., Jernigan, R.L., Abe, A. 'Conformational energies of n-alkanes and the random configuration of higher homologs including polymethylene.' *J. Am. Chem. Soc.*, Vol. **88**, p631-639 (1966).
6. Flory, P.J., Suter, U.W. 'Conformational energy and configurational statistics of polypropylene.' *Macromolecules*, Vol. **8**, p765-776 (1975).
7. Mark, J.E., DeBolt, L., Welsh, W.J. 'Conformational energies and unperturbed chain dimensions of polysilane and poly(dimethylsilane).' *Macromolecules*, Vol. **19**, p2978-2983 (1986).
8. Mark, J.E. 'Dipole moments of dimethylsiloxane chains.' *J. Chem. Phys.*, Vol. **49**, p1398-1402 (1968).
9. Suter, U. 'Conformational characteristics of poly(methylvinylketones) and of simple model ketones.' *J. Am. Chem. Soc.*, Vol. **101**, p6481-6496 (1979).
10. Brant, D.A., Flory, P.J. 'The configuration of random polypeptide chains. II. Theory.' *J. Am. Chem Soc.*, Vol. **87**, p2791-2800 (1965).
11. Cowie, J.M.G., *Polymers: Chemistry and Physics of Modern Materials*, Intertext Books (1973).
12. Guggenheim, E.A., 'A proposed simplification in the procedure for computing electric dipole moments.' *Trans. Far. Soc.*, Vol. **45**, p714-720 (1949).
13. Onsager, L., 'Electric moments of molecules in liquids.' *J. Am. Chem. Soc.*, Vol. **58**, p1486-1493 (1936).
14. A synthesis and degradative study of some silicon-carbon polymers, D. Jones, PhD thesis, University of Aston (1974).

15. Boury, B., Corriu, R.J.P., Douglas, W.E. 'Poly(carbosilane) precursors of silicon carbide: The effect of cross-linking on ceramic residue.' *Chem. Mater.*, Vol. **3**, p487-489 (1991).
16. Gundyrev, A.A., Nametkin, N.S., Panchenkov, G.M., Topchiev, A.V. 'The dielectric permeability and dipole moments of certain organosilicon compounds.' *Doklady Akad. Nauk. SSSR.*, Vol. **129**, p1325-1327 (1959).
17. Gundyrev, A.A., 'Dielectric constants and dipole moments of some silicon-organic compounds.' *Issled. V obl. Kremniorgan. Soedin. Sintez I Fiz.-Khim Svoista Akad. Nauk. SSSR*, Vol. **16**, p235-242 (1962).
18. Kartsev, G.N., Syrkin, K., Mironov, V.F., Chernyshev, E.A. 'The dipole moments of certain organosilicon compounds.' *Doklady Akad. Nauk. SSSR*, Vol. **122**, p99-102 (1958).
19. Knoth, W.H., Lindsey, R.V. '1,1,3,3-tetramethyl-1,3-disilacyclobutane.' *J. Org. Chem.*, Vol. **23**, p1392 (1958).
20. Kriner, W.A. 'The preparation of cyclic siliconmethylene compounds.' *J. Org. Chem.*, Vol. **29**, p1601-1606 (1964).
21. Chmielecka, J., Stanczyk, W. 'Synthesis of 1,1,3,3-tetramethyl-1,3-disilacyclobutanes using lithium metal or organolithium reagents.' *Synlett*, Vol. **1**, p334 (1990).
22. Andrianov, K.A., Pakhomov, V.I., Gel'perina, V.M., Semenova, G.A. 'Synthesis of polydimethylsilylenes and polydimethylsilacetylenes.' *Polym. Sci. USSR Vysokomolekuliarnye soedinenia*, Vol. **8**, p1793-1797 (1966).
23. Ching, A.C., Speiler, J.L. 'Method of preparing alpha-unsaturated organosilicon compounds.' U.K. Patent No. 1245555.
24. McCrum, N.G., Read, B.E., Williams, G., *Anelastic and dielectric effects in polymeric solids*, Wiley, New York (1967).
25. Scott, A., Scheraga, H.A., 'A method for calculating internal rotation barriers.' *J. Chem. Phys.*, Vol. **42**, p2209-2215 (1965).
26. Atkins, P.W., *Physical chemistry*, Oxford University Press (1986).
27. Damewood, J.R., West, R. 'Structure calculations for silane polymers: Polysilane and poly(dimethylsilane).' *Macromolecules*, Vol. **18**, p159-164 (1985).
28. Fjeldberg, T., Seip, R., Lappert, M.F., Thorne, A.J. 'The molecular structure of gaseous bis(trimethylsilyl)methane, $\text{CH}_2(\text{Si}(\text{CH}_3)_3)_2$, as determined by electron diffraction: An unusually large SiCSi angle.' *J. Mol. Struct.*, Vol. **99**, p295-302 (1983).

29. Kriegsmann, H. 'Spectroscopic investigations of silicon compounds. II. Spectroscopic investigation of the Si-X-Si bond angle.' *Z. Elektrochem*, Vol. **8**, p1088-1094 (1957).
30. Hummel, J.P., Stackhouse, J., Mislow, K. 'Conformational analysis of polysilanes by the empirical force field method.' *Tetrahedron*, Vol. **33**, p1925-1930 (1977).
31. Ketelaar, J., *Chemical constitution*, Elsevier, Amsterdam (1953).
32. Mark, J.E., Ko, J.H. 'Configuration-dependent properties of poly(dimethylsilmethylene) chains. Correlation of theory and experiment.' *Macromolecules*, Vol. **8**, p874-878 (1975).
33. Calculations performed by author.
34. Mark, J.E., Ko, J.H. 'Configuration-dependent properties of poly(dimethylsilmethylene) chains. Experimental results.' *Macromolecules*, Vol. **8**, p869-874 (1975).
35. Kartsev, G.N., Syrkin, Y.K. 'Dipole moments of some organosilicon compounds.' *Izvest. Akad. Nauk. SSSR, Otdel. Khim. Nauk.*, Vol. **2**, p348-349 (1960).
36. Tribble, M.T., Allinger, N.L. 'Conformational analysis-LXXXIII. Calculation of the structures and energies of silanes by the method of molecular mechanics.' *Tetrahedron*, Vol. **28**, p2147-2156 (1972).
37. Streitwieser, A., Heathcock, C.H., *Introduction to organic chemistry*, Macmillan, New York (1985).
38. Sutton, C., Mark, J.E. 'Dipole moments of dimethylsiloxane oligomers and poly(dimethylsiloxane).' *J. Chem. Phys.*, Vol. **54**, p5011-5014 (1971).
39. Calculations performed by author.
40. Weyenberg, D.R., Nelson, L.E. 'Pt-catalysed reactions of silacyclobutanes and 1,3-disilacyclobutanes.' *J. Org. Chem.*, Vol. **30**, p2168-2121 (1965).
41. Bamford, W.R., Lovie, J.C., Watt, J.A.C. 'Preparation and properties of polysilmethylenes: Use of various compounds of group VIII metal catalysts.' *J. Chem Soc. (C)*, p1137-1140 (1966).
42. Nelkon, M., Parker, P., *Advanced level physics*, Heinemann (1982).
43. Debye, P., *Polar molecules*, Chem. Catalog., New York (1929).
44. Cole, R.H., Cole, K.S. 'Dispersion and absorption in dielectrics. Alternating current characteristics.' *J. Chem. Phys.* Vol. **9**, p341-351 (1941).
45. Davidson, D.W., Cole, R.H. 'Dielectric relaxation in glycerine.' *J. Chem. Phys.*, Vol. **18**, p1417 (1950).

46. Eyring, H. 'Viscosity, plasticity and diffusion (a) examples of absolute reaction rates.' J. Chem. Phys., Vol. 4, p283-291 (1936).
47. Interaction of metal salts with polyethers, F. Hakiempoor, PhD thesis, University of Aston (1985).
48. Handbook of chemistry and physics (52nd edition), The chemical rubber company (1971-1972).
49. Adachi, H., Adachi, K., Ishida, Y., Kotaka, K. 'Dielectric relaxation of poly(dimethylsiloxane).' J. Polym. Sci. Polm. Phys. Ed., Vol. 17, p851-857 (1979).
50. Dielectric relaxation of polysiloxanes and Kerr effect of p-phenylene vinylene oligomers, A.A. Goodwin, PhD thesis, University of Aston (1987).
51. Synder, R.G., Poore, M.W. 'Conformational Structure of Polyethylene Chains from the Infrared Spectroscopy of Partially Deuterated Polymer.' Macromolecules, Vol. 8, p708 (1973).
52. Ishigure, K., Ohashi, H., Tabata, Y., Oshima K. '¹⁹F and ¹H Nuclear Magnetic Resonances of Chlorotrifluorethylene-isobuthylene Copolymers.' Macromolecules, 9, p290 (1976).
53. Yoon, D.A., Suter, U.W., Flory, P.J. 'Conformational Characteristics of Poly(methylacrylate).' Macromolecules, 8, p784 (1975).
54. Yoon, D.A., Flory, P.J. 'Analysis of Nuclear Resonance Spectra of Protons in Predominantly Isotactic Polystyrene.' Macromolecules, 10, p562 (1977).
55. Tonelli, F.C., et al. 'Calculated and Measured ¹³C NMR Chemical Shifts of the 2,4,6-trichloroheptanes and their Implications for the ¹³C NMR Spectra of Poly(vinyl chloride).' Macromolecules, 12, p78 (1978).
56. Methods of Experimental Physics Vol. 16A. Academic Press Inc. (1980).
57. Beevers, M.S., Elliot, D.A., Williams, G. 'Molecular motion in melt samples of poly(propylene glycol) studied using dielectric and Kerr effect relaxation techniques.' Polymer, Vol. 21, p13-19 (1980).

APPENDIX A

THE USE OF EXPERIMENTAL TECHNIQUES TO DETERMINE CONFORMATIONAL BEHAVIOUR

A.1. Introduction

Presented in this appendix are a number of important experimental methods which have been used to determine the conformational behaviour of polymer molecules. They include infrared spectroscopy, high resolution N.M.R. spectroscopy and calorimetry techniques.

A.2 Infrared Spectroscopy

In many cases most of the infrared spectroscopic data regarding the conformation of a polymer is lost due to the overlap of the multitude of absorption bands produced by these large molecules to form continua. This usually limits the use of infrared spectroscopy as an analytical tool to investigate their conformational behaviour. However, in some situations this complexity may be by-passed by using deuterium substitution in order to uncouple and isolate a single vibration whose frequency exhibits a strong conformational dependence. In this way some aspects of the conformational structure of a polymer may be revealed from its infrared spectrum.

The infrared spectrum of deuterated polyethylene⁵¹ containing a low concentration (approx. 5%) of CD₂ groups is illustrated in Figure (A-1). In this spectrum the bands associated with the presence of trans-trans and trans-gauche bonds appear in the region 800-500 cm⁻¹.

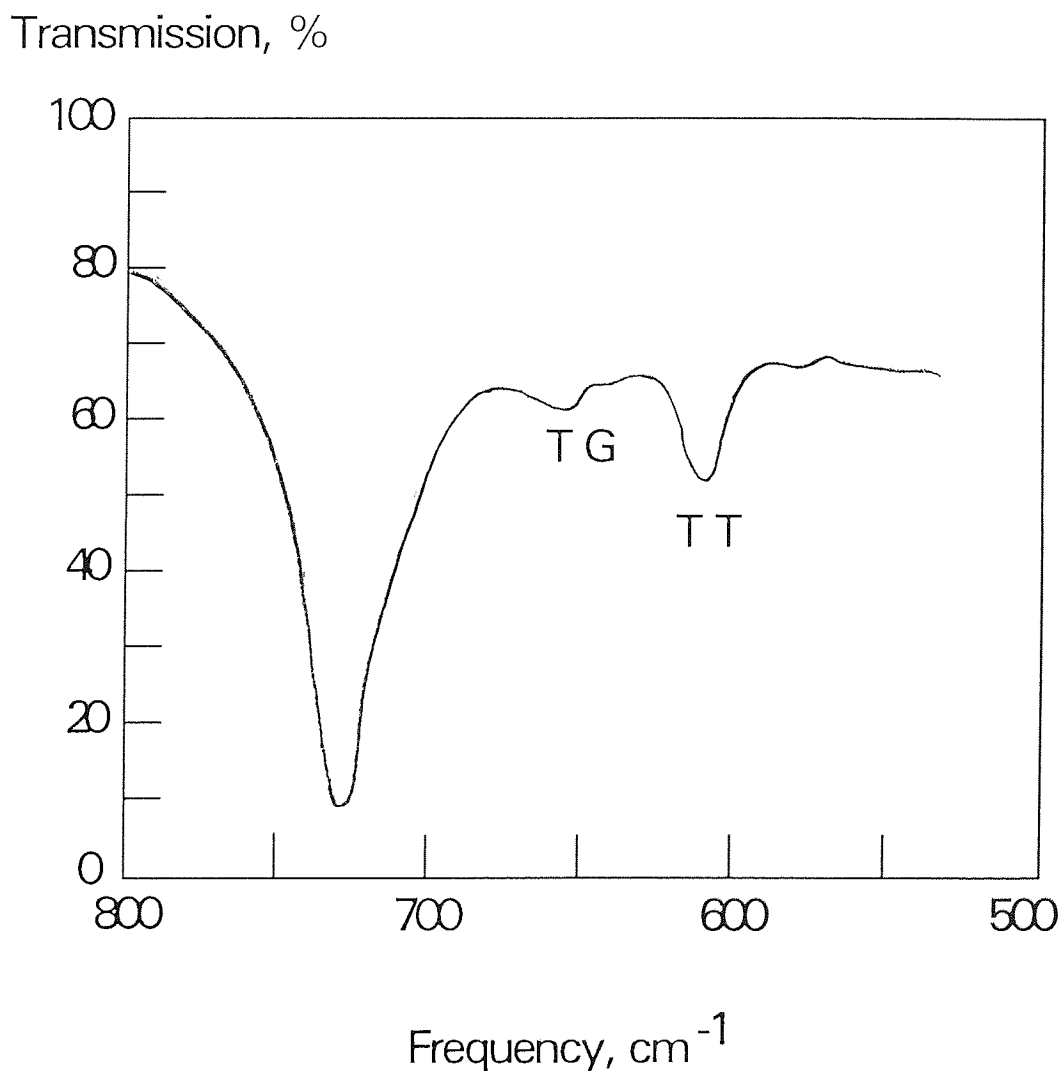


Figure (A-1). Infrared spectrum of CD₂-doped polyethylene⁵¹ at 120°C.

In this case the vibration of interest is a methylene rocking mode which for a CH₂ group is essentially the motion of the hydrogen atoms. The mass

effect resulting from deuterium substitution reduces the frequency of this mode by a factor of approximately $2^{-1/2}$ so that the rocking mode of an isolated CD_2 group in an extended chain occurs at a frequency $\sim 620 \text{ cm}^{-1}$, well below the absorption band for the methylene rocking mode in the undeuterated polymer chain. Because of the mild coupling between the CD_2 group and its two immediate CH_2 neighbours, the frequency of the CD_2 rocking mode is significantly dependent upon the conformation of the bonds connecting these neighbours to the CD_2 group. If the adjoining bonds are both trans, the frequency of the rocking mode is 622 cm^{-1} . However, when one bond is in the trans conformation while the other is in the gauche conformation, the frequency of the rocking mode occurs at 652 cm^{-1} .

When this technique is applied to polymers over a range of temperatures, the ratio of the concentration of TT and TG pairs can be determined. In the case of polyethylene, as the temperature is increased there is a significant increase in the concentration of the TG pairs even before the melting point of the polymer is reached. In the liquid state, the ratio of the concentration of TT and TG pairs can be determined, and is found to be somewhat higher than that calculated using the rotational isomeric state model². Thus this method can not only be used to identify bond conformers but also to measure their relative concentrations.

This same technique has been employed to study the conformational behaviour of crystalline polyethylene. For this purpose, the spectra of

samples doped with CD_2CD_2 entities provides additional information in that the rocking mode frequencies of this isotopic impurity are dependent upon the conformation of three adjoining bonds.

A very useful quantity, the spectroscopic entropy, may also be determined from infrared spectroscopy. When this quantity is compared with the value determined from measurements of the heat capacity of a substance (see section A.3.), any disagreement between the two can indicate the presence of a rotational barrier to rotation.

A.3. High Resolution N.M.R. Spectroscopy

Polymer molecules may exist in any or all of their possible conformations at any one time. The rate of their interconversion between different conformational states is quite rapid when compared to the N.M.R. timescale. In general, the freezing out of conformers at low temperatures, in order to slow this rate of interconversion and observe their N.M.R. spectra, has not been feasible for polymers since the rotational barriers between different conformers is usually small. An additional difficulty arises from the poor resolution obtained from polymers in solution. For these reasons, the use of N.M.R. data to obtain conformational information for polymers has not been as successful as for smaller organic molecules.

However, some information regarding their conformational behaviour may be obtained from the measurement of the coupling constants related to the polymers structure. An example of the conformational data obtained from

N.M.R. coupling constants is the study of the ^{19}F and ^1H N.M.R. spectra of chlorotrifluoroethylene-isobutylene alternating copolymers⁵². A section of chlorotrifluoroethylene-isobutylene is illustrated in Figure (A-2). By assuming a familiar three-fold rotational potential for the bond between the $\text{C}(\text{Cl})(\text{F})$ and CH_2 skeletal carbon atoms, the possible conformational states for this bond are simply trans(t), gauche⁺(g⁺) and gauche⁻(g⁻).

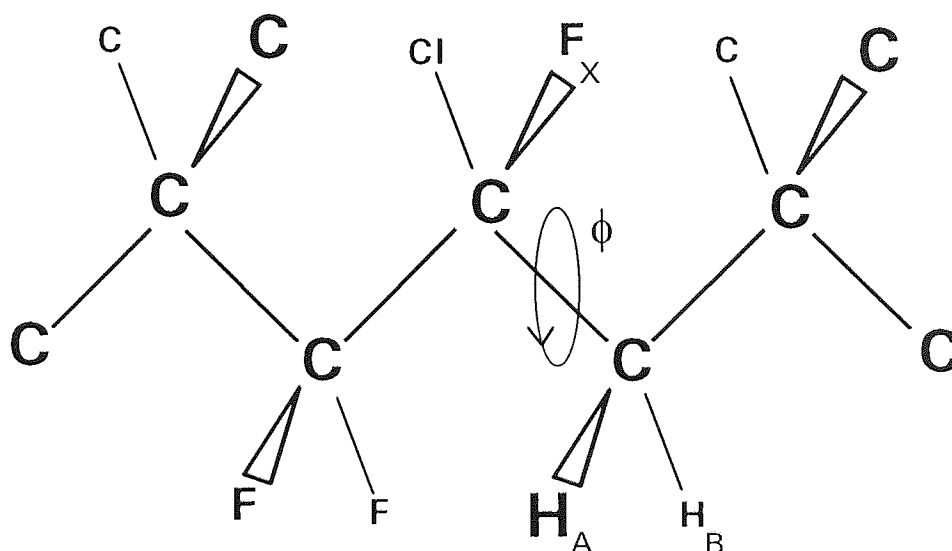


Figure (A-2). Trans conformation of a section of chlorotrifluoroethylene-isobutylene copolymer.

The observed H-F coupling constants⁵² for this structure are $J_{\text{AX}} = 0.5 \pm 1$ Hz and $J_{\text{BX}} = 33.5 \pm 1$ Hz. These values are in fact the conformationally averaged coupling constants for the three conformations t, g⁺ and g⁻. By assigning a probability factor to each conformational state, the specific values for the trans and gauche couplings may be individually

determined. In the case of the above example, calculations have indicated $J_g \ll J_t$ suggesting a dominance of trans conformations for these particular bonds in the structure.

An alternative approach to correlating N.M.R. coupling constants and conformational behaviour is to predict the magnitude of the coupling between atoms from conformational populations based on the rotational isomeric state approximation⁵³. This type of investigation has been undertaken by several workers including Flory and Yoon⁵⁴, and Tonelli et al⁵⁵.

A.3. Calorimetry

The determination of the enthalpy and entropy associated with flexible molecules from calorimetry measurements can uncover many facts regarding their conformational behaviour.

The enthalpy of combustion of most compounds may be determined by placing a sample of the compound in a bomb under a pressure of oxygen and igniting it. The bomb is enclosed in a calorimeter so that its change in temperature may be determined. Provided that the heat capacity of the system is known, the observed temperature increase corresponds to the amount of heat released by the combustion of the sample.

The entropy of a polymer may be determined calorimetrically by measuring its heat capacity. Most substances form crystals at absolute zero which are perfectly ordered, and hence the entropy of the substance may be assumed to be zero. By cooling the sample to as near absolute zero as

possible, then adding heat in measured increments and noting the temperature rise, the entropy of the sample may be determined up to room temperature which is adequate for most purposes.

When the calorimetric entropy, determined as above, and the spectroscopic entropy are compared, they are often found to be identical. Frequently, however, it is found that the calorimetric value is somewhat lower. These occurrences are usually the result of assuming free rotation about a single bond in the calculation of the calorimetric entropy. In real molecules a barrier to rotation often exists, the amount of restriction being dependent upon the height of the rotational barrier. Thus, a thermodynamic method for determining rotational barriers consists of calculating the barrier height which will bring the calorimetric and spectroscopic entropies into agreement. Teller and Topley⁵⁶ used this argument to suggest, as early as 1935, that in ethane a three-fold rotational barrier to rotation would reconcile most of the then available experimental data.

To date, the heights of many rotational barriers have subsequently been determined in this way.

APPENDIX B

COMPUTER SIMULATION OF POLY(DIMETHYLSILMETHYLENE) AND POLY(DIMETHYLSILETHENE)

B.1. Introduction

Presented in this appendix are the computer programs used to generate the conformational energy maps for poly(dimethylsilmethylene) and poly(dimethylsilethene), illustrated in Figures (4-3) and (5-8) respectively.

Both of the programs presented in this appendix were written in Vax Fortran and were run on the VAX 8650 mainframe computer in the Department of Computer Science, Aston University.

B.2. A Brief Description of the Important Subroutines

SUBROUTINES CCXYZ AND HHXYZ

These subroutines calculate the positions, in vectorial format (X,Y,Z), of all the atoms in Figures (4-2) and (5-6) relative to the first skeletal atom. By calculating the position of each atom in this way, the corresponding interatomic distances may be determined.

SUBROUTINE XX_DIST

This set of subroutines where XX may equal HH, SH, CH, CC, CH or SS calculates the interatomic distances of the hydrogen (H), silicon (S), carbon (C) atoms that are dependent upon the rotation angles ϕ_a and ϕ_b .

SUBROUTINE XX_ENERGY

These subroutines where XX may equal HH, SH, CH, CC, CH or SS calculate the interaction energies from the interatomic distances using the Lennard-Jones (6-12) potential.

SUBROUTINES E_TOR AND E_TOR1

These two subroutines calculate the contribution to the conformational energy from torsional rotations about ϕ_a and ϕ_b , and the branched methyl groups respectively.

SUBROUTINE T_MAT

This subroutine calculates the values of the transformation matrix from bond angle supplements ($180^\circ - \theta$, where $\theta = \text{Bond Angle}$) and bond rotation angles ϕ_a and ϕ_b , according to Eq. (2-20).

B.3. Computer Simulation of Poly(dimethylsilmethylene): Program Listing.

```
DIMENSION TMAT(3,3),TMAT1(3,3),TMAT2(3,3)
DIMENSION XYZ(3),CXYZ(3,5),HXYZ(3,22)
DIMENSION AXYZ(3,27),XPHI(4),XPHI1(4),APHI(6)
DIMENSION SC(6),SH(16),CC(9),CH(108),HH(138)
OPEN(1,FILE = 'ENERGY1.DAT',STATUS = 'NEW')
OPEN(2,FILE = 'ROTATE.DAT',STATUS = 'NEW')
XPI = 3.14159265359
XPHI(1) = 0.
XPHI(4) = 0.
CALL SET_XYZ(CXYZ,HXYZ)
DO 5 A = 0,360,10
XPHI(2) = A*(XPI/180.)
DO 10 B = 0,360,10
XPHI(3) = B*(XPI/180.)
ETOTAL = 100000000000.
CALL CCXYZ(CXYZ,XPHI,XYZ,TMAT,TMAT1)
CALL HHXYZ(CXYZ,HXYZ,XPHI,XYZ,TMAT,TMAT1)
CALL HHXYZ1(CXYZ,HXYZ,XPHI,XYZ,TMAT,TMAT1)
CALL ORG_XYZ(AXYZ,CXYZ,HXYZ)
CALL CC_DIST(CC,AXYZ)
CALL SC_DIST(SC,AXYZ)
CALL E_TOR(XPHI,ETOR)
CALL CC_ENERGY(CC,CCENERGY)
CALL SC_ENERGY(SC,SCENERGY)
DO 15 C = 0,120,5
XPHI1(1) = C*(XPI/180.)
DO 20 D = 0,120,5
XPHI1(2) = D*(XPI/180.)
DO 25 E = 0,120,5
XPHI1(3) = E*(XPI/180.)
DO 30 F = 0,120,5
XPHI1(4) = F*(XPI/180.)
CALL HHXYZ2(CXYZ,HXYZ,XPHI,XYZ,TMAT,TMAT1,XPHI1)
CALL HHXYZ3(CXYZ,HXYZ,XPHI,XYZ,TMAT,TMAT1,XPHI1)
CALL ORG1_XYZ(AXYZ,CXYZ,HXYZ)
CALL CH_DIST(CH,AXYZ)
CALL SH_DIST(SH,AXYZ)
CALL HH_DIST(HH,AXYZ)
CALL CH_ENERGY(CH,CHENERGY)
CALL SH_ENERGY(SH,SHENERGY)
CALL HH_ENERGY(HH,HHENERGY)
CALL E_TOR1(XPHI1,ETOR1)
ETOTAL1 = ETOR + ETOR1 + CCENERGY + SCENERGY + CHENERGY + SHENERGY +
HHENERGY
IF (ETOTAL1 .LT. ETOTAL) THEN
  ETOTAL = ETOTAL1
  APHI(1) = A
  APHI(2) = B
  APHI(3) = C
  APHI(4) = D
  APHI(5) = E
  APHI(6) = F
ENDIF
```

```

30 CONTINUE
25 CONTINUE
20 CONTINUE
15 CONTINUE
   CALL O_PUT(APHI,ETOTAL)
10 CONTINUE
5  CONTINUE
   CLOSE (1)
   CLOSE (2)
   END

```

```

SUBROUTINE TEST(AXYZ)
DIMENSION AXYZ(3,27)
AA = 3
BB = 23
CC = 5
DD = 23
YY = (AXYZ(1,AA)-AXYZ(1,BB))**2 + (AXYZ(2,AA)-AXYZ(2,BB))**2
YY = (YY + (AXYZ(3,AA)-AXYZ(3,BB))**2)**0.5
ZZ = (AXYZ(1,CC)-AXYZ(1,DD))**2 + (AXYZ(2,CC)-AXYZ(2,DD))**2
ZZ = (ZZ + (AXYZ(3,CC)-AXYZ(3,DD))**2)**0.5
PRINT*,YY,ZZ
RETURN
END

```

```

SUBROUTINE O_PUT(APHI,ETOTAL)
DIMENSION APhi(6)
XPI = 3.14159265359
WRITE(1,*) APhi(1),APhi(2),ETOTAL
WRITE(2,*) APhi(3),APhi(4),APhi(5),APhi(6)
PRINT*,APhi(1),APhi(2)
RETURN
END

```

```

SUBROUTINE HH_DIST(HH,AXYZ)
DIMENSION AXYZ(3,27),HH(138)
DO 5 A = 12,27
   HH(A-11) = (AXYZ(1,10)-AXYZ(1,A))**2 + (AXYZ(2,10)-AXYZ(2,A))**2
   HH(A-11) = (HH(A-11) + (AXYZ(3,10)-AXYZ(3,A))**2)**0.5
   HH(A+5) = (AXYZ(1,11)-AXYZ(1,A))**2 + (AXYZ(2,11)-AXYZ(2,A))**2
   HH(A+5) = (HH(A+5) + (AXYZ(3,11)-AXYZ(3,A))**2)**0.5
5  CONTINUE
DO 10 A = 14,27
   HH(A+19) = (AXYZ(1,12)-AXYZ(1,A))**2 + (AXYZ(2,12)-AXYZ(2,A))**2
   HH(A+19) = (HH(A+19) + (AXYZ(3,12)-AXYZ(3,A))**2)**0.5
   HH(A+33) = (AXYZ(1,13)-AXYZ(1,A))**2 + (AXYZ(2,13)-AXYZ(2,A))**2
   HH(A+33) = (HH(A+33) + (AXYZ(3,13)-AXYZ(3,A))**2)**0.5
10 CONTINUE
DO 15 A = 16,27
   HH(A+45) = (AXYZ(1,14)-AXYZ(1,A))**2 + (AXYZ(2,14)-AXYZ(2,A))**2
   HH(A+45) = (HH(A+45) + (AXYZ(3,14)-AXYZ(3,A))**2)**0.5
   HH(A+57) = (AXYZ(1,15)-AXYZ(1,A))**2 + (AXYZ(2,15)-AXYZ(2,A))**2
   HH(A+57) = (HH(A+57) + (AXYZ(3,15)-AXYZ(3,A))**2)**0.5
15 CONTINUE
DO 20 A = 19,27
   HH(A+66) = (AXYZ(1,16)-AXYZ(1,A))**2 + (AXYZ(2,16)-AXYZ(2,A))**2
   HH(A+66) = (HH(A+66) + (AXYZ(3,16)-AXYZ(3,A))**2)**0.5

```



```

HH(A + 75) = (AXYZ(1,17)-AXYZ(1,A))**2 + (AXYZ(2,17)-AXYZ(2,A))**2
HH(A + 75) = (HH(A + 75) + (AXYZ(3,17)-AXYZ(3,A))**2)**0.5
HH(A + 84) = (AXYZ(1,18)-AXYZ(1,A))**2 + (AXYZ(2,18)-AXYZ(2,A))**2
HH(A + 84) = (HH(A + 84) + (AXYZ(3,18)-AXYZ(3,A))**2)**0.5
20  CONTINUE
DO 25 A = 22,27
  HH(A + 90) = (AXYZ(1,19)-AXYZ(1,A))**2 + (AXYZ(2,19)-AXYZ(2,A))**2
  HH(A + 90) = (HH(A + 90) + (AXYZ(3,19)-AXYZ(3,A))**2)**0.5
  HH(A + 96) = (AXYZ(1,20)-AXYZ(1,A))**2 + (AXYZ(2,20)-AXYZ(2,A))**2
  HH(A + 96) = (HH(A + 96) + (AXYZ(3,20)-AXYZ(3,A))**2)**0.5
  HH(A + 102) = (AXYZ(1,21)-AXYZ(1,A))**2 + (AXYZ(2,21)-AXYZ(2,A))**2
  HH(A + 102) = (HH(A + 102) + (AXYZ(3,21)-AXYZ(3,A))**2)**0.5
25  CONTINUE
DO 30 A = 25,27
  HH(A + 105) = (AXYZ(1,22)-AXYZ(1,A))**2 + (AXYZ(2,22)-AXYZ(2,A))**2
  HH(A + 105) = (HH(A + 105) + (AXYZ(3,22)-AXYZ(3,A))**2)**0.5
  HH(A + 108) = (AXYZ(1,23)-AXYZ(1,A))**2 + (AXYZ(2,23)-AXYZ(2,A))**2
  HH(A + 108) = (HH(A + 108) + (AXYZ(3,23)-AXYZ(3,A))**2)**0.5
  HH(A + 111) = (AXYZ(1,24)-AXYZ(1,A))**2 + (AXYZ(2,24)-AXYZ(2,A))**2
  HH(A + 111) = (HH(A + 111) + (AXYZ(3,24)-AXYZ(3,A))**2)**0.5
30  CONTINUE
RETURN
END

SUBROUTINE SH_DIST(SH,AXYZ)
DIMENSION SH(16),AXYZ(3,27)
DO 5 A = 10,11
  SH(A-9) = (AXYZ(1,4)-AXYZ(1,A))**2 + (AXYZ(2,4)-AXYZ(2,A))**2
  SH(A-9) = (SH(A-9) + (AXYZ(3,4)-AXYZ(3,A))**2)**0.5
5  CONTINUE
DO 10 A = 14,15
  SH(A-11) = (AXYZ(1,2)-AXYZ(1,A))**2 + (AXYZ(2,2)-AXYZ(2,A))**2
  SH(A-11) = (SH(A-11) + (AXYZ(3,2)-AXYZ(3,A))**2)**0.5
10  CONTINUE
DO 15 A = 22,24
  SH(A-17) = (AXYZ(1,2)-AXYZ(1,A))**2 + (AXYZ(2,2)-AXYZ(2,A))**2
  SH(A-17) = (SH(A-17) + (AXYZ(3,2)-AXYZ(3,A))**2)**0.5
15  CONTINUE
DO 20 A = 25,27
  SH(A-17) = (AXYZ(1,2)-AXYZ(1,A))**2 + (AXYZ(2,2)-AXYZ(2,A))**2
  SH(A-17) = (SH(A-17) + (AXYZ(3,2)-AXYZ(3,A))**2)**0.5
20  CONTINUE
DO 25 A = 16,18
  SH(A-5) = (AXYZ(1,4)-AXYZ(1,A))**2 + (AXYZ(2,4)-AXYZ(2,A))**2
  SH(A-5) = (SH(A-5) + (AXYZ(3,4)-AXYZ(3,A))**2)**0.5
25  CONTINUE
DO 30 A = 19,21
  SH(A-5) = (AXYZ(1,4)-AXYZ(1,A))**2 + (AXYZ(2,4)-AXYZ(2,A))**2
  SH(A-5) = (SH(A-5) + (AXYZ(3,4)-AXYZ(3,A))**2)**0.5
30  CONTINUE
RETURN
END

SUBROUTINE CH_DIST(CH,AXYZ)
DIMENSION CH(108),AXYZ(3,27)
DO 5 A = 12,13
  CH(A-11) = (AXYZ(1,A)**2 + AXYZ(2,A)**2 + AXYZ(3,A)**2)**0.5

```

```

CH(A-9) = (AXYZ(1,5)-AXYZ(1,A))**2 + (AXYZ(2,5)-AXYZ(2,A))**2
CH(A-9) = (CH(A-9) + (AXYZ(3,5)-AXYZ(3,A))**2)**0.5
CH(A-7) = (AXYZ(1,6)-AXYZ(1,A))**2 + (AXYZ(2,6)-AXYZ(2,A))**2
CH(A-7) = (CH(A-7) + (AXYZ(3,6)-AXYZ(3,A))**2)**0.5
CH(A-5) = (AXYZ(1,7)-AXYZ(1,A))**2 + (AXYZ(2,7)-AXYZ(2,A))**2
CH(A-5) = (CH(A-5) + (AXYZ(3,7)-AXYZ(3,A))**2)**0.5
CH(A-3) = (AXYZ(1,8)-AXYZ(1,A))**2 + (AXYZ(2,8)-AXYZ(2,A))**2
CH(A-3) = (CH(A-3) + (AXYZ(3,8)-AXYZ(3,A))**2)**0.5
CH(A-1) = (AXYZ(1,9)-AXYZ(1,A))**2 + (AXYZ(2,9)-AXYZ(2,A))**2
CH(A-1) = (CH(A-1) + (AXYZ(3,9)-AXYZ(3,A))**2)**0.5
5  CONTINUE
DO 10 A = 10,11
CH(A + 3) = (AXYZ(1,3)-AXYZ(1,A))**2 + (AXYZ(2,3)-AXYZ(2,A))**2
CH(A + 3) = (CH(A + 3) + (AXYZ(3,3)-AXYZ(3,A))**2)**0.5
CH(A + 5) = (AXYZ(1,5)-AXYZ(1,A))**2 + (AXYZ(2,5)-AXYZ(2,A))**2
CH(A + 5) = (CH(A + 5) + (AXYZ(3,5)-AXYZ(3,A))**2)**0.5
CH(A + 7) = (AXYZ(1,6)-AXYZ(1,A))**2 + (AXYZ(2,6)-AXYZ(2,A))**2
CH(A + 7) = (CH(A + 7) + (AXYZ(3,6)-AXYZ(3,A))**2)**0.5
CH(A + 9) = (AXYZ(1,7)-AXYZ(1,A))**2 + (AXYZ(2,7)-AXYZ(2,A))**2
CH(A + 9) = (CH(A + 9) + (AXYZ(3,7)-AXYZ(3,A))**2)**0.5
CH(A + 11) = (AXYZ(1,8)-AXYZ(1,A))**2 + (AXYZ(2,8)-AXYZ(2,A))**2
CH(A + 11) = (CH(A + 11) + (AXYZ(3,8)-AXYZ(3,A))**2)**0.5
CH(A + 13) = (AXYZ(1,9)-AXYZ(1,A))**2 + (AXYZ(2,9)-AXYZ(2,A))**2
CH(A + 13) = (CH(A + 13) + (AXYZ(3,9)-AXYZ(3,A))**2)**0.5
10 CONTINUE
DO 15 A = 14,15
CH(A + 11) = (AXYZ(1,A)**2 + AXYZ(2,A)**2 + AXYZ(3,A)**2)**0.5
CH(A + 13) = (AXYZ(1,3)-AXYZ(1,A))**2 + (AXYZ(2,3)-AXYZ(2,A))**2
CH(A + 13) = (CH(A + 13) + (AXYZ(3,3)-AXYZ(3,A))**2)**0.5
CH(A + 15) = (AXYZ(1,6)-AXYZ(1,A))**2 + (AXYZ(2,6)-AXYZ(2,A))**2
CH(A + 15) = (CH(A + 15) + (AXYZ(3,6)-AXYZ(3,A))**2)**0.5
CH(A + 17) = (AXYZ(1,7)-AXYZ(1,A))**2 + (AXYZ(2,7)-AXYZ(2,A))**2
CH(A + 17) = (CH(A + 17) + (AXYZ(3,7)-AXYZ(3,A))**2)**0.5
CH(A + 19) = (AXYZ(1,8)-AXYZ(1,A))**2 + (AXYZ(2,8)-AXYZ(2,A))**2
CH(A + 19) = (CH(A + 19) + (AXYZ(3,8)-AXYZ(3,A))**2)**0.5
CH(A + 21) = (AXYZ(1,9)-AXYZ(1,A))**2 + (AXYZ(2,9)-AXYZ(2,A))**2
CH(A + 21) = (CH(A + 21) + (AXYZ(3,9)-AXYZ(3,A))**2)**0.5
15 CONTINUE
DO 20 A = 16,27
CH(A + 21) = (AXYZ(1,A)**2 + AXYZ(2,A)**2 + AXYZ(3,A)**2)**0.5
CH(A + 33) = (AXYZ(1,3)-AXYZ(1,A))**2 + (AXYZ(2,3)-AXYZ(2,A))**2
CH(A + 33) = (CH(A + 33) + (AXYZ(3,3)-AXYZ(3,A))**2)**0.5
CH(A + 45) = (AXYZ(1,5)-AXYZ(1,A))**2 + (AXYZ(2,5)-AXYZ(2,A))**2
CH(A + 45) = (CH(A + 45) + (AXYZ(3,5)-AXYZ(3,A))**2)**0.5
20 CONTINUE
DO 25 A = 19,27
CH(A + 54) = (AXYZ(1,6)-AXYZ(1,A))**2 + (AXYZ(2,6)-AXYZ(2,A))**2
CH(A + 54) = (CH(A + 54) + (AXYZ(3,6)-AXYZ(3,A))**2)**0.5
25 CONTINUE
DO 30 A = 16,18
CH(A + 66) = (AXYZ(1,7)-AXYZ(1,A))**2 + (AXYZ(2,7)-AXYZ(2,A))**2
CH(A + 66) = (CH(A + 66) + (AXYZ(3,7)-AXYZ(3,A))**2)**0.5
30 CONTINUE
DO 35 A = 22,27
CH(A + 63) = (AXYZ(1,7)-AXYZ(1,A))**2 + (AXYZ(2,7)-AXYZ(2,A))**2
CH(A + 63) = (CH(A + 63) + (AXYZ(3,7)-AXYZ(3,A))**2)**0.5
35 CONTINUE

```

```

DO 40 A = 16,21
  CH(A + 75) = (AXYZ(1,8)-AXYZ(1,A))**2 + (AXYZ(2,8)-AXYZ(2,A))**2
  CH(A + 75) = (CH(A + 75) + (AXYZ(3,8)-AXYZ(3,A))**2)**0.5
40  CONTINUE
DO 45 A = 25,27
  CH(A + 72) = (AXYZ(1,8)-AXYZ(1,A))**2 + (AXYZ(2,8)-AXYZ(2,A))**2
  CH(A + 72) = (CH(A + 72) + (AXYZ(3,8)-AXYZ(3,A))**2)**0.5
45  CONTINUE
DO 50 A = 16,24
  CH(A + 84) = (AXYZ(1,9)-AXYZ(1,A))**2 + (AXYZ(2,9)-AXYZ(2,A))**2
  CH(A + 84) = (CH(A + 84) + (AXYZ(3,9)-AXYZ(3,A))**2)**0.5
50  CONTINUE
RETURN
END

```

```

SUBROUTINE CC_DIST(CC,AXYZ)
DIMENSION CC(9),AXYZ(3,27)
CC(1) = (AXYZ(1,5)**2 + AXYZ(2,5)**2 + AXYZ(3,5)**2)**0.5
DO 5 A = 8,9
  CC(A-6) = (AXYZ(1,A)**2 + AXYZ(2,A)**2 + AXYZ(3,A)**2)**0.5
5  CONTINUE
DO 10 A = 6,7
  CC(A-2) = (AXYZ(1,5)-AXYZ(1,A))**2 + (AXYZ(2,5)-AXYZ(2,A))**2
  CC(A-2) = (CC(A-2) + (AXYZ(3,5)-AXYZ(3,A))**2)**0.5
10 CONTINUE
DO 15 A = 8,9
  CC(A-2) = (AXYZ(1,6)-AXYZ(1,A))**2 + (AXYZ(2,6)-AXYZ(2,A))**2
  CC(A-2) = (CC(A-2) + (AXYZ(3,6)-AXYZ(3,A))**2)**0.5
  CC(A) = (AXYZ(1,7)-AXYZ(1,A))**2 + (AXYZ(2,7)-AXYZ(2,A))**2
  CC(A) = (CC(A) + (AXYZ(3,7)-AXYZ(3,A))**2)**0.5
15 CONTINUE
RETURN
END

```

```

SUBROUTINE SC_DIST(SC,AXYZ)
DIMENSION SC(6),AXYZ(3,27)
SC(1) = (AXYZ(1,4)**2 + AXYZ(2,4)**2 + AXYZ(3,4)**2)**0.5
SC(2) = (AXYZ(1,5)-AXYZ(1,2))**2 + (AXYZ(2,5)-AXYZ(2,2))**2
SC(2) = (SC(2) + (AXYZ(3,5)-AXYZ(3,2))**2)**0.5
DO 5 A = 6,7
  SC(A-3) = (AXYZ(1,4)-AXYZ(1,A))**2 + (AXYZ(2,4)-AXYZ(2,A))**2
  SC(A-3) = (SC(A-3) + (AXYZ(3,4)-AXYZ(3,A))**2)**0.5
5  CONTINUE
DO 10 A = 8,9
  SC(A-3) = (AXYZ(1,2)-AXYZ(1,A))**2 + (AXYZ(2,2)-AXYZ(2,A))**2
  SC(A-3) = (SC(A-3) + (AXYZ(3,2)-AXYZ(3,A))**2)**0.5
10 CONTINUE
RETURN
END

```

```

SUBROUTINE CH_ENERGY(CH,CHENERGY)
DIMENSION CH(108)
CHENERGY = 0.
A3 = 5.63*(10**4)
C3 = 127.
DO 5 A = 1,108
  CHENERGY = CHENERGY + (A3/(CH(A)**12))-(C3/(CH(A)**6))

```

```

5  CONTINUE
   RETURN
   END

   SUBROUTINE HH_ENERGY(HH,HHENERGY)
   DIMENSION HH(138)
   HHENERGY = 0.
   A2 = 7.27*(10**3)
   C2 = 47.1
   DO 5 A = 1,138
     HHENERGY = HHENERGY + (A2/(HH(A)**12))-(C2/(HH(A)**6))
5  CONTINUE
   RETURN
   END

   SUBROUTINE CC_ENERGY(CC,CCENERGY)
   DIMENSION CC(9)
   CCENERGY = 0.
   A1 = 3.95*(10**5)
   C1 = 363.
   DO 5 A = 1,9
     CCENERGY = CCENERGY + (A1/(CC(A)**12))-(C1/(CC(A)**6))
5  CONTINUE
   RETURN
   END

   SUBROUTINE SC_ENERGY(SC,SCENERGY)
   DIMENSION SC(6)
   SCENERGY = 0.
   A4 = 1.71*(10**6)
   C4 = 1050.
   DO 5 A = 1,6
     SCENERGY = SCENERGY + (A4/(SC(A)**12))-(C4/(SC(A)**6))
5  CONTINUE
   RETURN
   END

   SUBROUTINE SH_ENERGY(SH,SHENERGY)
   DIMENSION SH(16)
   SHENERGY = 0.
   A5 = 2.62*(10**5)
   C5 = 371.4
   DO 5 A = 1,16
     SHENERGY = SHENERGY + (A5/(SH(A)**12))-(C5/(SH(A)**6))
5  CONTINUE
   RETURN
   END

   SUBROUTINE E_TOR(XPHI,ETOR)
   DIMENSION XPHI(4)
   ETOR = 0.
   DO 5 A = 2,3
     ETOR = ETOR + (0.5/2)*(1-COS(3.*XPHI(A)))
5  CONTINUE
   RETURN
   END

```

```

SUBROUTINE E_TOR1(XPHI1,ETOR1)
DIMENSION XPHI1(4)
ETOR1 = 0.
DO 5 A = 1,4
  ETOR1 = ETOR1 + (0.5/2)*(1-COS(3.*XPHI1(A)))
5  CONTINUE
RETURN
END

SUBROUTINE ORG_XYZ(AXYZ,CXYZ,HXYZ)
DIMENSION AXYZ(3,27),CXYZ(3,5),HXYZ(3,22)
DO 5 A = 1,5
  AXYZ(1,A) = CXYZ(1,A)
  AXYZ(2,A) = CXYZ(2,A)
  AXYZ(3,A) = CXYZ(3,A)
5  CONTINUE
DO 10 A = 1,3
  AXYZ(A,6) = HXYZ(A,2)
  AXYZ(A,7) = HXYZ(A,7)
  AXYZ(A,8) = HXYZ(A,4)
  AXYZ(A,9) = HXYZ(A,9)
  AXYZ(A,10) = HXYZ(A,1)
  AXYZ(A,11) = HXYZ(A,6)
  AXYZ(A,12) = HXYZ(A,3)
  AXYZ(A,13) = HXYZ(A,8)
  AXYZ(A,14) = HXYZ(A,5)
  AXYZ(A,15) = HXYZ(A,10)
10 CONTINUE
RETURN
END

SUBROUTINE ORG1_XYZ(AXYZ,CXYZ,HXYZ)
DIMENSION AXYZ(3,27),CXYZ(3,5),HXYZ(3,22)
DO 5 A = 1,3
  AXYZ(A,16) = HXYZ(A,11)
  AXYZ(A,17) = HXYZ(A,12)
  AXYZ(A,18) = HXYZ(A,13)
  AXYZ(A,19) = HXYZ(A,14)
  AXYZ(A,20) = HXYZ(A,15)
  AXYZ(A,21) = HXYZ(A,16)
  AXYZ(A,22) = HXYZ(A,17)
  AXYZ(A,23) = HXYZ(A,18)
  AXYZ(A,24) = HXYZ(A,19)
  AXYZ(A,25) = HXYZ(A,20)
  AXYZ(A,26) = HXYZ(A,21)
  AXYZ(A,27) = HXYZ(A,22)
5  CONTINUE
RETURN
END

SUBROUTINE HHXYZ3(CXYZ,HXYZ,XPHI,XYZ,TMAT,TMAT1,XPHI1)
DIMENSION CXYZ(3,5),HXYZ(3,22),XPHI(4),XYZ(3)
DIMENSION TMAT(3,3),TMAT1(3,3),XPHI1(4)
XPI = 3.14159265359
THETA1 = 67.6*(XPI/180.)
THETA2 = 56.8*(XPI/180.)
THETA3 = 70.*(XPI/180.)

```

```

XYZ(1) = 1.101
XYZ(2) = 0.
XYZ(3) = 0.
DO 5 A = 1,2
  IF (A .EQ. 1) THEN
    ZPHI1 = XPHI1(3)-(2.15*(XPI/180.))
    ZPHI = XPHI(1)
    CALL T_MAT(TMAT,ZPHI,THETA1)
    DO 10 B = 1,3
      DO 15 C = 1,3
        TMAT1(B,C) = TMAT(B,C)
15      CONTINUE
10      CONTINUE
    ZPHI = XPHI(2)
    CALL T_MAT(TMAT,ZPHI,THETA2)
    CALL T_SQR(TMAT,TMAT1)
    ZPHI = XPHI(3) + (122.93*(XPI/180.))
    CALL T_MAT(TMAT,ZPHI,THETA3)
    CALL T_SQR(TMAT,TMAT1)
  ENDIF
  IF (A .EQ. 2) THEN
    ZPHI1 = XPHI1(4) + (2.15*(XPI/180.))
    ZPHI = XPHI(1)
    CALL T_MAT(TMAT,ZPHI,THETA1)
    DO 20 B = 1,3
      DO 25 C = 1,3
        TMAT1(B,C) = TMAT(B,C)
25      CONTINUE
20      CONTINUE
    ZPHI = XPHI(2)
    CALL T_MAT(TMAT,ZPHI,THETA2)
    CALL T_SQR(TMAT,TMAT1)
    ZPHI = XPHI(3) + (237.07*(XPI/180.))
    CALL T_MAT(TMAT,ZPHI,THETA3)
    CALL T_SQR(TMAT,TMAT1)
  ENDIF
DO 30 D = 1,3
  IF (D .EQ. 1) THEN
    ZPHI = ZPHI1
    CALL T_MAT(TMAT,ZPHI,THETA3)
    CALL T_SQR1(TMAT,TMAT1)
  ENDIF
  IF (D .EQ. 2) THEN
    ZPHI = (120.*(XPI/180.)) + ZPHI1
    CALL T_MAT(TMAT,ZPHI,THETA3)
    CALL T_SQR1(TMAT,TMAT1)
  ENDIF
  IF (D .EQ. 3) THEN
    ZPHI = (240.*(XPI/180.)) + ZPHI1
    CALL T_MAT(TMAT,ZPHI,THETA3)
    CALL T_SQR1(TMAT,TMAT1)
  ENDIF
  XXX = 0.
  YYY = 0.
  ZZZ = 0.
DO 35 B = 1,3
  XXX = XXX + TMAT(1,B)*XYZ(B)

```

```

        YYY = YYY + TMAT(2,B)*XYZ(B)
        ZZZ = ZZZ + TMAT(3,B)*XYZ(B)
35    CONTINUE
    IF (A .EQ. 1) THEN
        HXYZ(1,D + 16) = XXX + HXYZ(1,4)
        HXYZ(2,D + 16) = YYY + HXYZ(2,4)
        HXYZ(3,D + 16) = ZZZ + HXYZ(3,4)
    ENDIF
    IF (A .EQ. 2) THEN
        HXYZ(1,D + 19) = XXX + HXYZ(1,9)
        HXYZ(2,D + 19) = YYY + HXYZ(2,9)
        HXYZ(3,D + 19) = ZZZ + HXYZ(3,9)
    ENDIF
30    CONTINUE
5    CONTINUE
    RETURN
    END

SUBROUTINE HHXYZ2(CXYZ,HXYZ,XPHI,XYZ,TMAT,TMAT1,XPHI1)
DIMENSION CXYZ(3,5),HXYZ(3,22),XPHI(4),XYZ(3)
DIMENSION TMAT(3,3),TMAT1(3,3),XPHI1(4)
XPI = 3.14159265359
THETA1 = 70. *(XPI/180.)
XYZ(1) = 1.101
XYZ(2) = 0.
XYZ(3) = 0.
DO 5 A = 1,2
    IF (A .EQ. 1) THEN
        ZPHI1 = XPHI1(1)-(2.15*(XPI/180.))
        ZPHI = XPHI(1) + (122.93*(XPI/180.))
        CALL T_MAT(TMAT,ZPHI,THETA1)
        DO 10 B = 1,3
            DO 15 C = 1,3
                TMAT1(B,C) = TMAT(B,C)
15            CONTINUE
10        CONTINUE
    ENDIF
    IF (A .EQ. 2) THEN
        ZPHI1 = XPHI1(2) + (2.15*(XPI/180.))
        ZPHI = XPHI(1) + (237.07*(XPI/180.))
        CALL T_MAT(TMAT,ZPHI,THETA1)
        DO 20 B = 1,3
            DO 25 C = 1,3
                TMAT1(B,C) = TMAT(B,C)
25            CONTINUE
20        CONTINUE
    ENDIF
DO 30 D = 1,3
    IF (D .EQ. 1) THEN
        ZPHI = ZPHI1
        CALL T_MAT(TMAT,ZPHI,THETA1)
        CALL T_SQR1(TMAT,TMAT1)
    ENDIF
    IF (D .EQ. 2) THEN
        ZPHI = (120. *(XPI/180.)) + ZPHI1
        CALL T_MAT(TMAT,ZPHI,THETA1)
        CALL T_SQR1(TMAT,TMAT1)

```

```

ENDIF
IF (D .EQ. 3) THEN
  ZPHI = (240. *(XPI/180.)) + ZPHI1
  CALL T_MAT(TMAT,ZPHI,THETA1)
  CALL T_SQR1(TMAT,TMAT1)
ENDIF
XXX = 0.
YYY = 0.
ZZZ = 0.
DO 35 B = 1,3
  XXX = XXX + TMAT(1,B) * XYZ(B)
  YYY = YYY + TMAT(2,B) * XYZ(B)
  ZZZ = ZZZ + TMAT(3,B) * XYZ(B)
35  CONTINUE
IF (A .EQ. 1) THEN
  HXYZ(1,D + 10) = XXX + HXYZ(1,2)
  HXYZ(2,D + 10) = YYY + HXYZ(2,2)
  HXYZ(3,D + 10) = ZZZ + HXYZ(3,2)
ENDIF
IF (A .EQ. 2) THEN
  HXYZ(1,D + 13) = XXX + HXYZ(1,7)
  HXYZ(2,D + 13) = YYY + HXYZ(2,7)
  HXYZ(3,D + 13) = ZZZ + HXYZ(3,7)
ENDIF
30  CONTINUE
5  CONTINUE
RETURN
END

SUBROUTINE HHXYZ1(CXYZ,HXYZ,XPHI,XYZ,TMAT,TMAT1)
DIMENSION CXYZ(3,5),HXYZ(3,22),XPHI(4),XYZ(3)
DIMENSION TMAT(3,3),TMAT1(3,3)
XPI = 3.14159265359
THETA1 = 67.6 *(XPI/180.)
THETA2 = 56.8 *(XPI/180.)
THETA3 = 70. *(XPI/180.)
THETA4 = 71. *(XPI/180.)
DO 5 A = 1,4
  ZPHI = XPHI(A)
  IF (A .EQ. 1) THEN
    XYZ(1) = 1.874
    XYZ(2) = 0.
    XYZ(3) = 0.
    ZPHI = ZPHI + (237.07 *(XPI/180.))
    CALL T_MAT(TMAT,ZPHI,THETA3)
  ENDIF
  IF (A .EQ. 2) THEN
    XYZ(1) = 1.101
    XYZ(2) = 0.
    XYZ(3) = 0.
    YPHI = XPHI(1)
    CALL T_MAT(TMAT,YPHI,THETA1)
  DO 10 B = 1,3
    DO 15 C = 1,3
      TMAT1(B,C) = TMAT(B,C)
15    CONTINUE
10  CONTINUE

```



```

        ZPHI = ZPHI + (230.5*(XPI/180.))
        CALL T_MAT(TMAT,ZPHI,THETA4)
        CALL T_SQR1(TMAT,TMAT1)
    ENDIF
    IF (A .EQ. 3) THEN
        XYZ(1) = 1.874
        XYZ(2) = 0.
        XYZ(3) = 0.
        YPHI = XPHI(2)
        CALL T_MAT(TMAT,YPHI,THETA2)
        CALL T_SQR(TMAT,TMAT1)
        ZPHI = ZPHI + (237.07*(XPI/180.))
        CALL T_MAT(TMAT,ZPHI,THETA3)
        CALL T_SQR1(TMAT,TMAT1)
    ENDIF
    IF (A .EQ. 4) THEN
        XYZ(1) = 1.101
        XYZ(2) = 0.
        XYZ(3) = 0.
        YPHI = XPHI(3)
        CALL T_MAT(TMAT,YPHI,THETA1)
        CALL T_SQR(TMAT,TMAT1)
        ZPHI = ZPHI + (230.5*(XPI/180.))
        CALL T_MAT(TMAT,ZPHI,THETA4)
        CALL T_SQR(TMAT,TMAT1)
    ENDIF
    XXX = 0.
    YYY = 0.
    ZZZ = 0.
    DO 20 B = 1,3
        XXX = XXX + TMAT(1,B)*XYZ(B)
        YYY = YYY + TMAT(2,B)*XYZ(B)
        ZZZ = ZZZ + TMAT(3,B)*XYZ(B)
20    CONTINUE
    HXYZ(1,A + 6) = XXX + CXYZ(1,A + 1)
    HXYZ(2,A + 6) = YYY + CXYZ(2,A + 1)
    HXYZ(3,A + 6) = ZZZ + CXYZ(3,A + 1)
5    CONTINUE
    RETURN
    END

SUBROUTINE HHXYZ(CXYZ,HXYZ,XPHI,XYZ,TMAT,TMAT1)
DIMENSION CXYZ(3,5),HXYZ(3,22),XPHI(4),XYZ(3)
DIMENSION TMAT(3,3),TMAT1(3,3)
XPI = 3.14159265359
THETA1 = 67.6*(XPI/180.)
THETA2 = 56.8*(XPI/180.)
THETA3 = 70.*(XPI/180.)
THETA4 = 71.*(XPI/180.)
DO 5 A = 1,4
    ZPHI = XPHI(A)
    IF (A .EQ. 1) THEN
        XYZ(1) = 1.874
        XYZ(2) = 0.
        XYZ(3) = 0.
        ZPHI = ZPHI + (122.93*(XPI/180.))
        CALL T_MAT(TMAT,ZPHI,THETA3)

```

```

ENDIF
IF (A .EQ. 2) THEN
  XYZ(1) = 1.101
  XYZ(2) = 0.
  XYZ(3) = 0.
  YPHI = XPHI(1)
  CALL T_MAT(TMAT,YPHI,THETA1)
  DO 10 B = 1,3
    DO 15 C = 1,3
      TMAT1(B,C) = TMAT(B,C)
15    CONTINUE
10    CONTINUE
  ZPHI = ZPHI + (129.5*(XPI/180.))
  CALL T_MAT(TMAT,ZPHI,THETA4)
  CALL T_SQR1(TMAT,TMAT1)
ENDIF
IF (A .EQ. 3) THEN
  XYZ(1) = 1.874
  XYZ(2) = 0.
  XYZ(3) = 0.
  YPHI = XPHI(2)
  CALL T_MAT(TMAT,YPHI,THETA2)
  CALL T_SQR(TMAT,TMAT1)
  ZPHI = ZPHI + (122.93*(XPI/180.))
  CALL T_MAT(TMAT,ZPHI,THETA3)
  CALL T_SQR1(TMAT,TMAT1)
ENDIF
IF (A .EQ. 4) THEN
  XYZ(1) = 1.101
  XYZ(2) = 0.
  XYZ(3) = 0.
  YPHI = XPHI(3)
  CALL T_MAT(TMAT,YPHI,THETA1)
  CALL T_SQR(TMAT,TMAT1)
  ZPHI = ZPHI + (129.5*(XPI/180.))
  CALL T_MAT(TMAT,ZPHI,THETA4)
  CALL T_SQR1(TMAT,TMAT1)
ENDIF
XXX = 0.
YYY = 0.
ZZZ = 0.
DO 20 B = 1,3
  XXX = XXX + TMAT(1,B)*XYZ(B)
  YYY = YYY + TMAT(2,B)*XYZ(B)
  ZZZ = ZZZ + TMAT(3,B)*XYZ(B)
20 CONTINUE
HXYZ(1,A + 1) = XXX + CXYZ(1,A + 1)
HXYZ(2,A + 1) = YYY + CXYZ(2,A + 1)
HXYZ(3,A + 1) = ZZZ + CXYZ(3,A + 1)
5 CONTINUE
RETURN
END

SUBROUTINE CCXYZ(CXYZ,XPHI,XYZ,TMAT,TMAT1)
DIMENSION CXYZ(3,5),XPHI(4),XYZ(3)
DIMENSION TMAT(3,3),TMAT1(3,3)
XPI = 3.14159265359

```

```

THETA1 = 67.6*(XPI/180.)
THETA2 = 56.8*(XPI/180.)
DO 5 A = 1,3
  ZPHI = XPHI(A)
  IF (A .EQ. 1) THEN
    XYZ(1) = 1.889
    XYZ(2) = 0.
    XYZ(3) = 0.
    CALL T_MAT(TMAT,ZPHI,THETA1)
    DO 10 B = 1,3
      DO 15 C = 1,3
        TMAT1(B,C) = TMAT(B,C)
15      CONTINUE
10      CONTINUE
    ENDIF
    IF (A .EQ. 2) THEN
      XYZ(1) = 1.889
      XYZ(2) = 0.
      XYZ(3) = 0.
      CALL T_MAT(TMAT,ZPHI,THETA2)
      CALL T_SQR(TMAT, TMAT1)
    ENDIF
    IF (A .EQ. 3) THEN
      XYZ(1) = 1.889
      XYZ(2) = 0.
      XYZ(3) = 0.
      CALL T_MAT(TMAT,ZPHI,THETA1)
      CALL T_SQR(TMAT, TMAT1)
    ENDIF
    XXX = 0.
    YYY = 0.
    ZZZ = 0.
    DO 20 B = 1,3
      XXX = XXX + TMAT(1,B)*XYZ(B)
      YYY = YYY + TMAT(2,B)*XYZ(B)
      ZZZ = ZZZ + TMAT(3,B)*XYZ(B)
20    CONTINUE
      CXYZ(1,A + 2) = XXX + CXYZ(1,A + 1)
      CXYZ(2,A + 2) = YYY + CXYZ(2,A + 1)
      CXYZ(3,A + 2) = ZZZ + CXYZ(3,A + 1)
5    CONTINUE
  RETURN
END

```

```

SUBROUTINE SET_XYZ(CXYZ,HXYZ)
DIMENSION CXYZ(3,5),HXYZ(3,16)
CXYZ(1,1) = 0.
CXYZ(2,1) = 0.
CXYZ(3,1) = 0.
CXYZ(1,2) = 1.889
CXYZ(2,2) = 0.
CXYZ(3,2) = 0.
HXYZ(1,1) = -0.35845
HXYZ(2,1) = 0.662168
HXYZ(3,1) = -0.803274
HXYZ(1,6) = -0.35845
HXYZ(2,6) = 0.662168

```

```

HXYZ(3,6) = 0.803274
RETURN
END

```

```

SUBROUTINE T_MAT(TMAT,ZPHI,THETA)
DIMENSION TMAT(3,3)
TMAT(1,1) = COS(THETA)
TMAT(1,2) = SIN(THETA)
TMAT(1,3) = 0.
TMAT(2,1) = SIN(THETA)*COS(ZPHI)
TMAT(2,2) = -(COS(THETA)*COS(ZPHI))
TMAT(2,3) = SIN(ZPHI)
TMAT(3,1) = SIN(THETA)*SIN(ZPHI)
TMAT(3,2) = -(COS(THETA)*SIN(ZPHI))
TMAT(3,3) = -COS(ZPHI)
RETURN
END

```

```

SUBROUTINE T_SQR(TMAT,TMAT1)
DIMENSION TMAT(3,3),TMAT1(3,3),TMAT2(3,3)
DO 5 C = 1,3
  DO 10 A = 1,3
    SUM0 = 0.
    DO 15 B = 1,3
      SUM0 = SUM0 + TMAT1(C,B)*TMAT(B,A)
15    CONTINUE
      TMAT2(C,A) = SUM0
10    CONTINUE
5    CONTINUE
DO 20 A = 1,3
  DO 25 B = 1,3
    TMAT(A,B) = TMAT2(A,B)
    TMAT1(A,B) = TMAT2(A,B)
25    CONTINUE
20    CONTINUE
RETURN
END

```

```

SUBROUTINE T_SQR1(TMAT,TMAT1)
DIMENSION TMAT(3,3),TMAT1(3,3),TMAT2(3,3)
DO 5 C = 1,3
  DO 10 A = 1,3
    SUM0 = 0.
    DO 15 B = 1,3
      SUM0 = SUM0 + TMAT1(C,B)*TMAT(B,A)
15    CONTINUE
      TMAT2(C,A) = SUM0
10    CONTINUE
5    CONTINUE
DO 20 A = 1,3
  DO 25 B = 1,3
    TMAT(A,B) = TMAT2(A,B)
25    CONTINUE
20    CONTINUE
RETURN
END

```

B.4. Computer Simulation of Poly(dimethylsilethene): Program Listing.

```
DIMENSION TMAT(3,3),TMAT1(3,3),TMAT2(3,3)
DIMENSION XYZ(3),CXYZ(3,8),HXYZ(3,28),XPHI1(6)
DIMENSION AXYZ(3,36),XPHI(7),RPHI(6),APHI(8)
DIMENSION SS(1),SC(16),SH(40),CC(31),CH(194),HH(211)
OPEN(1,FILE='ENERGY1.DAT',STATUS='NEW')
OPEN(2,FILE='ROTATE.DAT',STATUS='NEW')
XPI=3.14159265359
DO 5 A=1,8.
XPHI1(A)=0.
5 CONTINUE
CALL SET_XYZ(CXYZ)
THETAX1=58.*(XPI/180.)
THETAX2=61.*(XPI/180.)
DO 10 A=0,360,10
XPHI(4)=A*(XPI/180.)
DO 15 B=0,360,10
XPHI(5)=B*(XPI/180.)
ETOTAL=1000000000000
CALL CCXYZ(CXYZ,XPHI,XYZ,TMAT,TMAT1,THETAX1)
CALL HHXYZA(CXYZ,HXYZ,XPHI,XYZ,TMAT,TMAT1)
CALL HHXYZ(CXYZ,HXYZ,XPHI,XYZ,TMAT,TMAT1,THETAX1)
CALL HHXYZ1(CXYZ,HXYZ,XPHI,XYZ,TMAT,TMAT1,THETAX1)
CALL HHXYZ2(CXYZ,HXYZ,XPHI,XYZ,TMAT,TMAT1,THETAX1,THETAX2)
CALL HHXYZ3(CXYZ,HXYZ,XPHI,XYZ,TMAT,TMAT1,THETAX1,THETAX2)
CALL SS_DIST(SS,AXYZ)
CALL SC_DIST(SC,AXYZ)
CALL CC_DIST(CC,AXYZ)
CALL E_TOR(XPHI,ETOR)
DO 20 C=0,120,5
XPHI(1)=C*(XPI/180.)
DO 25 D=0,120,5
XPHI(2)=D*(XPI/180.)
DO 30 E=0,120,5
XPHI(3)=E*(XPI/180.)
DO 35 F=0,120,5
XPHI(4)=F*(XPI/180.)
DO 40 G=0,120,5
XPHI(5)=G*(XPI/180.)
DO 45 H=0,120,5
XPHI(6)=H*(XPI/180.)
CALL HHXYZ5(CXYZ,HXYZ,XPHI,XPHI1,XYZ,TMAT,TMAT1,THETAX1)
CALL HHXYZ4(CXYZ,HXYZ,XPHI,XPHI1,XYZ,TMAT,TMAT1,THETAX1)
CALL HHXYZ6(CXYZ,HXYZ,XPHI,XPHI1,XYZ,TMAT,TMAT1)
CALL A_XYZ(AXYZ,CXYZ,HXYZ)
CALL SS_ENERGY(SS,SSEN)
CALL SC_ENERGY(SC,SCEN)
CALL CC_ENERGY(CC,CCEN)
CALL SH_DIST(SH,AXYZ)
CALL CH_DIST(CH,AXYZ)
CALL HH_DIST(HH,AXYZ)
CALL SH_ENERGY(SH,SHEN)
CALL CH_ENERGY(CH,CHEN)
CALL HH_ENERGY(HH,HHEN)
CALL E_TOR1(XPHI1,ETOR1)
```

```

ETOTAL1 = ETOR + ETOR1 + SSEN + SCEN + SHEN + CCEN + HHEN + CHEN
IF (ETOTAL1 .LT. ETOTAL) THEN
  ETOTAL = ETOTAL1
  APhi(1) = A
  APhi(2) = B
  APhi(3) = C
  APhi(4) = D
  APhi(5) = E
  APhi(6) = F
  APhi(7) = G
  APhi(8) = H
ENDIF
45 CONTINUE
40 CONTINUE
35 CONTINUE
30 CONTINUE
25 CONTINUE
20 CONTINUE
CALL OUT_PUT(APHI,ETOTAL)
15 CONTINUE
10 CONTINUE
CLOSE (1)
CLOSE (2)
END

```

```

SUBROUTINE O_PUT(APHI,ETOTAL)
DIMENSION APhi(8)
XPI = 3.14159265359
WRITE(1, *) APhi(1),APhi(2),ETOTAL
WRITE(2, *) APhi(3),APhi(4),APhi(5),APhi(6),APhi(7),APhi(8)
PRINT*,APhi(1),APhi(2)
RETURN
END

```

```

SUBROUTINE SS_DIST(SS,XYZ)
DIMENSION SS(1),XYZ(3,36)
SS(1) = (XYZ(1,2)-XYZ(1,8))**2 + (XYZ(2,2)-XYZ(2,8))**2
SS(1) = (SS(1) + (XYZ(3,2)-XYZ(3,8))**2)**0.5
RETURN
END

```

```

SUBROUTINE SC_DIST(SC,XYZ)
DIMENSION SC(16),XYZ(3,36)
DO 5 A = 6,7
  SC(A-5) = (XYZ(1,2)-XYZ(1,A))**2 + (XYZ(2,2)-XYZ(2,A))**2
  SC(A-5) = (SC(A-5) + (XYZ(3,2)-XYZ(3,A))**2)**0.5
5 CONTINUE
DO 10 A = 11,14
  SC(A-8) = (XYZ(1,2)-XYZ(1,A))**2 + (XYZ(2,2)-XYZ(2,A))**2
  SC(A-8) = (SC(A-8) + (XYZ(3,2)-XYZ(3,A))**2)**0.5
10 CONTINUE
DO 15 A = 9,10
  SC(A-2) = (XYZ(1,5)-XYZ(1,A))**2 + (XYZ(2,5)-XYZ(2,A))**2
  SC(A-2) = (SC(A-2) + (XYZ(3,5)-XYZ(3,A))**2)**0.5
15 CONTINUE
DO 20 A = 13,14
  SC(A-4) = (XYZ(1,5)-XYZ(1,A))**2 + (XYZ(2,5)-XYZ(2,A))**2
  SC(A-4) = (SC(A-4) + (XYZ(3,5)-XYZ(3,A))**2)**0.5

```

```

20  CONTINUE
    DO 25 A = 3,4
        SC(A + 8) = (AXYZ(1,8)-AXYZ(1,A))**2 + (AXYZ(2,8)-AXYZ(2,A))**2
        SC(A + 8) = (SC(A + 8) + (AXYZ(3,8)-AXYZ(3,A))**2)**0.5
25  CONTINUE
    DO 30 A = 9,12
        SC(A + 4) = (AXYZ(1,8)-AXYZ(1,A))**2 + (AXYZ(2,8)-AXYZ(2,A))**2
        SC(A + 4) = (SC(A + 4) + (AXYZ(3,8)-AXYZ(3,A))**2)**0.5
30  CONTINUE
    RETURN
    END

    SUBROUTINE SH_DIST(SH,AXYZ)
    DIMENSION SH(40),AXYZ(3,36)
    DO 5 A = 17,18
        SH(A-16) = (AXYZ(1,2)-AXYZ(1,A))**2 + (AXYZ(2,2)-AXYZ(2,A))**2
        SH(A-16) = (SH(A-16) + (AXYZ(3,2)-AXYZ(3,A))**2)**0.5
5   CONTINUE
    DO 10 A = 25,36
        SH(A-22) = (AXYZ(1,2)-AXYZ(1,A))**2 + (AXYZ(2,2)-AXYZ(2,A))**2
        SH(A-22) = (SH(A-22) + (AXYZ(3,2)-AXYZ(3,A))**2)**0.5
10  CONTINUE
    DO 15 A = 19,24
        SH(A-4) = (AXYZ(1,5)-AXYZ(1,A))**2 + (AXYZ(2,5)-AXYZ(2,A))**2
        SH(A-4) = (SH(A-4) + (AXYZ(3,5)-AXYZ(3,A))**2)**0.5
15  CONTINUE
    DO 20 A = 31,36
        SH(A-10) = (AXYZ(1,5)-AXYZ(1,A))**2 + (AXYZ(2,5)-AXYZ(2,A))**2
        SH(A-10) = (SH(A-10) + (AXYZ(3,5)-AXYZ(3,A))**2)**0.5
20  CONTINUE
    DO 25 A = 15,16
        SH(A + 12) = (AXYZ(1,8)-AXYZ(1,A))**2 + (AXYZ(2,8)-AXYZ(2,A))**2
        SH(A + 12) = (SH(A + 12) + (AXYZ(3,8)-AXYZ(3,A))**2)**0.5
25  CONTINUE
    DO 30 A = 19,30
        SH(A + 10) = (AXYZ(1,8)-AXYZ(1,A))**2 + (AXYZ(2,8)-AXYZ(2,A))**2
        SH(A + 10) = (SH(A + 10) + (AXYZ(3,8)-AXYZ(3,A))**2)**0.5
30  CONTINUE
    RETURN
    END

    SUBROUTINE CC_DIST(CC,AXYZ)
    DIMENSION CC(31),AXYZ(3,36)
    DO 5 A = 11,14
        CC(A-10) = (AXYZ(1,3)-AXYZ(1,A))**2 + (AXYZ(2,3)-AXYZ(2,A))**2
        CC(A-10) = (CC(A-10) + (AXYZ(3,3)-AXYZ(3,A))**2)**0.5
5   CONTINUE
    DO 10 A = 6,7
        CC(A-1) = (AXYZ(1,3)-AXYZ(1,A))**2 + (AXYZ(2,3)-AXYZ(2,A))**2
        CC(A-1) = (CC(A-1) + (AXYZ(3,3)-AXYZ(3,A))**2)**0.5
10  CONTINUE
    CC(7) = (AXYZ(1,4)-AXYZ(1,7))**2 + (AXYZ(2,4)-AXYZ(2,7))**2
    CC(7) = (CC(7) + (AXYZ(3,4)-AXYZ(3,7))**2)**0.5
    DO 15 A = 9,10
        CC(A-1) = (AXYZ(1,4)-AXYZ(1,A))**2 + (AXYZ(2,4)-AXYZ(2,A))**2
        CC(A-1) = (CC(A-1) + (AXYZ(3,4)-AXYZ(3,A))**2)**0.5
15  CONTINUE
    DO 20 A = 13,14

```

```

    CC(A-3) = (AXYZ(1,4)-AXYZ(1,A))**2 + (AXYZ(2,4)-AXYZ(2,A))**2
    CC(A-3) = (CC(A-3) + (AXYZ(3,4)-AXYZ(3,A))**2)**0.5
20  CONTINUE
    DO 25 A = 9,10
        CC(A + 3) = (AXYZ(1,6)-AXYZ(1,A))**2 + (AXYZ(2,6)-AXYZ(2,A))**2
        CC(A + 3) = (CC(A + 3) + (AXYZ(3,6)-AXYZ(3,A))**2)**0.5
25  CONTINUE
    DO 30 A = 13,14
        CC(A + 1) = (AXYZ(1,6)-AXYZ(1,A))**2 + (AXYZ(2,6)-AXYZ(2,A))**2
        CC(A + 1) = (CC(A + 1) + (AXYZ(3,6)-AXYZ(3,A))**2)**0.5
30  CONTINUE
    DO 35 A = 9,12
        CC(A + 7) = (AXYZ(1,7)-AXYZ(1,A))**2 + (AXYZ(2,7)-AXYZ(2,A))**2
        CC(A + 7) = (CC(A + 7) + (AXYZ(3,7)-AXYZ(3,A))**2)**0.5
35  CONTINUE
    DO 40 A = 11,14
        CC(A + 9) = (AXYZ(1,9)-AXYZ(1,A))**2 + (AXYZ(2,9)-AXYZ(2,A))**2
        CC(A + 9) = (CC(A + 9) + (AXYZ(3,9)-AXYZ(3,A))**2)**0.5
40  CONTINUE
    DO 45 A = 11,14
        CC(A + 13) = (AXYZ(1,10)-AXYZ(1,A))**2 + (AXYZ(2,10)-AXYZ(2,A))**2
        CC(A + 13) = (CC(A + 13) + (AXYZ(3,10)-AXYZ(3,A))**2)**0.5
45  CONTINUE
    DO 50 A = 13,14
        CC(A + 15) = (AXYZ(1,11)-AXYZ(1,A))**2 + (AXYZ(2,11)-AXYZ(2,A))**2
        CC(A + 15) = (CC(A + 15) + (AXYZ(3,11)-AXYZ(3,A))**2)**0.5
50  CONTINUE
    DO 55 A = 13,14
        CC(A + 17) = (AXYZ(1,12)-AXYZ(1,A))**2 + (AXYZ(2,12)-AXYZ(2,A))**2
        CC(A + 17) = (CC(A + 17) + (AXYZ(3,12)-AXYZ(3,A))**2)**0.5
55  CONTINUE
    RETURN
    END

SUBROUTINE CH_DIST(CH,AXYZ)
DIMENSION CH(194),AXYZ(3,36)
DO 5 A = 17,36
    CH(A-16) = (AXYZ(1,3)-AXYZ(1,A))**2 + (AXYZ(2,3)-AXYZ(2,A))**2
    CH(A-16) = (CH(A-16) + (AXYZ(3,3)-AXYZ(3,A))**2)**0.5
5  CONTINUE
    DO 10 A = 17,36
        CH(A + 4) = (AXYZ(1,4)-AXYZ(1,A))**2 + (AXYZ(2,4)-AXYZ(2,A))**2
        CH(A + 4) = (CH(A + 4) + (AXYZ(3,4)-AXYZ(3,A))**2)**0.5
10  CONTINUE
    DO 15 A = 15,16
        CH(A + 26) = (AXYZ(1,6)-AXYZ(1,A))**2 + (AXYZ(2,6)-AXYZ(2,A))**2
        CH(A + 26) = (CH(A + 26) + (AXYZ(3,6)-AXYZ(3,A))**2)**0.5
15  CONTINUE
    DO 20 A = 19,36
        CH(A + 24) = (AXYZ(1,6)-AXYZ(1,A))**2 + (AXYZ(2,6)-AXYZ(2,A))**2
CH(A + 24) = (CH(A + 24) + (AXYZ(3,6)-AXYZ(3,A))**2)**0.5
        CH(A + 24) = (CH(A + 24) + (AXYZ(3,6)-AXYZ(3,A))**2)**0.5
20  CONTINUE
    DO 25 A = 15,16
        CH(A + 46) = (AXYZ(1,7)-AXYZ(1,A))**2 + (AXYZ(2,7)-AXYZ(2,A))**2
        CH(A + 46) = (CH(A + 46) + (AXYZ(3,7)-AXYZ(3,A))**2)**0.5
25  CONTINUE
    DO 30 A = 19,36

```



```

      CH(A + 44) = (AXYZ(1,7)-AXYZ(1,A))**2 + (AXYZ(2,7)-AXYZ(2,A))**2
      CH(A + 44) = (CH(A + 44) + (AXYZ(3,7)-AXYZ(3,A))**2)**0.5
30  CONTINUE
      DO 35 A = 15,18
      CH(A + 66) = (AXYZ(1,9)-AXYZ(1,A))**2 + (AXYZ(2,9)-AXYZ(2,A))**2
      CH(A + 66) = (CH(A + 66) + (AXYZ(3,9)-AXYZ(3,A))**2)**0.5
35  CONTINUE
      DO 40 A = 22,36
      CH(A + 63) = (AXYZ(1,9)-AXYZ(1,A))**2 + (AXYZ(2,9)-AXYZ(2,A))**2
      CH(A + 63) = (CH(A + 63) + (AXYZ(3,9)-AXYZ(3,A))**2)**0.5
40  CONTINUE
      DO 45 A = 15,21
      CH(A + 85) = (AXYZ(1,10)-AXYZ(1,A))**2 + (AXYZ(2,10)-AXYZ(2,A))**2
      CH(A + 85) = (CH(A + 85) + (AXYZ(3,10)-AXYZ(3,A))**2)**0.5
45  CONTINUE
      DO 50 A = 25,36
      CH(A + 82) = (AXYZ(1,10)-AXYZ(1,A))**2 + (AXYZ(2,10)-AXYZ(2,A))**2
      CH(A + 82) = (CH(A + 82) + (AXYZ(3,10)-AXYZ(3,A))**2)**0.5
50  CONTINUE
      DO 55 A = 15,27
      CH(A + 104) = (AXYZ(1,11)-AXYZ(1,A))**2 + (AXYZ(2,11)-AXYZ(2,A))**2
      CH(A + 104) = (CH(A + 104) + (AXYZ(3,11)-AXYZ(3,A))**2)**0.5
55  CONTINUE
      DO 60 A = 31,36
      CH(A + 101) = (AXYZ(1,11)-AXYZ(1,A))**2 + (AXYZ(2,11)-AXYZ(2,A))**2
      CH(A + 101) = (CH(A + 101) + (AXYZ(3,11)-AXYZ(3,A))**2)**0.5
60  CONTINUE
      DO 65 A = 15,24
      CH(A + 123) = (AXYZ(1,12)-AXYZ(1,A))**2 + (AXYZ(2,12)-AXYZ(2,A))**2
      CH(A + 123) = (CH(A + 123) + (AXYZ(3,12)-AXYZ(3,A))**2)**0.5
65  CONTINUE
      DO 70 A = 28,36
      CH(A + 120) = (AXYZ(1,12)-AXYZ(1,A))**2 + (AXYZ(2,12)-AXYZ(2,A))**2
      CH(A + 120) = (CH(A + 120) + (AXYZ(3,12)-AXYZ(3,A))**2)**0.5
70  CONTINUE
      DO 75 A = 15,30
      CH(A + 142) = (AXYZ(1,13)-AXYZ(1,A))**2 + (AXYZ(2,13)-AXYZ(2,A))**2
      CH(A + 142) = (CH(A + 142) + (AXYZ(3,13)-AXYZ(3,A))**2)**0.5
75  CONTINUE
      DO 80 A = 34,36
      CH(A + 139) = (AXYZ(1,13)-AXYZ(1,A))**2 + (AXYZ(2,13)-AXYZ(2,A))**2
      CH(A + 139) = (CH(A + 139) + (AXYZ(3,13)-AXYZ(3,A))**2)**0.5
80  CONTINUE
      DO 85 A = 15,33
      CH(A + 161) = (AXYZ(1,14)-AXYZ(1,A))**2 + (AXYZ(2,14)-AXYZ(2,A))**2
      CH(A + 161) = (CH(A + 161) + (AXYZ(3,14)-AXYZ(3,A))**2)**0.5
85  CONTINUE
      RETURN
      END

      SUBROUTINE HH_DIST(HH,AXYZ)
      DIMENSION HH(211),AXYZ(3,36)
      DO 5 A = 17,36
      HH(A-16) = (AXYZ(1,15)-AXYZ(1,A))**2 + (AXYZ(2,15)-AXYZ(2,A))**2
      HH(A-16) = (HH(A-16) + (AXYZ(3,15)-AXYZ(3,A))**2)**0.5
      HH(A + 4) = (AXYZ(1,16)-AXYZ(1,A))**2 + (AXYZ(2,16)-AXYZ(2,A))**2
      HH(A + 4) = (HH(A + 4) + (AXYZ(3,16)-AXYZ(3,A))**2)**0.5
5  CONTINUE

```

```

DO 10 A = 19,36
  HH(A + 22) = (AXYZ(1,17)-AXYZ(1,A))**2 + (AXYZ(2,17)-AXYZ(2,A))**2
  HH(A + 22) = (HH(A + 22) + (AXYZ(3,17)-AXYZ(3,A))**2)**0.5
  HH(A + 40) = (AXYZ(1,18)-AXYZ(1,A))**2 + (AXYZ(2,18)-AXYZ(2,A))**2
  HH(A + 40) = (HH(A + 40) + (AXYZ(3,18)-AXYZ(3,A))**2)**0.5
10  CONTINUE
DO 15 A = 22,36
  HH(A + 55) = (AXYZ(1,19)-AXYZ(1,A))**2 + (AXYZ(2,19)-AXYZ(2,A))**2
  HH(A + 55) = (HH(A + 55) + (AXYZ(3,19)-AXYZ(3,A))**2)**0.5
  HH(A + 70) = (AXYZ(1,20)-AXYZ(1,A))**2 + (AXYZ(2,20)-AXYZ(2,A))**2
  HH(A + 70) = (HH(A + 70) + (AXYZ(3,20)-AXYZ(3,A))**2)**0.5
  HH(A + 85) = (AXYZ(1,21)-AXYZ(1,A))**2 + (AXYZ(2,21)-AXYZ(2,A))**2
  HH(A + 85) = (HH(A + 85) + (AXYZ(3,21)-AXYZ(3,A))**2)**0.5
15  CONTINUE
DO 20 A = 25,36
  HH(A + 97) = (AXYZ(1,22)-AXYZ(1,A))**2 + (AXYZ(2,22)-AXYZ(2,A))**2
  HH(A + 97) = (HH(A + 97) + (AXYZ(3,22)-AXYZ(3,A))**2)**0.5
  HH(A + 109) = (AXYZ(1,23)-AXYZ(1,A))**2 + (AXYZ(2,23)-AXYZ(2,A))**2
  HH(A + 109) = (HH(A + 109) + (AXYZ(3,23)-AXYZ(3,A))**2)**0.5
  HH(A + 121) = (AXYZ(1,24)-AXYZ(1,A))**2 + (AXYZ(2,24)-AXYZ(2,A))**2
  HH(A + 121) = (HH(A + 121) + (AXYZ(3,24)-AXYZ(3,A))**2)**0.5
20  CONTINUE
DO 25 A = 28,36
  HH(A + 130) = (AXYZ(1,25)-AXYZ(1,A))**2 + (AXYZ(2,25)-AXYZ(2,A))**2
  HH(A + 130) = (HH(A + 130) + (AXYZ(3,25)-AXYZ(3,A))**2)**0.5
  HH(A + 139) = (AXYZ(1,26)-AXYZ(1,A))**2 + (AXYZ(2,26)-AXYZ(2,A))**2
  HH(A + 139) = (HH(A + 139) + (AXYZ(3,26)-AXYZ(3,A))**2)**0.5
  HH(A + 148) = (AXYZ(1,27)-AXYZ(1,A))**2 + (AXYZ(2,27)-AXYZ(2,A))**2
  HH(A + 148) = (HH(A + 148) + (AXYZ(3,27)-AXYZ(3,A))**2)**0.5
25  CONTINUE
DO 30 A = 31,36
  HH(A + 154) = (AXYZ(1,28)-AXYZ(1,A))**2 + (AXYZ(2,28)-AXYZ(2,A))**2
  HH(A + 154) = (HH(A + 154) + (AXYZ(3,28)-AXYZ(3,A))**2)**0.5
  HH(A + 160) = (AXYZ(1,29)-AXYZ(1,A))**2 + (AXYZ(2,29)-AXYZ(2,A))**2
  HH(A + 160) = (HH(A + 160) + (AXYZ(3,29)-AXYZ(3,A))**2)**0.5
  HH(A + 166) = (AXYZ(1,30)-AXYZ(1,A))**2 + (AXYZ(2,30)-AXYZ(2,A))**2
  HH(A + 166) = (HH(A + 166) + (AXYZ(3,30)-AXYZ(3,A))**2)**0.5
30  CONTINUE
DO 35 A = 34,36
  HH(A + 169) = (AXYZ(1,31)-AXYZ(1,A))**2 + (AXYZ(2,31)-AXYZ(2,A))**2
  HH(A + 169) = (HH(A + 169) + (AXYZ(3,31)-AXYZ(3,A))**2)**0.5
  HH(A + 172) = (AXYZ(1,32)-AXYZ(1,A))**2 + (AXYZ(2,32)-AXYZ(2,A))**2
  HH(A + 172) = (HH(A + 172) + (AXYZ(3,32)-AXYZ(3,A))**2)**0.5
  HH(A + 175) = (AXYZ(1,33)-AXYZ(1,A))**2 + (AXYZ(2,33)-AXYZ(2,A))**2
  HH(A + 175) = (HH(A + 175) + (AXYZ(3,33)-AXYZ(3,A))**2)**0.5
35  CONTINUE
RETURN
END

SUBROUTINE TEST(AXYZ,AA,BB)
DIMENSION AXYZ(3,36)
YY = (AXYZ(1,AA)-AXYZ(1,BB))**2 + (AXYZ(2,AA)-AXYZ(2,BB))**2
YY = (YY + (AXYZ(3,AA)-AXYZ(3,BB))**2)**0.5
ZZ = (AXYZ(1,CC)-AXYZ(1,DD))**2 + (AXYZ(2,CC)-AXYZ(2,DD))**2
ZZ = (ZZ + (AXYZ(3,CC)-AXYZ(3,DD))**2)**0.5
PRINT*,YY
RETURN
END

```

```

SUBROUTINE A_XYZ(AXYZ,CXYZ,HXYZ)
DIMENSION AXYZ(3,36),CXYZ(3,8),HXYZ(3,28)
DO 5 A = 1,8
  AXYZ(1,A) = CXYZ(1,A)
  AXYZ(2,A) = CXYZ(2,A)
  AXYZ(3,A) = CXYZ(3,A)
5  CONTINUE
DO 10 A = 1,3
  AXYZ(A,9) = HXYZ(A,1)
  AXYZ(A,10) = HXYZ(A,2)
  AXYZ(A,11) = HXYZ(A,4)
  AXYZ(A,12) = HXYZ(A,3)
  AXYZ(A,13) = HXYZ(A,5)
  AXYZ(A,14) = HXYZ(A,6)
  AXYZ(A,15) = HXYZ(A,7)
  AXYZ(A,16) = HXYZ(A,8)
  AXYZ(A,17) = HXYZ(A,9)
  AXYZ(A,18) = HXYZ(A,10)
  AXYZ(A,19) = HXYZ(A,23)
  AXYZ(A,20) = HXYZ(A,24)
  AXYZ(A,21) = HXYZ(A,25)
  AXYZ(A,22) = HXYZ(A,26)
  AXYZ(A,23) = HXYZ(A,27)
  AXYZ(A,24) = HXYZ(A,28)
  AXYZ(A,25) = HXYZ(A,11)
  AXYZ(A,26) = HXYZ(A,12)
  AXYZ(A,27) = HXYZ(A,13)
  AXYZ(A,28) = HXYZ(A,14)
  AXYZ(A,29) = HXYZ(A,15)
  AXYZ(A,30) = HXYZ(A,16)
  AXYZ(A,31) = HXYZ(A,17)
  AXYZ(A,32) = HXYZ(A,18)
  AXYZ(A,33) = HXYZ(A,19)
  AXYZ(A,34) = HXYZ(A,20)
  AXYZ(A,35) = HXYZ(A,21)
  AXYZ(A,36) = HXYZ(A,22)
10 CONTINUE
RETURN
END

SUBROUTINE K_BOND(XEN,ANG1,ANG2)
XEN = 0.
XEN = 4*(0.017652/2.)*(ANG1-122.5)**2
XEN = XEN + (4*(0.017652/2.)*(ANG2-118.4)**2)
RETURN
END

SUBROUTINE CH_ENERGY(CH,CHENERGY)
DIMENSION CH(194)
CHENERGY = 0.
A3 = 5.63*(10**4)
C3 = 127.
AA3 = 6.39*(10**4)
CC3 = 158.8
DO 5 A = 1,80
  CHENERGY = CHENERGY + (AA3/(CH(A)**12))-(CC3/(CH(A)**6))
5  CONTINUE

```

```

DO 10 A = 81,194
  CHENERGY = CHENERGY + (A3/(CH(A)**12))-(C3/(CH(A)**6))
10  CONTINUE
RETURN
END

SUBROUTINE HH_ENERGY(HH,HHENERGY)
DIMENSION HH(211)
HHENERGY = 0.
A2 = 7.27*(10**3)
C2 = 47.1
DO 5 A = 1,211
  HHENERGY = HHENERGY + (A2/(HH(A)**12))-(C2/(HH(A)**6))
5  CONTINUE
RETURN
END

SUBROUTINE CC_ENERGY(CC,CCENERGY)
DIMENSION CC(31)
CCENERGY = 0.
A1 = 3.95*(10**5)
C1 = 363.
AA1 = 4.48*(10**5)
CC1 = 447.2
AA2 = 5.1*(10**5)
CC2 = 552.9
DO 5 A = 1,4
  CCENERGY = CCENERGY + (AA1/(CC(A)**12))-(C1/(CC(A)**6))
5  CONTINUE
DO 10 A = 5,7
  CCENERGY = CCENERGY + (AA2/(CC(A)**12))-(C2/(CC(A)**6))
10  CONTINUE
DO 15 A = 8,19
  CCENERGY = CCENERGY + (AA1/(CC(A)**12))-(C1/(CC(A)**6))
15  CONTINUE
DO 20 A = 20,31
  CCENERGY = CCENERGY + (A1/(CC(A)**12))-(C1/(CC(A)**6))
20  CONTINUE
RETURN
END

SUBROUTINE SC_ENERGY(SC,SCENERGY)
DIMENSION SC(16)
SCENERGY = 0.
A4 = 1.71*(10**6)
C4 = 1050.
AA4 = 1.96*(10**6)
CC4 = 1300.
DO 5 A = 1,2
  SCENERGY = SCENERGY + (AA4/(SC(A)**12))-(CC4/(SC(A)**6))
5  CONTINUE
DO 10 A = 3,10
  SCENERGY = SCENERGY + (A4/(SC(A)**12))-(C4/(SC(A)**6))
10  CONTINUE
DO 15 A = 11,12
  SCENERGY = SCENERGY + (AA4/(SC(A)**12))-(CC4/(SC(A)**6))
15  CONTINUE
DO 20 A = 13,16

```

```

    SCENERGY = SCENERGY + (A4/(SC(A)**12))-(C4/(SC(A)**6))
20  CONTINUE
    RETURN
    END

```

```

SUBROUTINE SH_ENERGY(SH,SHENERGY)
DIMENSION SH(40)
SHENERGY = 0.
A5 = 2.62*(10**5)
C5 = 371.4
DO 5 A = 1,40
    SHENERGY = SHENERGY + (A5/(SH(A)**12))-(C5/(SH(A)**6))
5  CONTINUE
    RETURN
    END

```

```

SUBROUTINE SS_ENERGY(SS,SSENERGY)
DIMENSION SS(1)
SSENERGY = 0.
A6 = 7.26*(10**6)
C6 = 3060.0
    SSENERGY = SSENERGY + (A6/(SS(1)**12))-(C6/SS(1)**6))
    RETURN
    END

```

```

SUBROUTINE E_TOR(XPHI,ETOR)
DIMENSION XPHI(7)
ETOR = 0.
DO 5 A = 4,5
    ETOR = ETOR + (0.0/2)*(1-COS(3.*XPHI(A)-3.14259))
5  CONTINUE
    RETURN
    END

```

```

SUBROUTINE E_TOR1(XPHI1,ETOR1)
DIMENSION XPHI1(6)
ETOR1 = 0.
DO 5 A = 1,6
    ETOR1 = ETOR1 + (0.5/2)*(1-COS(3.*XPHI1(A)))
5  CONTINUE
    RETURN
    END

```

```

SUBROUTINE HHXYZA(CXYZ,HXYZ,XPHI,XYZ,TMAT,TMAT1)
DIMENSION CXYZ(3,8),HXYZ(3,28),XPHI(7),XYZ(3)
DIMENSION TMAT(3,3),TMAT1(3,3)
XPI = 3.14159265359
THETA1 = 70.*(XPI/180.)
XYZ(1) = 1.87
XYZ(2) = 0.
XYZ(3) = 0.
DO 5 A = 1,2
    ZPHI = XPHI(1)
    IF (A .EQ. 1) THEN
        ZPHI = ZPHI + (121.319*(XPI/180.))
        CALL T_MAT(TMAT,ZPHI,THETA1)
    ENDIF
    IF (A .EQ. 2) THEN

```

```

        ZPHI = ZPHI + (238.681*(XPI/180.))
        CALL T_MAT(TMAT,ZPHI,THETA1)
    ENDIF
    XXX = 0.
    YYY = 0.
    ZZZ = 0.
    DO 10 B = 1,3
        XXX = XXX + TMAT(1,B)*XYZ(B)
        YYY = YYY + TMAT(2,B)*XYZ(B)
        ZZZ = ZZZ + TMAT(3,B)*XYZ(B)
10    CONTINUE
        HXYZ(1,A) = XXX + CXYZ(1,2)
        HXYZ(2,A) = YYY + CXYZ(2,2)
        HXYZ(3,A) = ZZZ + CXYZ(3,2)
5    CONTINUE
    RETURN
    END

SUBROUTINE HHXYZ6(CXYZ,HXYZ,XPHI,XPHI1,XYZ,TMAT,TMAT1)
    DIMENSION CXYZ(3,8),HXYZ(3,28),XPHI(7),XYZ(3)
    DIMENSION TMAT(3,3),TMAT1(3,3),XPHI1(6)
    XPI = 3.14159265359
    THETA2 = 70.*(XPI/180.)
    THETA3 = 71.*(XPI/180.)
    XYZ(1) = 1.1
    XYZ(2) = 0.
    XYZ(3) = 0.
    DO 5 A = 1,2
        IF (A .EQ. 1) THEN
            ZPHI1 = XPHI1(5)-0.63*(XPI/180.)
            ZPHI = XPHI(1) + (121.319*(XPI/180.))
            CALL T_MAT(TMAT,ZPHI,THETA2)
            DO 10 B = 1,3
                DO 15 C = 1,3
                    TMAT1(B,C) = TMAT(B,C)
15                CONTINUE
10            CONTINUE
        ENDIF
        IF (A .EQ. 2) THEN
            ZPHI1 = XPHI1(6) + 0.63*(XPI/180.)
            ZPHI = XPHI(1) + (238.681*(XPI/180.))
            CALL T_MAT(TMAT,ZPHI,THETA2)
            DO 20 B = 1,3
                DO 25 C = 1,3
                    TMAT1(B,C) = TMAT(B,C)
25                CONTINUE
20            CONTINUE
        ENDIF
        DO 30 D = 1,3
            IF (D .EQ. 1) THEN
                ZPHI = ZPHI1
                CALL T_MAT(TMAT,ZPHI,THETA3)
                CALL T_SQR1(TMAT,TMAT1)
            ENDIF
            IF (D .EQ. 2) THEN
                ZPHI = (120.*(XPI/180.)) + ZPHI1
                CALL T_MAT(TMAT,ZPHI,THETA3)

```

```

        CALL T_SQR1(TMAT, TMAT1)
    ENDIF
    IF (D .EQ. 3) THEN
        ZPHI = (240. * (XPI/180.)) + ZPHI1
        CALL T_MAT(TMAT, ZPHI, THETA3)
        CALL T_SQR1(TMAT, TMAT1)
    ENDIF
    XXX = 0.
    YYY = 0.
    ZZZ = 0.
    DO 35 B = 1, 3
        XXX = XXX + TMAT(1, B) * XYZ(B)
        YYY = YYY + TMAT(2, B) * XYZ(B)
        ZZZ = ZZZ + TMAT(3, B) * XYZ(B)
35    CONTINUE
    IF (A .EQ. 1) THEN
        HXYZ(1, D + 22) = XXX + HXYZ(1, 1)
        HXYZ(2, D + 22) = YYY + HXYZ(2, 1)
        HXYZ(3, D + 22) = ZZZ + HXYZ(3, 1)
    ENDIF
    IF (A .EQ. 2) THEN
        HXYZ(1, D + 25) = XXX + HXYZ(1, 2)
        HXYZ(2, D + 25) = YYY + HXYZ(2, 2)
        HXYZ(3, D + 25) = ZZZ + HXYZ(3, 2)
    ENDIF
30    CONTINUE
5    CONTINUE
    RETURN
    END

```

```

SUBROUTINE HHXYZ5(CXYZ, HXYZ, XPHI, XPHI1, XYZ, TMAT, TMAT1, THETA1)
DIMENSION CXYZ(3, 8), HXYZ(3, 28), XPHI(7), XYZ(3)
DIMENSION TMAT(3, 3), TMAT1(3, 3), XPHI1(6)
XPI = 3.14159265359
THETA2 = 70. * (XPI/180.)
THETA3 = 71. * (XPI/180.)
XYZ(1) = 1.1
XYZ(2) = 0.
XYZ(3) = 0.
DO 5 A = 1, 2
    IF (A .EQ. 1) THEN
        ZPHI1 = XPHI1(1) - 0.63 * (XPI/180.)
        ZPHI = XPHI(1)
        CALL T_MAT(TMAT, ZPHI, THETA2)
        DO 10 B = 1, 3
            DO 15 C = 1, 3
                TMAT1(B, C) = TMAT(B, C)
15            CONTINUE
10        CONTINUE
        ZPHI = XPHI(2)
        CALL T_MAT(TMAT, ZPHI, THETA1)
        CALL T_SQR(TMAT, TMAT1)
        ZPHI = XPHI(3)
        CALL T_MAT(TMAT, ZPHI, THETA1)
        CALL T_SQR(TMAT, TMAT1)
        ZPHI = XPHI(4)
        CALL T_MAT(TMAT, ZPHI, THETA2)
        CALL T_SQR(TMAT, TMAT1)

```

```

ZPHI = XPHI(5)
CALL T_MAT(TMAT,ZPHI,THETAX1)
CALL T_SQR(TMAT,TMAT1)
ZPHI = XPHI(6)
CALL T_MAT(TMAT,ZPHI,THETAX1)
CALL T_SQR(TMAT,TMAT1)
ZPHI = XPHI(7) + (121.319*(XPI/180.))
CALL T_MAT(TMAT,ZPHI,THETA2)
CALL T_SQR(TMAT,TMAT1)
ENDIF
IF (A .EQ. 2) THEN
  ZPHI1 = XPHI1(2) + 0.63*(XPI/180.)
  ZPHI = XPHI(1)
  CALL T_MAT(TMAT,ZPHI,THETA2)
  DO 20 B = 1,3
    DO 25 C = 1,3
      TMAT1(B,C) = TMAT(B,C)
25     CONTINUE
20     CONTINUE
  ZPHI = XPHI(2)
  CALL T_MAT(TMAT,ZPHI,THETAX1)
  CALL T_SQR(TMAT,TMAT1)
  ZPHI = XPHI(3)
  CALL T_MAT(TMAT,ZPHI,THETAX1)
  CALL T_SQR(TMAT,TMAT1)
  ZPHI = XPHI(4)
  CALL T_MAT(TMAT,ZPHI,THETA2)
  CALL T_SQR(TMAT,TMAT1)
  ZPHI = XPHI(5)
  CALL T_MAT(TMAT,ZPHI,THETAX1)
  CALL T_SQR(TMAT,TMAT1)
  ZPHI = XPHI(6)
  CALL T_MAT(TMAT,ZPHI,THETAX1)
  CALL T_SQR(TMAT,TMAT1)
  ZPHI = XPHI(7) + (238.681*(XPI/180.))
  CALL T_MAT(TMAT,ZPHI,THETA2)
  CALL T_SQR(TMAT,TMAT1)
ENDIF
DO 30 D = 1,3
  IF (D .EQ. 1) THEN
    ZPHI = ZPHI1
    CALL T_MAT(TMAT,ZPHI,THETA3)
    CALL T_SQR1(TMAT,TMAT1)
  ENDIF
  IF (D .EQ. 2) THEN
    ZPHI = (120.*(XPI/180.)) + ZPHI1
    CALL T_MAT(TMAT,ZPHI,THETA3)
    CALL T_SQR1(TMAT,TMAT1)
  ENDIF
  IF (D .EQ. 3) THEN
    ZPHI = (240.*(XPI/180.)) + ZPHI1
    CALL T_MAT(TMAT,ZPHI,THETA3)
    CALL T_SQR1(TMAT,TMAT1)
  ENDIF
  XXX = 0.
  YYY = 0.
  ZZZ = 0.
  DO 35 B = 1,3

```



```

        XXX = XXX + TMAT(1,B)*XYZ(B)
        YYY = YYY + TMAT(2,B)*XYZ(B)
        ZZZ = ZZZ + TMAT(3,B)*XYZ(B)
35    CONTINUE
        IF (A .EQ. 1) THEN
            HXYZ(1,D + 16) = XXX + HXYZ(1,5)
            HXYZ(2,D + 16) = YYY + HXYZ(2,5)
            HXYZ(3,D + 16) = ZZZ + HXYZ(3,5)
        ENDIF
        IF (A .EQ. 2) THEN
            HXYZ(1,D + 19) = XXX + HXYZ(1,6)
            HXYZ(2,D + 19) = YYY + HXYZ(2,6)
            HXYZ(3,D + 19) = ZZZ + HXYZ(3,6)
        ENDIF
30    CONTINUE
5    CONTINUE
    RETURN
    END

SUBROUTINE HHXYZ4(CXYZ,HXYZ,XPHI,XPHI1,XYZ,TMAT,TMAT1,THETAX1)
DIMENSION CXYZ(3,8),HXYZ(3,28),XPHI(7),XYZ(3)
DIMENSION TMAT(3,3),TMAT1(3,3),XPHI1(6)
XPI = 3.14159265359
THETA2 = 70.*(XPI/180.)
THETA3 = 71.*(XPI/180.)
XYZ(1) = 1.1
XYZ(2) = 0.
XYZ(3) = 0.
DO 5 A = 1,2
    IF (A .EQ. 1) THEN
        ZPHI1 = XPHI1(3)-0.63*(XPI/180.)
        ZPHI = XPHI(1)
        CALL T_MAT(TMAT,ZPHI,THETA2)
        DO 10 B = 1,3
            DO 15 C = 1,3
                TMAT1(B,C) = TMAT(B,C)
15            CONTINUE
10        CONTINUE
        ZPHI = XPHI(2)
        CALL T_MAT(TMAT,ZPHI,THETAX1)
        CALL T_SQR(TMAT,TMAT1)
        ZPHI = XPHI(3)
        CALL T_MAT(TMAT,ZPHI,THETAX1)
        CALL T_SQR(TMAT,TMAT1)
        ZPHI = XPHI(4) + (121.319*(XPI/180.))
        CALL T_MAT(TMAT,ZPHI,THETA2)
        CALL T_SQR(TMAT,TMAT1)
    ENDIF
    IF (A .EQ. 2) THEN
        ZPHI1 = XPHI1(4) + 0.63*(XPI/180.)
        ZPHI = XPHI(1)
        CALL T_MAT(TMAT,ZPHI,THETA2)
        DO 20 B = 1,3
            DO 25 C = 1,3
                TMAT1(B,C) = TMAT(B,C)
25            CONTINUE
20        CONTINUE
        ZPHI = XPHI(2)

```

```

CALL T_MAT(TMAT,ZPHI,THETAX1)
CALL T_SQR(TMAT,TMAT1)
ZPHI = XPHI(3)
CALL T_MAT(TMAT,ZPHI,THETAX1)
CALL T_SQR(TMAT,TMAT1)
ZPHI = XPHI(4) + (238.681*(XPI/180.))
CALL T_MAT(TMAT,ZPHI,THETA2)
CALL T_SQR(TMAT,TMAT1)
ENDIF
DO 30 D = 1,3
  IF (D .EQ. 1) THEN
    ZPHI = ZPHI1
    CALL T_MAT(TMAT,ZPHI,THETA3)
    CALL T_SQR1(TMAT,TMAT1)
  ENDIF
  IF (D .EQ. 2) THEN
    ZPHI = (120.*(XPI/180.)) + ZPHI1
    CALL T_MAT(TMAT,ZPHI,THETA3)
    CALL T_SQR1(TMAT,TMAT1)
  ENDIF
  IF (D .EQ. 3) THEN
    ZPHI = (240.*(XPI/180.)) + ZPHI1
    CALL T_MAT(TMAT,ZPHI,THETA3)
    CALL T_SQR1(TMAT,TMAT1)
  ENDIF
  XXX = 0.
  YYY = 0.
  ZZZ = 0.
  DO 35 B = 1,3
    XXX = XXX + TMAT(1,B)*XYZ(B)
    YYY = YYY + TMAT(2,B)*XYZ(B)
    ZZZ = ZZZ + TMAT(3,B)*XYZ(B)
35  CONTINUE
  IF (A .EQ. 1) THEN
    HXYZ(1,D + 10) = XXX + HXYZ(1,3)
    HXYZ(2,D + 10) = YYY + HXYZ(2,3)
    HXYZ(3,D + 10) = ZZZ + HXYZ(3,3)
  ENDIF
  IF (A .EQ. 2) THEN
    HXYZ(1,D + 13) = XXX + HXYZ(1,4)
    HXYZ(2,D + 13) = YYY + HXYZ(2,4)
    HXYZ(3,D + 13) = ZZZ + HXYZ(3,4)
  ENDIF
30  CONTINUE
5   CONTINUE
RETURN
END

SUBROUTINE
HHXYZ3(CXYZ,HXYZ,XPHI,XYZ,TMAT,TMAT1,THETAX1,THETA2)
DIMENSION CXYZ(3,8),HXYZ(3,28),XPHI(7),XYZ(3)
DIMENSION TMAT(3,3),TMAT1(3,3)
XPI = 3.14159265359
THETA2 = 70.*(XPI/180.)
XYZ(1) = 1.09
XYZ(2) = 0.
XYZ(3) = 0.
ZPHI = XPHI(1)

```

```

CALL T_MAT(TMAT,ZPHI,THETA2)
DO 5 B=1,3
  DO 10 C=1,3
    TMAT1(B,C) = TMAT(B,C)
10  CONTINUE
5  CONTINUE
ZPHI = XPHI(2)
CALL T_MAT(TMAT,ZPHI,THETAX1)
CALL T_SQR(TMAT,TMAT1)
ZPHI = XPHI(3)
CALL T_MAT(TMAT,ZPHI,THETAX1)
CALL T_SQR(TMAT,TMAT1)
ZPHI = XPHI(4)
CALL T_MAT(TMAT,ZPHI,THETA2)
CALL T_SQR(TMAT,TMAT1)
DO 15 A=5,6
  ZPHI = XPHI(A)
  IF (A .EQ. 5) THEN
    ZPHI = ZPHI + XPI
    CALL T_MAT(TMAT,ZPHI,THETAX2)
    CALL T_SQR1(TMAT,TMAT1)
  ENDIF
  IF (A .EQ. 6) THEN
    YPHI = XPHI(5)
    CALL T_MAT(TMAT,YPHI,THETAX1)
    CALL T_SQR(TMAT,TMAT1)
    ZPHI = ZPHI + XPI
    CALL T_MAT(TMAT,ZPHI,THETAX2)
    CALL T_SQR1(TMAT,TMAT1)
  ENDIF
  XXX = 0.
  YYY = 0.
  ZZZ = 0.
  DO 20 B=1,3
    XXX = XXX + TMAT(1,B)*XYZ(B)
    YYY = YYY + TMAT(2,B)*XYZ(B)
    ZZZ = ZZZ + TMAT(3,B)*XYZ(B)
20  CONTINUE
  HXYZ(1,A+4) = XXX + CXYZ(1,A+1)
  HXYZ(2,A+4) = YYY + CXYZ(2,A+1)
  HXYZ(3,A+4) = ZZZ + CXYZ(3,A+1)
15  CONTINUE
RETURN
END

```

```

SUBROUTINE
HHXYZ2(CXYZ,HXYZ,XPHI,XYZ,TMAT,TMAT1,THETAX1,THETAX2)
DIMENSION CXYZ(3,8),HXYZ(3,28),XPHI(7),XYZ(3)
DIMENSION TMAT(3,3),TMAT1(3,3)
XPI = 3.14159265359
THETA2 = 70. *(XPI/180.)
XYZ(1) = 1.09
XYZ(2) = 0.
XYZ(3) = 0.
ZPHI = XPHI(1)
CALL T_MAT(TMAT,ZPHI,THETA2)
DO 5 B=1,3
  DO 10 C=1,3

```

```

    TMAT1(B,C) = TMAT(B,C)
10  CONTINUE
5   CONTINUE
    DO 15 A = 2,3
      ZPHI = XPHI(A)
      IF (A .EQ. 2) THEN
        ZPHI = ZPHI + XPI
        CALL T_MAT(TMAT,ZPHI,THETAX2)
        CALL T_SQR1(TMAT,TMAT1)
      ENDIF
      IF (A .EQ. 3) THEN
        CALL T_MAT(TMAT,ZPHI,THETAX1)
        CALL T_SQR(TMAT,TMAT1)
        ZPHI = ZPHI + XPI
        CALL T_MAT(TMAT,ZPHI,THETAX2)
        CALL T_SQR1(TMAT,TMAT1)
      ENDIF
      XXX = 0.
      YYY = 0.
      ZZZ = 0.
      DO 20 B = 1,3
        XXX = XXX + TMAT(1,B)*XYZ(B)
        YYY = YYY + TMAT(2,B)*XYZ(B)
        ZZZ = ZZZ + TMAT(3,B)*XYZ(B)
20  CONTINUE
      HXYZ(1,A + 5) = XXX + CXYZ(1,A + 1)
      HXYZ(2,A + 5) = YYY + CXYZ(2,A + 1)
      HXYZ(3,A + 5) = ZZZ + CXYZ(3,A + 1)
15  CONTINUE
    RETURN
    END

SUBROUTINE HHXYZ1(CXYZ,HXYZ,XPHI,XYZ,TMAT,TMAT1,THETAX1)
DIMENSION CXYZ(3,8),HXYZ(3,28),XPHI(7),XYZ(3)
DIMENSION TMAT(3,3),TMAT1(3,3)
XPI = 3.14159265359
THETA2 = 70. *(XPI/180.)
ZPHI = XPHI(1)
CALL T_MAT(TMAT,ZPHI,THETA2)
DO 5 B = 1,3
  DO 10 C = 1,3
    TMAT1(B,C) = TMAT(B,C)
10  CONTINUE
5   CONTINUE
    ZPHI = XPHI(2)
    CALL T_MAT(TMAT,ZPHI,THETAX1)
    CALL T_SQR(TMAT,TMAT1)
    ZPHI = XPHI(3)
    CALL T_MAT(TMAT,ZPHI,THETAX1)
    CALL T_SQR(TMAT,TMAT1)
    ZPHI = XPHI(4)
    CALL T_MAT(TMAT,ZPHI,THETA2)
    CALL T_SQR(TMAT,TMAT1)
    DO 15 A = 5,6
      ZPHI = XPHI(A)
      CALL T_MAT(TMAT,ZPHI,THETAX1)
      CALL T_SQR(TMAT,TMAT1)
15  CONTINUE

```

```

XYZ(1) = 1.87
XYZ(2) = 0.
XYZ(3) = 0.
DO 20 A = 1,2
  IF (A .EQ. 1) THEN
    ZPHI = XPHI(7) + (121.319*(XPI/180.))
    CALL T_MAT(TMAT,ZPHI,THETA2)
    CALL T_SQR1(TMAT,TMAT1)
  ENDIF
  IF (A .EQ. 2) THEN
    ZPHI = XPHI(7) + (238.681*(XPI/180.))
    CALL T_MAT(TMAT,ZPHI,THETA2)
    CALL T_SQR1(TMAT,TMAT1)
  ENDIF
  XXX = 0.
  YYY = 0.
  ZZZ = 0.
  DO 25 B = 1,3
    XXX = XXX + TMAT(1,B)*XYZ(B)
    YYY = YYY + TMAT(2,B)*XYZ(B)
    ZZZ = ZZZ + TMAT(3,B)*XYZ(B)
25  CONTINUE
  HXYZ(1,A + 4) = XXX + CXYZ(1,8)
  HXYZ(2,A + 4) = YYY + CXYZ(2,8)
  HXYZ(3,A + 4) = ZZZ + CXYZ(3,8)
20  CONTINUE
RETURN
END

SUBROUTINE HHXYZ(CXYZ,HXYZ,XPHI,XYZ,TMAT,TMAT1,THETA2)
DIMENSION CXYZ(3,8),HXYZ(3,28),XPHI(7),XYZ(3)
DIMENSION TMAT(3,3),TMAT1(3,3)
XPI = 3.14159265359
THETA2 = 70.*(XPI/180.)
ZPHI = XPHI(1)
CALL T_MAT(TMAT,ZPHI,THETA2)
DO 5 B = 1,3
  DO 10 C = 1,3
    TMAT1(B,C) = TMAT(B,C)
10  CONTINUE
5  CONTINUE
ZPHI = XPHI(2)
CALL T_MAT(TMAT,ZPHI,THETA2)
CALL T_SQR(TMAT,TMAT1)
ZPHI = XPHI(3)
CALL T_MAT(TMAT,ZPHI,THETA2)
CALL T_SQR(TMAT,TMAT1)
XYZ(1) = 1.87
XYZ(2) = 0.
XYZ(3) = 0.
DO 15 A = 1,2
  IF (A .EQ. 1) THEN
    ZPHI = XPHI(4)
    ZPHI = ZPHI + (121.319*(XPI/180.))
    CALL T_MAT(TMAT,ZPHI,THETA2)
    CALL T_SQR1(TMAT,TMAT1)
  ENDIF
  IF (A .EQ. 2) THEN

```

```

        ZPHI = XPHI(4)
        ZPHI = ZPHI + (238.681*(XPI/180.))
        CALL T_MAT(TMAT,ZPHI,THETA2)
        CALL T_SQR1(TMAT,TMAT1)
    ENDIF
    XXX = 0.
    YYY = 0.
    ZZZ = 0.
    DO 20 B = 1,3
        XXX = XXX + TMAT(1,B)*XYZ(B)
        YYY = YYY + TMAT(2,B)*XYZ(B)
        ZZZ = ZZZ + TMAT(3,B)*XYZ(B)
20    CONTINUE
    HXYZ(1,A + 2) = XXX + CXYZ(1,5)
    HXYZ(2,A + 2) = YYY + CXYZ(2,5)
    HXYZ(3,A + 2) = ZZZ + CXYZ(3,5)
15    CONTINUE
    RETURN
    END

SUBROUTINE CCXYZ(CXYZ,XPHI,XYZ,TMAT,TMAT1,THETAX1)
DIMENSION CXYZ(3,8),XPHI(7),XYZ(3)
DIMENSION TMAT(3,3),TMAT1(3,3)
XPI = 3.14159265359
THETA2 = 70.*(XPI/180.)
DO 5 A = 1,6
    ZPHI = XPHI(A)
    IF (A .EQ. 1) THEN
        XYZ(1) = 1.85
        XYZ(2) = 0.
        XYZ(3) = 0.
        CALL T_MAT(TMAT,ZPHI,THETA2)
        DO 10 B = 1,3
            DO 15 C = 1,3
                TMAT1(B,C) = TMAT(B,C)
15            CONTINUE
10        CONTINUE
    ENDIF
    IF (A .EQ. 2) THEN
        XYZ(1) = 1.34
        XYZ(2) = 0.
        XYZ(3) = 0.
        CALL T_MAT(TMAT,ZPHI,THETAX1)
        CALL T_SQR(TMAT,TMAT1)
    ENDIF
    IF (A .EQ. 3) THEN
        XYZ(1) = 1.85
        XYZ(2) = 0.
        XYZ(3) = 0.
        CALL T_MAT(TMAT,ZPHI,THETAX1)
        CALL T_SQR(TMAT,TMAT1)
    ENDIF
    IF (A .EQ. 4) THEN
        XYZ(1) = 1.85
        XYZ(2) = 0.
        XYZ(3) = 0.
        CALL T_MAT(TMAT,ZPHI,THETA2)
        CALL T_SQR(TMAT,TMAT1)

```

```

ENDIF
IF (A .EQ. 5) THEN
  XYZ(1) = 1.34
  XYZ(2) = 0.
  XYZ(3) = 0.
  CALL T_MAT(TMAT,ZPHI,THETAX1)
  CALL T_SQR(TMAT,TMAT1)
ENDIF
IF (A .EQ. 6) THEN
  XYZ(1) = 1.85
  XYZ(2) = 0.
  XYZ(3) = 0.
  CALL T_MAT(TMAT,ZPHI,THETAX1)
  CALL T_SQR(TMAT,TMAT1)
ENDIF
XXX = 0.
YYY = 0.
ZZZ = 0.
DO 20 B = 1,3
  XXX = XXX + TMAT(1,B)*XYZ(B)
  YYY = YYY + TMAT(2,B)*XYZ(B)
  ZZZ = ZZZ + TMAT(3,B)*XYZ(B)
20  CONTINUE
  CXYZ(1,A + 2) = XXX + CXYZ(1,A + 1)
  CXYZ(2,A + 2) = YYY + CXYZ(2,A + 1)
  CXYZ(3,A + 2) = ZZZ + CXYZ(3,A + 1)
5  CONTINUE
RETURN
END

SUBROUTINE SET_XYZ(CXYZ)
DIMENSION CXYZ(3,8)
CXYZ(1,1) = 0.
CXYZ(2,1) = 0.
CXYZ(3,1) = 0.
CXYZ(1,2) = 1.89
CXYZ(2,2) = 0.
CXYZ(3,2) = 0.
RETURN
END

SUBROUTINE T_MAT(TMAT,ZPHI,THETA)
DIMENSION TMAT(3,3)
TMAT(1,1) = COS(THETA)
TMAT(1,2) = SIN(THETA)
TMAT(1,3) = 0.
TMAT(2,1) = SIN(THETA)*COS(ZPHI)
TMAT(2,2) = -(COS(THETA)*COS(ZPHI))
TMAT(2,3) = SIN(ZPHI)
TMAT(3,1) = SIN(THETA)*SIN(ZPHI)
TMAT(3,2) = -(COS(THETA)*SIN(ZPHI))
TMAT(3,3) = -COS(ZPHI)
RETURN
END

SUBROUTINE T_SQR(TMAT,TMAT1)
DIMENSION TMAT(3,3),TMAT1(3,3),TMAT2(3,3)
DO 5 C = 1,3

```

```

        DO 10 A = 1,3
          SUM0 = 0.
          DO 15 B = 1,3
            SUM0 = SUM0 + TMAT1(C,B)*TMAT(B,A)
15      CONTINUE
          TMAT2(C,A) = SUM0
10      CONTINUE
5       CONTINUE
        DO 20 A = 1,3
          DO 25 B = 1,3
            TMAT(A,B) = TMAT2(A,B)
            TMAT1(A,B) = TMAT2(A,B)
25      CONTINUE
20      CONTINUE
        RETURN
        END

```

```

SUBROUTINE T_SQR1(TMAT, TMAT1)
DIMENSION TMAT(3,3), TMAT1(3,3), TMAT2(3,3)
DO 5 C = 1,3
  DO 10 A = 1,3
    SUM0 = 0.
    DO 15 B = 1,3
      SUM0 = SUM0 + TMAT1(C,B)*TMAT(B,A)
15    CONTINUE
      TMAT2(C,A) = SUM0
10    CONTINUE
5     CONTINUE
  DO 20 A = 1,3
    DO 25 B = 1,3
      TMAT(A,B) = TMAT2(A,B)
25    CONTINUE
20    CONTINUE
  RETURN
END

```


APPENDIX C

COMPUTER PROGRAMS

C.1. Introduction

The computer programs employed in the analysis of experimental and theoretical data are presented in this appendix. Each program is accompanied by an outline of its function together with a list of the parameters required as input by the program. All the programs were written in QBasic and were run on an IBM AT personal computer.

C.2. Davidson-Cole Analysis

This program calculates theoretical values of dielectric permittivity and dielectric loss, at a series of spot frequencies in the range $100-10^5$, for particular values of β , ϵ_0 , ϵ_i and the frequency corresponding to maximum loss, f_{\max} . The program requires as input the following data:

1. Values of the Davidson-Cole empirical distribution factor, β .
2. The limiting low frequency permittivity, ϵ_0 .
3. The limiting high frequency permittivity, ϵ_i .
4. The frequency corresponding to maximum loss, f_{\max} .

Using the first input value of β , the value of f_{\max} , and the equation (8-32), the program is able to calculate a value of τ_1 . This permits the program to calculate a value of ϕ (from $\text{Tan}\phi = \omega\tau_1$) at each spot frequency. Equations

(8-30) and (8-31) are then used to calculate the values of ϵ' and ϵ'' . The results of the calculations are then displayed on the screen with the option of producing a hard copy.

Computer Program Listing

```

'           Theoretical Evaluation of Dielectric Loss
'           Equations Using Various Models
'
'           Written by Dr. M.S.Beevers,
'           Department of Chemical Engineering and Applied Chemistry,
'           Aston University, Birmingham, B4 7ET.
'
'           Converted to QBasic by David J. Elsby
'
DIM  freqs(25),logfreqs(25),eloss(25),eperm(25),ordinate(25),abscissa(25)
DECLARE SUB  intro      (ans,modelname$)
DECLARE SUB  initialise (reqs(),logfreqs(),nfreq,tau,elow,ehigh)
DECLARE SUB  display1  (modelname$,freqs(),eloss(),eperm(),logfreqs(),
                        nfreq,fmax,emax,beta)

DECLARE SUB  debye     (freqs(),eloss(),eperm(),nfreq,tau,elow,ehigh)
DECLARE SUB  normalise (freqs(),eloss(),nfreq,fmax,emax)
DECLARE SUB  cole      (freqs(),eloss(),eperm(),nfreq,tau,elow,ehigh,beta)
DECLARE SUB  davidson  (freqs(),eloss(),eperm(),nfreq,tau,elow,ehigh,
                        beta)
'
'***Main Program Routine***
CALL intro      (ans,modelname$)
CALL initialise (freqs(),logfreqs(),nfreq,tau,elow,ehigh)
IF (ans = 1) THEN
    CALL debye   (freqs(),eloss(),eperm(),nfreq,tau,elow,ehigh)
    CALL normalise (freqs(),eloss(),nfreq,fmax,emax)
    CALL display1 (modelname$,freqs(),eloss(),eperm(),logfreqs(),
                  nfreq,fmax,emax,beta)
END IF
IF (ans = 2) THEN
    CLS
    LINE (150, 140) - (490, 180), 1, BF
    LINE (150, 140)-(490, 180), 15, B
    LOCATE 12, 22
    INPUT "Enter a value of Beta ? ", beta
    CALL cole      (freqs(),eloss(),eperm(),nfreq,tau,elow,ehigh,beta)
    CALL normalise (freqs(),eloss(),nfreq,fmax,emax)

```

```

CALL display1 (modelname$,freqs(),eloss(),eperm(),logfreqs(),
              nfreq,fmax,emax,beta)
END IF
IF (ans = 3) THEN
  CLS
  LINE (150, 140)-(490, 180), 1, BF
  LINE (150, 140)-(490, 180), 15, B
  LOCATE 12, 22
  INPUT "Enter a value of Gamma ? ", beta
  CALL davidson (freqs(),eloss(),eperm(),nfreq,tau,elow,ehigh,
               beta)
  CALL normalise (freqs(),eloss(),nfreq,fmax,emax)
  CALL display1 (modelname$,freqs(),eloss(),eperm(),logfreqs(),
               nfreq,fmax,emax,beta)
END IF
END
'
'***Cole-Cole-Analysis***
SUB cole (freqs(),eloss(),eperm(),nfreq,tau,elow,ehigh,beta)
  CLS
  pi = 3.14159
  sbeta = SIN(beta * pi / 2)
  cbeta = COS(beta * pi / 2)
  FOR i = 1 TO nfreq
    wrad = 2 * pi * freqs(i)
    eloss(i) = (elow - ehight) * (wrad * tau) ^ beta * sbeta
    eloss(i) = eloss(i) / (1 + 2 * ((wrad * tau) ^ beta) * cbeta +
    (wrad * tau) ^ (2 * beta))
    eperm(i) = (elow - ehight) * (1 + (wrad * tau) ^ beta * cbeta)
    eperm(i) = eperm(i) / (1 + 2 * ((wrad * tau) ^ beta) * cbeta +
    (wrad * tau) ^ (2 * beta))
    eperm(i) = eperm(i) + ehight
  NEXT i
END SUB
'
'***Davidson-Cole-Analysis***
SUB davidson (freqs(),eloss(),eperm(),nfreq,tau,elow,ehight,beta)
  CLS
  pi = 3.14159
  FOR i = 1 TO nfreq
    wrad = 2 * pi * freqs(i)
    phi = ATN(wrad * tau)
    cphi = COS(phi)
    sphigamma = SIN(phi * beta)
    cphigamma = COS(phi * beta)
    eloss(i) = (elow - ehight) * (cphi ^ beta) * sphigamma
  
```

```

        eperm(i) = ((elow - ehigh) * (cphi ^ beta) * cphigamma) + ehigh
    NEXT i
END SUB
'
'***Debye-Analysis***
SUB debye (freqs(),eloss(),eperm(),nfreq,tau,elow,ehigh)
    CLS
    pi = 3.14159
    FOR i = 1 TO nfreq
        wrad = 2 * pi * freqs(i)
        eloss(i) = ((elow - ehigh) * wrad * tau) / (1 + wrad * wrad * tau *
        tau)
        eperm(i) = ehigh + (elow - ehigh) / (1 + wrad * wrad * tau * tau)
    NEXT i
END SUB
'
'***Display-Results***
SUB display (modelname$,freqs(),eloss(),eperm(),logfreqs(),nfreq,fmax,
            emax,beta)
    CLS
    LINE (2, 2)-(636, 346), 1, BF
    LINE (2, 2)-(636, 346), 15, B
    IF (modelname$ = "-Debye Model-") THEN
        LOCATE 2, 17
        PRINT "Dielectric Relaxation : "; modelname$
    END IF
    IF (modelname$ = "-Cole-Cole Model-") THEN
        LOCATE 2, 6
        PRINT "Dielectric Relaxation : "; modelname$
        LOCATE 2, 55
        PRINT "Beta ="; beta
        ELSE PRINT ""
    END IF
    IF (modelname$ = "-Davidson-Cole Model-") THEN
        LOCATE 2, 6
        PRINT "Dielectric Relaxation : "; modelname$
        LOCATE 2, 55
        PRINT "Gamma ="; beta
        ELSE PRINT ""
    END IF
    LOCATE 4, 6
    PRINT "Frequency (Hz)"
    LOCATE 4, 27
    PRINT "Log f (Hz)"
    LOCATE 4, 47
    PRINT "Loss"

```

```

LOCATE 4, 62
PRINT "Permittivity"
FOR i = 1 TO nfreq
  LOCATE 5 + i, 9
  PRINT freqs(i)
  LOCATE 5 + i, 27
  PRINT logfreqs(i)
  LOCATE 5 + i, 43
  PRINT eloss(i)
  LOCATE 5 + i, 63
  PRINT eperm(i)
NEXT i
LOCATE 21, 6
PRINT "Emax =", emax
LOCATE 21, 30
PRINT "Fmax (Hz) =", fmax,
LOCATE 23, 6
INPUT "Do you require a print out of the results...(Y/N) ? ", prn$
IF (prn$ = "y" OR prn$ = "Y") THEN
  LOCATE 23, 6
  PRINT "Press 'PrtSc' on keyboard (right of the F12 function
  button)"
  SLEEP 15
END IF
LOCATE 23, 6
PRINT "
LOCATE 23, 6
PRINT "Press any key to continue...."
DO
  key$ = INKEY$
LOOP WHILE LEN(key$) = 0
RUN
END SUB
'
'***Initialise-Parameters***
SUB initialise (freqs(),logfreqs(),nfreq,tau,elow,ehigh)
CLS
LINE (10, 10)-(630, 220), 1, BF
LINE (10, 10)-(630, 220), 15, B
pi = 3.14159
LOCATE 3, 4
INPUT "Enter centre frequency (Hz) ? ", cenfreq
wrad = 2 * pi * cenfreq
tau = 1 / wrad
LOCATE 6, 4
INPUT "Enter zero frequency dielectric permittivity ? ", elow

```

```

LOCATE 9, 4
INPUT "Enter optical or high frequency dielectric permittivity ? ",
      ehigh
WHILE test% = 0
LOCATE 12, 4
INPUT "Number of frequencies (multiples of 3, plus 1, max. 13) ? ",
      nfreq$
nfreq = VAL(nfreq$)
IF ((nfreq - 1) / 3) - INT((nfreq - 1) / 3) = 0 THEN
  test% = 1
END IF
IF ((nfreq - 1) / 3) - INT((nfreq - 1) / 3) <> 0 THEN
  BEEP
END IF
IF ((nfreq - 1) / 3) - INT((nfreq - 1) / 3) > 13 THEN
  BEEP
END IF
WEND
FOR i = 1 TO ((nfreq - 1) / 3)
  freqs(1 + 3 * (i - 1)) = 1 * 10 ^ i
  freqs(2 + 3 * (i - 1)) = 2 * 10 ^ i
  freqs(3 + 3 * (i - 1)) = 5 * 10 ^ i
NEXT i
freqs(nfreq) = 10 ^ (((nfreq - 1) / 3) + 1)
FOR i = 1 TO nfreq
  logfreqs(i) = .4342936 * LOG(freqs(i))
NEXT i
END SUB
'
'***Introduction-Screen***
SUB intro (ans,modelname$)
  CLS
  SCREEN 9
  COLOR , 9
  LINE (50, 50)-(590, 300), 1, BF
  LINE (50, 50)-(590, 300), 15, B
  LOCATE 18, 14
  PRINT "Which model do you require...(1-4) "
  LOCATE 8, 14
  PRINT "1 : Debye model (single relaxation time)"
  LOCATE 10, 14
  PRINT "2 : Cole-Cole model (symmetrical distribution)"
  LOCATE 12, 14
  PRINT "3 : Davidson-Cole model (asymmetrical distribution)"
  LOCATE 14, 14
  PRINT "4 : Exit program"

```

```

LOCATE 18, 48
INPUT ans$
ans = VAL(ans$)
WHILE (ans < 1) OR (ans > 4)
    LOCATE 20, 14
    PRINT "**** Choice invalid ! ****"
    BEEP
    SLEEP 1.5
    LOCATE 20, 14
    PRINT "**** Please try again ! ****"
    LOCATE 18, 48
    INPUT ans$
    ans = VAL(ans$)
WEND
IF (ans = 1) THEN
    modelname$ = "-Debye Model-"
END IF
IF (ans = 2) THEN
    modelname$ = "-Cole-Cole Model-"
END IF
IF (ans = 3) THEN
    modelname$ = "-Davidson-Cole Model-"
END IF
IF (ans = 4) THEN
    CLS
    LINE (150, 140)-(490, 180), 1, BF
    LINE (150, 140)-(490, 180), 15, B
    LOCATE 12, 22
    PRINT "Are you sure you want to quit...(Y/N) ?"
    BEEP
    DO
        key$ = INKEY$
    LOOP WHILE LEN(key$) = 0
    IF (key$ <> "Y" AND key$ <> "y") THEN
        CLS
        RUN
    END IF
    CLS
    END
END IF
END SUB
'
'***Normalise-Dielectric-Loss***
SUB normalise (freqs(),eloss(),nfreq,fmax,emax)
CLS
maxloss = 0

```

```

FOR i = 1 TO nfreq
  IF (eloss(i) > maxloss) THEN
    maxloss = eloss(i)
    fmax = freqs(i)
  END IF
NEXT i
emax = INT(1000 * maxloss) / 1000
FOR i = 1 TO nfreq
  eloss(i) = eloss(i) / maxloss
NEXT i
END SUB

```

C.3. Calculation of the Characteristic Ratio and the Dipole Moment Ratio of Poly(dimethylsilmethylene)

This program was used to calculate the characteristic ratio and dipole moment ratio of poly(dimethylsilmethylene). The calculations were carried out according to Eq. (4-13) and Eq. (4-16) respectively. The calculations may be performed on chains of different lengths and at different temperatures.

Computer Program Listings

```

'
'           Calculation of the Characteristic Ratio
'           and the Dipole Moment Ratio for
'           poly(dimethylsilmethylene).
'
'
'           Written by D. J. Elsby
'           Department of Chemical Engineering and Applied
'           Chemistry, Aston University, Birmingham, B4 7ET.
'
'
DIM gmat1#(15,15),gmat#(15,15),temp1#(15,15)
DIM gmata#(15,15),gmatb#(15,15),umata#(3,3),umatb#(3,3)
DIM tmata1#(3,3),tmata2#(3,3),tmata3#(3,3)
DIM matb1#(3,3),tmatb2#(3,3),tmatb3#(3,3)
DIM temp2#(15,15),temp3#(15,15),temp4#(15,15),utemp1#(3,3)
DIM temp#(3,3),umat#(3,3),zmat#(3,3),emat#(3,3)
DIM bmat#(9,9),jstar1#(3),jnorm1#(3),jtemp1#(3)
DIM jstar2#(15),jnorm2#(15),jtemp2#(15),jtemp3#(15)
DIM xyz#(3),amat#(3,9)

```



```

DECLARE SUB intro (polynome$,ans)
DECLARE SUB setgmat (gmat1#(),tmat1#(),tmat2#(),tmat3#(),emat#(),
emat#(),xyz#(),polynome$,ans)

DECLARE SUB sqr1 (umat#(),umata#(),umatb#())
DECLARE SUB sqr2 (gmat#(),gmata#(),gmatb#())
DECLARE SUB UMATSQR (umat#(),umata#(),zpart#,scale,bond)
DECLARE SUB GMATSQR (gmat#(),gmat1#(),gmata#(),vector#,scale,
bond)
DECLARE SUB RESULTS (xyz#(),vector#,zpart#,bond,znum,temp,
polynome$,ans2)

emat#(1,1) = 1
emat#(1,2) = 0
emat#(1,3) = 0
emat#(2,1) = 0
emat#(2,2) = 1
emat#(2,3) = 0
emat#(3,1) = 0
emat#(3,2) = 0
emat#(3,3) = 1
CALL intro(polynome$, ans)
gascon = 8.31441
tmatb1#(1,1) = 0.3811
tmatb1#(1,2) = 0.9245
tmatb1#(1,3) = 0
tmatb1#(2,1) = 0.9245
tmatb1#(2,2) = -0.3811
tmatb1#(2,3) = 0
tmatb1#(3,1) = 0
tmatb1#(3,2) = 0
tmatb1#(3,3) = -1
tmatb2#(1,1) = 0.3811
tmatb2#(1,2) = 0.9245
tmatb2#(1,3) = 0
tmatb2#(2,1) = -0.3907
tmatb2#(2,2) = 0.16105
tmatb2#(2,3) = 0.9063
tmatb2#(3,1) = 0.8379
tmatb2#(3,2) = -0.34537
tmatb2#(3,3) = 0.4226
tmatb3#(1,1) = 0.3811
tmatb3#(1,2) = 0.9245
tmatb3#(1,3) = 0
tmatb3#(2,1) = -0.3907
tmatb3#(2,2) = 0.16105
tmatb3#(2,3) = -0.9063

```

```

tmatb3#(3,1) = -0.83792
tmatb3#(3,2) = 0.34537
tmatb3#(3,3) = 0.4226
tmata1#(1,1) = 0.54756
tmata1#(1,2) = 0.83676
tmata1#(1,3) = 0
tmata1#(2,1) = 0.83676
tmata1#(2,2) = -0.54756
tmata1#(2,3) = 0
tmata1#(3,1) = 0
tmata1#(3,2) = 0
tmata1#(3,3) = -1
tmata2#(1,1) = 0.54756
tmata2#(1,2) = 0.83676
tmata2#(1,3) = 0
tmata2#(2,1) = -0.3536
tmata2#(2,2) = 0.23141
tmata2#(2,3) = 0.9063
tmata2#(3,1) = 0.7584
tmata2#(3,2) = -0.4963
tmata2#(3,3) = 0.4226
tmata3#(1,1) = 0.54756
tmata3#(1,2) = 0.83676
tmata3#(1,3) = 0
tmata3#(2,1) = -0.3536
tmata3#(2,2) = 0.2314
tmata3#(2,3) = -0.9063
tmata3#(3,1) = -0.7584
tmata3#(3,2) = 0.49626
tmata3#(3,3) = 0.4226
IF (ans = 1) THEN
  xyza#(1) = 1.89
  xyza#(2) = 0
  xyza#(3) = 0
  xyzb#(1) = 1.89
  xyzb#(2) = 0
  xyzb#(3) = 0
END IF
IF (ans = 2) THEN
  xyza#(1) = -0.6
  xyza#(2) = 0
  xyza#(3) = 0
  xyzb#(1) = 0.6
  xyzb#(2) = 0
  xyzb#(3) = 0
END IF

```

```

CLS
SCREEN 9
COLOR , 9
LINE (50, 50)-(590, 150), 1, BF
LINE (50, 50)-(590, 150), 15, B
LOCATE 6, 10
INPUT "Enter the Temperature for the Calculations (K)"; temp
alpha = 0.97 * EXP(-164 / (gascon * temp))
beta = 0.91 * EXP(-287 / (gascon * temp))
gamma = .85 * EXP(-369 / (gascon * temp))
umata#(1,1) = 1
umata#(1,2) = alpha
umata#(1,3) = alpha
umata#(2,1) = alpha
umata#(2,2) = beta
umata#(2,3) = gamma
umata#(3,1) = alpha
umata#(3,2) = gamma
umata#(3,3) = beta
umatb#(1,1) = 1
umatb#(1,2) = 1
umatb#(1,3) = 1
umatb#(2,1) = 1
umatb#(2,2) = 1
umatb#(2,3) = 0
umatb#(3,1) = 1
umatb#(3,2) = 0
umatb#(3,3) = 1
LOCATE 9, 10
INPUT "Enter the Number of Matrix Squares Required"; bond
CALL setgmat (gmat1#(),tmatb1#(),tmatb2#(),tmatb3#(),emat#(),emat#(),
             xyzb#(), polyname$, ans)
CALL setgmat (gmata#(),tmata1#(),tmata2#(),tmata3#(),umata#(),emat#(),
             xyza#(),polyname$,ans)
CALL setgmat (gmatb#(),tmatb1#(),tmatb2#(),tmatb3#(),umatb#(),emat#(),
             xyzb#(),polyname$,ans)
CALL sqr1 (umat#(),umata#(),umatb#())
CALL sqr2 (gmat#(),gmata#(),gmatb#())
CALL UMATSQR (umat#(),umata#(),zpart#,scale,bond)
CALL GMATSQR (gmat#(),gmat1#(),gmata#(),vector#,scale,bond)
CALL RESULTS (xyza#(),vector#,zpart#,bond,znum,temp,polyname$,
             ans2)

SUB GMATSQR (temp2#(),gmat1#(),gmata#(),vector#,scale,bond)
  DIM jstar2#(15),jnorm2#(15),jtemp2#(15),jtemp3#(15)
  DIM temp3#(15, 15), sum0 AS DOUBLE

```

```

CLS
LINE (150, 140)-(490, 220), 1, BF
LINE (150, 140)-(490, 220), 15, B
LOCATE 12, 22
PRINT "Processing Subroutine GMATSQR"
LOCATE 14, 22
PRINT "Please wait....."
FOR z = 1 TO bond
  FOR c = 1 TO 15
    FOR a = 1 TO 15
      sum0 = 0
      FOR B = 1 TO 15
        sum0 = sum0 + (temp2#(c, B) * temp2#(B, a))
      NEXT B
      temp3#(c, a) = sum0
    NEXT a
  NEXT c
  FOR a = 1 TO 15
    FOR B = 1 TO 15
      temp2#(a, B) = temp3#(a, B)
    NEXT B
  NEXT a
NEXT z
FOR c = 1 TO 15
  FOR a = 1 TO 15
    sum0 = 0
    FOR B = 1 TO 15
      sum0 = sum0 + (gmat1#(c, B) * temp2#(B, a))
    NEXT B
    temp3#(c, a) = sum0
  NEXT a
NEXT c
FOR c = 1 TO 15
  FOR a = 1 TO 15
    sum0 = 0
    FOR B = 1 TO 15
      sum0 = sum0 + (temp3#(c, B) * gmata#(B, a))
    NEXT B
    temp2#(c, a) = sum0
  NEXT a
NEXT c
vector# = temp2#(1, 13) + temp2#(1, 14) + temp2#(1, 15)
END SUB

```

```

SUB intro (polyname$,ans)
  CLS
  SCREEN 9
  COLOR , 9
  LINE (50, 50)-(590, 300), 1, BF
  LINE (50, 50)-(590, 300), 15, B
  LOCATE 18, 14
  PRINT "Please Select Which Option You Require (1-3) "
  LOCATE 8, 14
  PRINT "1 : Calculate Characteristic Ratio"
  LOCATE 11, 14
  PRINT "2 : Calculate Dipole Moment Ratio"
  LOCATE 14, 14
  PRINT "3 : Exit Program"
  LOCATE 18, 58
  INPUT ans$
  ans = VAL(ans$)
  WHILE (ans < 1) OR (ans > 3)
    LOCATE 20, 14
    PRINT "**** Choice invalid ! ****"
    BEEP
    SLEEP 1.5
    LOCATE 20, 14
    PRINT "**** Please try again ! ****"
    LOCATE 18, 58
    INPUT ans$
    ans = VAL(ans$)
  WEND
  IF (ans = 1) THEN
    polyname$ = "-Poly(dimethylsiloxane)-"
  END IF
  IF (ans = 2) THEN
    polyname$ = "-Poly(dimethylsilimethylene)-"
  END IF
  IF (ans = 3) THEN
    CLS
    LINE (150, 140)-(490, 180), 1, BF
    LINE (150, 140)-(490, 180), 15, B
    LOCATE 12, 22
    PRINT "Are you sure you want to quit...(Y/N) ?"
    BEEP
    DO
      key$ = INKEY$
    LOOP WHILE LEN(key$) = 0
    IF (key$ <> "Y" AND key$ <> "y") THEN
      CLS

```

```

        RUN
    END IF
    CLS
    END
END IF
END SUB

SUB RESULTS (xyz#(),vector#,zpart#,bond,znum,temp,polynome$,ans2)
    CLS
    SCREEN 9
    COLOR , 9
    LINE (50, 50)-(590, 300), 1, BF
    LINE (50, 50)-(590, 300), 15, B
    LOCATE 7, 14
    znum = 2 * (1 + (2 ^ bond))
    ratio = (2 * (1 / zpart#) * vector#) / (znum * (xyz#(1) ^ 2))
    PRINT "Results for"
    LOCATE 7, 30
    PRINT polynome$
    IF (ans2 = 1) THEN
        LOCATE 10, 14
        PRINT "Characteristic Ratio is"
    END IF
    IF (ans2 = 2) THEN
        LOCATE 10, 14
        PRINT "Dipole Moment Ratio is"
    END IF
    LOCATE 10, 40
    PRINT ratio
    LOCATE 13, 14
    PRINT "Number of Bonds in the Chain is"
    LOCATE 13, 47
    PRINT znum
    LOCATE 16, 14
    PRINT "Temperature Used in the Calculations is"
    LOCATE 16, 55
    PRINT temp
    LOCATE 16, 60
    PRINT "K"
    LOCATE 19, 14
    PRINT "Press any key to Continue....."
    DO
        key$ = INKEY$
    LOOP WHILE LEN(key$) = 0
    RUN
END SUB

```

```

SUB setgmat (temp1#(),tmat1#(),tmat2#(),tmat3#(),temp#(),emat#(),xyz#(),
            polyname$, ans)
DIM sum1 AS DOUBLE, sum2 AS DOUBLE, sum3 AS DOUBLE, sum4 AS
    DOUBLE, sum5 AS DOUBLE, sum6 AS DOUBLE, sum7 AS DOUBLE
DIM sum8 AS DOUBLE, sum9 AS DOUBLE, sum10 AS DOUBLE, sum11 AS
    DOUBLE, sum12 AS DOUBLE
DIM amat#(3,9),bmat#(9,9),zmatsqr AS DOUBLE
CLS
LINE (150, 140)-(490, 220), 1, BF
LINE (150, 140)-(490, 220), 15, B
LOCATE 12, 22
PRINT "Processing Subroutine SETMAT"
LOCATE 14, 22
PRINT "Please wait....."
zmatsqr = (xyz#(1) ^ 2 + xyz#(2) ^ 2 + xyz#(3) ^ 2)
FOR a = 1 TO 3
    FOR B = 1 TO 3
        amat#(a, B) = temp#(a, 1) * xyz#(B)
        amat#(a, B + 3) = temp#(a, 2) * xyz#(B)
        amat#(a, B + 6) = temp#(a, 3) * xyz#(B)
        bmat#(a, B) = temp#(1, 1) * emat#(a, B)
        bmat#(a, B + 3) = temp#(1, 2) * emat#(a, B)
        bmat#(a, B + 6) = temp#(1, 3) * emat#(a, B)
        bmat#(a + 3, B) = temp#(2, 1) * emat#(a, B)
        bmat#(a + 3, B + 3) = temp#(2, 2) * emat#(a, B)
        bmat#(a + 3, B + 6) = temp#(2, 3) * emat#(a, B)
        bmat#(a + 6, B) = temp#(3, 1) * emat#(a, B)
        bmat#(a + 6, B + 3) = temp#(3, 2) * emat#(a, B)
        bmat#(a + 6, B + 6) = temp#(3, 3) * emat#(a, B)
        temp1#(a, B) = temp#(a, B)
        temp1#(a + 12, B + 12) = temp#(a, B)
        temp1#(a + 3, B + 12) = temp#(1, B) * xyz#(a)
        temp1#(a + 6, B + 12) = temp#(2, B) * xyz#(a)
        temp1#(a + 9, B + 12) = temp#(3, B) * xyz#(a)
        temp1#(a, B + 12) = (zmatsqr / 2) * temp#(a, B)
    NEXT B
NEXT a
FOR c = 1 TO 3
    FOR a = 1 TO 3
        sum1 = 0
        sum2 = 0
        sum3 = 0
        sum4 = 0
        sum5 = 0
        sum6 = 0

```

```

sum7 = 0
sum8 = 0
sum9 = 0
sum10 = 0
sum11 = 0
sum12 = 0
FOR B = 1 TO 3
    sum1 = sum1 + amat#(c, B) * tmat1#(B, a)
    sum2 = sum2 + amat#(c, B + 3) * tmat2#(B, a)
    sum3 = sum3 + amat#(c, B + 6) * tmat3#(B, a)
    sum4 = sum4 + bmat#(c, B) * tmat1#(B, a)
    sum5 = sum5 + bmat#(c, B + 3) * tmat2#(B, a)
    sum6 = sum6 + bmat#(c, B + 6) * tmat3#(B, a)
    sum7 = sum7 + bmat#(c + 3, B) * tmat1#(B, a)
    sum8 = sum8 + bmat#(c + 3, B + 3) * tmat2#(B, a)
    sum9 = sum9 + bmat#(c + 3, B + 6) * tmat3#(B, a)
    sum10 = sum10 + bmat#(c + 6, B) * tmat1#(B, a)
    sum11 = sum11 + bmat#(c + 6, B + 3) * tmat2#(B, a)
    sum12 = sum12 + bmat#(c + 6, B + 6) * tmat3#(B, a)
NEXT B
temp1#(c, a + 3) = sum1
temp1#(c, a + 6) = sum2
temp1#(c, a + 9) = sum3
temp1#(c + 3, a + 3) = sum4
temp1#(c + 3, a + 6) = sum5
temp1#(c + 3, a + 9) = sum6
temp1#(c + 6, a + 3) = sum7
temp1#(c + 6, a + 6) = sum8
temp1#(c + 6, a + 9) = sum9
temp1#(c + 9, a + 3) = sum10
temp1#(c + 9, a + 6) = sum11
temp1#(c + 9, a + 9) = sum12
NEXT a
NEXT c
END SUB

SUBsqr1 (umat#(),umata#(),umatb#())
CLS
LINE (150, 140)-(490, 220), 1, BF
LINE (150, 140)-(490, 220), 15, B
LOCATE 12, 22
PRINT "Processing Subroutine SETSQR1"
LOCATE 14, 22
PRINT "Please wait....."
FOR c = 1 TO 3
    FOR a = 1 TO 3

```



```

        sum0 = 0
        FOR B = 1 TO 3
            sum0 = sum0 + umata#(c, B) * umatb#(B, a)
        NEXT B
        umat#(c, a) = sum0
    NEXT a
NEXT c
END SUB

```

```

SUB sqr2 (gmat#(),gmata#(),gmatb#())
CLS
LINE (150, 140)-(490, 220), 1, BF
LINE (150, 140)-(490, 220), 15, B
LOCATE 12, 22
PRINT "Processing Subroutine SETSQR2"
LOCATE 14, 22
PRINT "Please wait....."
FOR c = 1 TO 15
    FOR a = 1 TO 15
        sum0 = 0
        FOR B = 1 TO 15
            sum0 = sum0 + gmata#(c, B) * gmatb#(B, a)
        NEXT B
        gmat#(c, a) = sum0
    NEXT a
NEXT c
END SUB

```

```

SUB UMATSQR (zmat#(), umata#(), zpart#, scale, bond)
DIM utemp1#(3,3)
DIM jtemp1#(3),jstar1#(3),jnorm1#(3)
DIM zlam AS DOUBLE, sum0 AS DOUBLE, zmax AS DOUBLE
CLS
LINE (150, 140)-(490, 220), 1, BF
LINE (150, 140)-(490, 220), 15, B
LOCATE 12, 22
PRINT "Processing Subroutine UMATSQR"
LOCATE 14, 22
PRINT "Please wait....."
FOR z = 1 TO bond
    FOR c = 1 TO 3
        FOR a = 1 TO 3
            sum0 = 0
            FOR B = 1 TO 3
                sum0 = sum0 + (zmat#(c, B) * zmat#(B, a))
            NEXT B

```

```

        utemp1#(c, a) = sum0
    NEXT a
NEXT c
FOR a = 1 TO 3
    FOR B = 1 TO 3
        zmat#(a, B) = utemp1#(a, B)
    NEXT B
NEXT a
NEXT z
FOR c = 1 TO 3
    FOR a = 1 TO 3
        sum0 = 0
        FOR B = 1 TO 3
            sum0 = sum0 + (zmat#(c, B) * umata#(B, a))
        NEXT B
        utemp1#(c, a) = sum0
    NEXT a
NEXT c
FOR a = 1 TO 3
    FOR B = 1 TO 3
        zmat#(a, B) = utemp1#(a, B)
    NEXT B
NEXT a
zpart# = zmat#(1, 1) + zmat#(1, 2) + zmat#(1, 3)
END SUB

```

C.4. Calculation of the Characteristic Ratio of Poly(dimethylsilethane)

This program was used to calculate the characteristic ratio of poly(dimethylsilethane). The calculations were carried out according to Eq. (6-5). The calculations may be performed on chains with different lengths.

Computer Program Listing

```

·           Calculation of the Characteristic Ratio
·           of poly(dimethylsilethane).
·
·           Written by D. J. Elsby
·           Department of Chemical Engineering and Applied
·           Chemistry, Aston University, Birmingham, B4 7ET.

```

```

DIM  gmat1#(15,15),gmat#(15,15),temp1#(15,15)

```

```

DIM    gmata#(15,15),gmatb#(15,15),gmatc#(15,15),gmatd#(15,15),
       gmate#(15,15)
DIM    umata#(3,3),umatb#(3,3),umate#(3,3),umatc#(3,3),umatd#(3,3),umate#(3,3)
DIM    tmata1#(3,3),tmata2#(3,3),tmata3#(3,3)
DIM    tmatb1#(3,3),tmatb2#(3,3),tmatb3#(3,3)
DIM    tmatc1#(3,3),tmatc2#(3,3),tmatc3#(3,3)
DIM    tmatd1#(3,3),tmatd2#(3,3),tmatd3#(3,3)
DIM    tmate1#(3,3),tmate2#(3,3),tmate3#(3,3)
DIM    temp2#(15,15),temp3#(15,15),temp4#(15,15),utemp1#(3,3)
DIM    temp#(3,3),umat#(3,3),zmat#(3,3),emat#(3,3),bmat#(9,9),
       amat#(3,9)
DIM    xyz#(3), xyza#(3), xyzb#(3), xyzc#(3), xyzd#(3), xyze#(3)

DECLARE SUB  intro      (polyname$,ans)
DECLARE SUB  setgmat    (gmat1#(),tmat1#(),tmat2#(),tmat3#(),
                        emat#(),emat#(),xyz#(),ans)
DECLARE SUB  sqr1      (umat#(),umata#(),umatb#(),umatc#())
DECLARE SUB  sqr2      (gmat#(),gmata#(),gmatb#(),gmatc#())
DECLARE SUB  umatsqr   (umat#(),umata#(),umatb#(),zpart#,bond)
DECLARE SUB  gmatsqr   (gmat#(),gmat1#(),gmata#(),gmatb#(),
                        vector#,bond)
DECLARE SUB  results   (xyza#(),xyzb#(),xyzc#(),vector#,zpart#,
                        bond,ans)

emat#(1,1) = 1
emat#(1,2) = 0
emat#(1,3) = 0
emat#(2,1) = 0
emat#(2,2) = 1
emat#(2,3) = 0
emat#(3,1) = 0
emat#(3,2) = 0
emat#(3,3) = 1
CALL intro(polyname$, ans)
IF (ans = 1) THEN
    xyza#(1) = 1.53
    xyza#(2) = 0
    xyza#(3) = 0
END IF
IF (ans = 2) THEN
    xyza#(1) = 0
    xyza#(2) = 0
    xyza#(3) = 0
END IF
tmata1#(1,1) = 0.3746
tmata1#(1,2) = 0.9272
tmata1#(1,3) = 0

```

```

tmata1#(2,1) = 0.9272
tmata1#(2,2) = -0.3746
tmata1#(2,3) = 0
tmata1#(3,1) = 0
tmata1#(3,2) = 0
tmata1#(3,3) = -1
tmata2#(1,1) = 0.3746
tmata2#(1,2) = 0.9272
tmata2#(1,3) = 0
tmata2#(2,1) = -0.4636
tmata2#(2,2) = 0.1873
tmata2#(2,3) = 0.866
tmata2#(3,1) = 0.803
tmata2#(3,2) = -0.3244
tmata2#(3,3) = 0.5
tmata3#(1,1) = 0.3746
tmata3#(1,2) = 0.9272
tmata3#(1,3) = 0
tmata3#(2,1) = -0.4636
tmata3#(2,2) = 0.1873
tmata3#(2,3) = -0.866
tmata3#(3,1) = -0.803
tmata3#(3,2) = 0.3244
tmata3#(3,3) = 0.5
umata#(1,1) = 1
umata#(1,2) = 0
umata#(1,3) = 0
umata#(2,1) = 1
umata#(2,2) = 0
umata#(2,3) = 0
umata#(3,1) = 1
umata#(3,2) = 0
umata#(3,3) = 0
IF (ans = 1) THEN
  xyzb#(1) = 1.89
  xyzb#(2) = 0
  xyzb#(3) = 0
END IF
IF (ans = 2) THEN
  xyzb#(1) = 0
  xyzb#(2) = 0
  xyzb#(3) = 0
END IF
tmatb1#(1,1) = 0.342
tmatb1#(1,2) = 0.9397
tmatb1#(1,3) = 0

```

```

tmatb1#(2,1) = 0397
tmatb1#(2,2) = 0.342
tmatb1#(2,3) = 0
tmatb1#(3,1) = 0
tmatb1#(3,2) = 0
tmatb1#(3,3) = -1
tmatb2#(1,1) = 0.342
tmatb2#(1,2) = 0.9397
tmatb2#(1,3) = 0
tmatb2#(2,1) = -0.4698
tmatb2#(2,2) = 0.171
tmatb2#(2,3) = 0.866
tmatb2#(3,1) = 0.8138
tmatb2#(3,2) = -0.2962
tmatb2#(3,3) = 0.5
tmatb3#(1,1) = 0.342
tmatb3#(1,2) = 0.9397
tmatb3#(1,3) = 0
tmatb3#(2,1) = -0.4698
tmatb3#(2,2) = 0.171
tmatb3#(2,3) = -0.866
tmatb3#(3,1) = -0.8138
tmatb3#(3,2) = 0.2962
tmatb3#(3,3) = 0.5
umatb#(1,1) = 1
umatb#(1,2) = 1
umatb#(1,3) = 1
umatb#(2,1) = 0
umatb#(2,2) = 0
umatb#(2,3) = 0
umatb#(3,1) = 0
umatb#(3,2) = 0
umatb#(3,3) = 0
IF (ans = 1) THEN
  xyzc#(1) = 1.89
  xyzc#(2) = 0
  xyzc#(3) = 0
END IF
IF (ans = 2) THEN
  xyzc#(1) = 0
  xyzc#(2) = 0
  xyzc#(3) = 0
END IF
tmatc1#(1,1) = 0.3746
tmatc1#(1,2) = 0.9272
tmatc1#(1,3) = 0

```

```

tmatc1#(2,1) = 0.9272
tmatc1#(2,3) = 0
tmatc1#(3,1) = 0
tmatc1#(3,2) = 0
tmatc1#(3,3) = -1
tmatc2#(1,1) = 0.3746
tmatc2#(1,2) = 0.9272
tmatc2#(1,3) = 0
tmatc2#(2,1) = -0.4636
tmatc2#(2,2) = 0.1873
tmatc2#(2,3) = 0.866
tmatc2#(3,1) = 0.803
tmatc2#(3,2) = -0.3244
tmatc2#(3,3) = 0.5
tmatc3#(1,1) = 0.3746
tmatc3#(1,2) = 0.9272
tmatc3#(1,3) = 0
tmatc3#(2,1) = -0.4636
tmatc3#(2,2) = 0.1873
tmatc3#(2,3) = -0.866
tmatc3#(3,1) = -0.803
tmatc3#(3,2) = 0.3244
tmatc3#(3,3) = 0.5
umatc#(1,1) = 1
umatc#(1,2) = 1
umatc#(1,3) = 1
umatc#(2,1) = 1
umatc#(2,2) = 1
umatc#(2,3) = 0.5
umatc#(3,1) = 1
umatc#(3,2) = 0.5
umatc#(3,3) = 1
CLS
LINE (120, 140)-(530, 180), 1, BF
LINE (120, 140)-(530, 180), 15, B
LOCATE 12, 18
INPUT "Enter the Number of Matrix Squares Required"; bond
CALL setgmat (gmat1#(),tmatc1#(),tmatc2#(),tmatc3#(),emat#(),
emat#(),xyza#(),ans)
CALL setgmat (gmata#(),tmata1#(),tmata2#(),tmata3#(),umata#(),
emat#(),xyza#(),ans)
CALL setgmat (gmatb#(),tmatb1#(),tmatb2#(),tmatb3#(),umatb#(),
emat#(),xyzb#(),ans)
CALL setgmat (gmatc#(),tmatc1#(),tmatc2#(),tmatc3#(),umatc#(),
emat#(),xyzc#(),ans)
CALL sqr1 (umat#(),umata#(),umatb#(),umatc#())

```

```

CALL  sqr2      (gmat#(),gmata#(),gmatb#(),gmatc#())
CALL  umatsqr  (umat#(),umata#(),umatb#(),zpart#,bond)
CALL  gmatsqr  (gmat#(),gmat1#(),gmata#(),gmatb#(),vector#,bond)
CALL  results  (xyza#(),xyzb#(),xyzc#(),vector#,zpart#,bond,ans)
SUB   gmatsqr  (temp2#(),gmat1#(),gmata#(),gmatb#(),vector#,bond)
DIM   jstar2#(15),jnrm2#(15),jtemp2#(15),jtemp3#(15)
DIM   temp3#(15, 15), sum0 AS DOUBLE
CLS
LINE (150, 140)-(490, 220), 1, BF
LINE (150, 140)-(490, 220), 15, B
LOCATE 12, 22
PRINT "Processing Subroutine GMATSQR"
LOCATE 14, 22
PRINT "Please wait....."
FOR z = 1 TO bond
  FOR c = 1 TO 15
    FOR a = 1 TO 15
      sum0 = 0
      FOR B = 1 TO 15
        sum0 = sum0 + (temp2#(c, B) * temp2#(B, a))
      NEXT B
      temp3#(c, a) = sum0
    NEXT a
  NEXT c
  FOR a = 1 TO 15
    FOR B = 1 TO 15
      temp2#(a, B) = temp3#(a, B)
    NEXT B
  NEXT a
NEXT z
FOR c = 1 TO 15
  FOR a = 1 TO 15
    sum0 = 0
    FOR B = 1 TO 15
      sum0 = sum0 + (gmat1#(c, B) * temp2#(B, a))
    NEXT B
    temp3#(c, a) = sum0
  NEXT a
NEXT c
FOR c = 1 TO 15
  FOR a = 1 TO 15
    sum0 = 0
    FOR B = 1 TO 15
      sum0 = sum0 + (temp3#(c, B) * gmata#(B, a))
    NEXT B
    temp2#(c, a) = sum0
  NEXT a
NEXT c

```

```

NEXT a
NEXT c
FOR c = 1 TO 15
  FOR a = 1 TO 15
    sum0 = 0
    FOR B = 1 TO 15
      sum0 = sum0 + (temp2#(c, B) * gmatb#(B, a))
    NEXT B
    temp3#(c, a) = sum0
  NEXT a
NEXT c
vector# = temp3#(1, 13) + temp3#(1, 14) + temp3#(1, 15)
END SUB

```

```

SUB intro (polynome$,ans)
  CLS
  SCREEN 9
  COLOR , 9
  LINE (50, 50)-(590, 300), 1, BF
  LINE (50, 50)-(590, 300), 15, B
  LOCATE 19, 14
  PRINT "Please Select Which Option You Require (1-3) "
  LOCATE 7, 14
  PRINT "Poly(dimethylsilethane)"
  LOCATE 10, 14
  PRINT "1 : Calculation of Characteristic Ratio"
  LOCATE 13, 14
  PRINT "2 : Calculation of Dipole Moment Ratio"
  LOCATE 16, 14
  PRINT "3 : Exit program"
  LOCATE 19, 58
  INPUT ans$
  ans = VAL(ans$)
  WHILE (ans < 1) OR (ans > 3)
    LOCATE 21, 14
    PRINT "**** Choice invalid ! ****"
    BEEP
    SLEEP 1.5
    LOCATE 21, 14
    PRINT "*** Please try again ! ***"
    LOCATE 19, 58
    INPUT ans$
    ans = VAL(ans$)
  WEND
  IF (ans = 3) THEN
    CLS

```



```

LINE (150, 140)-(490, 180), 1, BF
LINE (150, 140)-(490, 180), 15, B
LOCATE 12, 22
PRINT "Are you sure you want to quit...(Y/N) ?"
BEEP
DO
    key$ = INKEY$
LOOP WHILE LEN(key$) = 0
IF (key$ <> "Y" AND key$ <> "y") THEN
    CLS
    RUN
END IF
CLS
END
END IF
END SUB

```

```

SUB results (xyza#(),xyzb#(),xyzc#(),vector#,zpart#,bond,ans)
CLS
SCREEN 9
COLOR , 9
LINE (50, 50)-(590, 300), 1, BF
LINE (50, 50)-(590, 300), 15, B
znum1 = 3 * (2 ^ bond + 1)
znum = (2 ^ bond + 1) * (xyza#(1) ^ 2 + xyzb#(1) ^ 2 + xyzc#(1) ^ 2)
ratio = (2 * (1 / zpart#) * vector#) / znum
LOCATE 7, 14
PRINT "Poly(dimethylsilethane)"
IF (ans = 1) THEN
    LOCATE 10, 14
    PRINT "Characteristic Ratio is"
END IF
IF (ans = 2) THEN
    LOCATE 10, 14
    PRINT "Dipole Moment Ratio is"
END IF
LOCATE 10, 40
PRINT ratio
LOCATE 13, 14
PRINT "Number of Bonds in the Chain is"
LOCATE 13, 47
PRINT znum1
LOCATE 19, 14
PRINT "Press any key to Continue....."
DO
    key$ = INKEY$

```

```

LOOP WHILE LEN(key$) = 0
RUN
END SUB

SUB setgmat (temp1#(),tmat1#(),tmat2#(),tmat3#(),temp#(),
            emat#(),xyz#(),ans)
DIM sum1 AS DOUBLE, sum2 AS DOUBLE, sum3 AS DOUBLE, sum4 AS
    DOUBLE, sum5 AS DOUBLE, sum6 AS DOUBLE, sum7 AS DOUBLE
DIM sum8 AS DOUBLE, sum9 AS DOUBLE, sum10 AS DOUBLE, sum11 AS
    DOUBLE, sum12 AS DOUBLE
DIM amat#(3,), bmat#(9,9), zmatsqr AS DOUBLE
CLS
LINE (150, 140)-(490, 220), 1, BF
LINE (150, 140)-(490, 220), 15, B
LOCATE 12, 22
PRINT "Processing Subroutine SETMAT"
LOCATE 14, 22
PRINT "Please wait....."
zmatsqr = (xyz#(1) ^ 2 + xyz#(2) ^ 2 + xyz#(3) ^ 2)
FOR a = 1 TO 3
    FOR B = 1 TO 3
        amat#(a, B) = temp#(a, 1) * xyz#(B)
        amat#(a, B + 3) = temp#(a, 2) * xyz#(B)
        amat#(a, B + 6) = temp#(a, 3) * xyz#(B)
        bmat#(a, B) = temp#(1, 1) * emat#(a, B)
        bmat#(a, B + 3) = temp#(1, 2) * emat#(a, B)
        bmat#(a, B + 6) = temp#(1, 3) * emat#(a, B)
        bmat#(a + 3, B) = temp#(2, 1) * emat#(a, B)
        bmat#(a + 3, B + 3) = temp#(2, 2) * emat#(a, B)
        bmat#(a + 3, B + 6) = temp#(2, 3) * emat#(a, B)
        bmat#(a + 6, B) = temp#(3, 1) * emat#(a, B)
        bmat#(a + 6, B + 3) = temp#(3, 2) * emat#(a, B)
        bmat#(a + 6, B + 6) = temp#(3, 3) * emat#(a, B)
        temp1#(a, B) = temp#(a, B)
        temp1#(a + 3, B + 12) = temp#(1, B) * xyz#(a)
        temp1#(a + 6, B + 12) = temp#(2, B) * xyz#(a)
        temp1#(a + 9, B + 12) = temp#(3, B) * xyz#(a)
        temp1#(a, B + 12) = (zmatsqr / 2) * temp#(a, B)
    NEXT B
NEXT a
FOR c = 1 TO 3
    FOR a = 1 TO 3
        sum1 = 0
        sum2 = 0
        sum3 = 0
    
```

```

sum4 = 0
sum5 = 0
sum6 = 0
sum7 = 0
sum8 = 0
sum9 = 0
sum10 = 0
sum11 = 0
sum12 = 0
FOR B = 1 TO 3
    sum1 = sum1 + amat#(c, B) * tmat1#(B, a)
    sum2 = sum2 + amat#(c, B + 3) * tmat2#(B, a)
    sum3 = sum3 + amat#(c, B + 6) * tmat3#(B, a)
    sum4 = sum4 + bmat#(c, B) * tmat1#(B, a)
    sum5 = sum5 + bmat#(c, B + 3) * tmat2#(B, a)
    sum6 = sum6 + bmat#(c, B + 6) * tmat3#(B, a)
    sum7 = sum7 + bmat#(c + 3, B) * tmat1#(B, a)
    sum8 = sum8 + bmat#(c + 3, B + 3) * tmat2#(B, a)
    sum9 = sum9 + bmat#(c + 3, B + 6) * tmat3#(B, a)
    sum10 = sum10 + bmat#(c + 6, B) * tmat1#(B, a)
    sum11 = sum11 + bmat#(c + 6, B + 3) * tmat2#(B, a)
    sum12 = sum12 + bmat#(c + 6, B + 6) * tmat3#(B, a)
NEXT B
temp1#(c, a + 3) = sum1
temp1#(c, a + 6) = sum2
temp1#(c, a + 9) = sum3
temp1#(c + 3, a + 3) = sum4
temp1#(c + 3, a + 6) = sum5
temp1#(c + 3, a + 9) = sum6
temp1#(c + 6, a + 3) = sum7
temp1#(c + 6, a + 6) = sum8
temp1#(c + 6, a + 9) = sum9
temp1#(c + 9, a + 3) = sum10
temp1#(c + 9, a + 6) = sum11
temp1#(c + 9, a + 9) = sum12
NEXT a
NEXT c
END SUB

SUB  sqr1 (umat#(),umata#(),umatb#(),umatc#())
    DIM utemp1#(3,3),utemp2#(3,3)
    CLS
    LINE (150, 140)-(490, 220), 1, BF
    LINE (150, 140)-(490, 220), 15, B
    LOCATE 12, 22
    PRINT "Processing Subroutine SETSQR1"

```

```

LOCATE 14, 22
PRINT "Please wait....."
FOR c = 1 TO 3
  FOR a = 1 TO 3
    sum0 = 0
    FOR B = 1 TO 3
      sum0 = sum0 + umata#(c, B) * umatb#(B, a)
    NEXT B
    utemp1#(c, a) = sum0
  NEXT a
NEXT c
FOR c = 1 TO 3
  FOR a = 1 TO 3
    sum0 = 0
    FOR B = 1 TO 3
      sum0 = sum0 + utemp1#(c, B) * umatc#(B, a)
    NEXT B
    umat#(c, a) = sum0
  NEXT a
NEXT c
END SUB

```

```

SUB  sqr2 (gmat#(),gmata#(),gmatb#(),gmatc#())
DIM  gtemp1#(15,15),gtemp2#(15,15)
CLS
LINE (150, 140)-(490, 220), 1, BF
LINE (150, 140)-(490, 220), 15, B
LOCATE 12, 22
PRINT "Processing Subroutine SETSOR2"
LOCATE 14, 22
PRINT "Please wait....."
FOR c = 1 TO 15
  FOR a = 1 TO 15
    sum0 = 0
    FOR B = 1 TO 15
      sum0 = sum0 + gmata#(c, B) * gmatb#(B, a)
    NEXT B
    gtemp1#(c, a) = sum0
  NEXT a
NEXT c
FOR c = 1 TO 15
  FOR a = 1 TO 15
    sum0 = 0
    FOR B = 1 TO 15
      sum0 = sum0 + gtemp1#(c, B) * gmatc#(B, a)
    NEXT B

```

```

        gmat#(c, a) = sum0
    NEXT a
NEXT c
END SUB

```

```

SUB  umatsqr (zmat#(),umata#(),umatb#(),zpart#,bond)
    DIM utemp1#(3,3),utemp2#(3,3)
    DIM jtemp1#(3),jstar1#(3),jnorm1#(3)
    DIM zlam AS DOUBLE, sum0 AS DOUBLE, zmax AS DOUBLE
    CLS
    LINE (150, 140)-(490, 220), 1, BF
    LINE (150, 140)-(490, 220), 15, B
    LOCATE 12, 22
    PRINT "Processing Subroutine UMATSQR"
    LOCATE 14, 22
    PRINT "Please wait....."
    FOR z = 1 TO bond
        FOR c = 1 TO 3
            FOR a = 1 TO 3
                sum0 = 0
                FOR B = 1 TO 3
                    sum0 = sum0 + (zmat#(c, B) * zmat#(B, a))
                NEXT B
                utemp1#(c, a) = sum0
            NEXT a
        NEXT c
        FOR a = 1 TO 3
            FOR B = 1 TO 3
                zmat#(a, B) = utemp1#(a, B)
            NEXT B
        NEXT a
    NEXT z
    FOR c = 1 TO 3
        FOR a = 1 TO 3
            sum0 = 0
            FOR B = 1 TO 3
                sum0 = sum0 + (zmat#(c, B) * umata#(B, a))
            NEXT B
            utemp1#(c, a) = sum0
        NEXT a
    NEXT c
    FOR c = 1 TO 3
        FOR a = 1 TO 3
            sum0 = 0
            FOR B = 1 TO 3
                sum0 = sum0 + (utemp1#(c, B) * umatb#(B, a))

```

```

        NEXT B
        utemp2#(c, a) = sum0
    NEXT a
NEXT c
FOR a = 1 TO 3
    FOR B = 1 TO 3
        zmat#(a, B) = utemp2#(a, B)
    NEXT B
NEXT a
zpart# = zmat#(1, 1) + zmat#(1, 2) + zmat#(1, 3)
END SUB

```

C.5. Calculation of the Characteristic Ratio and the Dipole Moment of Poly(2,2,5,5-tetramethyl-1-oxa-2,5-disilapentane)

This program was used to calculate the characteristic ratio and the dipole moment ratio of poly(2,2,5,5-tetramethyl-1-oxa-2,2,5,5-disilapentane). The calculations were carried out according to Eq. (6-12) and Eq. (6-13) respectively. The calculations may be performed on chains of different lengths.

Computer Program Listing

```

'           Calculation of Characteristic Ratio
'           and Dipole Moment Ratio for
'           poly(2,2,5,5-tetramethyl-1-oxa-2,5-disilapentane).
'
'           Written by D. J. Elsby
'           Department of Chemical Engineering and Applied
'           Chemistry, Aston University, Birmingham, B4 7ET.

DIM  gmat1#(15,15),gmat#(15,5),temp1#(15,5)
DIM  gmata#(15,15),gmatb#(15,15),gmatc#(15,15),gmatd#(15,15),
      gmate#(15,15)
DIM  umata#(3,3),umatb#(3,3),umatac#(3,3),umatd#(3,3),umate#(3,3)
DIM  tmata1#(3,3),tmata2#(3,3),tmata3#(3,3)
DIM  tmatb1#(3,3),tmatb2#(3,3),tmatb3#(3,3)
DIM  tmatc1#(3,3),tmatc2#(3,3),tmatc3#(3,3)
DIM  tmatd1#(3,3),tmatd2#(3,3),tmatd3#(3,3)
DIM  tmate1#(3,3),tmate2#(3,3),tmate3#(3,3)

```

```

DIM   temp2#(15,15),temp3#(15,15),temp4#(15,15),utemp1#(3,3)
DIM   temp#(3,3),umat#(3,3),zmat#(3,3),emat#(3,3),bmat#(9,9),amat#(3,9)
DIM   xyz#(3),xyza#(3),xyzb#(3),xyzc#(3),xyzd#(3),xyze#(3)

```

```

DECLARE SUB  intro      (polynome$,ans)
DECLARE SUB  setgmat    (gmat1#(),tmat1#(),tmat2#(),tmat3#(),emat#(),
                        emat#(),xyz#(),ans)
DECLARE SUB  sqr1       (umat#(),umata#(),umatb#(),umate#(),umate#(),
                        umate#())
DECLARE SUB  sqr2       (gmat#(),gmata#(),gmatb#(),gmatc#(),
                        gmatd#(),gmate#())
DECLARE SUB  umatsqr    (umat#(),umata#(),umatb#(),umate#(),umate#(),
                        umate#(),zpart#,bond)
DECLARE SUB  gmatsqr    (gmat#(),gmat1#(),gmata#(),gmatb#(),
                        gmatc#(),gmatd#(),vector#,bond)

DECLARE SUB  results    (xyza#(),xyzb#(),xyzc#(),xyzd#(),xyze#(),
                        vector#,zpart#,bond,ans)

```

```

emat#(1,1) = 1
emat#(1,2) = 0
emat#(1,3) = 0
emat#(2,1) = 0
emat#(2,2) = 1
emat#(2,3) = 0
emat#(3,1) = 0
emat#(3,2) = 0
emat#(3,3) = 1

```

```
CALL intro(polynome$, ans)
```

```
IF (ans = 1) THEN
```

```
  xyza#(1) = 1.64
```

```
  xyza#(2) = 0
```

```
  xyza#(3) = 0
```

```
END IF
```

```
IF (ans = 2) THEN
```

```
  xyza#(1) = -0.6
```

```
  xyza#(2) = 0
```

```
  xyza#(3) = 0
```

```
END IF
```

```
tmata1#(1,1) = 0.342
```

```
tmata1#(1,2) = 0.9397
```

```
tmata1#(1,3) = 0
```

```
tmata1#(2,1) = 0.9397
```

```
tmata1#(2,2) = -0.342
```

```
tmata1#(2,3) = 0
```

```

tmata1#(3,1) = 0
tmata1#(3,2) = 0
tmata1#(3,3) = -1
tmata2#(1,1) = 0.342
tmata2#(1,2) = 0.9397
tmata2#(1,3) = 0
tmata2#(2,1) = -0.4698
tmata2#(2,2) = 0.171
tmata2#(2,3) = 0.866
tmata2#(3,1) = 0.8138
tmata2#(3,2) = -0.2962
tmata2#(3,3) = 0.5
tmata3#(1,1) = 0.342
tmata3#(1,2) = 0.9397
tmata3#(1,3) = 0
tmata3#(2,1) = -0.4698
tmata3#(2,2) = 0.171
tmata3#(2,3) = -0.866
tmata3#(3,1) = -0.8138
tmata3#(3,2) = 0.2962
tmata3#(3,3) = 0.5
umata#(1,1) = 1
umata#(1,2) = 1
umata#(1,3) = 1
umata#(2,1) = 1
umata#(2,2) = 1
umata#(2,3) = 1
umata#(3,1) = 1
umata#(3,2) = 1
umata#(3,3) = 1
IF (ans = 1) THEN
  xyzb#(1) = 1.89
  xyzb#(2) = 0
  xyzb#(3) = 0
END IF
IF (ans = 2) THEN
  xyzb#(1) = 0
  xyzb#(2) = 0
  xyzb#(3) = 0
END IF
tmatb1#(1,1) = 0.3746
tmatb1#(1,2) = 0.9272
tmatb1#(1,3) = 0
tmatb1#(2,1) = 0.9272
tmatb1#(2,2) = -0.3746
tmatb1#(2,3) = 0

```



```

tmatb1#(3,1) = 0
tmatb1#(3,2) = 0
tmatb1#(3,3) = -1
tmatb2#(1,1) = 0.3746
tmatb2#(1,2) = 0.9272
tmatb2#(1,3) = 0
tmatb2#(2,1) = -0.4636
tmatb2#(2,2) = 0.1873
tmatb2#(2,3) = 0.866
tmatb2#(3,1) = 0.803
tmatb2#(3,2) = -0.3244
tmatb2#(3,3) = 0.5
tmatb3#(1,1) = 0.3746
tmatb3#(1,2) = 0.9272
tmatb3#(1,3) = 0
tmatb3#(2,1) = -0.4636
tmatb3#(2,2) = 0.1873
tmatb3#(2,3) = -0.866
tmatb3#(3,1) = -0.803
tmatb3#(3,2) = 0.3244
tmatb3#(3,3) = 0.5
umatb#(1,1) = 1
umatb#(1,2) = 1
umatb#(1,3) = 1
umatb#(2,1) = 1
umatb#(2,2) = 1
umatb#(2,3) = 0
umatb#(3,1) = 1
umatb#(3,2) = 0
umatb#(3,3) = 1
IF (ans = 1) THEN
  xyzc#(1) = 1.53
  xyzc#(2) = 0
  xyzc#(3) = 0
END IF
IF (ans = 2) THEN
  xyzc#(1) = 0
  xyzc#(2) = 0
  xyzc#(3) = 0
END IF
tmatc1#(1,1) = 0.3746
tmatc1#(1,2) = 0.9272
tmatc1#(1,3) = 0
tmatc1#(2,1) = 0.9272
tmatc1#(2,2) = -0.3746
tmatc1#(2,3) = 0

```

```

tmatc1#(3,1) = 0
tmatc1#(3,2) = 0
tmatc1#(3,3) = -1
tmatc2#(1,1) = 0.3746
tmatc2#(1,2) = 0.9272
tmatc2#(1,3) = 0
tmatc2#(2,1) = -0.4636
tmatc2#(2,2) = 0.1873
tmatc2#(2,3) = 0.866
tmatc2#(3,1) = 0.803
tmatc2#(3,2) = -0.3244
tmatc2#(3,3) = 0.5
tmatc3#(1,1) = 0.3746
tmatc3#(1,2) = 0.9272
tmatc3#(1,3) = 0
tmatc3#(2,1) = -0.4636
tmatc3#(2,2) = 0.1873
tmatc3#(2,3) = -0.866
tmatc3#(3,1) = -0.803
tmatc3#(3,2) = 0.3244
tmatc3#(3,3) = 0.5
umatc#(1,1) = 1
umatc#(1,2) = 0
umatc#(1,3) = 0
umatc#(2,1) = 1
umatc#(2,2) = 0
umatc#(2,3) = 0
umatc#(3,1) = 1
umatc#(3,2) = 0
umatc#(3,3) = 0
IF (ans = 1) THEN
  xyzd#(1) = 1.89
  xyzd#(2) = 0
  xyzd#(3) = 0
END IF
IF (ans = 2) THEN
  xyzd#(1) = 0
  xyzd#(2) = 0
  xyzd#(3) = 0
END IF
tmatd1#(1,1) = 0.342
tmatd1#(1,2) = 0.9397
tmatd1#(1,3) = 0
tmatd1#(2,1) = 0.9397
tmatd1#(2,2) = -0.342
tmatd1#(2,3) = 0

```

```

tmatd1#(3,1) = 0
tmatd1#(3,2) = 0
tmatd1#(3,3) = -1
tmatd2#(1,1) = 0.342
tmatd2#(1,2) = 0.9397
tmatd2#(1,3) = 0
tmatd2#(2,1) = -0.4698
tmatd2#(2,2) = 0.171
tmatd2#(2,3) = 0.866
tmatd2#(3,1) = 0.8138
tmatd2#(3,2) = -0.2962
tmatd2#(3,3) = 0.5
tmatd3#(1,1) = 0.342
tmatd3#(1,2) = 0.9397
tmatd3#(1,3) = 0
tmatd3#(2,1) = -0.4698
tmatd3#(2,2) = 0.171
tmatd3#(2,3) = -0.866
tmatd3#(3,1) = -0.8138
tmatd3#(3,2) = 0.2962
tmatd3#(3,3) = 0.5
umatd#(1,1) = 1
umatd#(1,2) = 1
umatd#(1,3) = 1
umatd#(2,1) = 0
umatd#(2,2) = 0
umatd#(2,3) = 0
umatd#(3,1) = 0
umatd#(3,2) = 0
umatd#(3,3) = 0
IF (ans = 1) THEN
  xyze#(1) = 1.64
  xyze#(2) = 0
  xyze#(3) = 0
END IF
IF (ans = 2) THEN
  xyze#(1) = 0.6
  xyze#(2) = 0
  xyze#(3) = 0
END IF
tmate1#(1,1) = 0.7986
tmate1#(1,2) = 0.6018
tmate1#(1,3) = 0
tmate1#(2,1) = 0.6018
tmate1#(2,2) = -0.7986
tmate1#(2,3) = 0

```

```

tmate1#(3,1) = 0
tmate1#(3,2) = 0
tmate1#(3,3) = -1
tmate2#(1,1) = 0.7986
tmate2#(1,2) = 0.6018
tmate2#(1,3) = 0
tmate2#(2,1) = -0.3009
tmate2#(2,2) = 0.3993
tmate2#(2,3) = 0.866
tmate2#(3,1) = 0.5212
tmate2#(3,2) = -0.6916
tmate2#(3,3) = 0.5
tmate3#(1,1) = 0.7986
tmate3#(1,2) = 0.6018
tmate3#(1,3) = 0
tmate3#(2,1) = -0.3009
tmate3#(2,2) = 0.3993
tmate3#(2,3) = -0.866
tmate3#(3,1) = -0.5212
tmate3#(3,2) = 0.6936
tmate3#(3,3) = 0.5
umate#(1,1) = 1
umate#(1,2) = 1
umate#(1,3) = 1
umate#(2,1) = 1
umate#(2,2) = 1
umate#(2,3) = 0
umate#(3,1) = 1
umate#(3,2) = 0
umate#(3,3) = 1
CLS
LINE (120, 140)-(530, 180), 1, BF
LINE (120, 140)-(530, 180), 15, B
LOCATE 12, 18
INPUT "Enter the Number of Matrix Squares Required"; bond
CALL setgmat (gmat1#(),tmate1#(),tmate2#(),tmate3#(),emat#(),
emat#(),xyze#(),ans)
CALL setgmat (gmata#(),tmata1#(),tmata2#(),tmata3#(),umata#(),
emat#(),xyza#(),ans)
CALL setgmat (gmatb#(),tmatb1#(),tmatb2#(),tmatb3#(),umatb#(),
emat#(),xyzb#(),ans)
CALL setgmat (gmatc#(),tmatc1#(),tmatc2#(),tmatc3#(),umatc#(),
emat#(),xyzc#(),ans)
CALL setgmat (gmatd#(),tmatd1#(),tmatd2#(),tmatd3#(),umatd#(),
emat#(),xyzd#(),ans)
CALL setgmat (gmate#(),tmate1#(),tmate2#(),tmate3#(),umate#(),

```

```

                                emat#(),xyze#(),ans)
CALL  sqr1      (umat#(),umata#(),umatb#(),umate#(),umate#())
CALL  sqr2      (gmat#(),gmata#(),gmatb#(),gmatc#(),gmatd#(),gmate#())
CALL  umatsqr   (umat#(),umata#(),umatb#(),umate#(),umate#(),zpart#,
                bond)
CALL  gmatsqr   (gmat#(),gmat1#(),gmata#(),gmatb#(),gmatc#(),
                gmatd#(),vector#,bond)
CALL  results   (xyza#(),xyzb#(),xyzc#(),xyzd#(),xyze#(),vector#,zpart#,
                bond,ans)

SUB    gmatsqr  (temp2#(),gmat1#(),gmata#(),gmatb#(),gmatc#(),
                gmatd#(),vector#,bond)
DIM    jstar2#(15),jnorm2#(15),jtemp2#(15),jtemp3#(15)
DIM    temp3#(15, 5), sum0 AS DOUBLE
CLS
LINE (150, 140)-(490, 220), 1, BF
LINE (150, 140)-(490, 220), 15, B
LOCATE 12, 22
PRINT "Processing Subroutine GMATSQR"
LOCATE 14, 22
PRINT "Please wait....."
FOR z = 1 TO bond
  FOR c = 1 TO 15
    FOR a = 1 TO 15
      sum0 = 0
      FOR B = 1 TO 15
        sum0 = sum0 + (temp2#(c, B) * temp2#(B, a))
      NEXT B
      temp3#(c, a) = sum0
    NEXT a
  NEXT c
  FOR a = 1 TO 15
    FOR B = 1 TO 15
      temp2#(a, B) = temp3#(a, B)
    NEXT B
  NEXT a
NEXT z
FOR c = 1 TO 15
  FOR a = 1 TO 15
    sum0 = 0
    FOR B = 1 TO 15
      sum0 = sum0 + (gmat1#(c, B) * temp2#(B, a))
    NEXT B
    temp3#(c, a) = sum0
  NEXT a
NEXT c

```

```

FOR c = 1 TO 15
  FOR a = 1 TO 15
    sum0 = 0
    FOR B = 1 TO 15
      sum0 = sum0 + (temp3#(c, B) * gmata#(B, a))
    NEXT B
    temp2#(c, a) = sum0
  NEXT a
NEXT c
FOR c = 1 TO 15
  FOR a = 1 TO 15
    sum0 = 0
    FOR B = 1 TO 15
      sum0 = sum0 + (temp2#(c, B) * gmatb#(B, a))
    NEXT B
    temp3#(c, a) = sum0
  NEXT a
NEXT c
FOR c = 1 TO 15
  FOR a = 1 TO 15
    sum0 = 0
    FOR B = 1 TO 15
      sum0 = sum0 + (temp3#(c, B) * gmatc#(B, a))
    NEXT B
    temp2#(c, a) = sum0
  NEXT a
NEXT c
FOR c = 1 TO 15
  FOR a = 1 TO 15
    sum0 = 0
    FOR B = 1 TO 15
      sum0 = sum0 + (temp2#(c, B) * gmatd#(B, a))
    NEXT B
    temp3#(c, a) = sum0
  NEXT a
NEXT c
vector# = temp3#(1, 13) + temp3#(1, 14) + temp3#(1, 15)
END SUB

```

```

SUB intro (polyname$,ans)
  CLS
  SCREEN 9
  COLOR , 9
  LINE (50, 50)-(590, 300), 1, BF
  LINE (50, 50)-(590, 300), 15, B
  LOCATE 19, 14

```

```

PRINT "Please Select Which Option You Require (1-3) "
LOCATE 7, 14
PRINT "Poly(2,2,5,5-tetramethyl-1-oxa-2,7-disilapentane)"
LOCATE 10, 14
PRINT "1 : Calculation of Characteristic Ratio"
LOCATE 13, 14
PRINT "2 : Calculation of Dipole Moment Ratio"
LOCATE 16, 14
PRINT "3 : Exit program"
LOCATE 19, 58
INPUT ans$
ans = VAL(ans$)
WHILE (ans < 1) OR (ans > 3)
  LOCATE 21, 14
  PRINT "**** Choice invalid ! ****"
  BEEP
  SLEEP 1.5
  LOCATE 21, 14
  PRINT "*** Please try again ! ***"
  LOCATE 19, 58
  INPUT ans$
  ans = VAL(ans$)
WEND
IF (ans = 3) THEN
  CLS
  LINE (150, 140)-(490, 180), 1, BF
  LINE (150, 140)-(490, 180), 15, B
  LOCATE 12, 22
  PRINT "Are you sure you want to quit...(Y/N) ?"
  BEEP
  DO
    key$ = INKEY$
  LOOP WHILE LEN(key$) = 0
  IF (key$ <> "Y" AND key$ <> "y") THEN
    CLS
    RUN
  END IF
  CLS
  END
END IF
END SUB

SUB results (xyza#(),xyzb#(),xyzc#(),xyzd#(),xyze#(),vector#,zpart#,
            bond,ans)

CLS
SCREEN 9

```

```

COLOR , 9
LINE (50, 50)-(590, 300), 1, BF
LINE (50, 50)-(590, 300), 15, B
znum1 = 5 * (2 ^ bond + 1)
znum = (2 ^ bond + 1) * (xyza#(1) ^ 2 + xyzb#(1) ^ 2 + xyzc#(1) ^ 2
      + xyzd#(1) ^ 2 + xyze#(1) ^ 2)
ratio = (2 * (1 / zpart#) * vector#) / znum
LOCATE 7, 14
PRINT "Poly(2,2,5,5-tetramethyl-1-oxa-2,5-disilapentane)"
IF (ans = 1) THEN
  LOCATE 10, 14
  PRINT "Characteristic Ratio is"
END IF
IF (ans = 2) THEN
  LOCATE 10, 14
  PRINT "Dipole Moment Ratio is"
END IF
LOCATE 10, 40
PRINT ratio
LOCATE 13, 14
PRINT "Number of Bonds in the Chain is"
LOCATE 13, 47
PRINT znum1
LOCATE 19, 14
PRINT "Press any key to Continue....."
DO
  key$ = INKEY$
LOOP WHILE LEN(key$) = 0
RUN
END SUB

SUB setgmat (temp1#(),tmat1#(),tmat2#(),tmat3#(),temp#(),emat#(),
            xyz#(),ans)
  DIM sum1 AS DOUBLE, sum2 AS DOUBLE, sum3 AS DOUBLE, sum4 AS
    DOUBLE, sum5 AS DOUBLE, sum6 AS DOUBLE, sum7 AS DOUBLE
  DIM sum8 AS DOUBLE, sum9 AS DOUBLE, sum10 AS DOUBLE, sum11 AS
    DOUBLE, sum12 AS DOUBLE
  DIM amat#(3,9), bmat#(9,9), zmatsqr AS DOUBLE
  CLS
  LINE (150, 140)-(490, 220), 1, BF
  LINE (150, 140)-(490, 220), 15, B
  LOCATE 12, 22
  PRINT "Processing Subroutine SETMAT"
  LOCATE 14, 22
  PRINT "Please wait....."
  zmatsqr = (xyz#(1) ^ 2 + xyz#(2) ^ 2 + xyz#(3) ^ 2)

```



```

FOR a = 1 TO 3
  FOR B = 1 TO 3
    amat#(a, B) = temp#(a, 1) * xyz#(B)
    amat#(a, B + 3) = temp#(a, 2) * xyz#(B)
    amat#(a, B + 6) = temp#(a, 3) * xyz#(B)
    bmat#(a, B) = temp#(1, 1) * emat#(a, B)
    bmat#(a, B + 3) = temp#(1, 2) * emat#(a, B)
    bmat#(a, B + 6) = temp#(1, 3) * emat#(a, B)
    bmat#(a + 3, B) = temp#(2, 1) * emat#(a, B)
    bmat#(a + 3, B + 3) = temp#(2, 2) * emat#(a, B)
    bmat#(a + 3, B + 6) = temp#(2, 3) * emat#(a, B)
    bmat#(a + 6, B) = temp#(3, 1) * emat#(a, B)
    bmat#(a + 6, B + 3) = temp#(3, 2) * emat#(a, B)
    bmat#(a + 6, B + 6) = temp#(3, 3) * emat#(a, B)
    temp1#(a, B) = temp#(a, B)
    temp1#(a + 12, B + 12) = temp#(a, B)
    temp1#(a + 3, B + 12) = temp#(1, B) * xyz#(a)
    temp1#(a + 6, B + 12) = temp#(2, B) * xyz#(a)
    temp1#(a + 9, B + 12) = temp#(3, B) * xyz#(a)
    temp1#(a, B + 12) = (zmat1qr / 2) * temp#(a, B)
  NEXT B
NEXT a
FOR c = 1 TO 3
  FOR a = 1 TO 3
    sum1 = 0
    sum2 = 0
    sum3 = 0
    sum4 = 0
    sum5 = 0
    sum6 = 0
    sum7 = 0
    sum8 = 0
    sum9 = 0
    sum10 = 0
    sum11 = 0
    sum12 = 0
    FOR B = 1 TO 3
      sum1 = sum1 + amat#(c, B) * tmat1#(B, a)
      sum2 = sum2 + amat#(c, B + 3) * tmat2#(B, a)
      sum3 = sum3 + amat#(c, B + 6) * tmat3#(B, a)
      sum4 = sum4 + bmat#(c, B) * tmat1#(B, a)
      sum5 = sum5 + bmat#(c, B + 3) * tmat2#(B, a)
      sum6 = sum6 + bmat#(c, B + 6) * tmat3#(B, a)
      sum7 = sum7 + bmat#(c + 3, B) * tmat1#(B, a)
      sum8 = sum8 + bmat#(c + 3, B + 3) * tmat2#(B, a)
      sum9 = sum9 + bmat#(c + 3, B + 6) * tmat3#(B, a)
    NEXT B
  NEXT a
NEXT c

```

```

        sum10 = sum10 + bmat#(c + 6, B) * tmat1#(B, a)
        sum11 = sum11 + bmat#(c + 6, B + 3) * tmat2#(B, a)
        sum12 = sum12 + bmat#(c + 6, B + 6) * tmat3#(B, a)
    NEXT B
    temp1#(c, a + 3) = sum1
    temp1#(c, a + 6) = sum2
    temp1#(c, a + 9) = sum3
    temp1#(c + 3, a + 3) = sum4
    temp1#(c + 3, a + 6) = sum5
    temp1#(c + 3, a + 9) = sum6
    temp1#(c + 6, a + 3) = sum7
    temp1#(c + 6, a + 6) = sum8
    temp1#(c + 6, a + 9) = sum9
    temp1#(c + 9, a + 3) = sum10
    temp1#(c + 9, a + 6) = sum11
    temp1#(c + 9, a + 9) = sum12
NEXT a
NEXT c
END SUB

SUB  sqr1 (umat#(),umata#(),umatb#(),umatc#(),umatd#(),umate#())
    DIM utemp1#(3,3),utemp2#(3,3)
    CLS
    LINE (150, 140)-(490, 220), 1, BF
    LINE (150, 140)-(490, 220), 15, B
    LOCATE 12, 22
    PRINT "Processing Subroutine SETSQR1"
    LOCATE 14, 22
    PRINT "Please wait....."
    FOR c = 1 TO 3
        FOR a = 1 TO 3
            sum0 = 0
            FOR B = 1 TO 3
                sum0 = sum0 + umata#(c, B) * umatb#(B, a)
            NEXT B
            utemp1#(c, a) = sum0
        NEXT a
    NEXT c
    FOR c = 1 TO 3
        FOR a = 1 TO 3
            sum0 = 0
            FOR B = 1 TO 3
                sum0 = sum0 + utemp1#(c, B) * umatc#(B, a)
            NEXT B
            utemp2#(c, a) = sum0
        NEXT a
    NEXT a

```

```

NEXT c
FOR c = 1 TO 3
  FOR a = 1 TO 3
    sum0 = 0
    FOR B = 1 TO 3
      sum0 = sum0 + utemp2#(c, B) * umatd#(B, a)
    NEXT B
    utemp1#(c, a) = sum0
  NEXT a
NEXT c
FOR c = 1 TO 3
  FOR a = 1 TO 3
    sum0 = 0
    FOR B = 1 TO 3
      sum0 = sum0 + utemp1#(c, B) * umate#(B, a)
    NEXT B
    umat#(c, a) = sum0
  NEXT a
NEXT c
END SUB

SUB  sqr2 (gmat#(),gmata#(),gmatb#(),gmatc#(),gmatd#(),gmate#())
DIM gtemp1#(15,15),gtemp2#(15,15)
CLS
LINE (150, 140)-(490, 220), 1, BF
LINE (150, 140)-(490, 220), 15, B
LOCATE 12, 22
PRINT "Processing Subroutine SETSQR2"
LOCATE 14, 22
PRINT "Please wait....."
FOR c = 1 TO 15
  FOR a = 1 TO 15
    sum0 = 0
    FOR B = 1 TO 15
      sum0 = sum0 + gmata#(c, B) * gmatb#(B, a)
    NEXT B
    gtemp1#(c, a) = sum0
  NEXT a
NEXT c
FOR c = 1 TO 15
  FOR a = 1 TO 15
    sum0 = 0
    FOR B = 1 TO 15
      sum0 = sum0 + gtemp1#(c, B) * gmatc#(B, a)
    NEXT B
    gtemp2#(c, a) = sum0
  NEXT a
NEXT c

```

```

    NEXT a
NEXT c
FOR c = 1 TO 15
    FOR a = 1 TO 15
        sum0 = 0
        FOR B = 1 TO 15
            sum0 = sum0 + gtemp2#(c, B) * gmatd#(B, a)
        NEXT B
        gtemp1#(c, a) = sum0
    NEXT a
NEXT c
FOR c = 1 TO 15
    FOR a = 1 TO 15
        sum0 = 0
        FOR B = 1 TO 15
            sum0 = sum0 + gtemp1#(c, B) * gmate#(B, a)
        NEXT B
        gmat#(c, a) = sum0
    NEXT a
NEXT c
END SUB

SUB  umatsqr (zmat#(),umata#(),umatb#(),umate#(),umatd#(),zpart#,bond)
    DIM utemp1#(3,3),utemp2#(3,3)
    DIM jtemp1#(3),jstar1#(3),jnorm1#(3)
    DIM zlam AS DOUBLE, sum0 AS DOUBLE, zmax AS DOUBLE
    CLS
    LINE (150, 140)-(490, 220), 1, BF
    LINE (150, 140)-(490, 220), 15, B
    LOCATE 12, 22
    PRINT "Processing Subroutine UMATSQR"
    LOCATE 14, 22
    PRINT "Please wait....."
    FOR z = 1 TO bond
        FOR c = 1 TO 3
            FOR a = 1 TO 3
                sum0 = 0
                FOR B = 1 TO 3
                    sum0 = sum0 + (zmat#(c, B) * zmat#(B, a))
                NEXT B
                utemp1#(c, a) = sum0
            NEXT a
        NEXT c
    FOR a = 1 TO 3
        FOR B = 1 TO 3
            zmat#(a, B) = utemp1#(a, B)
        NEXT B
    NEXT a
NEXT z
END SUB

```

```

        NEXT B
    NEXT a
NEXT z
FOR c = 1 TO 3
    FOR a = 1 TO 3
        sum0 = 0
        FOR B = 1 TO 3
            sum0 = sum0 + (zmat#(c, B) * umata#(B, a))
        NEXT B
        utemp1#(c, a) = sum0
    NEXT a
NEXT c
FOR c = 1 TO 3
    FOR a = 1 TO 3
        sum0 = 0
        FOR B = 1 TO 3
            sum0 = sum0 + (utemp1#(c, B) * umatb#(B, a))
        NEXT B
        utemp2#(c, a) = sum0
    NEXT a
NEXT c
FOR c = 1 TO 3
    FOR a = 1 TO 3
        sum0 = 0
        FOR B = 1 TO 3
            sum0 = sum0 + (utemp2#(c, B) * umatc#(B, a))
        NEXT B
        utemp1#(c, a) = sum0
    NEXT a
NEXT c
FOR c = 1 TO 3
    FOR a = 1 TO 3
        sum0 = 0
        FOR B = 1 TO 3
            sum0 = sum0 + (utemp1#(c, B) * umatd#(B, a))
        NEXT B
        utemp2#(c, a) = sum0
    NEXT a
NEXT c
FOR a = 1 TO 3
    FOR B = 1 TO 3
        zmat#(a, B) = utemp2#(a, B)
    NEXT B
NEXT a
zpart# = zmat#(1, 1) + zmat#(1, 2) + zmat#(1, 3)
END SUB

```

APPENDIX D

DIELECTRIC RELAXATION OF THE POLYMER SYSTEM

PPG2025 + 1 MOLE %HgCl₂

D.1. Introduction

To establish the performance and reliability of the dielectric cell described in Chapter 9, the dielectric relaxation of the polymer system PPG2025 + 1 mole %HgCl₂, which had previously been studied by Hakiempoor⁴⁷, was investigated. A description of the apparatus and the experimental techniques involved in the investigation can be found in section 9.3 and section 9.4 of Chapter 9. Presented in this appendix are the dielectric loss results for that system.

D.2. Dielectric Loss Results

The variation of ϵ'' with respect to $\log f/(\text{Hz})$, at various temperatures, is shown as a series of normalised plots for the polymer system PPG2025 + 1 mole %HgCl₂, in Figure (D-1).

The presence of a broad α -type relaxation process for this system is readily discernible. A secondary relaxation process occurring at a lower frequency, shown only in some of the curves, is also present. This secondary relaxation process has been observed in previous investigations⁵¹ of PPG2025 polymer systems.

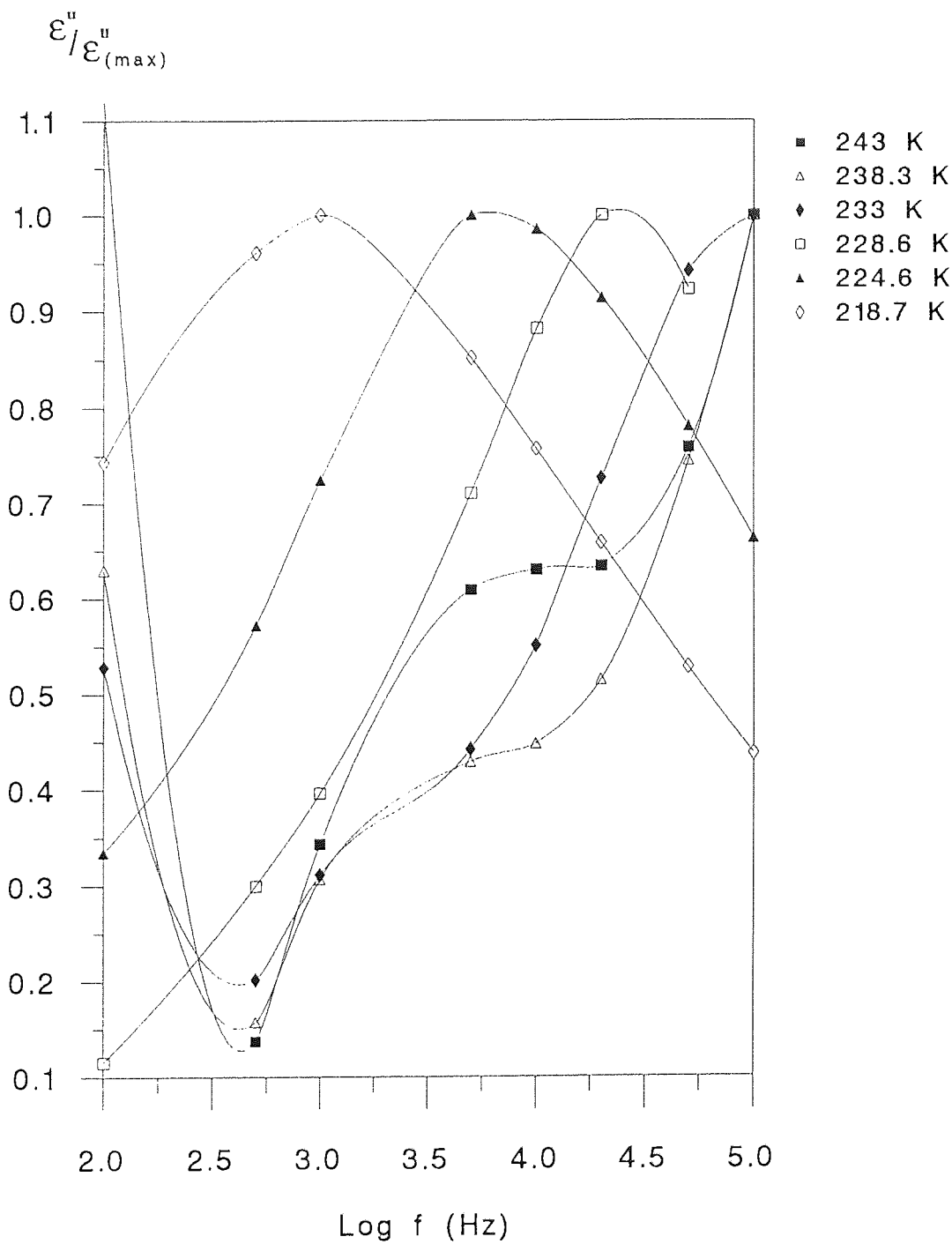


Figure (D-1). Frequency dependence of $\epsilon''/\epsilon''_{(max)}$ for the polymer system PPG2025 + 1 mole % HgCl₂.

D.3. Conclusion

The dielectric relaxation results for PPG2025 + 1 mole %HgCl₂ obtained from the application of the dielectric cell were compared with those published by Hakiempoor⁴⁷. Since both sets of results were in agreement as to the shape of the loss curves and also the temperature at which the dielectric loss occurred, it was concluded that the dielectric cell was suitable for use in this project.

APPENDIX E

SPECIFICATIONS OF THE DIELECTRIC CELL

E.1. Factors Effecting the Design of the Dielectric Cell

The dielectric cell used in this project was designed for use with a small quantity of polymer sample. When dealing with small sample volumes, it is important to design a cell that will produce a significant difference between the capacitance readings taken when the cell is empty, to readings taken when the cell contains a sample. This is necessary to take reliable dielectric readings. Taking this factor in to account, the dimensions of the dielectric cell were designed to produce a difference in capacitance of around $15\mu\text{F}$ for a polymer sample whose relative dielectric constant is around 2.5.

A further consideration when investigating the dielectric properties of polymers at low temperatures is sample contraction. If the sample contracts to the extent that it no longer occupies an area of the cell that is subjected to the electric field, then a significant error will be inherent in the results obtained. To counteract this effect, the cell was designed with an earthed guard ring, within which the sample was not subjected to an electric field. The sample in this region of the dielectric cell acted as a reservoir to compensate for any sample contraction.

E.2. Dimensions of the Cell

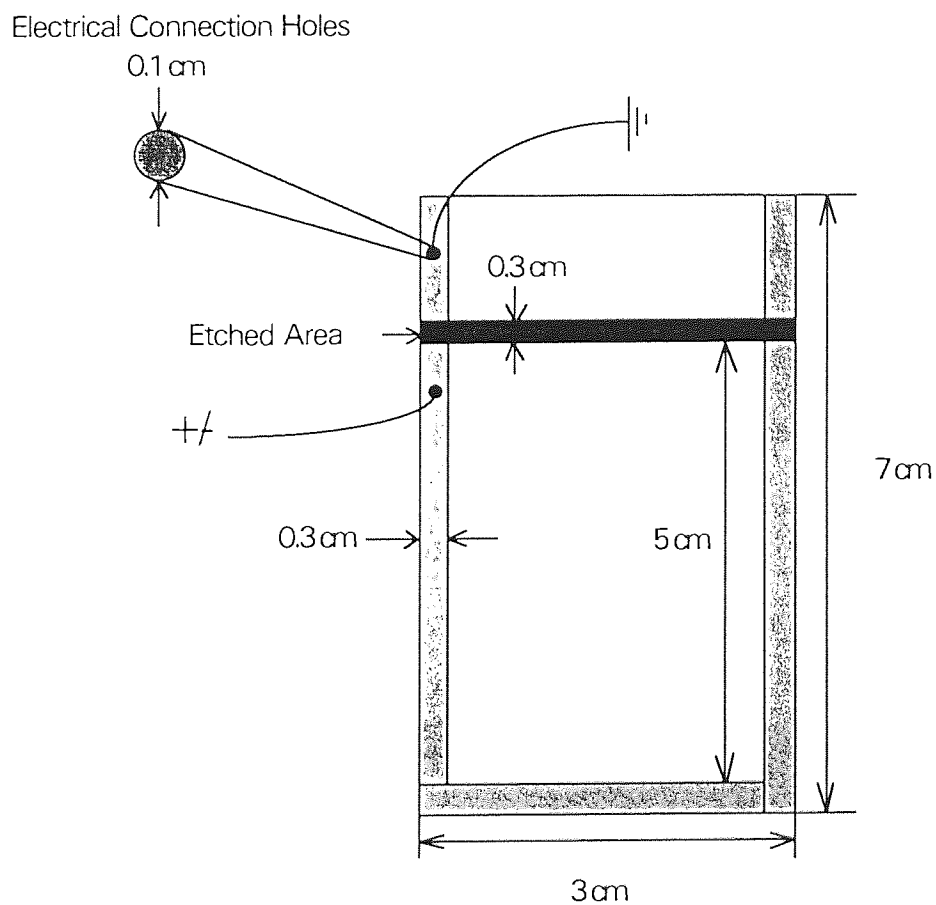


Figure (E-1). Schematic illustration of one plate of the dielectric cell.

The dielectric cell consisted of two plates with the dimensions specified in Figure (E-1). The distance of separation between the plates was 0.1 cm. The total sample volume of the cell was 1.6 cm^3 .

APPENDIX F

EXPERIMENTAL DIELECTRIC DATA

The experimental dielectric data used to generate the dielectric loss curves in Figures (10-1) and (10-2) for Dow polymer samples 10423-1 and 10423-9 are tabulated in Tables (F-1) and (F-2) respectively.

Table (F-1). Sample 10423-1 ($M_w = 28000$).

Temperature (K)	198	198	193	193	188	188
Frequency (Hz)	C_p (pF)	Tan δ	C_p (pF)	Tan δ	C_p (pF)	Tan δ
100	12.57	1.9E-02	12.02	1.6E-02	12.36	1.7E-02
200	11.82	1.5E-02	11.56	1.3E-02	11.67	1.3E-02
500	10.99	1.3E-02	10.85	1.2E-02	10.9	1.0E-02
1000	10.52	1.1E-02	10.41	9.8E-03	10.4	7.8E-03
2000	10.17	9.5E-03	10.12	8.0E-03	9.99	1.1E-02
4000	9.95	7.5E-03	9.82	1.9E-02	9.65	3.6E-02
7000	9.82	1.8E-02	9.66	2.8E-02	9.44	4.1E-02
10000	9.73	2.5E-02	9.51	3.7E-02	9.3	4.3E-02
20000	9.56	3.5E-02	9.38	4.1E-02	9.13	4.4E-02
70000	9.25	4.0E-02	9.02	3.9E-02	8.81	3.9E-02
100000	9.18	4.1E-02	8.93	3.7E-02	8.77	3.6E-02

Table (F-1). Continued.....

Temperature (K)	183	183	179	179
Frequency (Hz)	C_p (pF)	Tan δ	C_p (pF)	Tan δ
100	12.03	1.7E-02	11.9	1.6E-02
200	11.49	1.3E-02	11.47	1.5E-02
500	10.8	9.2E-03	10.88	1.9E-02
1000	10.25	1.2E-02	10.35	6.6E-02
2000	9.77	4.9E-02	9.82	8.9E-02
4000	9.35	6.2E-02	9.35	9.0E-02
7000	9.11	6.2E-02	9.09	8.7E-02
10000	8.9	6.0E-02	8.9	8.0E-02
20000	8.73	5.5E-02	8.65	6.8E-02
70000	8.41	4.4E-02	8.33	5.0E-02
100000	8.37	3.9E-02	8.23	4.7E-02

Table (F-2). Sample 10423-9 ($M_w = 46000$).

Temperature (K)	205	205	197	197	193	193
Frequency (Hz)	C_p (pF)	Tan δ	C_p (pF)	Tan δ	C_p (pF)	Tan δ
100	11.36	3.5E-02	11.4	2.9E-02	11.44	2.5E-02
200	10.66	3.1E-02	10.69	2.6E-02	10.74	2.3E-02
500	9.99	2.7E-02	10.05	2.4E-02	10.1	2.0E-02
700	9.8	2.5E-02	9.84	1.9E-02	9.92	1.6E-02
1000	9.64	2.3E-02	9.67	1.5E-02	9.73	1.3E-02
2000	9.29	1.9E-02	9.35	1.2E-02	9.42	7.3E-03
5000	8.97	1.5E-02	9.03	8.3E-03	9.06	2.9E-02
7000	8.89	1.2E-02	8.93	2.4E-02	8.97	3.4E-02
10000	8.78	7.3E-02	8.82	3.3E-02	8.85	3.8E-02
20000	8.64	2.8E-02	8.67	3.8E-02	8.69	3.8E-02
50000	8.42	3.7E-02	8.44	3.5E-02	8.47	3.2E-02
100000	8.36	3.7E-02	8.37	3.1E-02	8.41	2.5E-02

Table (F-2). Continued.....

Temperature (K)	187	187	183	183
Frequency (Hz)	C_p (pF)	Tan δ	C_p (pF)	Tan δ
100	12.05	2.6E-02	12.1	2.8E-02
200	11.34	2.2E-02	11.4	2.5E-02
500	10.57	1.9E-02	10.63	2.1E-02
700	10.32	1.6E-02	10.43	1.8E-02
1000	10.07	1.2E-02	10.13	5.0E-02
2000	9.69	4.2E-02	9.75	7.6E-02
5000	9.26	5.5E-02	9.31	8.1E-02
7000	9.14	5.7E-02	9.19	7.8E-02
10000	8.99	5.6E-02	9.02	7.3E-02
20000	8.8	4.9E-02	8.83	6.0E-02
50000	8.55	3.9E-02	8.58	4.6E-02
100000	8.46	3.1E-02	8.52	3.9E-02